MAR 26 1928

BUREAU OF STANDARDS JOURNAL OF RESEARCH

Vol. 1 AUGUST, 1928 No. 2

CONTENTS

RP. No.	TITLE AND AUTHOR	Page
6	Some measurements of the transmission of ultra-violet radiation through various kinds of fabrics. W. W. Coblentz, R. Stair, and C. W. Schoffstall	105
7	Tinting strength of pigments. H. D. Bruce	125
8	Wave-length measurements in the arc and spark spectra of hafnium. William F. Meggers	151
9	Tests of the effect of brackets in reinforced concrete rigid frames. Frank E. Richart	189
10	Accelerated laboratory corrosion test methods for zinc-coated steel. Edward C. Groesbeck and William A. Tucker	255

DEPARTMENT OF COMMERCE
BUREAU OF STANDARDS
George K. Burgess, Director

BUREAU OF STANDARDS JOURNAL OF RESEARCH

August, 1928
Vol. 1, No. 2

PRICE, 25 CENTS
$2.75 PER YEAR ON SUBSCRIPTION
Sold only by the Superintendent of Documents, U. S. Government Printing Office
Washington, D. C.

UNITED STATES
GOVERNMENT PRINTING OFFICE
WASHINGTON
1928

Announcement

BUREAU OF STANDARDS JOURNAL OF RESEARCH

Beginning July, 1928, a new periodical to be known as the BUREAU OF STANDARDS JOURNAL OF RESEARCH supersedes and continues the two series of research publications heretofore issued under the designations "Scientific Papers of the Bureau of Standards," and "Technologic Papers of the Bureau of Standards."

Forty-four volumes of the two superseded series have been published. The 22 volumes of scientific papers issued by the bureau (since 1904) contain some 572 research papers on fundamental science, and the 22 volumes of technologic papers (issued since 1910) contain some 370 research papers on applied science.

The new BUREAU OF STANDARDS JOURNAL OF RESEARCH will publish the results of the bureau's researches (both theoretical and experimental). It is expected the monthly issues will range from 100 to 300 pages, an average issue containing about 200 pages. Subscriptions ($2.75 per year, United States, Canada, and Mexico) should be placed direct with the Superintendent of Documents, Government Printing Office, Washington, D. C. ($3.50 for foreign subscriptions).

Shortly after each month's JOURNAL is published, reprints of the separate articles contained may be purchased from the Superintendent of Documents.

SOME MEASUREMENTS OF THE TRANSMISSION OF ULTRA-VIOLET RADIATION THROUGH VARIOUS FABRICS

By W. W. Coblentz, R. Stair, and C. W. Schoffstall

ABSTRACT

In this paper measurements are described of the transmission of ultra-violet and visible radiation through fabrics made of various kinds of material—cotton, natural silk, rayon (artificial silk), linen, and wool.

The source of radiation was a quartz mercury arc lamp from which ultra-violet radiation was obtained by filtration through a Corning purple glass 986A, and the visible radiation was isolated by filtration through a yellowish-green glass.

By examining black and white samples of the same material, it was possible to eliminate the effect of the radiation transmitted through the openings between the individual threads and thus determine the amount of radiation transmitted directly through the yarn.

Fabrics of close-weave and open-weave (twill, satin, voile) material were examined. The results obtained on these different weaves are in agreement in showing that, comparing materials having the same weight, there is practically no difference in the amount of ultra-violet transmitted through bleached samples of cotton, linen, viscose rayon, and the rayon made by the cellulose acetate process.

The fresh, white, natural silk is almost as transparent as bleached cotton, while wool is only about half as transparent to ultra-violet solar radiation as bleached cotton.

In all cases when the fabric is dyed, or slightly yellowed with age, the ultra-violet transmission through the thread is greatly decreased. Hence, as is to be expected in comparing various kinds of dyed fabrics, the one having the largest openings between the threads transmits the most ultra-violet.

CONTENTS

	Page
I. Introduction	106
II. Experimental procedure	107
III. Discussion of the transmission data on fabrics	117
1. Cotton fabrics	119
2. Linen fabrics	119
3. Silk fabrics	119
4. Wool fabrics	120
5. Rayon fabrics	120
6. Concluding remarks	122
IV. Transparency of feathers and animal tissue	123

100438°—28—1

I. INTRODUCTION

An important utilitarian problem is the transparency or opacity of fabrics to solar radiation: (1) Great transparency when it is desired to expose the body to the short wave length ultra-violet rays which have a therapeutic value, and (2) great opacity when it is desired to shield the body from excessive amounts of these rays, as, for example, the clothing and head gear of troops and expeditions in tropical countries.

Incidentally the problem promises to be of especial interest optically in connection with the question of the transmission of light through an optically inhomogenous medium in the form of a twisted thread which consists of a great many strands of homogenous material (cellulose) having a low coefficient of absorption when undyed and usually a rather high coefficient of selective absorption when dyed.

As a result of internal reflection within the individual fibers or single threads (if it is artificial material), a large part of the incident radiation is returned upon its original path, and if the absorption is low, an appreciable amount of the remainder is transmitted either directly through, or by successive total reflection within, the individual strands of the yarn.

From our earlier studies of thin films of cellulose [1] either as a lacquer or as a covering for airplane fabrics, it was found that a slight discoloration, caused by exposure to ultra-violet radiation, greatly decreases the transmission of these rays. From this observation, and also from the fact that fabrics are usually colored with dyes that absorb the ultra-violet, it was recently indicated [2] that there is no justification for advocating rayon (artificial silk) in preference to natural silk, cotton, or linen fabrics as a therapeutic medium for transmitting ultra-violet rays. In fact, as shown in the present paper, if any preference is to be given to the composition of the fabric, instead of the kind of weave, then the material of pure white cellulose (cotton and regenerated cellulose rayon) is somewhat better than wool and natural silk for transmitting the ultra-violet rays.

II. EXPERIMENTAL PROCEDURE

Since the material examined was inhomogeneous, causing a relatively large scattering of the light, it was impracticable to determine the spectral transmission with a spectroradiometer. Moreover, for the purposes of the present inquiry it was sufficient to determine the transmission of the fabric for the band of ultra-violet radiation between 290 and 320 mμ (which rays are known to have a therapeutic value) relative to the transmission of a spectral region of

[1] Coblentz and Kahler, B. S. Sci. Paper No. 342, **15**, p. 215; 1919.
[2] Coblentz, Physical Therapeutics, **45**, p. 407; 1927. Coblentz, Trans. Illum. Eng. Soc., **23**, p. 247; 1927.

longer wave lengths in the yellow-green of the visible spectrum, where selective absorption is less pronounced or nonexistent, which condition obtains in white fabrics.

Using a 110-volt quartz mercury arc as a source, an image of the burner was focused by means of a quartz lens of 18 cm focal length upon a Bi-Ag thermopile [3] having a surface 3 by 9 mm (see fig. 1a). This was covered with a window of quartz 2.5 mm in thickness to exclude long wave length, low-temperature radiation from the cloth, which may become heated [4] when exposed to the quartz lamp, and consequently radiate to the thermopile. This effect was found negligible in the case of thin material which did not absorb much of the incident radiation.

The cloth under examination was placed directly over this quartz window in order to have it as close as possible to the thermopile receiver, so as to intercept as much as possible of the radiation which emanates diffusely from the underside of the cloth. In order to have reproducible conditions, the cloth was held flat by placing over it the glass which was used for isolating either the ultra-violet or visible radiation.

The filter for isolating the ultra-violet radiation at 250 to 400 mμ consisted of a plate of Corning purple glass G986A, which is quite opaque to the visible and the infra-red rays. The ultra-violet spectral transmission of this glass is depicted in Figure 1, as observed when the sample was new. After it had been exposed to ultra-violet radiation from the quartz mercury arc lamp in the course of these and other measurements, the transmission remained practically unchanged. However, the effect of prolonged exposure to ultra-violet radiation is to decrease the transmission of this screen in the extreme ultra-violet wave lengths. That such a change was not sufficient to affect our work was determined by measurements on the same samples of fabrics at the beginning and at the completion of this investigation. For some of our measurements we used a combination of G986A and a piece of window glass, No. 4, by means of which filter the ultra-violet is separated into two bands, at 250 to 310 mμ and 310 to 400 mμ, respectively, as shown on Figure 1.

The filter used for isolating the yellow and green in the visible spectrum consisted of a greenish-yellow glass, shade No. 3 of Willsonweld (or Bausch and Lomb) glass, which is opaque to the ultra-violet and the infra-red (see fig. 1). Usually no transmission measurements were made on colored fabrics, because this screen is not monochromatic and, hence, is best adapted for measurements on white and black fabrics.

In order to obtain the amount of ultra-violet and visible radiation transmitted through the openings between the thread, measurements

[3] Coblentz and Kahler, B. S. Sci. Paper No. 378, **16**, p. 233; 1920.
[4] Coblentz, B. S. Bull. No. 196, **9**, p. 283; 1913.

were made on white and on black samples of the same kind of cloth, the black threads having practically zero transmission. In some cases the cloth was dyed black, and since the same results were obtained by the two methods, when the samples were small it was quicker to blacken part of the fabric by means of india ink. Repeated tests showed that the blackening of the threads with india ink (Higgins drawing ink) was satisfactory.

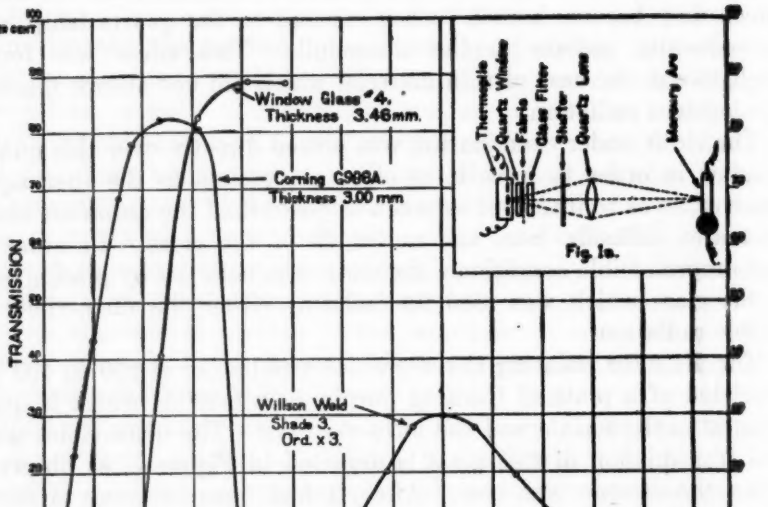

FIG. 1

The electric current generated by means of the thermopile when exposed to radiation was measured by means of an ironclad Thomson galvanometer.[5] By noting the galvanometer deflection, with and without the cloth placed over the thermopile receiver, the percentage of transmission was obtained. These values for both the ultra-violet and the visible region of the spectrum are assembled in Tables 1 and 2.[6]

[5] Coblentz, B. S. Bull. No. 282, **13**, p. 423; 1916.

[6] Information on the use of thermopiles, etc., in radiometry, is given in B. S. Bulls. Nos. 85, 188, 229, 282, 319, 378, and 413, obtainable from the Superintendent of Documents, Washington, D. C.

TABLE 1.—*Percentage of transmission of ultra-violet radiation through various substances*

TABLE 1.—*Percentage of transmission of ultra-violet radiation through various substances*

[Columns 2, 3, and 4 give the total transmission through the threads and intervening spaces]

Sample No.	Observed transmission, in per cent				Transmission through thread in per cent		Description of material					
	250 to 400 mμ	250 to 310 mμ	310 to 400 mμ	Through interstices	250 to 310 mμ	310 to 400 mμ	Mark or type	Weave	Color	Thread count: Warp	Thread count: Filler	Weight
												Oz. per sq. yd.
COTTON (CELLULOSE)												
24S	13.1	10.4	15.7	2.2	8.4	13.8	Muslin	Plain	White	83	80	4.6
10H	10.0	6.9	13.0	2.6	4.4	10.7	Shirting	do	do	91	84	3.4
7b	24.0	21.1	26.7	3.9	17.9	23.7	Balloon	do	do	126	128	1.6
5H	19.0	16.4	21.3	5.0	12.0	17.2	Batiste	do	do	97	96	2.0
4H	34.0	31.3	37.0	17.5	16.7	23.7	Nainsook	do	do	97	77	2.0
23S	13.2	10.2	15.9	1.7	8.7	14.4	Broadcloth	do	do	105	58	3.7
3B	23.0	20.7	25.2	3.9	17.5	22.2	do	do	do	124	66	2.8
30L	7.3	4.5	9.9	.8	3.8	9.2	Handkerchief	do	do	50	47	5.8
3M	27.5	24.5	30.2	13.4	12.8	19.4	Mesh	Leno	do	36	40	4.2
WOOL												
39F	8.4	3.8	12.7	0.3	3.5	12.4	Worsted serge	Twill	White	91	72	3.8
54R	7.5	2.6	13.3	.1	2.5	13.2	Worsted rep	Plain	do	80	45	4.5
54F	11.5	5.4	15.4	.7	4.7	14.8	Worsted flannel	Twill	do	92	72	4.0
LINEN (CELLULOSE AND LIGNOSE)												
5L	26.8	25.1	28.3	12.8	14.1	17.8	Handkerchief	Plain	White	90	90	2.2
6L	8.3	5.7	10.7	1.3	4.5	9.5	Napkin	Damask	do	72	96	4.4
7L	15.3	12.9	16.9	3.5	9.7	13.9	Tablecloth	do	do			
8L	10.0	7.8	11.7	3.5	4.5	8.5	Towel	Huckaback	do	60	42	5.0
9L	5.5	4.0	6.9	2.5	1.5	4.5	do	do	do	75	35	7.8

TABLE 1.—*Percentage of transmission of ultra-violet radiation through various substances*—Continued

[Columns 2, 3, and 4 give the total transmission through the threads and intervening spaces]

Sample No.	Observed transmission, in per cent				Transmission through thread in per cent		Description of material					
	250 to 400 mμ	250 to 310 mμ	310 to 400 mμ	Through interstices	250 to 310 mμ	310 to 400 mμ	Mark or type	Weave	Color	Thread count		Weight
										Warp	Filler	
												Oz. per sq. yd.
SILK												
2	16.2	12.1	20.0	3.0	9.4	17.5	Unweighted	Plain	White	100	105	1.8
7H	21.0	15.7	24.7	4.2	12.0	21.4	Parachute	do	do	130	86	1.4
4	20.0	14.0	25.2	2.9	11.4	23.0	Crêpe, unweighted	do	do	135	80	2.0
RAYON (CELLULOSE ACETATE)												
4	60.0	59.0	61.0	43.0	28.1	31.6	Voile	Plain	White	63	66	1.4
3c	25.0	20.5	29.0	1.5	19.3	27.9	Dress goods	do	do	105	54	3.0
2H	12.5	12.1	13.2	.3	11.8	12.9	Satin	Twill	Tan	120	72	2.5
1	15.3	11.0	19.1	1.3	9.8	18.0	Twill	do	White	125	100	2.3
5	16.0	10.3	21.3	.3	10.0	21.1	Satin	do	do	105	115	2.7
RAYON (VISCOSE, CELLULOSE)												
10	61.0	61.0	61.0	5.1	20.4	20.4	Voile	Plain	Light yellow	62	52	1.2
12a	17.5	12.0	22.6	.1	11.9	22.5	Rep	Rep	White	120	54	4.4
13	29.0	24.3	32.0	2.7	22.2	30.1	Satin	Satin	do	144	80	2.0
RAYON (NITROCELLULOSE)												
14	20.1	17.5	22.5	0.1	17.4	22.4	Satin	Satin	White	164	125	2.6
RAYON (CUPRAMMONIUM)												

RAYON (CUPRAMMONIUM)

15	25.0	22.6	27.1	6.0	17.7	22.4	Crêpe	Crêpe	White	79	66	2.7
16	26.8	23.6	29.7	9.0	16.1	22.8	Taffeta		do	158	84	1.9
16a	13.1	12.7	13.4	9.0	4.1	4.8	do		Brown	158	84	1.9

FEATHERS

Sample No.	Observed transmission, in per cent			Description of material
	250 to 400 mμ	250 to 310 mμ	310 to 400 mμ	
1	21.8	19.4	24.0	Catbird wing feather (primary).
2	35.2	34.8	35.6	Do.
3	28.5	27.6	29.4	Do.
4	26.5	21.2	31.3	White ibis wing feather (primary).
5	28.9	22.1	35.2	White ibis wing feather (secondary).
6	52.1	48.0	56.0	White swan feather (secondary).
7	11.7	7.1	16.0	White pigeon wing feather (primary).
8	19.4	16.7	19.9	Brown turkey feather.
9	17.9	17.4	18.4	Do.
10	14.2	13.3	15.1	Do.
11	26.4	22.8	29.8	Barred plymouth rock chicken feather.
12	26.5	24.3	28.5	Woodpecker wing feather (primary).
13	31.1	28.8	33.3	Woodpecker wing feather (secondary).
14	24.0	21.5	26.3	Do.
15	23.3	14.9	31.0	Brownish-red chicken wing feather (primary).
16	15.5	12.6	18.2	Brownish-red chicken wing feather (secondary).
17	23.6	22.5	24.8	Black chicken wing feather (secondary).

ANIMAL TISSUE

1	31.0	26.0	39.0	Outer wall of chicken intestine. Thickness 0.05 mm.
2	36.0	34.0	43.0	Do.

TABLE 2.—*Transmission in per cent of the total ultra-violet and visible radiation observed through various fabrics, using screen G986A for columns 2, 3, and 4, and the screen transmitting visible radiation for column 5*

COTTON (CELLULOSE)

Sample No.	Observations of total ultra-violet transmitted through thread and interstices	Observations of ultra-violet transmitted through interstices	Transmission of ultra-violet through thread in per cent	Observations of total visibility transmitted through thread and interstices	Ratio U. V. / Vis.	Description of material					
						Mark or type	Weave	Color	Thread count		Weight
									Warp	Filler	
											Oz. per sq. yd.
14H	16.0	2.5	13.8	24.0	63	Shirting	Plain	White	82	74	2.8
12H	9.5	1.1	8.5	19.0	47	do	do	do	88	82	3.8
13H	16.0	2.0	14.3	22.0	70	do	do	do	80	74	3.0
29S	7.6	4.5	3.2			do	do	Light tan	70	44	6.4
10H	10.0	2.6	7.6	19.0	45	do	do	White	91	84	3.4
16H	23.5	4.7	19.7	29.0	77	do	do	do	107	92	2.0
9S	3.9	2.4	1.5			Romper cloth	do	Green	56	47	7.2
10S	6.9	2.4	4.6			do	do	Linen	53	45	4.7
15H	15.0	1.0	14.2	20.5	72	Shirting	do	White	87	76	3.0
7B	24.0	3.9	20.9	30.0	77	Balloon	do	do	126	128	1.6
7	8.4	3.9	4.7	20.0	28	do	do	Natural	126	128	1.6
24S	13.1	2.2	11.1	21.5	57	Muslin	do	White	83	80	4.6
23S	13.2	1.7	11.7	19.0	66	Broadcloth	do	do	105	58	3.7
3B	23.0	3.9	19.9	26.7	84	Broadcloth (mercerized)	do	do	124	66	2.8
27S	21.0	6.8	15.2			Nainsook	do	Orchid	67	58	4.5
4H	34.0	17.5	20.0	39.0	77	do	do	White	97	77	2.0
5H	19.0	5.0	14.7	26.5	65	Batiste	do	do	97	96	2.0
8	7.8	.2	7.6	13.0	59	Duck	do	do	92	26	7.0
14S	3.2	.5	2.7			Sateen (mercerized)	Satin	Light tan	83	66	3.4
12S	18.0	9.5	9.4			Crêpe	Crêpe	Yellow	78	40	3.5
16S	.2	.03	.2			Khaki	Twill	Khaki	100	78	5.9
18S	14.0	3.8	10.6			Pongee	Plain	Light blue	72	66	2.6
19S	16.5	3.8	13.2			do	do	Light pink	72	70	2.6
21S	21.0	3.8	17.9	26.5	76	do	do	White	73	68	2.6
22S	14.0	3.8	10.6			do	do	Rose	70	70	2.5

28S	7.9	.03	7.9			Flannel (outing)	do	Light pink	50	44	4.3
32S	10.4	.7	9.8	17.5	58	Stocking		White			
2S	48.0	40.0	13.3			Voile	Plain	Light yellow	53	50	1.7
3H	52.0	42.0	17.2			do	do	Light blue	66	55	1.8
5S	27.0	15.5	13.6			Cotton-silk dress goods	Crêpe	Dark rose	90	90	1.6
6S	27.0	13.0	16.1			do	Plain	Lavender	96	86	1.7
3S	32.0	21.5	13.4			Cotton-rayon	do	Rose	66	50	2.1
26S	13.0	3.5	9.8	22.0	51	Handkerchief	do	White	52	50	4.3
30L	7.3	.8	6.6	15.3	45	do	do	do	50	47	5.8
3M	27.5	13.4	16.3	33.8	69	Mesh	Leno	do	36	40	4.2
						SILK					
3	21.0	3.8	17.9	32.0	61	Crêpe, unweighted	Plain	White	192	90	1.7
4	20.0	2.9	17.6	30.0	63	do	do	do	135	80	2.0
1S	10.0	.9	9.2			Crêpe (flat)	Crêpe	Reddish orange	75	180	1.6
37S	25.0	10.5	16.2			Dress goods	Plain	Lavender	73	160	1.1
6[1]	10.0	2.6	7.6	25.0	33	Crêpe, weighted	do	White	210	90	2.0
5[1]	6.0	1.1	5.0	18.0	29	Taffeta, unweighted	do	do	122	90	2.4
7H	21.0	4.2	17.5	30.0	65	Parachute	do	do	130	86	1.4
2	16.2	3.0	13.6	26.0	57	do	do	do	100	105	1.8
11S	22.5	8.5	15.3			Dress goods	do	Lavender	126	78	1.3
36S	67.0	55.0	26.7	72.0	71	Crêpe (georgette)	Crêpe	White	92	80	.6
13S	18.5	5.9	13.4			Silk-rayon	Satin	Pink	130	54	2.9
						WOOL					
35B	18.5	3.7	15.4	36.0	46	Worsted batiste	Plain	White	63	62	2.6
35C	11.0	2.4	8.8	31.0	30	Worsted crêpe	Crêpe	do	50	50	4.8
35H	15.0	2.6	12.7	32.5	41	Worsted henrietta	Plain	do	56	87	2.8
39C	12.5	1.0	11.6	28.0	43	Worsted crêpeline	Crêpe	do	82	72	3.5
39F	8.4	.3	8.1	27.0	30	Worsted serge	Twill	do	91	72	3.8
54C	3.3	.2	3.1	19.0	16.5	Worsted cheviot	do	do	35	30	8.2
54F	11.5	.7	10.9	28.5	39	Worsted flannel	do	do	92	72	4.0
54G	4.4	.03	4.4	19.0	23	do	do	do	70	48	5.6
35S	.7	.0	.7			do	Plain	Green	32	36	8.8
54R	7.5	.1	7.4	24.0	31	Worsted rep	do	White	80	45	4.5
11H	.8	.1	.7			Worsted serge	Twill	Navy blue	45	50	7.2
10	2.2	.5	1.7	13.0	13.6	do	do	White	60	54	7.0
7S	15.0	7.4	8.2	30.0	33.6	do	do	do	70	60	3.7
8S	7.9	1.0	7.0	20.0	36	Wool-cotton serge	do	do	58	52	4.7
6H	3.0					Worsted suiting	Plain	Dark gray	44	36	6.2

[1] Samples yellowed with age.

TABLE 2.—*Transmission in per cent of the total ultra-violet and visible radiation observed through various fabrics, using screen G986A for columns 2, 3, and 4, and the screen transmitting visible radiation for column 5*—Continued

WOOL—Continued

Sample No.	Observations of total ultra-violet transmitted through thread and interstices	Observations of ultra-violet transmitted through interstices	Transmission of ultra-violet through thread in per cent	Observations of total visibility transmitted through thread and interstices	Ratio U. V. / Vis.	Description of material					
						Mark or type	Weave	Color	Thread count		Weight
									Warp	Filler	
											Oz. per sq. yd.
8A	15.5	2.2	13.6	33.0	43	Worsted dress goods	Plain	Cream	57	90	3.0
8B	13.5					do	do	Pink	60	85	3.1
8C	21.0	8.3	13.9	37.0	44	do	do	Cream	64	60	2.8
8D	14.0					do	do	Light tan	66	60	2.9
9N	18.0	9.5	9.4	30.0	41	Worsted (silk filling)	do	Greyish white	68	60	2.2
9-4	17.5					do	do	Blue	68	60	2.2
9-3	16.0					do	do	Rose	68	60	2.2
15S	3.0	2.5	.5			Wool-cotton suiting	do	Dark linen	40	40	6.6
						LINEN (CELLULOSE AND LIGNOSE)					
9	5.5	1.3	4.3	13.0	36	Airplane	Plain	Natural	102	99	3.8
9B	13.5	1.3	12.4	22.0	59	do	do	White	102	99	3.8
5L	26.8	12.8	16.1	29.2	85	Handkerchief	do	do	90	90	2.2
6L	8.3	1.3	7.1	12.6	62	Napkin	Damask	do	72	96	4.4
7L	15.3	3.5	12.2	19.3	75	Tablecloth	do	do			
8L	10.0	3.5	6.7	13.7	64	Towel	Huckaback	do	60	42	5.0
9L	5.5	2.5	3.1	12.4	30	do	do	do	75	35	7.8
4S	7.9	3.3	4.8			French linen	Plain	Light red	50	45	4.2

RAYON (CELLULOSE ACETATE)

I	14.0	1.3	12.9	23.5	57	Twill	Twill	White	125	100	2.3
II	3.0	1.3	1.7			do	do	Yellow	125	100	2.3
III	2.2	1.3	.7			do	do	Gold	125	100	2.3
5	16.0	.3	15.8	25.0	64	Satin	do	White	105	115	2.7
W13	8.1	1.5	6.7			do	Satin	Orange	100	112	2.6
2H	12.5	.3	12.2			do	Twill	Tan	120	72	2.5
12	14.0	1.5	12.7			Bedspread	do	Rose	90	72	3.3
6	17.5	.7	16.9			Dress goods	do	Light lavender	79	80	3.4
3C	25.0	1.5	23.9	32.8	75	do	Plain	White	105	54	3.0
W20	21.0	4.3	17.5			do	Twill	Pink	130	92	2.0
W613	2.7	1.6	1.1			Satin	Satin	Orange	170	120	3.0
11	12.0					Bedspread	Twill	Light lavender	90	72	3.3
WA43	17.5	4.2	13.9			Moire	Plain corded	Light blue	150	50	3.6
WA10	10.5	3.1	7.6			Chiffon taffeta	Plain	Green	160	78	2.4
W36	45.0	41.0	6.8			Chiffon crêpe	do	Orchid	92	85	1.5
101	49.0	35.0	21.6			Chiffon	do	Green	82	85	1.7
100R	58.0	47.0	20.8			Voile	do	Red	62	62	1.4
100Y	60.0	47.0	24.5			do	do	Yellow	62	62	1.4
100G	55.0	47.0	15.1			do	do	Light green	62	62	1.4
1H	55.0	49.0	11.8			do	do	Blue	66	62	1.4
4	60.0	43.0	29.8			do	do	White	63	66	1.4
2	33.0	25.0	10.7	41.0	50	Plain knit	Knit	do			
1A[1]	38.0	23.0	19.5	45.0	68	do	do	do			
1B	32.5	23.0	12.3			do	do	Cream			
1C	31.0	23.0	10.4			do	do	Dark cream			
1D	30.0	23.0	9.1			do	do	Light peach			
1E	27.0	23.0	5.2			do	do	Light yellow			
1F	24.5	23.0	1.9			do	do	Yellow			

RAYON (VISCOSE, CELLULOSE)

13	29.0	2.7	27.0	33.0	87	Satin	Satin	White	144	80	2.0
12A	17.5	.1	17.4	25.0	70	Rep	Rep	do	120	54	4.4
12	11.0	.1	10.9			do	do	Rose	120	54	4.4
1	26.0	12.0	15.9			Plain knit	Knit	Cream			
11A	52.0	39.0	21.3	56.0	76	Voile	Plain	White	67	65	1.5
11	54.0	45.0	16.4			do	do	Turquoise blue	67	65	1.5
10	61.0	51.0	20.4			do	do	Light yellow	62	52	1.2
10B	59.0	51.0	16.3			do	do	Light blue	62	52	1.2
34S	38.0					Stocking		Black			

[1] Samples 1A to 1F are knitted from 150 denier yarn, 30 wales and 35 courses to the inch.

TABLE 2.—*Transmission in per cent of the total ultra-violet and visible radiation observed through various fabrics, using screen G986A for columns 2, 3, and 4, and the screen transmitting visible radiation for column 5*—Continued

RAYON (NITROCELLULOSE)

Sample No.	Observations of total ultra-violet transmitted through thread and interstices	Observations of ultra-violet transmitted through interstices	Transmission of ultra-violet through thread in per cent	Observations of total visibility transmitted through thread and interstices	Ratio U. V. / Vis.	Description of material					
						Mark or type	Weave	Color	Thread count		Weight
									Warp	Filler	
											Oz. per sq. yd.
14	20.1	0.1	20.0	25.5	79	Satin	Satin	White	164	125	2.6
RAYON (CUPRAMMONIUM)											
15	25.0	6.0	20.2	31.2	75	Crêpe	Crêpe	White	79	66	2.7
16	26.8	9.0	19.5	32.3	76	Taffeta	Plain	do	158	84	1.9
16A	13.1	9.0	4.5			do	do	Brown	158	84	1.9

III. DISCUSSION OF THE TRANSMISSION DATA ON FABRICS

Under this caption is given a summary (Tables 1 and 2) of the observations on the transmission of ultra-violet and visible radiation through various fabrics; also a comparative analysis of a few of these observations on samples typical of the group.

As already stated, by examining the same weave of cloth, white (in most cases bleached) and dyed black, it was possible to measure the transmission through the openings between the individual threads and thus determine the amount of radiation transmitted directly through the thread. Columns 2 and 5 of Table 2 give the amount transmitted through the fabric as a whole.

In this manner it was possible to study close-weave and open-weave (for example, twill, satin, and voile) material and determine quantitatively the amount of ultra-violet and visible radiation transmitted through the various kinds of yarn, composed of cotton, of natural silk, of rayon (artificial silk), of linen, and of wool.

Starting with an open-weave fabric (for example, a voile weave), as is perfectly obvious, the fewer the threads per unit area the higher the transmission. But even in this case, by blackening the fabric with a dye it was possible to determine the amount of radiation obstructed or transmitted by the thread. As shown in Table 2, the transmission of radiation (for example, viscose rayon, voile No. 11a; cellulose acetate rayon, celanese 1H; silk georgette, 36S) through open-weave fabrics is 55 to 65 per cent, of which amount 40 to 55 per cent is transmitted through the openings between the thread. Deducting the amount transmitted through the openings between the threads, the ratio of the ultra-violet relative to the visible transmitted through the yarn ranges from 70 to 75 per cent. This is in good agreement with the measurements on similar, closely woven material (for example, the satin weaves of viscose, etc.), showing that the method is reliable.

In Table 1 are given the observed transmissions, in per cent of the total incident radiation of wave lengths at 250 to 310 mμ and 310 to 400 mμ. The data given in columns 6 and 7 of this table are interesting in showing that these materials are more opaque in the shorter wave lengths than in the longer wave lengths of the ultra-violet. This is to be expected, of course, from our spectral transmission measurements, using homogeneous films of material and monochromatic radiation.

The data given in columns 2 and 5 of Table 1 are the same as given in columns 2 and 3 of Table 2. The data in column 2 of Table 1 are the observed measurements of the whole ultra-violet spectral region at 250 to 400 mμ, and, as is to be expected, they

are about the average of the observed transmissions of the two components (250 to 310 mμ and 310 to 400 mμ) of this spectral region.

Columns 6 and 7 in Table 1 and the column 4 in Table 2 give the percentage of ultra-violet incident on the thread that is transmitted through the thread. These values are obtained by deducting from the observed transmissions in column 2 the amount of radiation transmitted through the openings between the threads (column 3 of Table 2) as determined by measurements on the blackened material. For example, since the sample of white muslin, 24S, transmitted 2.2 per cent through the holes between the threads, 97.8 per cent of the total area was occupied by the threads. Hence, referring to Table 1 $(10.4-2.2)\div 97.8=8.4$ per cent is the amount of ultra-violet of wave lengths 250 to 310 mμ transmitted through the threads of this sample of muslin.

In the same manner the visible radiation transmitted through the thread might be obtained from column 5. However, it seemed instructive to record also the ratio of the transmissions of the ultra-violet to the visible (columns 2 and 5) after deducting the amount transmitted through the interstices. These ratios are given in column 6. They serve as a measure of the absorption in the ultra-violet. For example, they show very effectively that the ultra-violet transmission ranges from 14 per cent (wool No. 10) to 87 per cent (viscose satin No. 13) of that of the visible spectrum. Furthermore, these ratios show that the ultra-violet transmission relative to the visible is much higher (70 to 87 per cent) for the pure white cellulose (cotton and viscose rayon) than the cellulose acetate rayon, which gives ratios of 50 to 75 per cent. Of course, the absolute values of the ultra-violet transmissions of the threads given in column 4 of Table 2 also show this condition, but this method of recording the data accentuates errors of observation which are eliminated to some extent by taking ratios, which serves as a check on the accuracy of the measurements.

As is to be expected, since there are probably no narrow absorption bands, the transmissions of these wide bands of spectral radiation represent averages which approximate the values that would be obtained from monochromatic transmission curves. For example, the sample of cotton, 30L, has the following gradually increasing transmissions of 3.8, 9.2, and 15.3 per cent, respectively, for the spectral regions of 240 to 310 mμ, 310 to 400 mμ, and 400 to 750 mμ.

Considered as a whole, these data show the much greater absorption of the short wave length ultra-violet rays than those in the visible spectrum; and they disclose quite conspicuously the very rapid increase in absorption of these short wave-length rays by a slight discoloration or tinting of the fabric—as, for example, the unbleached

cotton or the yellowing of the (natural) silk fabric—in comparison with the bleached cotton or white silk. Further examples are the dyed samples of cellulose acetate twill (I, II, III) and those of the open-weave rayon fabric (1a to 1b), which was dyed different shades of yellow.

1. COTTON FABRICS

Taking the opposite extreme, of closely woven fabrics, only 1 to 4 per cent of the total incident radiation is transmitted through the interstices, while a surprisingly large amount of ultra-violet and visible radiation is transmitted through the thread.

For example, a thin-bleached cotton fabric (7b in Table 2) transmitted 24 per cent of the total incident ultra-violet radiation, of which amount only 3.9 per cent of the incident radiation was transmitted through the openings between the yarn. The ratio of ultra-violet to visible is 77 per cent, showing that the bleached material absorbed but little ultra-violet, relative to the visible rays. In marked contrast, the unbleached cotton material (No. 7) transmitted only 8.4 per cent of the ultra-violet, of which amount 3.9 per cent passed through the interstices.

As a wearing material the white cotton nainsook, 4H, and the cotton batiste, 5H, have a high transmission of ultra-violet radiation, amounting to about 20 per cent, most of which passed through the thread, showing the great transparency of the bleached cotton thread to ultra-violet radiation.

2. LINEN FABRICS

The samples of linen which were bleached were found to be highly transparent to ultra-violet radiation, but the transmission of the unbleached material was low. In general, it appears that the average bleached sample of linen transmits about as much of the ultra-violet as bleached cotton.

3. SILK FABRICS

The natural silks, when not yellowed with age, have a high transmission of ultra-violet radiation. For example, a white silk crêpe (No. 4 in Table 2) transmitted 20 per cent of the ultra-violet, of which amount less than 3 per cent passed through the interstices. Similarly, the plain woven silk, 7H, had a high transmission. However, the transmission of ultra-violet radiation relative to visible radiation through natural silk is distinctly lower than through cotton, the ratio being of the order 60 to 65 per cent in comparison with 65 to 84 per cent through cotton. Moreover, the ultra-violet rays (and to a less extent the longer wave lengths) are greatly absorbed by natural silk that is yellowed with age.

4. WOOL FABRICS

Some of the most transparent white wool fabrics (serge, 8S) examined by us transmitted only about one-half as much ultra-violet as the most transparent cotton yarns. Some samples (for example, a cream-colored worsted, 8A) compared favorably with the best silks in transparency, while one sample (a worsted, 8C) transmitted 21 per cent, of which 8.3 per cent passed through the

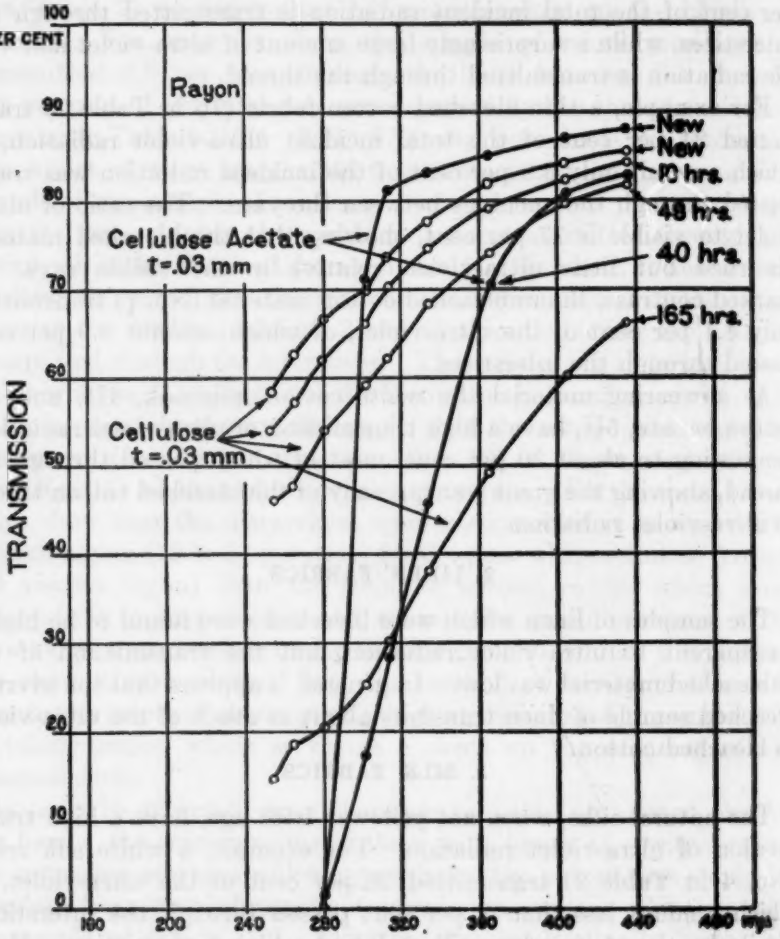

FIG. 2

interstices. The transmission of ultra-violet relative to visible radiation of a number of samples was 44 per cent, which is a good showing in comparison with 65 to 84 per cent through cotton.

5. RAYON FABRICS

Rayon (formerly known as "artificial silk") is the generic name of filaments made from various solutions of modified cellulose, which is obtained commercially from cotton linters and from wood pulp. We

have examined rayons made by the following processes: (1) Nitrocellulose or chardonnet, (2) cuprammonium, (3) viscose, and (4) cellulose acetate—the latter under the trade name celanese.

In Figure 2 is shown the spectral transmission of thin homogeneous films of different kinds of rayon before and after exposure to ultra-violet light. When new, the pure cellulose and the cellulose acetate differ but little in transmission of radiation of wave lengths greater than 300 mμ, which includes the most of the short wave length solar radiation that has an activating, vitalizing, therapeutic action.

Our tests show that, on an average, viscose and cuprammonium rayon transmit practically as much ultra-violet radiation as the most transparent samples of white cotton, having a ratio of transmission of ultra-violet to visible radiation amounting to 70 per cent (viscose rep, 12a, Table 2) in comparison with 65 to 84 per cent through cotton. One sample of white satin viscose rayon (13) even excelled cotton, having a relative transmission of ultra-violet to visible amounting to 87 per cent. This seemed so unusually high that the observations were repeated with especial care. The new ratio of ultra-violet to visible was found to be 88 per cent, verifying the earlier measurements. This is probably to be expected in view of the fact that the viscose rayon thread is composed of a number of long, practically untwisted filaments, while the cotton thread is composed of numerous short filaments which scatter the radiation.

The average cellulose acetate rayon fabric appears to be as transparent as the pure cellulose, whether in the form of cotton or viscose. But some samples (for example, the cellulose acetate rayon satin, 5, and twill, I) transmit only 13 to 16 per cent of the incident ultra-violet light. This is observed also in the open-weave fabrics of cellulose acetate rayon, 1a and 2. One very thin sample of the acetate rayon (No. 4) transmitted 29.8 per cent of the incident ultra-violet radiation.

In all cases the transmission of the ultra-violet relative to the visible through white cellulose acetate rayon is distinctly lower than that observed through cotton and through viscose rayon, ranging from 50 to 75 per cent as compared with 65 to 87 per cent through the pure cellulose fabrics. This is to be expected from the measurements on the homogeneous film of the acetate rayon, which shows strong absorption in the ultra-violet.

From Tables 1 and 2 it appears that, after deducting the light transmitted through the openings between the threads, the percentage of transmission of ultra-violet radiation through the bleached, white threads are as follows:

Viscose rayon varies from 16 to 27 per cent.
Cotton varies from 14 to 21 per cent.
Cellulose acetate rayon varies from 11 to 29 per cent.

Silk varies from 14 to 18 per cent.
Linen varies from 7 to 16 per cent.
Wool varies from 5 to 15 per cent.

The great variation in transmission (11 to 29 per cent) of ultra-violet through the cellulose acetate rayon is no doubt owing to the high absorption of this material at 300 mμ (see fig. 2), which produces a great variation in transparency for a small variation in thickness.

6. CONCLUDING REMARKS

As distinctly emphasized in the beginning of this paper, in order to obtain a reliable comparison between the various kinds of materials of which the fabrics are made it is necessary to examine black and white samples of the same cloth; also to examine different kinds of weaves; and finally to determine the effect of dyes. The latter would be an interminable undertaking, hence we have not examined very deeply into it. However, we have tabulated sufficient data to demonstrate the rapid decrease in transmission of ultra-violet radiation by red, orange, yellow, green, and tan colored dyes (pink seems to be an exception), which render these yarns almost, if not completely, opaque to ultra-violet radiation. Even a slight yellowing with age decreases the ultra-violet transmission.

Our measurements show that, after deducting for the openings between the threads, the transmission through the thread, especially when dyed, is only of the order of about 5 to 10 per cent. When one considers that the thread usually occupies from 95 to 99 per cent of the total space, a transmission of only 10 per cent of the total incident light is insignificant, and, since it is usually not practicable to have all fabrics uncolored, it is evident that the real gain in transparency to ultra-violet radiation is obtained by using an open-weave fabric. On this basis fabrics made of silk and the heavy wool yarns compare favorably with cotton and rayon for transmitting the ultra-violet. Evidently the question of the composition of the material for transmitting the ultra-violet is overestimated. This is illustrated in Table 2, in which white samples of cellulose acetate rayon (Twill I, II, III, and the open mesh, 1a to 1b) were dyed different shades of yellow, resulting in a rapid decrease in transmission from 20 per cent to less than 2 per cent through the latter fabric.

The foregoing discussion relates to the transmission of a single layer of fabric. In passing through two (or more) layers, as would be the case when more than one garment is worn, the transmission of ultra-violet radiation (also the visible radiation) is greatly decreased. This is shown by actual measurements on a sample of cotton broad cloth (similar to sample 3B of Table 2), as follows:

1 thickness transmitted 21.5 per cent.
2 thicknesses transmitted 8.0 per cent.
3 thicknesses transmitted 2.9 per cent.
4 thicknesses transmitted 1.7 per cent.

Whether there is justification for current opinion as to the importance of exposing the body to ultra-violet (solar) radiation remains to be determined. For young children, under proper medical supervision, it is known to be beneficial. But from the fact that adults have lived, fully clothed and in health all these years prior to the present discussion of the subject, it would appear that it requires but a small amount of these ultra-violet rays to keep the body in health; and that, until we know more about the biological effects of excessive amounts of ultra-violet rays, it would be wise to be cautious in exposing our food as well as our bodies to ultra-violet radiation. A note of warning has already been sounded by Price [7] regarding the injury that may result from missuse of the ultra-violet rays in aotivating foods.

In conclusion, it is relevant to refer to these data in connection with the question of shielding the body from ultra-violet and visible solar radiation, which is an important problem in the Tropics. As shown in a previous paper,[8] the best reflector for sunlight is a closely woven white fabric. To prevent heat radiation from falling upon the head, the underside of headgear may be painted with aluminum paint, suitable provision having been made for ventilation, as in the well-known helmets worn in the Tropics. For protecting the body from the ultra-violet rays transmitted through the outer clothing (which should be white in order to have a high reflecting power), the inner garment may be made of thin, closely woven yarn, of wool or cotton, dyed (red or khaki) with a substance that absorbs the ultra-violet. Obviously there are other applications, but it seems beyond the scope of this paper to attempt a further interpretation of the data at this time.

IV. TRANSPARENCY OF FEATHERS AND ANIMAL TISSUE

In connection with the foregoing measurements on fabrics, it was of interest to determine the transmission of radiation through feathers. The information obtained is of interest in connection with the problem of irradiating fowls with ultra-violet light.

For convenience and accuracy, the measurements were made on continuous areas (free from interstices) of large-sized primary and secondary wing coverts. The body feathers would be thinner and individually (that is, not overlapping) would be more transparent.

The data obtained are given in Table 2. They are interesting in showing a fairly high transmission, even for the colored feathers. The feather from the white swan was an unusually fine specimen

[7] Price, J. Amer. Dental Assn., **13**, p. 1765; 1926.

[8] Coblentz, B. S. Bull. No. 196, **9**, p. 283; 1913. Coblentz and Hughes, B. S. Tech. Paper No. 254, **18**, p. 171; 1924.

that was quite translucent and homogeneous, without interstices, as viewed through a reading glass.

The sample of animal tissue examined consisted of the thin outer wall of the intestine of a freshly killed chicken. The material, 0.05 mm in thickness, was placed between two plates of quartz and the edges sealed to retain the moisture. The data are of interest in connection with the question of the penetration of ultra-violet radiation into the body, for therapeutic purposes.[9]

WASHINGTON, February 14, 1928.

[9] As this paper goes through the press a similar research by Hirst, King, and Lamaert, Soc. of Dyers and Colorists, 44, p. 109; April, 1928; practically confirms our work on the transmission of ultra-violet radiation through various fabrics, previously reported in B. S. Tech. News Bulletin, No. 126, of October, 1927.

TINTING STRENGTH OF PIGMENTS

By H. D. Bruce

ABSTRACT

In this paper there is presented a discussion of the tinting strength of pigments. It is not primarily proposed herein to offer a new method for estimating and expressing tinting strength, but rather to aid in clarifying ideas on the subject, so that when the science of colorimetrics has been further advanced a rational means for appraising this valuable property may be the more easily developed.

The necessity for considering the tinting strength of chromatic pigments as a two-factor property is shown. A distinction between the tinting strength of whites and of blacks is drawn. New names for three differentiated factors involved in tinting are offered, namely, chromatic, darkening, and brightening strengths. A method for treating these properties photometrically or spectrophotometrically and of indicating their relative magnitude by numerical indices is suggested. Tabular and graphical data are presented.

In connection with and incidental to the subject of tinting, certain empirical formulas have been developed in the argument which may be used for computing the proper mixture of white pigment with pigment of another color in order to obtain a tint of some desired brightness or colorimetric purity.

The procedure employed in this work for specifying color in the monochromatic terms of dominant wave length, purity, and brightness is set forth with concise explanation in an appendix.

CONTENTS

	Page
I. Introduction	125
II. Discussion of tinting strength	128
III. Experimental data	132
IV. Discussion of data	140
1. Pigments other than white	140
2. White pigments	143
V. Appendix	145

I. INTRODUCTION

The color of a paint is the result of a very complex relationship between the optical properties of the pigment particles, the color and refractive index of the vehicle, the ratio of pigment to vehicle, the conditions of observation and illumination, and often the surface covered. Upon the optical properties of the particles depends the pigment's power to diffuse, transmit, selectively absorb, and disperse incident light. These optical properties are determined not only by

the chemical nature and refractive index, but in a large measure by the size, shape, and texture of the individual grains.

In examining pigments for their value in decorative paints and enamels, where color and tinting strength are primary considerations, chemical composition may be of quite minor importance as compared with physical properties. For example, two chrome yellows, both C. P. lead chromate, may differ so considerably in physical structure that under otherwise identical conditions they will form tints quite unlike in appearance and depth of shade. (Throughout this discussion, the term "depth of shade" or "depth of tint" will be used without rigorous definition to designate the common conception of degree of tint upon which tinting or color strength depends. The terms "tinting strength" and "color strength" are used synonymously in the literature.) It naturally follows that the strength of pigments should be evaluated by physical means, with no great reliance placed upon the results of chemical analysis.

At present the following procedure for determining the tinting strength of pigments is usually employed. A small quantity of the sample to be tested is accurately weighed, transferred to a large glass slab, and mixed by spatula with a measured volume of bleached linseed oil. A weighed amount of zinc oxide is then added and the mixture rubbed with a flat-bottomed muller in an arbitrarily specified manner. An equal weight of a selected standard is treated in the same way. Dabs of each tint are then compared side by side on a glass slide. From the relative depths of shade of the two tints the relative color strengths of the two samples are judged.

There are several objections to this method of testing tinting strength. The method does not readily lend itself to precise quantitative evaluation. To overcome this objection, it has been suggested that the standard should be assigned a value in tinting strength of 1.0, and that the unknown be varied in amount to match exactly the depth of shade produced by the standard. The ratio of the amount of unknown used to the amount of standard would then be taken as the numerical value of the strength of the unknown sample of pigment. There is also Ostwald's suggestion that the strength of color can be measured by the ratio in which chromatic and white pigment may be mixed before the chroma is just apparently gone. These suggestions involve cut and try processes which are so laborious and tedious that they are probably rarely or never used.

Another serious objection is that pigments of different hues can not accurately be visually compared as to depth of tint. Their contrast in hue need not be great to be objectionable, for very slight variations in hue often make decisions of relative strengths unreliable. Thus, in judging between a yellow and an orange yellow, several observers might differ as to which is the stronger.

A comparison of the tinting strengths of different pigments at various dilutions with a standard white, adjudged by our present methods, may reveal another real objection, the variability of tinting strengths in their relative order. In Figure 1 are plotted for two chrome yellow pastes two series of tints made by rubbing out each with zinc oxide in varying proportions. The brightnesses of the tints are plotted as ordinates and the compositions of the pigment mixtures as abscissas. Chrome yellow *A* was a good grade of medium chrome yellow; *B* was a dark chrome yellow selected because it was known to be somewhat coarse. Observe that the curves cross. If plotted to infinity, 100 per cent yellow, they would end at 33.4 per cent brightness for *B*, and at 46.4 per cent for *A*. On the assumption that the

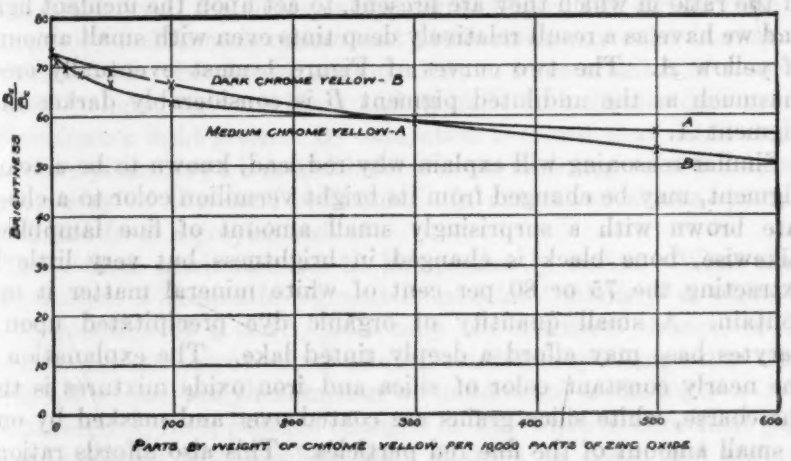

FIG. 1.—*Brightness-composition curves, for two series of yellow tints, illustrating the crossing of these curves*

darker the tint the stronger is the tinting substance (the validity of this assumption will be discussed later) which pigment, *A* or *B*, is the stronger? One laboratory working at a ratio of 500 to 10,000 would report *B* to be the stronger; another laboratory working at a ratio of 100 to 10,000 would report *A* to be the stronger. The answer depends solely upon the proportion of white to yellow pigment.

The explanation of this variability in relative tinting strengths lies in the relative grain sizes of the white and of the yellow pigments. Zinc oxide is a sublimed product composed of very minute grains. Chrome yellows are precipitated products which may or may not be very fine. As a powder is ground increasingly fine, the surface of a constant weight becomes increasingly great, and the more surface that may be exposed to incident light the greater will be the tinting strength. Furthermore, as pointed out by Briggs,[1] the possible tendency of the small particles to adhere to the surfaces

[1] T. R. Briggs, J. Phys. Chem., **22**, p. 223; 1918.

of the larger ones may be another factor of importance. The average particle size of the chrome yellow *B* was probably comparatively great, and the zinc oxide particles tended to coat over the larger yellow surfaces, and thus to produce an appearance approximating that of the white coating material. The resulting degree of apparent whiteness would, of course, depend on other factors, such as the opacities of the two pigments and their powers to diffuse light. As more and more chrome yellow is added, it is obvious that more yellow surface will be exposed with an increase in the proportion of yellow light reflected. If the particles of chrome yellow *A* are sufficiently small, little or no coating by the fine white may occur. Thus, the yellow and white particles would have equal opportunity, in the ratio in which they are present, to act upon the incident light, and we have as a result relatively deep tints even with small amounts of yellow *A*. The two curves of Figure 1 must eventually cross, inasmuch as the undiluted pigment *B* is considerably darker than pigment *A*.

Similar reasoning will explain why red lead, known to be a coarse pigment, may be changed from its bright vermilion color to a chocolate brown with a surprisingly small amount of fine lampblack. Likewise, bone black is changed in brightness but very little by extracting the 75 or 80 per cent of white mineral matter it may contain. A small quantity of organic dye precipitated upon a barytes base may afford a deeply tinted lake. The explanation of the nearly constant color of silica and iron oxide mixtures is that the coarse, white silica grains are coated over and masked by only a small amount of the fine red particles. This also affords rational ground for the preference for coarse mineral blacks over fine lampblacks when the tinting strengths of white pigments are used as indications of their hiding powers. For certainly, in such a measurement, the white should coat and hide the black rather than the reverse.

II. DISCUSSION OF TINTING STRENGTH

The American Society for Testing Materials has adopted the following definition of tinting strength: "The power of coloring a given quantity of paint or pigment selected as a medium standard for estimating such power." This definition is in accord with the common conception of color strength among paint men generally, but it is not definite enough to permit its use as a basis for a measurement of tinting strength.

What is meant by the term "power of coloring"? Offhand, one might suggest "power to change the degree of color." However, this definition fails when one considers the American Society for Testing Materials definition for color, "A generic term referring

inclusively to all the colors of the spectrum, white and black, and all the tints, shades, and hues which may be produced by their admixture." According to this definition, a gray, a red, and a pink are three separate and distinct colors, and one may not be said to possess a greater degree of color than another.

It is generally understood that there are three attributes by which color is characterized. These are hue, brilliance, and saturation. According to the latest nomenclature these terms belong to the psychological side of the phenomenon of color, the corresponding stimulus terms being, respectively, dominant wave length, brightness, and purity. By hue is meant that attribute of certain colors in respect of which they differ characteristically from the gray of the same brilliance.[2] In this quality, for example, red differs from a green. By brilliance is meant that attribute of any color in respect of which it may be classed as equivalent to some member of a series of grays ranging between black and white.[2] In brilliance dark green differs from a light green. By saturation is meant that attribute of all colors possessing a hue which determines their degree of difference from a gray of the same brilliance.[2] In saturation a pure spectral red differs from a grayish red.

These three attributes can be independently varied. What then occurs when a chromatic pigment is used for "coloring" a white in the production of a tint? Does only one attribute change, or do some two, or all three? And what effect does any change that may occur have upon the phenomenon we understand as tinting?

Considering, first, possible changes in hue when a chromatic pigment is diluted with a white, such changes do occur and are not necessarily due to any lack of perfect neutrality of the white, although the so-called whites are invariably not strictly neutral but incline to yellowish, bluish, etc. When a chromatic pigment is diluted with a white one, light rays internally transmitted within a paint film or pigment mass will have a shorter mean path through selectively absorbing grains before reflection into the atmosphere, because of the interspersion of the highly diffusing and refracting white grains. Merwin [3] has pointed out that one effect of this will be the shifting of the dominant radiation in the direction of maximum spectral absorption. Merwin has shown also, that because of the preferential scattering of light by fine particles the presence of very fine white pigment may cause a migration of the hue toward the violet end of the spectrum.

Enough has been said to show that real changes in hue often do occur when chromatic pigments are mixed with white pigments to

[2] J. Opt. Soc. Am. and Rev. Sci. Inst., 6, No. 6, p. 534; August, 1922.

[3] "Optical properties and theory of color of pigments and paints," Proc. Am. Soc. Test. Mats., 17, Pt. II, p. 496; 1917.

form tints. Do these changes play any part in our conception of tinting? Hue is the name for a psychological sensation which so differs from the sensation of gray as to permit such designation as reddish or yellowish. It must be sharply distinguished from saturation which is the sensation produced by the apparent intensity of the hue. A color either evokes a hue or it does not. Thus, a red and a pink may differ in saturation but be of the same hue, and it can not properly be said that one possesses more hue than the other. The physical measure of the hue of a yellow tint might be 580 mμ, of a red 680 mμ. But the red pigment would not have more strength than the yellow by virtue of its being red, or vice versa. Hue and tinting strength are not interdependent qualities. It is true that two observers might argue vehemently over the relative depths of two tints, a bluish green and a yellowish green. The differences in hue would prejudice the individual opinions, but this is due to a peculiarity of the psychological method of judging. The observers make their judgments from different points of view, each subconsciously preferring a different hue and probably basing his opinion largely upon the saturation of the colors with respect to this preferred hue. Hue desired is a matter of individual taste, and color and coloring efficiency must be considered separately.

Let us now observe how saturation and brilliance change during the process of "coloring" a white pigment in the production of a tint. It is obvious that both of these attributes do change. In the first place, a black pigment added to a white certainly produces a gray of intermediate brilliance. In the second place, any given color may be considered a mixture of pure color with gray, and the saturation of the color by definition depends upon its departure from gray. Make a tint, then, by adding to any given chromatic color an additional proportion of gray and the saturation will necessarily be diminished.

The important question, now, is whether a tint is formed from the white by admixture with another color because of an increase of saturation, because of a reduction of brilliance, or because of a change in both of these attributes.

Let us consider for the moment only achromatic pigments; that is, blacks and whites, evoking no hue and, therefore, possessing zero saturation. Any change on mixing these colors will be in the main a change in brilliance. Gardner, in "Paint Technology and Tests," says of mineral black: "It contains a comparatively low percentage of carbon, and consequently has low tinting value." Langton (London), in "Blacks and Pitches," says of bone blacks: "Acid-washed black has a very deep, black colour, and in consequence of its fine state of division a great deal of colour strength." Toch, in "Chemistry and Technology of Paint," says in regard to mineral

blacks: "As they possess very little tinctorial power it is more advantageous to use a 200-mesh silica tinted with lampblack." The point to which attention is called in each of these quotations is that the blacks are considered to possess tinting or color strength. The same usage is general throughout the literature, and any definition or discussion of tinting strength must conform to this generally accepted opinion that blacks do possess tinting strength by virtue of their power to decrease the brilliance of a white.

In the case of tinting with chromatic pigments both the brilliance and the saturation usually change. The conditions under which tints can be made with change in saturation but without change in brilliance must be specially selected. Consider Figures 1 and 13. In these figures the physical analogues of brilliance and saturation have been employed; namely, brightness and purity, respectively. Brilliance bears a linear relationship to the logarithm of the brightness according to Fechner's law, and whatever the relationship between saturation and purity this correlative use of the terms is permissible for our immediate discussion in which colors of nearly the same dominant wave length are being considered. It may be observed from Figure 1 that at about the ratio of 300 to 10,000 the two chrome yellow tints have the same brightness. From Figure 13, however, we observe that at this ratio the medium yellow has a very much higher purity than the dark. Show these two particular tints to color men with the question, "Which pigment is the stronger tinter?" and the typical answer would be, "Well, they differ a little in tone, but I'd say *A* is the stronger." Undoubtedly *A*, the medium chrome yellow, should be considered to possess the greater tinting strength. Of course, there is only one point on the two brightness-composition curves where the two would coincide, but in this special event there would be a difference in the strength of the two tints which would depend solely upon purity or saturation. Thus, it must be admitted that saturation as well as brilliance is a factor in the determination of tinting strength.

Indeed, it may be argued that, aside from the case of black pigments which are admittedly used in tinting to diminish brilliance, saturation alone is the factor upon which tinting depends. According to these arguments, if a painter adds a red pigment to a white to obtain a tint he does so for the sole purpose of producing a product which will appear reddish. The accompanying decrease in brilliance because of absorption of blue and green rays is not the painter's aim, but is, indeed, a necessary evil attending his method of producing a red color. Had he some other practical way to produce a red tint without lessening the brilliance he probably would utilize this alternative method.

However, it is generally true that, when a white is tinted with any other color than black, both brilliance and saturation change. It is possible that these two attributes are mentally combined into one sensation which has been called the depth of tint. It does seem, however, that if there is any psychological tendency toward combination, it is certainly not perfect, for of two tints of the same hue varying in both brilliance and saturation it is extremely difficult to select the deeper. Accordingly, it seems necessary that the two attributes be considered separately and a distinction made between the power of a pigment to alter the brilliance of a white and its power to alter the saturation of a white.

The relationship between brightness and brilliance has been fairly well determined. Fechner's expression for this relationship is $S = A \log I + c$, where S = the brilliance sensation, I = the brightness stimulus, and A and c are equating constants. Colorimetric purity is a physical quantity defined as the ratio

$$\frac{B_A}{B_A + B_w}$$

where B_A is the brightness of the homogeneous constituent and B_w is the brightness of the white light in a mixture of homogeneous and white light which matches the particular color in question. As such a physical quantity, purity can be numerically stated and easily treated. On the other hand, the relationship between purity and saturation is not thoroughly known, and it is not yet possible to represent saturation by a numerical designation. This lack of information abruptly checks our logical derivation of a means of expressing tinting strength in the most suitable and desirable way, on the basis of the degree of saturation possessed by the tint.

III. EXPERIMENTAL DATA

In this study of tinting considerable experimental work has been carried out in the endeavor to ascertain just how the brightness and the purity are altered when the proportion in which a white pigment is mixed with a pigment of another color is varied. Many series of tints were made up from one chosen standard white, each series being made from a different pigment in combination with the white, and consisting of several steps, grading from the untinted white through darker and purer colors, to the undiluted test pigment. Each test pigment was ground on a roller mill or thoroughly rubbed out by muller and stone with sufficient bleached linseed oil to form a paste of rather thin consistency. The standard white was a good grade of zinc oxide ground on a roller mill to a paste containing 25 per cent of oil by weight. To form each tint small portions of these pastes were accurately weighed and mixed in the glass weighing bottle

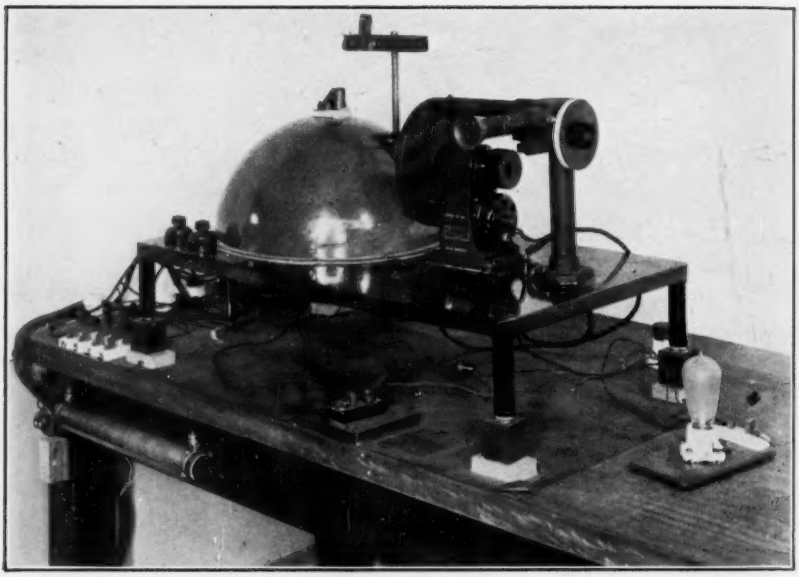

FIG. 2.—*Spectrophotometer on which color measurements were made*

UNIV. OF MICH.

with a stirring rod. The resulting tinted pastes were prepared for the color measurement by incasing a layer thick enough to be opaque between selected glass microscope slides.

The color measurements were made with a spectrophotometer. The particular color analyzer used in this investigation is shown in Figure 2. From the data of the spectrophotometric curves, which are reproduced in Figures 3 to 11, inclusive, the color of each tint was computed in terms of its dominant wave length, purity, and relative

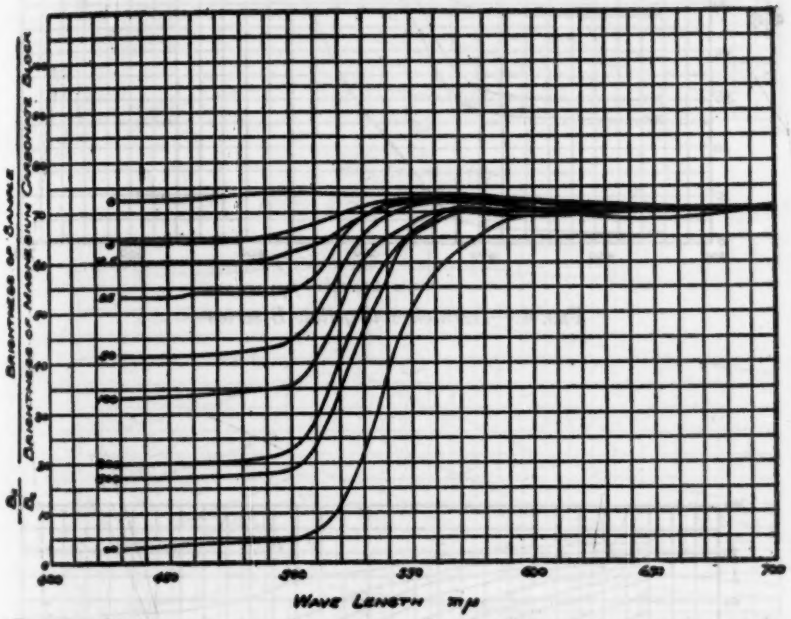

FIG. 3.—*Medium chrome yellow series. Spectrophotometric curves for a zinc oxide paint paste, a medium chrome yellow paste, and seven tints made by their admixture in various proportions*

The curve numbered 0 is for the zinc oxide; the curve ∞ is for the undiluted yellow; the curve 500 is for a paste made by mixing 500 parts of the chrome yellow pigment with 10,000 parts of the zinc oxide; etc., for the other curves.

brightness (reflection for sunlight).[4] The relative brightnesses of the gray series were measured by means of a Martens photometer.[5] This was preferred for this purpose to the spectrophotometer because of its greater simplicity and precision. In Figure 12 are plotted brightness-composition curves for several series, and in Figure 13 are plotted purity-composition curves. Each curve, beginning at the point representing the white, slopes away at a characteristic rate and approaches asymptotically the brightness or the purity, respectively, of the undiluted solid color.

[4] Vid. Appendix for the method used to make these computations.
[5] Illustrated in B. S. Tech. Paper No. 306, p. 175; 1926.

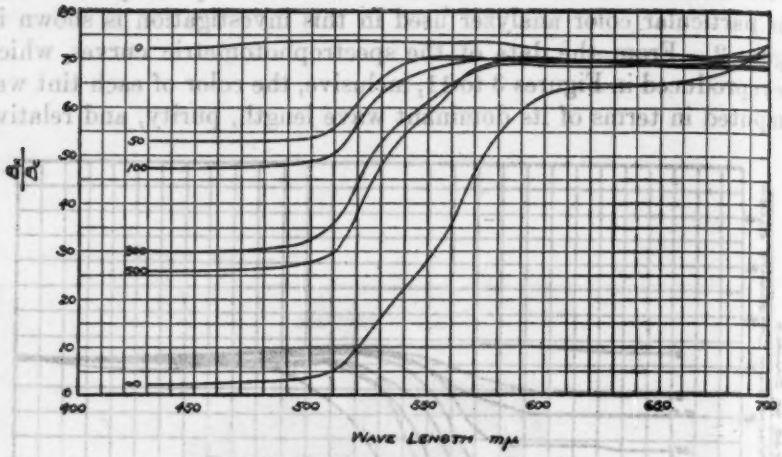

FIG. 4.—*Dark chrome yellow B series*

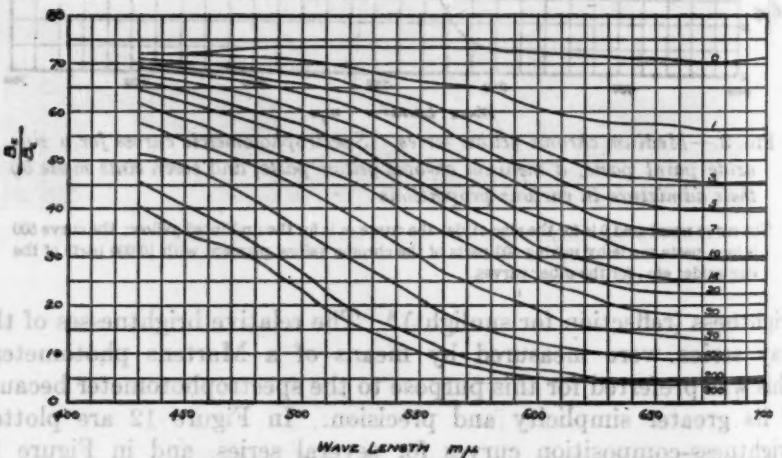

FIG. 5.—*Prussian blue series*

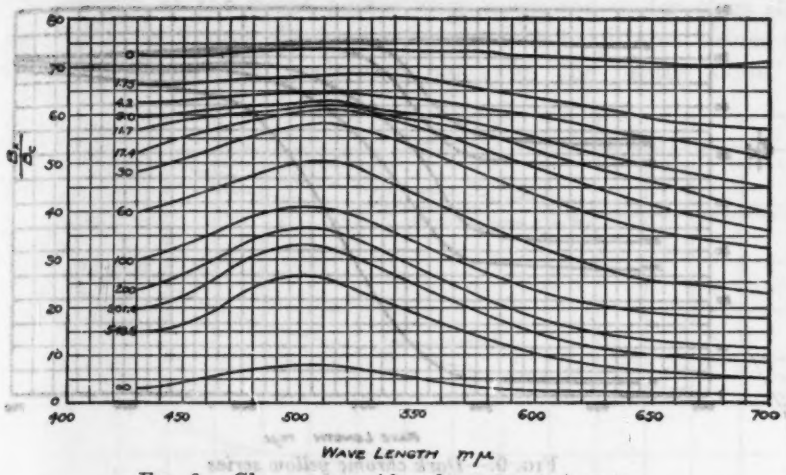

FIG. 6.—*Chrome green (first determination) series*

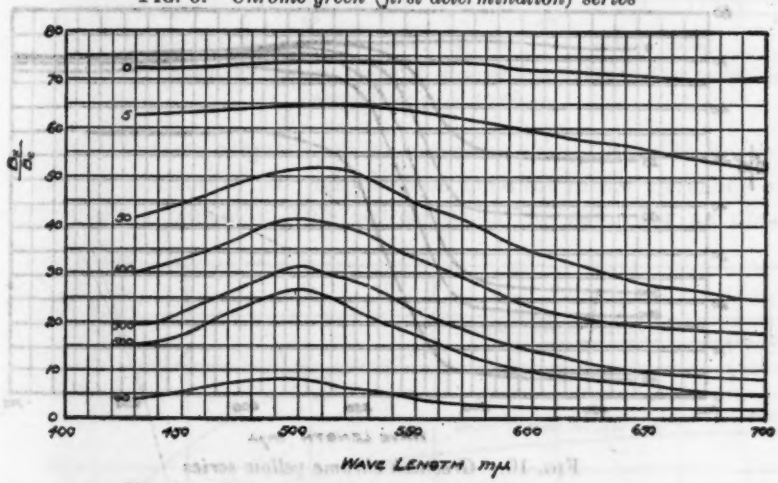

FIG. 7.—*Chrome green (second determination) series*

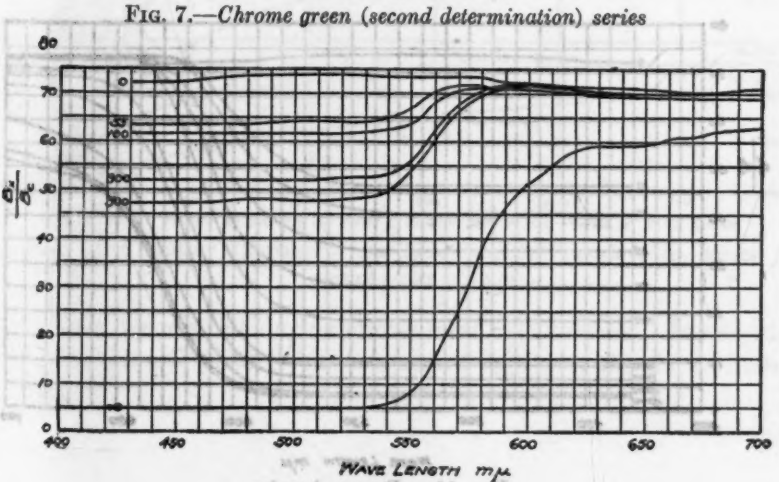

FIG. 8.—*Red lead series*

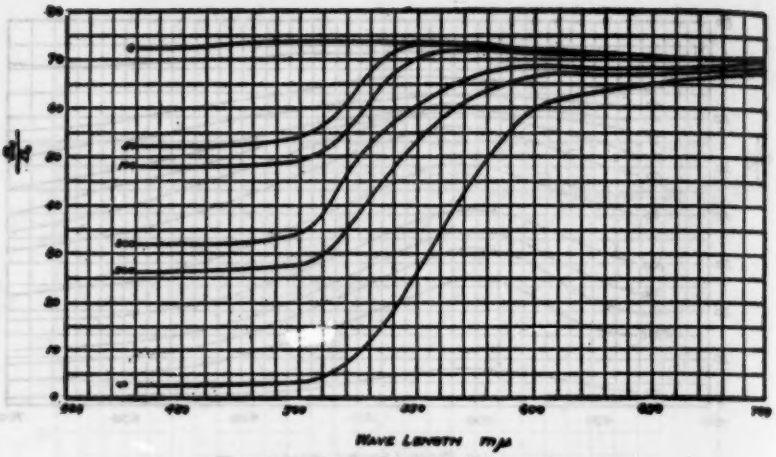

FIG. 9.—*Dark chrome yellow series*

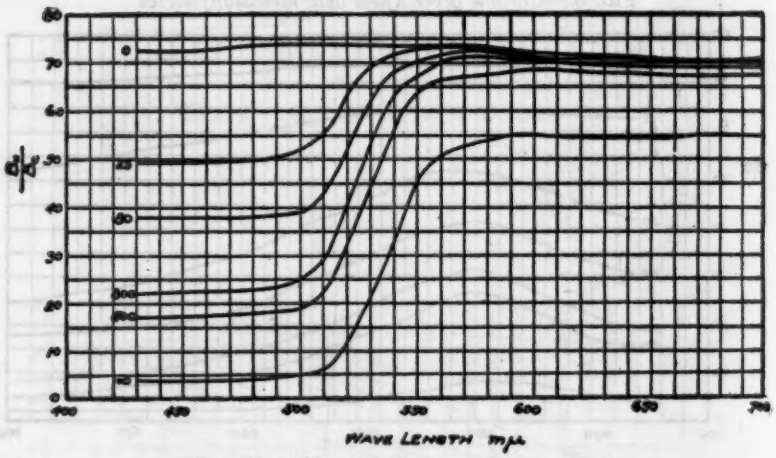

FIG. 10.—*Greenish chrome yellow series*

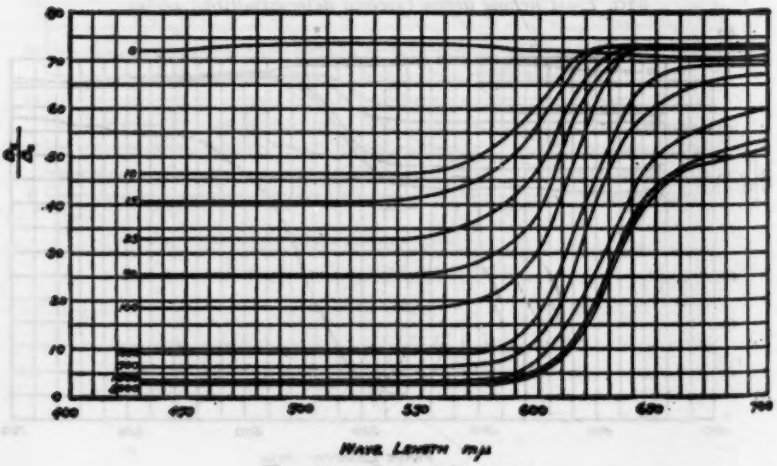

FIG. 11.—*Para red series*

Inasmuch as the paint pastes were measured under glass slides, the brightness figures obtained were not true brightness values relative to a magnesium carbonate block for the pastes alone. To

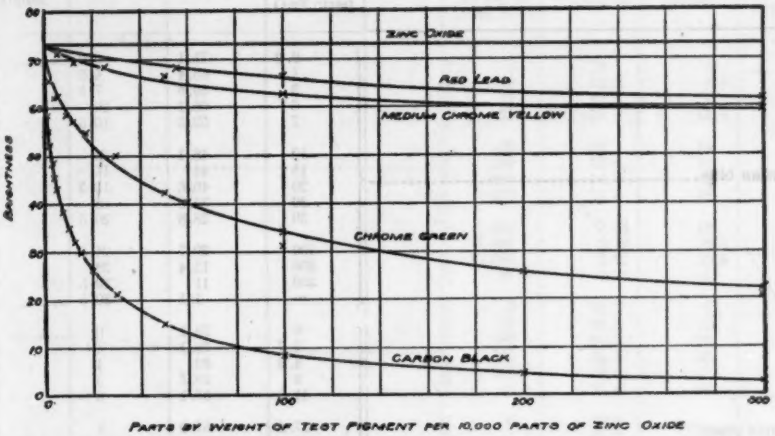

FIG. 12.—*Typical brightness pigment composition relationship curves for several series of tints*

obtain these true brightnesses a correction would have to be applied for the proportion of the light lost on account of the presence of the cover glass. However, this correction is the same for all observa-

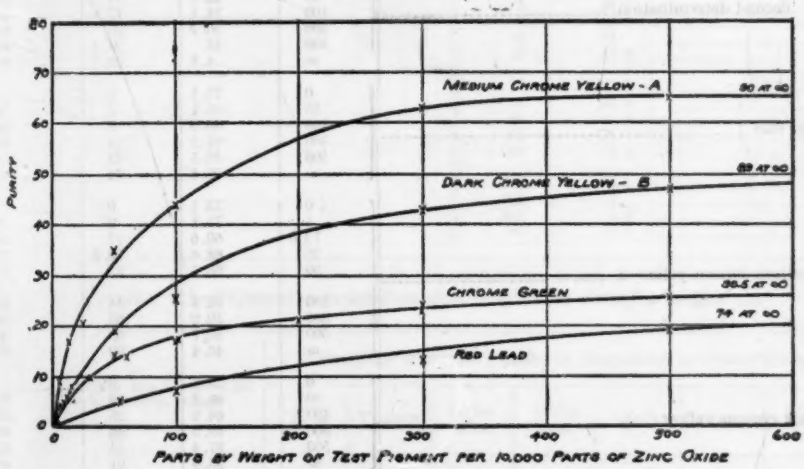
MEDIUM CHROME YELLOW - A
DARK CHROME YELLOW - B
CHROME GREEN
RED LEAD
PURITY
PARTS BY WEIGHT OF TEST PIGMENT PER 10,000 PARTS OF ZINC OXIDE

FIG. 13.—*Typical colorimetric purity-composition relationship curves for several series of tints*

tions and cancels out during subsequent calculations. It has, therefore, not been applied to the brightness figures of the data which will follow.

TABLE 1.—*Tint composition and color data*

Test pigment	Parts test pigment per 10,000 parts ZnO	Percentage brightness	Percentage purity	Dominant wave length
Prussian blue	0.0	73.1	0.0	----------
	1	65.4	4.5	484
	3	59.6	7.5	484
	5	56.1	10	485
	7	52.5	10.5	484
	10	48.1	12	483
	15	44	14	483
	20	40.6	15.5	483
	30	35.8	18	482
	50	28.8	20.5	481
	100	20.7	24.5	479
	200	13.4	28	476
	300	11	29.5	475
	∞	1.1	[1] 30.5	----------
Chrome green: First determination	0	73.1	0	----------
	1.7	66.1	3	492
	4.2	62	4	490
	9	58.5	5	490
	11.7	57.1	6	492
	17.4	54.9	8	492
	30	50.1	10	492
	60	40.4	14	492
	100	31.1	17	492
	200	25.9	21	493
	301.6	22.6	24	493
	548.5	16.6	25	493
	∞	4.8	30.5	494
Second determination	0	73.1	0	----------
	5	62.2	4	491
	50	42.6	14	493
	100	34.1	17	496
	300	20.9	23	493
	500	16	25.5	492
	∞	4.8	30.5	494
Red lead	0	73.1	0	----------
	55	68.1	5	590
	100	66.5	7	590
	300	61.5	13	590
	500	59.5	19	590
	∞	23.6	74	600
Medium chrome yellow A	0	73.1	0	----------
	5	71.1	9	580
	12.5	69.6	17	580
	25	68.6	20.5	577
	50	66.5	35	575
	100	62.8	44	580
	300	59.2	63	581
	500	56.7	65	582
	∞	46.4	90	586
Dark chrome yellow	0	73.1	0	----------
	50	66.8	19	580
	100	64.9	25	581
	300	58.9	46	581
	500	57.4	54	583
	∞	35.9	91	588
Chrome yellow greenish	0	73.1	0	----------
	25	68.5	26	581
	80	64.9	39	580
	300	60.1	59	580
	500	55.7	67	582
	∞	39.1	87	584

[1] Assumed.

TABLE 1.—*Tint composition and color data*—Continued

Test pigment	Parts test pigment per 10,000 parts ZnO	Percentage brightness	Percentage purity	Dominant wave length
Para red	0	73.1	0	----------
	10	52.2	8.5	615
	15	47.5	11	610
	25	39.9	14.5	615
	50	32.7	19	620
	100	25.4	24	620
	300	14.7	34	624
	500	11.5	39	627
	1,000	7.34	46	624
	5,000	5.70	50.5	626
	10,000	5.61	50.8	625
	∞	5.21	51	626
Dark chrome yellow B	0	73.1	0	----------
	50	68.8	21	581
	100	66.3	25	582
	300	58.9	43	582
	500	52.8	47	584
	∞	33.4	89	589
Carbon black	0	73.1	----------	----------
	.1	68.2	----------	----------
	.2	66.8	----------	----------
	.3	64.6	----------	----------
	.4	63.9	----------	----------
	.5	62.4	----------	----------
	1	58.6	----------	----------
	1.5	55.2	----------	----------
	2	52.4	----------	----------
	3	48.8	----------	----------
	4	45.8	----------	----------
	5	43.4	----------	----------
	7.5	38.6	----------	----------
	10	35	----------	----------
	12.5	32.2	----------	----------
	15	29.9	----------	----------
	20	26.2	----------	----------
	30	21.4	----------	----------
	50	15.1	----------	----------
	100	8.4	----------	----------
	200	4.5	----------	----------
	300	3	----------	----------
	500	2.3	----------	----------
	∞	1.5	----------	----------

TABLE 2.—*Pigment composition and brightness data for gray tints*

Parts of carbon black per 10,000 parts of white pigment	Percentage brightness relative to magnesium carbonate block						
	TiO_2	Titanox	Litho-pone	White lead	ZnO	ZnS	Blanc fixe
0.00	76.9	79.1	78.3	76.6	76.2	77.7	60.8
0.25	----------	----------	----------	----------	----------	----------	38.8
1.00	----------	----------	----------	----------	----------	----------	24.9
2.47	60.6	53.8	52.3	48.3	50.8	58.9	15.1
6.25	----------	----------	----------	----------	----------	----------	6.76
10.72	45.9	36.2	34.5	28.4	32.3	43.5	4.24
24.73	35.3	24.5	23.1	17.8	20.8	31.9	2.29
44.59	27.2	17.3	15.8	11.2	14.1	23.6	1.77
71.21	21.4	12.4	11.0	7.6	9.9	18.2	1.63
104.29	17.4	9.0	8.0	5.0	7.1	14.1	1.59
∞	1.5	1.5	1.5	1.5	1.5	1.5	1.5

IV. DISCUSSION OF DATA

1. PIGMENTS OTHER THAN WHITE

After the data were secured in the manner described they were carefully studied for any possible orderly relationship, and it was ultimately concluded that the following empirical equations involving two arbitrary constants, α and β, are very close approximations to the laws governing the phenomena observed:

$$\frac{B_t - B_p}{B_w - B_p} = \alpha^{-\sqrt{c}} \tag{1}$$

$$1 - \frac{P_t}{P_p} = \beta^{-\sqrt{c}} \tag{2}$$

where B_t represents the brightness of any tint made by mixing c parts by weight of a test pigment of brightness B_p with 10,000 parts of a standard white of brightness B_w. The constants α and β are named, respectively, the darkening index and the chromatic index.

By the use of these equations any confusing influence due to a difference of initial brightnesses or of initial purities is avoided. The indices α and β are quantities so chosen that they do not vary throughout a range of tints no matter what the initial brightness or purity of the test pigment may be. The quantity $\frac{B_t - B_p}{B_w - B_p}$ is a measure of brightness on that scale on which the standard white has a brightness value of 1.0 and the undiluted test pigment a value of zero. Similarly, $\frac{P_t}{P_p}$ is the purity of any tint relative to the purity of the test pigment. It should obviously not be expected that a yellow pigment of 60 per cent brightness added to a white in increasing proportions could ever reduce this white to a brightness below 60 per cent. This would remain true even though the strength of the particular specimen of yellow were infinite.

There is some evidence that these equations do not hold for pigment mixtures which are very close in color to the test pigment. However, we are here concerned with tints—that is, relatively light colors—and these empirical equations hold well within our experimental precision over the requisite range.

Transforming equations (1) and (2) to their logarithmic forms

$$\log \frac{B_t - B_p}{B_w - B_p} = -\sqrt{c} \log \alpha \tag{3}$$

$$\log \left(1 - \frac{P_t}{P_p}\right) = -\sqrt{c} \log \beta \tag{4}$$

and plotting $-\sqrt{c}$ against $\log \frac{B_t - B_p}{B_w - B_p}$ and $\log \left(1 - \frac{P_t}{P_p}\right)$, respectively, straight lines result with their slopes equal to the logarithms of α and β, respectively.

In Figures 14 and 15 these straight lines have been plotted. The values of α and β for different pigments lie between 1 and infinity. The greater the value of α the greater is the darkening strength. The greater the value of β the greater is the chromatic strength. Thus, it may be observed from Figures 14 and 15 that red lead, very weak in tinting strength, has low values for both α and β. Para red, on the other hand, ordinarily a powerful pigment, has considerably larger values for its darkening and chromatic indices.

TABLE 3

Test pigment	Darkening index	Chromatic index	Test pigment	Darkening index	Chromatic index
Red lead	1.014	1.012	Chrome green	1.084	1.083
Dark chrome yellow B	1.026	1.036	Para red	1.136	1.067
Dark chrome yellow	1.027	1.040	Prussian blue	1.139	1.180
Greenish chrome yellow	1.029	1.068	Carbon black	1.266	
Medium chrome yellow A	1.044	1.064			

In Table 3 are summarized the numerical indices found for various pigments. It must be understood that these figures are in no way absolute, inasmuch as they depend upon the particular white pigment arbitrarily selected as the standard. It should be emphasized, also, that these indices are measured on a scale determined by the properties of the particular pigment, and therefore do not represent what might properly be considered absolute tinting strength even with the one white pigment. This absolute tinting strength, dependent upon the actual depth of a tint, is not constant for any one pigment, but varies with the concentration used. These facts are well illustrated by the curves of Figure 1 in comparison with those for the same pigments in Figure 14. The medium chrome yellow pigment has a larger darkening index than the dark yellow, so that its graph as plotted in Figure 14 on the basis of equation (3) falls distinctly below that for the darker pigment. The significance of this is that a small quantity of the lighter pigment has a relatively large effect and carried the tint much further toward the depth of color shown by the pigment itself, although the absolute effect may not be materially different from that given by an equal amount of the darker pigment. Furthermore, despite the fact that all of these eight pigments in Table 3 fall, when their strength is estimated in actual practice, in the same order as listed in the table, we are not at liberty to draw comparisons between pigments of different hues from the values of their chromatic indices. Thus, if it were possible to have a coarse Prussian blue of the same chromatic index as a medium chrome yellow, tints made from the same proportions of the two pigments mixed with a white, although of the same colorimetric purity, would not appear equally saturated and, therefore,

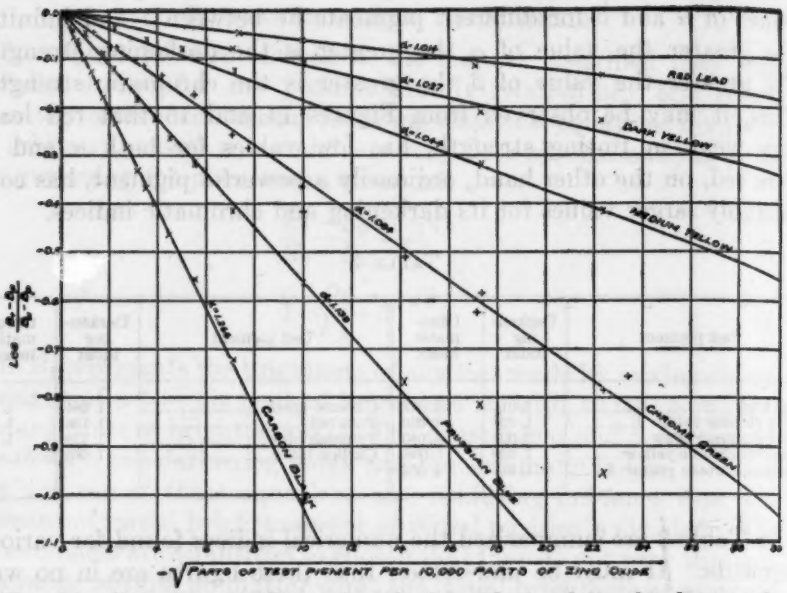

FIG. 14.—*Diagrammatic illustration of a logarithmic relationship between the brightness of a tint and its pigment composition*

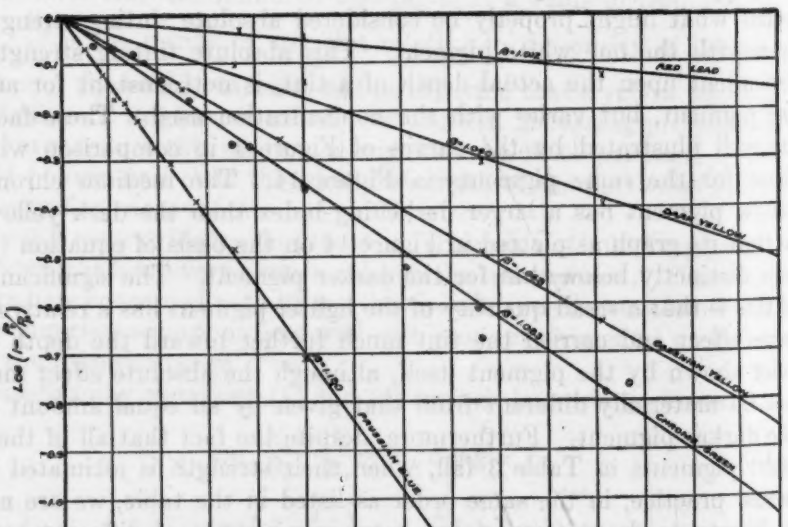

FIG. 15.—*Diagrammatic illustration of a logarithmic relationship between the colorimetric purity of a tint and its pigment composition*

not of the same depth of tint. The blue might be highly saturated and deeply tinted at a degree of purity at which the yellow might appear nearly white. It is, however, certainly permissible to contrast together all pigments of the same hue as all ultramarines or all yellow ochers, according to their chromatic indices. As it is probably never in actual practice required to compare as to tinting strength pigments of widely different hues, this restriction is perhaps after all not particularly stringent.

2. WHITE PIGMENTS

Heretofore attention has been confined to pigments other than whites. There exists a reason for this discrimination. A knowledge of the tinting strength of white pigments is arrived at by quite another process, differentiated from that used with other pigments by two important distinctions. One is that with whites a dark pigment must be used as the standard. The other is that in testing whites a large quantity of the test pigment is used with a small quantity of the standard, a procedure just the reverse of that employed for testing blacks and chromatic pigments. Thus, in estimating the tinting strength of a white lead a large portion is mixed as a paste with a small amount of the standard black. The depth of shade of the resulting gray is dependent upon that property of the standard black which we have called darkening strength. From the apparent darkening strength (*apparent* inasmuch as the actual darkening strength is that obtained only with the standard white) is derived by inference the power of the white to brighten. The two bear a reciprocal relationship to one another; the less the apparent darkening strength the greater the brightening strength. Thus, there is justification in defining γ, the index of brightening strength of white pigments as $\frac{1}{\alpha}$, where α is the darkening index of the black. As a result the index of brightening strength of a white pigment may be calculated from the following equation:

$$\frac{B_t - B_p}{B_w - B_p} = \gamma^{\sqrt{c}} \tag{5}$$

where B_t represents the brightness of any tint made by mixing c parts by weight of the standard black of brightness B_p with 10,000 parts of the white test pigment of brightness B_w. The constant, γ, is named the brightening index. γ varies between zero and unity. The greater the value of γ the greater will be the brightening strength.

Transposing equation (5) to its logarithmic form, $\log \frac{B_t - B_p}{B_w - B_p} = \sqrt{c} \log \gamma$, and plotting $\sqrt{c}$ against $\log \frac{B_t - B_p}{B_w - B_p}$, a straight line results which

passes through the origin with a slope equal to log γ. In Figure 16 several of these lines for various white pigments when mixed with a standard paste of carbon black have been plotted. Observe from Figure 16 how closely the experimental points fall upon the straight lines. No claim is made that the relationship should naturally and theoretically be linear. Indeed, a prolongation of these curves will reveal an actual upward curvature. What is claimed, however, and substantiated by Figure 16, is that the linear relationship is a very close and serviceable approach when confined to the realm of tints,

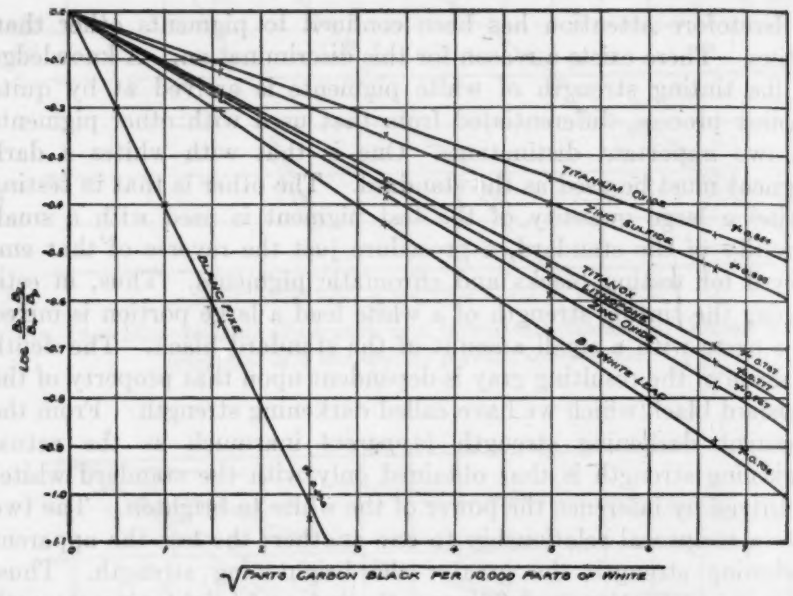

FIG. 16.—*Diagrammatic illustration of a logarithmic relationship between the brightness of a gray tint and its constituent parts of black and white pigments*

which as a specific and liberal approximation for this purpose may be considered to be above 20 per cent brightness. In Table 4 are summarized the numerical indices for individual samples of various white pigments.

TABLE 4

Test pigment	Index of brightening strength
Titanium oxide	0.854
Zinc sulphide	.833
Titanox	.787
Lithopone	.777
Zinc oxide	.767
BC white lead	.736
Blanc fixe	.388

The data in Table 4 and Figure 16 were obtained by mixing the various white pastes with a standard paste of carbon black. These pastes, both the whites and the black, had been prepared for other purposes by grinding the pigment on a roller mill not with linseed oil, but with a colorless nondrying mineral oil.

To illustrate the method for evaluating the constants of equations (1), (2), and (5), let us consider a concrete example. The index of chromatic strength of a given chrome green is to be measured. Equation (2) containing β, the chromatic index, is $1-\frac{P_t}{P_p}=\beta^{\sqrt{c}}$. This particular sample of chrome green pigment has a purity of 30.5 per cent as measured spectrophotometrically. P_p then is 0.305. A green tint is made by rubbing out some small amount of the green with a large amount of the standard white; say, 100 parts by weight of the green with 10,000 parts of the white. Quantity c is then 100. The purity of this tint, P_t, is measured and found to be 17 per cent. Equation (2) becomes

$$1-\frac{0.17}{0.305}=\beta^{-\sqrt{100}}$$

with β as the only unknown. Solving, $\beta=1.085$. This value is recorded for comparison with those of other chrome green pigments previously or subsequently tested.

Incidental to the subject of tinting strength, it is here interesting to note that equations (1), (2), and (5) provide means for predicting the purity and brightness that may be expected when two pigments, one of them white, are mixed in known proportions. Thus, assuming the index β to equal 1.085, as found above, what would be the purity of a tint composed of 200 parts of the same green with 10,000 of the white? Equation (2) becomes

$$1-\frac{P_t}{30.5}=1.085^{-\sqrt{200}}$$

P_t, the purity of the tint, is readily calculated to be 20.9 per cent. Actual measurements gave an observed value of 21 per cent for the purity. This is, perhaps, the first time that any attempt at precalculating the result of mixing pigments has been even approximately successful.

V. APPENDIX

By means of the spectrophotometer the spectral distribution of reflected light may be obtained in the form of a graph in which the portion of the incident light reflected has been plotted against wave length or frequency. The procedure that has been used in this inves-

tigation for converting a spectrophotometric curve into color specifications in terms of dominant wave length, purity, and brightness, is based upon the data given in the report of the Colorimetry Committee of the Optical Society of America, 1920–21.[6] For the purpose of showing how the computed values of brightness and purity were obtained the procedure will here be briefly presented.

When equal amounts of energy fall upon the retina of the eye as light of different wave lengths, quite different light intensities are experienced. This is because the human eye is not uniformly sensitive over the entire spectrum of radiant energy. In the ultra-violet the eye discerns no light whatever. Above this visibility rapidly mounts to a maximum in the greenish yellow and then falls again to zero in the infra-red. Consequently, when the brightness of a color is to be calculated from the spectrophotometric curve which represents the color, the relative values of visibility of the different wave lengths must be considered. A peak in the ultra-violet portion of the curve would add nothing to the brightness; a peak in the blue or red would add less than one in the green or yellow.

Furthermore, the brightness of a color is dependent upon the quality of the illuminating light. Thus, an orange might be very bright in sunlight but quite dark when viewed under a lamp deficient in yellow and red rays. Accordingly, in stating the brightness of a color, the character of the illumination must necessarily also be stated. White light is the common light for illumination, and brightness figures are usually calculated with reference to white light, which, for this purpose, has been specified as average noon sunlight.

A magnesium carbonate block has been found to reflect incident light almost nonselectively. Thus, the intensities of the various wave lengths of light reflected from a magnesium carbonate surface bear practically the same ratios to one another as they did in the incident light. Moreover, magnesium carbonate in air is one of the brightest of substances. A magnesium carbonate block makes, therefore, a very serviceable standard with which to compare samples in color examination. Observations with the spectrophotometer give for each wave length observed the ratio of the light reflected from the surface under examination to that reflected from magnesium carbonate; and a curve representing these ratios for wave lengths throughout the spectrum is the spectrophotometric or spectral reflection curve.

Considering one particular wave length, the greater its visibility, the greater the intensity of the incident light, and the greater the portion of the incident light reflected (the reflection factor) the greater will be the sensation of brightness caused by the reflected ray of that wave length. The contribution of that wave length to the

[6] J. Opt. Soc. Am. and Rev. Sci. Inst., 6, 6, p. 527; August, 1922.

brightness of the color may, therefore, be represented by *VIR*, the product of the visibility of the particular wave length under consideration (V)[7], the intensity of that wave length in white light (I)[8] and the reflection factor (R). If we take the reflection factor of the magnesium carbonate block as a unit, R is given directly by the spectral reflection curve. Values of the product *VI* prepared from tables given in the report of the optical society previously referred to and expressed in arbitrary units are given in Table 5.

TABLE 5.—*Spectral distribution of the visibility × intensity product for average noon sunlight*

Wave length	Visibility × intensity	Wave length	Visibility × intensity	Wave length	Visibility × intensity
mμ		mμ		mμ	
400	0.02	520	67.24	640	15.29
10	.07	30	83.89	50	9.17
20	.26	40	94.53	60	5.14
30	.80	50	99.65	70	2.57
440	1.76	560	99.01	680	1.34
50	3.26	70	93.73	90	.67
60	5.51	80	84.01	700	.33
70	8.70	90	71.66	10	.16
480	13.68	600	59.14	720	.07
90	20.68	10	46.67		
500	32.41	20	34.90		1,028.93
10	48.80	30	23.81		

The summation of the values of *VIR* for all wave lengths divided by the summation of *VI* (which is the value of *VIR* for magnesium carbonate, for which R is 1 by our choice of units) gives the ratio of the brightness of the color to the brightness of the magnesium carbonate block.

This process for measuring brightness spectrophotometrically may be summarized in the following three steps:

1. Spectral reflection data for the test sample are obtained by means of a spectrophotometer. These data are recorded as reflection factors relative to those from a magnesium carbonate block for wave lengths, varying by small intervals, such as 10 mμ, over the entire range of the visible spectrum.

2. Each reflection factor is multiplied by the corresponding *VI* value taken in Table 5.

3. The values of *VIR*, found in (2), for small regular intervals are added together and divided by the sum of the corresponding values of *VI*. (The *VIR* and the *VI* curves may be plotted and the areas inclosed by them measured by a planimeter instead of being computed as recommended above.)

[7] Ibid., second column, Table 2, p. 541. A table of visibility factors slightly different from that given in the report quoted has been since adopted as standard. See B. S. Sc. Paper No. 475, Table 3, last column, page 174; also Trans. Illum. Engrg. Soc., **19**, pp. 176 and 614; 1924; and **20**, p. 632; 1925.

[8] Ibid., first and fourth columns, Table 8, p. 563.

This ratio, *VIR* to *VI*, is the brightness of the test surface relative to the magnesium carbonate block.

For the simple specification of color (independent of brightness) two systems have been devised—the trichromatic and the monochromatic systems. In the trichromatic system the color is specified as equivalent to a mixture of certain percentages of three hypothetical elementary colors—red, green, and violet—so chosen that their combination in equal amounts would produce white light. In the monochromatic system the color is specified in terms of a homogeneous wave length, which evokes a hue identical with that of the test sample, and a certain purity of color which is the ratio between the brightness of the homogeneous wave length and the brightness of the total sample.

The relation between the two methods of specifying color is shown by the "color triangle," Figure 17.[9] The color triangle is laid out with ordinates representing the percentage of red and abscissas representing the percentage of violet, the remainder being green. The specification of color by dominant wave length and purity is represented by the radiating lines and curves centering about the vertex. In this particular chart, to facilitate reading, the straight lines which indicate the hues have been separated from the curves marking the purity values. For example, the color represented by the small circles may be specified either by the trichromatic method as made up of 20 per cent violet, 27 per cent red, and 53 per cent green or by the monochromatic method as having a dominant wave length of 510 mμ and a purity of 75 per cent.

The trichromatic method of specification is for our purpose only an auxiliary to the monochromatic; spectrophotometric data are converted first into trichromatic terms and then, by the aid of the color triangle, into terms of dominant wave length and purity.

The hue of an object is dependent upon the character of the illumination, just as we have seen is true in the case of brightness. A surface painted with red lead appears decidedly yellow under a mercury arc lamp. The change in color of cloth purchased under artificial light when brought into sunlight is a common experience. As a consequence the quality of the illuminating light has been arbitrarily specified for this purpose of color measurement as average noon sunlight.

It has been determined just how and to what relative extent light of any particular wave length would excite sensations of the red,

[9] This color triangle is similar to the one used in this work. It is reproduced through the courtesy of Carl W. Keuffel from a chart made by the Keuffel & Esser Co., plotted from data of Tables 14A and 14B in the colorimetry report previously referred to.

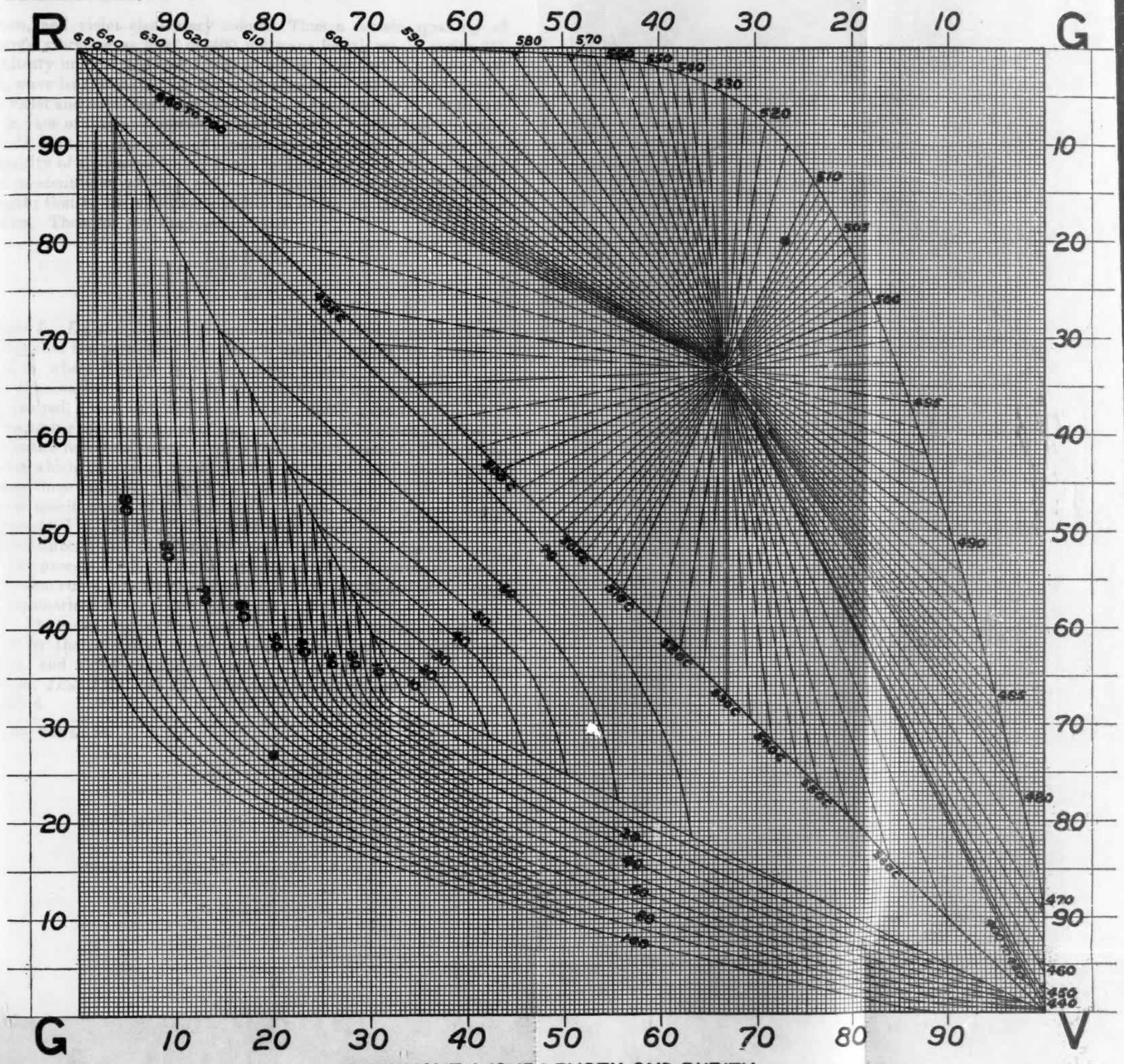

FIG. 17.—*Diagrammatic illustration of the relationship between the trichromatic and the monochromatic specifications of color*

green, and violet elementary colors. Thus a certain quantity of energy vibrating as light of 400 mμ wave length would excite 253 arbitrary units of the violet, but no red or green, while a ray of 600 mμ wave length containing the same amount of energy would excite no violet and much less green than red in the proportion of 196 to 510.

In view of this, any particular wave length of a reflection spectrum would excite an intensity of elementary color depending upon the intensity of that wave length in the incident light, on the portion of the incident light reflected, and on the excitation values of that wave length; that is, the vibration's ability to excite the three elementary colors. Thus, for any single wave length:

$$L_R = RIE_R$$
$$L_G = RIE_G$$
$$L_V = RIE_V$$

where L_R, L_G, and L_V are the amounts of the respective elementary colors that the particular wave length under consideration is equivalent to, where R is the reflection factor, where I is the intensity of the illumination, and where E_R, E_G, and E_V are the excitation values for the red, green, and violet elementary colors, respectively.

Summing up the portions of red, of violet, and of green colors over the entire reflection spectrum gives the relative amounts of the three colors which, combined, would produce the color under investigation. These three amounts reduced to a percentage basis are the trichromatic specifications of the test color. By the aid of the relationship represented in Figure 17 these trichromatic percentages can be converted directly into the monochromatic expression for the test color.

This process of converting the expression for a color from a spectral reflection curve into terms of dominant wave length and purity may be summarized in the following steps 4 to 7.

4. The mean intensity values for average noon sunlight are multiplied by the corresponding excitation values[10] for each of the red, green, and violet elementary colors. There result three separate curves, IE_R, IE_G, and IE_V, the data for which are tabulated in Table 6.

[10] Ibid. Table 6, p. 549.

TABLE 6.—*Spectral distribution of the excitation intensity product for average noon sunlight*

Wave length	IE_R	IE_G	IE_V	Wave length	IE_R	IE_G	IE_V
400	----------	----------	14, 168	550	44, 944	64, 872	1, 908
10	----------	----------	27, 279	60	48, 930	60, 690	1, 155
20	----------	----------	42, 980	70	52, 520	53, 768	728
30	----------	----------	66, 795	80	53, 040	42, 330	408
40	----------	567	82, 539	90	53, 500	29, 600	----------
450	----------	1, 448	85, 975	600	50, 490	19, 404	----------
60	----------	3, 686	81, 674	10	45, 276	11, 074	----------
70	----------	8, 181	70, 397	20	36, 375	5, 723	----------
80	1, 456	12, 688	49, 192	30	27, 360	2, 784	----------
90	4, 326	17, 830	23, 210	40	18, 525	950	----------
500	8, 798	27, 560	13, 038	650	11, 092	282	----------
10	16, 062	41, 642	9, 266	60	6, 256	----------	----------
20	24, 698	54, 060	6, 466	70	3, 620	----------	----------
30	32, 542	60, 632	4, 558	80	1, 947	----------	----------
40	39, 538	63, 918	3, 074	90+seq.	2, 349	----------	----------

5. The reflection factors from the spectral reflection curve from (1) are multiplied by the corresponding ordinates of each of the three curves from (4), Table 6. Three *RIE* curves result—one for the red, one for the green, and one for the violet.

6. The ordinates of each of the three curves from (5) are summed up. These three sums are then added together. The ratio of each sum to the total of the three is calculated. These ratios are the percentages of red, green, and violet in the reflected light.

7. The ratios from (6) of the red and the violet are plotted in the triangular graph (fig. 17) from which are read directly the purity and the dominant wave length of the sample color under examination.

The writer acknowledges with appreciation the assistance of P. H. Walker, I. G. Priest, and E. R. Weaver in this work.

WASHINGTON, January 8, 1927.

WAVE-LENGTH MEASUREMENTS IN THE ARC AND SPARK SPECTRA OF HAFNIUM

By W. F. Meggers

ABSTRACT

Using the purest available samples of hafnium salts the arc and spark spectra characteristic of this element were photographed with concave-grating and quartz-prism spectrographs. Wave-length measurements were made on about 2,100 lines, but 609 of these were discarded as impurities, identified mainly as columbium, zirconium, and titanium. Nearly 1,500 lines remain to describe the hafnium spectra between the wave-length limits 2155.72 A in the ultra-violet and 9250.27 in the infra-red. In this investigation an attempt has been made to improve upon an earlier description of these spectra, (1) by extending observations to shorter and to longer waves, (2) by increasing the precision of the wave-length measurements to ± 0.01 A, and (3) by making a more critical differentiation between lines characterizing neutral atoms (Hf I) and those ascribable to ionized atoms (Hf II). Comparison of these results with the earlier measurements of zirconium spectra proves that hafnium was invariably present as an unrecognized impurity. The most sensitive Hf I and Hf II lines for spectrochemical identification are tentatively selected. The stronger Hf II lines are identified with faint Fraunhofer lines in the sun's spectrum.

CONTENTS

		Page
I.	Introduction	151
II.	Procedure	153
III.	Results	155
IV.	Discussion	181
	1. Comparison with zirconium spectra	181
	2. Comparison with solar spectrum	185
	3. Persistent lines of hafnium	186

I. INTRODUCTION

In a letter addressed to Nature on January 20, 1923, D. Coster and G. v. Hevesy [1] announced the discovery of a chemical element having atomic No. 72. They proposed the name of "hafnium" (Hf) for this element because it was in Copenhagen (latin, Hafnia) that the discovery was made. This brilliant confirmation of the theoretical predictions of Prof. Niels Bohr was based on the evidence of Röntgen-ray spectra of zirconium minerals containing small amounts of hafnium, and was the first instance in which credit for the discovery of a new chemical element by spectroscopic methods was

[1] Coster and Hevesy, Nature, 111, p. 79; 1923.

transferred from optical spectra to the more accurately predictable Röntgen spectra. Shortly thereafter (March 10, 1923) H. N. Hansen and S. Werner [2] made the first announcement on the optical spectrum of hafnium. They published the wave lengths of 52 strong lines between 2500 A and 3500 A. This was followed by a list of 288 lines [3] covering the same interval, and then by 77 new lines [4] extending from 3505 A to 7240 A. A complete account of their researches on the optical spectrum of hafnium was published by Hansen and Werner [5] in "Communications to the Royal Academy of Denmark" of that year. The latter publication contained 807 lines ranging in wave length from 2253.98 A to 7240.9 A. The measurements were made relative to zirconium lines present as impurities, and a greater accuracy than about 0.05 A was not claimed. This list was reprinted in 1925 in a monograph by Prof. G. v. Hevesy [6] who also made a slight adjustment of the wave lengths. This appears to be, up to the present time, the only extensive list of hafnium lines, and no values laying claim to higher precision have been published. In March, 1926, Prof. H. Kayser [7] remarked in his Tabelle der Hauptlinien, "die Kenntnis von Hafnium scheint mir noch äusserst unvollkommen."

For several years the spectroscopy section of this bureau has had under investigation the structures of various spectra, especially to test, in successive periods of chemical elements, the alternation and displacement laws of spectroscopy and to determine the origin of the so-called *raies ultimes* which are the basis of spectrochemical analysis. Results for the first two long periods have already been published,[8] and some progress has been made with the next period,[9] in particular the elements lanthanum (57) and platinum (78). It is in this last-mentioned period that hafnium (72), the analogue of titanium and zirconium, finds its place, and it was believed that attempts to analyze its spectral structures should be preceded by a more careful description of the spectra. This was made possible through the kind generosity of Professors Bohr and Hevesy, who, in October, 1925, presented for this purpose two small samples of their hafnium salts. A detailed description of the hafnium arc and spark spectra derived from these samples is presented in this paper.

---

[2] Hansen and Werner, Nature, **111**, p. 322; 1923.
[3] Hansen and Werner, Nature, **112**, p. 618; 1923.
[4] Hansen and Werner, Nature, **112**, p. 900; 1923.
[5] Hansen and Werner, Kgl. Danske Vid Selskab. Math.-fysiske Medd., **V**, 8; 1923.
[6] Hevesy, Kgl. Danske Vid. Selskab. Math.-fysiske Medd., **VI**, 7; 1925.
[7] Kayser, Tabelle der Hauptlinien der Linienspektra aller Elemente, Julius Springer, Berlin, p. IV; 1926.
[8] Meggers, Kiess, and Walters, J. Opt. Soc. Am. and Rev. Sci. Inst., **9**, p. 355; 1924. Meggers and Kiess, ibid., **12**, p. 417; 1926.
[9] Meggers, J. Wash. Acad. Sci., **17**, p. 25; 1927. La I. Meggers, J. Opt. Soc. Am. and Rev. Sci. Inst., **14**, p. 191; 1927. La II. Laporte, Naturwissenschaften, **13**, p. 627; 1925. WI. Meggers and Laporte, Phys. Rev., **28**, p. 642; 1926. OaI, IrI, Pt I.

II. PROCEDURE

The two preparations of hafnium used are referred to as A and B. Most of the results were obtained with A, which the donors described as a very pure sample of about 0.3 g $HfOCl_2$+aq. containing a small amount of zirconium. From this the water of crystallization was carefully removed by Mr. Knowles, of this bureau. The dry salt weighed only 0.19 g and there were some misgivings as to how long it would last in the arc. The actual experience with it was very satisfactory, the small sample just sufficing to make more than 20 well-exposed arc and spark spectrograms. Sample B consisted of 1.4 g HfO_2 containing about 17 per cent ZrO_2. It was used only for making the long exposures necessary to record the infra-red spectrum. Further details as to the "purity" of these preparations, especially of A, are presented under "results" of the spectrum measurements.

For the economical use of this material in producing the maximum number of spectrograms, and in order to avoid the troublesome bands of carbon and cyanogen which are always present when salts are burned in arcs with carbon or graphite electrodes the samples were fused on silver electrodes. The silver rods were 6 mm in diameter. A minute quantity of the hafnium salt was placed on the lower electrode of the arc for each exposure. When the salt vapors were carrying a large part of the current the characteristic green color of the silver arc was more or less effectively replaced by a bluish white flame. The color of the arc served thus as an indicator of the exposure being obtained of the hafnium; if only the green color of silver could be seen the arc was broken and another small dose of hafnium salt administered. A small amount of the hafnium preparation was thus fused with the silver electrodes each time an arc exposure was made, so that the same electrodes could be used for the production of very satisfactory spark spectra. Arc and spark spectra were thus alternately photographed with a comparison spectrum of the iron arc between. The reverse ends of these silver electrodes were used for photographing comparison spectra of silver arcs and sparks alongside the corresponding exposures to hafnium and silver, thus permitting easy recognition and elimination of the electrode spectra of silver, of its impurities, and of atmospheric lines.

The arc spectrum was produced with a 220-volt direct current of 4 amperes. Higher currents were avoided on account of the danger of melting the silver electrodes. Furthermore, it was thought desirable to operate with relatively low current so as to increase the enhancement of spark lines on passing from arc to spark.

The source of the spark spectra was a high-potential condensed discharge between the identical electrodes which had just previously served as the source of hafnium arc spectra. A 40,000-volt transformer consuming about a kilowatt was employed. Condensers of 0.006 μf capacity were connected in parallel with the spark, while the self-induction usually inserted for the suppression of the air

lines was intentionally omitted with the hope that this procedure would permit an improvement in the differentiation between arc and spark lines. Hansen and Werner [10] concluded from their work on hafnium spectra that "the difference between the arc and spark spectrum is not very marked." The explanation is probably to be found in their sources; in that their arc spectra were obtained from intense direct-current carbon arcs using currents as high as 25 amperes while the spark spectra were produced with a 40 cm induction coil, a battery of Leyden jars of about 25,000 cm capacity (0.0278 μf) and a relatively large self-induction of about 0.0005 henry, the combined effect of which would undoubtedly be to make the spectral characteristics of the spark approach those of their intense arc. When our results are compared it is seen that the relative intensities of hafnium lines are really very sensitive to the conditions of excitation, and if these be properly chosen they permit a satisfactory separation of the true arc lines (characteristic of neutral atoms) from the spark lines (ascribed to ionized atoms).

The concave-grating and quartz-prism spectrographs of the Bureau of Standards were employed in making the spectrograms. The gratings and their use in a parallel-light mounting have been described in earlier papers,[11] the quartz spectrograph is a large autocollimating instrument—Hilger's type E_1. With a single setting of the latter instrument the ultra-violet between 2150 A and 2600 A was recorded on a 10-inch plate, the scale ranging from 1.8 A per mm to 3.0 A per mm. With the Hilger instrument three spectrograms of the hafnium arc and spark were obtained on Eastman 33 plates. Fourteen spectrograms covering the interval 2300 A to 9300 A were obtained in the first order of our concave gratings; the Rowland grating with 20,000 lines per inch giving a scale of about 3.6 A per mm being used between 2300 A and 7000 A, while the region from 6500 A to 9300 A was photographed with the Anderson grating with 7,500 lines per inch and scale of 10.4 A per mm.

Long photographic plates of extra thin glass, 40 cm long by 6 cm wide, some of which were obtained in 1925 from Doctor Schleussner in Frankfurt a. M. and some in 1927 from the Eastman Kodak Co. were used. These were coated with high-speed emulsions and their thinness permitted their bending so that satisfactory focus could be obtained throughout their length. To render the plates sensitive to the green, yellow, red, and infra-red spectral regions, they were bathed in photosensitizing solutions of pinaverdol, pinacyanol, dicyanin, and neocyanin, respectively, by the usual methods.[12]

All spectrograms were measured on the large Gaertner measuring machine which has been described in connection with earlier investigations of the same character.[13] The plates were measured from

[10] Hansen and Werner, see p. 10 of reference No. 4.
[11] Meggers and Burns, B. S. Sci. Papers (441), 18, p. 191; 1922.
[12] Walters and Davis, B. S. Sci. Papers (422), 17, p. 353; 1921.
[13] Kiess and Meggers, B. S. Sci. Papers (372), 16, p. 51; 1920.

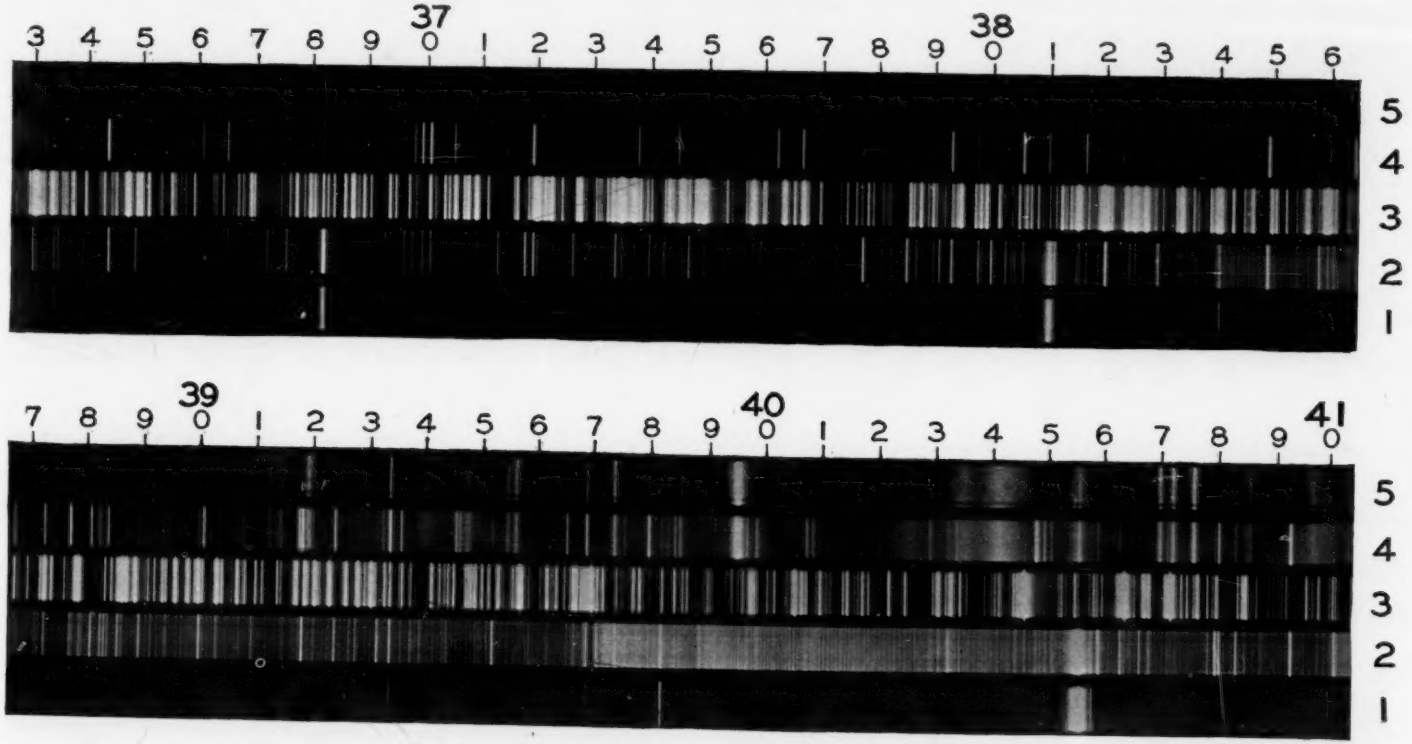

FIG. 1.—*Arc and spark spectra of hafnium and silver*

1, Arc spectrum of Ag; 2, arc spectrum of Ag+Hf; 3, arc spectrum of Fe; 4, spark spectrum of Ag+Hf; 5, spark spectrum of Ag. 3933, 3969, Ca^+; 3970, Hf band head; 3995, N^+; 3973, 4070, 4072, 4076, O^+

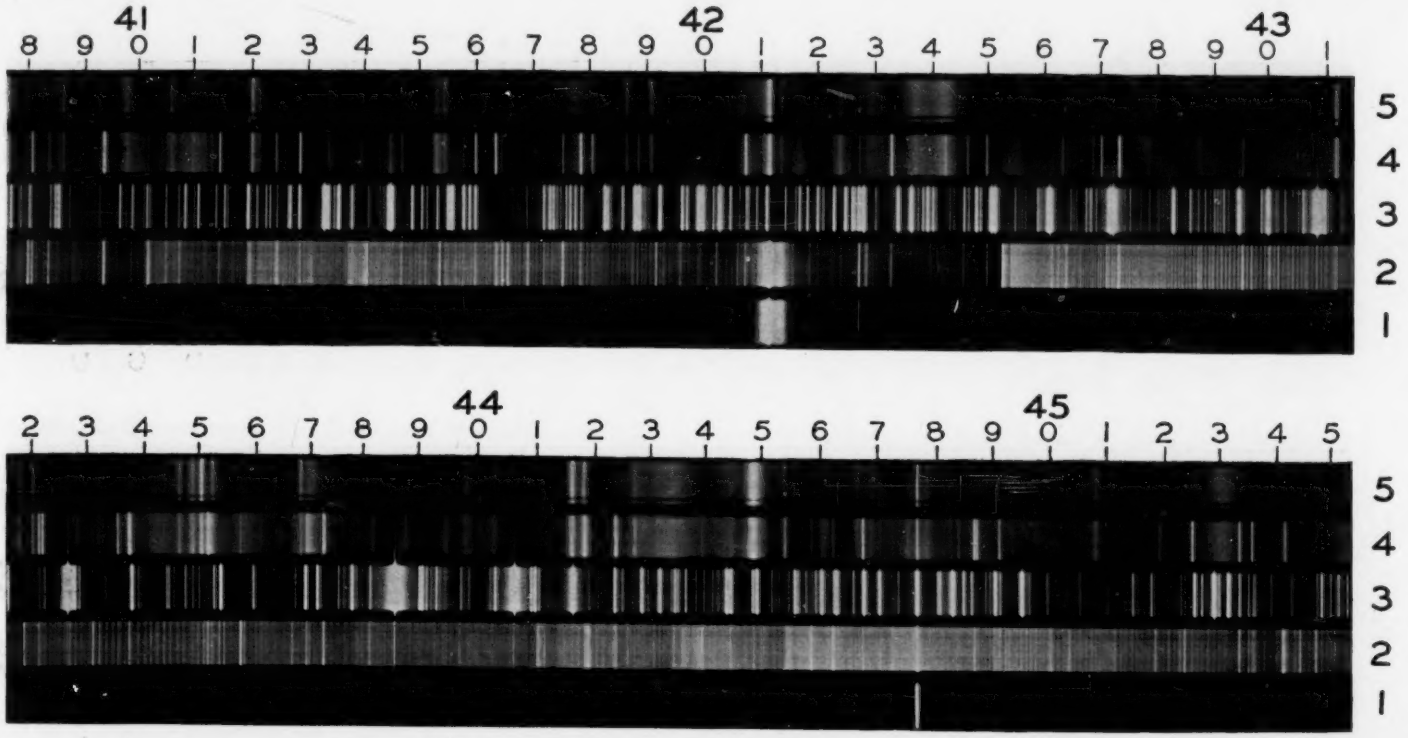

FIG. 2.—*Arc and spark spectra of hafnium and silver*

1, Arc spectrum of Ag; 2, arc spectrum of Ag+Hf; 3, arc spectrum of Fe; 4, spark spectrum of Ag+Hf; 5, spark spectrum of Ag. 4226, Ca; 4252, *Hf* band head; 4383, 4404, Fe; 4415, 4417, O^+; 4447, N^+

4404, Fe; 4415, 4417, O^+; 4447, N^+

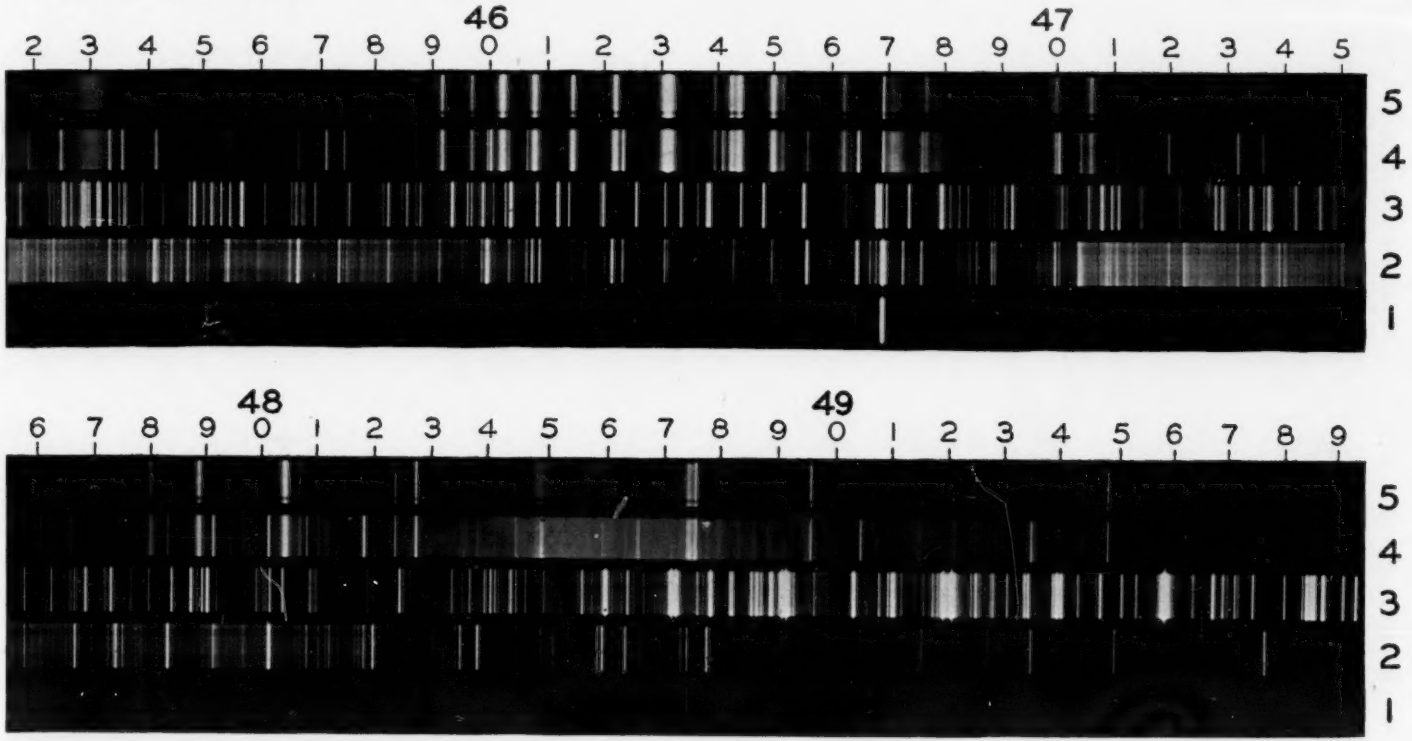

FIG. 3.—*Arc and spark spectra of hafnium and silver*

1, Arc spectrum of Ag; 2, arc spectrum of Ag+Hf; 3, arc spectrum of Fe; 4, spark spectrum of Ag+Hf; 5, spark spectrum of Ag. 4591, 4596, 4642, 4649, 4651, 4662, 4676, 4699, 4705, O^+; 4601, 4607, 4614, 4621, 4631, 4780, 4803, N^+; 4703, Hf band head

short to long waves and then in the opposite direction, settings on the spectral lines being recorded to 1 μ. So far as possible the wave lengths were determined by interpolation between the international secondary standards, but since these extend only from 6750 A to 3370 A the average values of other iron lines as compiled by Kayser and Konen [14] were used as standards down to 2324 A, beyond which the values for iron lines given by Schumacher [15] were selected as standards. The latter values are sadly in need of improvement. The first order spectra of wave lengths exceeding 6400 A were invariably measured relative to iron lines in the second order spectra which were photographed on removal of the Jena-red glass employed to absorb the second order hafnium spectra.

To illustrate the method of observing, and to exhibit some of the more striking features of the hafnium spectra, portions of the spectrograms are reproduced in Figures 1, 2, and 3.

III. RESULTS

When the wave-length measurements and computations of hafnium spectra were finally completed and compiled they totaled more than 2,100 lines ranging in wave from 2165 A to 9250 A. Forewarned that impurities were present, a systematic identification of these was begun by comparison with a list of *raies ultimes* of the chemical elements, the result of which was the detection of 17 different impurities. This does not include Ag, Cu, Na, K, Ca lines which originated with impurities in the silver electrodes because practically all of these were seen to be duplicated in the electrode comparison spectra and were, therefore, not measured. The zirconium lines showing in sample B (containing 17 per cent ZrO_2) contributed nothing to the list, because all of these lines were recognized from comparison spectra of zirconium metal. The complete wave-length list was next compared with the best available wave-length tables of the elements recognized as impurities, and all lines which could be ascribed with more or less certainty to the contaminations were struck from the list. In this way 609 lines were eliminated, the itemized list being as follows:

Columbium	357	Calcium	5
Zirconium	109	Silicon	5
Titanium	50	Aluminum	4
Tantalum	18	Magnesium	3
Iron	16	Rhodium	3
Tin	14	Lead	2
Copper	12	Barium	2
Manganese	10	Lanthanum	1
Palladium	7		

[14] Kayser and Konen, Handbuch der Spectroscopie, **VII**; 1924.
[15] Schumacher, Zeitschr. Wiss. Phot., **19**, p. 149; 1919.

As a further check on the elimination of lines due to impurities, my complete list of wave lengths was compared with Professor Kayser's Tabelle der Hauptlinien der Linien-spektra aller Elemente. This comparison disclosed a small number of additional coincidences with lines of other elements, such as cobalt, ruthenium, vanadium, molybdenum, and certain rare earth elements. Since each of these possesses a great abundance of lines, a considerable number of accidental coincidences may be expected, but no physical significance can be ascribed to them when the strongest and most sensitive lines are totally absent.

After eliminating all lines which could reasonably be ascribed to impurities, and a small number of faint lines resting on a single observation, the original list shrunk from 2,100 to slightly less than 1,500 lines. These are described in Table 1, where my wave lengths and intensities appear in the first and second columns, respectively. Each value is based upon at least two different spectrograms; about half of them depend on three observations, and many lines which appeared on overlapping spectrograms were measured on five plates. The probable errors of the mean of the latter are usually much less than 0.01 A, and it is believed that most of the values based on two or three observations are correct within 0.01 or 0.02 A. This is supported by the agreement of the impurity lines with the accurately measured wave lengths in spectra of the contaminating elements. Further evidence on the precision of these hafnium wave lengths will be deduced from Table 2 where some of my values are compared with accurate measurements of hafnium lines as unrecognized impurities in zirconium spectra.

My intensities are estimated on a scale of 1 to 100 so that the strong lines might stand out prominently and differences between the arc and spark might be more obvious. Unfortunately, the intensities of the spark exposure were not comparable with the arc for wave lengths greater than 6000 A. Beyond this point the intensities are mainly based on arc exposures made with the arc electrodes imaged on the spectrograph slit. Since the spectrograph is stigmatic the intensities of the lines in the center of the arc may be compared with those near the electrodes. Most of the lines are only slightly stronger near the poles than in the middle of the arc, but certain of them are very considerably enhanced, or make their appearance only at the cathode. Since the potential gradient in the arc is greatest near this electrode the conditions are here most favorable for the excitation of higher stage arc lines or of true spark lines. For lines between 6000 A and 7600 A, apart from those observed only at the pole of the arc, there is reason to believe that those which have intensity at least four times greater at the electrode than at the arc center may safely be assumed to be spark lines. It is a common

experience that the easily excited fundamental lines of neutral and of ionized atoms appear with great intensity in either arc or spark sources, but for the majority of the lines in Table 1 there is little or no doubt as to their correlation with Hf I and with Hf II spectra. Additional spectrograms with different exposures to the arc and spark, and stronger spark exposures in the red, would have made the differentiation still more positive. Attention is called to a group of lines between 2310 A and 2560 A which are abnormally enhanced in the spark. They must be ascribed either to Hf III or Hf IV spectra. It is noted also that these lines appear faintly or not at all in my arc and exhibit similar behavior in Hansen and Werner's spark, which is additional evidence that their spark was not especially well suited for the excitation of enhanced lines.

The wave lengths and intensities by Hansen and Werner are quoted in columns 3 and 4 of Table 1. In their original publication the wave lengths were expressed on the scale of Bachem's [16] zirconium wave lengths, since the zirconium lines appearing as impurities were regarded as convenient standards. Vahle,[17] who remeasured the zirconium arc spectrum with more care, found, on the average, somewhat larger values than Bachem, and explained the differences as errors in Bachem's scale, probably introduced by temperature shifts between his zirconium and iron exposures. The list of Hansen and Werner as reprinted by v. Hevesy is corrected to Vahle's scale and it is this corrected list which is quoted in Table 1. Although a greater accuracy than about 0.05 A was not claimed for their values, most of them appear to be well within this limit. The intensity estimates of Hansen and Werner were made on a scale of 1 to 6, which is perhaps too constricted a scale for a good gradation of intensities or differentiation of arc and spark lines. Band spectra from the carbon electrodes used by Hansen and Werner restricted the observation of hafnium lines in certain spectral regions, notably between 3750 A and 3890 A. On the other hand, the strongest silver lines from the electrodes used in securing my spectrograms appear to have obscured a few hafnium lines. For example, it appears that Hf lines at 2453 A, 2474 A, 3280 A, 3386 A, and 3682 A are covered or confused with silver lines on my plates. The greatest difficulty in describing the arc spectrum of hafnium arises from the band spectrum which probably originates with the oxides. Some of these bands are very strong and extremely complex over long spectral ranges. In many cases it is impossible to decide if faint lines belong to the Hf I or to the Hf O_2 spectrum.

In the last column of Table 1, some coincidences with other lines are noted. Certain of these may be real, at least in part, while others

[16] Bachem, Diss. Bonn; 1910.
[17] Vahle, Zeitschr. Wiss. Phot., 18, p. 84; 1918.

probably have no physical significance. The former class includes a considerable number of lines of impurities known to be present, but either the wave lengths or intensities are so discordant as to leave a suspicion that real hafnium lines also exist at or near these points in the spectrum. It was especially difficult to discard some of the approximate coincidences with columbium lines because the available wave lengths and intensities in the arc and spark spectra of columbium are not sufficiently reliable or extensive. Coincidences of the second kind, for example cobalt, ruthenium, molybdenum, vanadium, scandium, and yttrium are inclosed in parentheses since the probability is that they are purely accidental. A perfectly satisfactory description of hafnium spectra can not be made until much purer samples of hafnium salts become available. The ideal material for this purpose would be electrodes of spectroscopically pure hafnium metal and it is, perhaps, not unreasonable to hope for this in the future.

The unexplained symbols in Table 1 have the following significance:

h=hazy.
d=double.
c=complex.
n=band head.
l=shaded to long wave lengths.
p=part of band structure.
e=electrode line.
B. H.=band head.

TABLE 1.—*Arc and spark spectra of hafnium*

λ I. A.	Intensity		λ Hansen and Werner	Intensity		Notes
	Arc	Spark		Arc	Spark	
2155.72	--	5				
73.48	--	2				
74.32	--	4				
75.32	--	3				
78.49	--	2				
79.38	--	2				.4 Cu 4 4
83.48	--	10h				Hf III ?
89.59	--	1				.63 Cu 2 4
90.16	1	2				
90.36	--	4				
2195.41	--	15h				Hf III ?
2212.43	1	2				
13.53	--	20				Hf III ?
14.84	--	5				
21.86	--	1				
33.70	--	2				
34.60	1	20h				Hf III ?
35.45	--	2				
43.15	2	--				
54.01	4	6	3.98	2	4	
55.18	3	5	.11	1	3	
57.90	1	2				
58.70	1	2				
64.87	--	6h				Hf III ?
66.51	2	4	.51	1	3	
66.83	4	8	.81	2	4	
69.86	1	1				
73.14	3	6	.13	2	3	
77.15	10	10	.15	3	5	
83.00	1	--				

TABLE 1.—*Arc and spark spectra of hafnium*—Continued

λ I. A.	Intensity		λ Hansen and Werner	Intensity		Notes
	Arc	Spark		Arc	Spark	
83.56	--	5				
84.61	2	5	.57	1	2	
91.65	2	4	.64	1	2	
95.69	3	--				
97.76	--	1				(.8 La -- 7)
98.34	2	4	.34	--	2	
2298.77	1	1				
2302.08	1	2				
05.36	1	1				
10.21	--	10				Hf III ?
13.42	1	30	.43	--	1	Hf III ?
19.06	1	8	8.46	--	1	Hf III ?
21.13	4	3	.13	3	4½	
22.46	10	15	.44	4	5	
23.23	5	6	.23	3	4	
24.88	4	2	.86	3	4	
32.96	4	5	.95	2	3	
36.47	1	50	.44	--	2	Hf III ?
37.33	4	6	.33	3	4	
38.28	1	2				
39.67	--	?				Hf III ?
43.32	5	10	.32	4	4	
45.41	1	2				
47.45	8	25	.45	5	5	
51.22	10	30	.24	5	6	
53.04	2	--				
54.50	--	1				
55.49	--	20				Hf III ?
65.97	1	2	6.02	2	2	
71.40	1	2				
73.28	--	8				Hf III ?
77.57	--	20	.63	--	1	Hf III ?
80.29	5	10	.35	4	5	
81.00	2	6	.05	2	3	
83.55	1	30	.58	1	1	Hf III ?
93.21	3	5	.19	2	3	
93.36	5	10	.36	4	5	
2393.83	10	20	.81	4	5	.81Pb 5R 3R
2400.81	5	7	.80	4	4	
03.62	1	2	.61	1	2	(.6 Mo -- 4)
04.56	2	4	.57	2	3	
05.43	10	25	.43	4½	5½	
06.45	3	8	.43	3	4	
10.13	8	15	.13	5	6	
15.96	2	4				
17.23	--	1				
17.69	8	15	.67	5	6	.70 Sn 6R 3R
25.98	4	10	.95	4	4½	
28.99	2	5	.96	3	5	
33.56	5	15	.52	3	5	
34.76	2	5	.75	1	3	
41.05	1	2h	.04	1	2	
44.98	1	--				
47.25	10	20	.24	5	6	
49.44	5	10	.42	4	4½	
52.32	1	3	.28	2	3	
53.33	4	?Ag	.33	3	4½	
54.00	1	2	3.99	1	2	
54.60	--	1				
55.20	1	2	.18	1	2	
57.02	--	2h				
59.49	--	1	.43	--	2	
60.50	15	40	.47	6	6	
61.74	--	10				Hf III ?
63.97	--	5	.88	--	3	

TABLE 1.—*Arc and spark spectra of hafnium*—Continued

λ I. A.	Intensity		λ Hansen and Werner	Intensity		Notes			
	Arc	Spark		Arc	Spark				
64.19	20	75	.20	5	5½				
65.07	2	8	.08	3	3				
65.94	--	2							
66.84	--	2							
67.97	2	5							
69.18	8	20	.17	4½	6				
70.70	--	2							
73	?Ag	?Ag	.90	4	5	(.88	Ag	3	8)
78.57	1	5				.6	Ti	--	5
81.44	2	5	.41	2	3				
82.14	--	2							
82.67	2	--							
87.16	3	--							
90.89	--	1							
91.45	--	1							
94.44	1	3h	.38	--	2				
95.17	1	80	.15	1	3	Hf III ?			
96.99	10	20	7.04	5	5				
2498.61	--	1				(.58	Ru	3	5)
2500.75	2	8	.76	3	4				
01.42	--	2							
02.66	3	--	.68	4	3				
10.39	--	2	.44	--	2				
12.68	15	30	.72	6	5				
13.02	25	50	.03	6	5				
15.16	--	30				Hf III ?			
15.49	4	10	.51	4	4				
16.88	25	100	.89	6	6				
17.86	2	--	.88	1	2	(.87	Co	2R	2)
20.52	1	2h				(.53	Rh	2	10)
21.50	3	6	.50 (Cb)	3	4				
23.65	--	3							
31.20	10	25	.19	5	5				
32	--	--	.14	--	1				
32.97	2	3	.97	4	4				
34.34	--	5							
37.34	4	8	.34	5	5				
41.12	--	1							
41.86	--	2							
48.20	2	10	.20	4	4				
48	--	--	.54	1	2				
49	--	--	.00	--	1				
49.12	--	2	.14	--	2				
50.04	--	1							
50.72	--	1							
51.40	10	50	.40	5	6	.40	Cb	1	3
52.37	--	5				(.38	Sc II	3	8)
59.02	2	--							
59.20	5	15	.26	4	5				
60.32	--	1				(.28	Sc II	3	6)
60.75	--	10				Hf III ?			
63.62	5	15	.65 (Mn)	4	5	(.64	Mn	3	5)
67.45	--	5				.5	Ti	--	8
70.72	2	5	.73	2	3				
71.68	25	75	.72	5	6				
72.96	1	3	.97	1	2				
73.92	8	40	.94	5	5				
74.30	--	2							
74.88	2	--	.93	1	2	(.88	Co	2	8)
76.84	7	20	.85	5	5				
78.15	5	15	.19	5	5				
82.51	5	15	.52	5	5				
82.87	--	2							
87.95	--	1							
91.33	3	5	.33	5	5				

TABLE 1.—*Arc and spark spectra of hafnium*—Continued

λ I. A.	Intensity		λ Hansen and Werner	Intensity		Notes
	Arc	Spark		Arc	Spark	
95.61	--	4h	.61	1d	2	.6 Ag -- 3
2599.20	2	4	.18	1	2	
2602.68	3	--	.70	3	3	
02.86	2	--	.90	3	3	
03.50	2	1				
06.38	8	20	.42	5	5	
07.04	10	30	.06	5	5	
07.23	3	5	.31	2d	2	
08.47	5	1	.46	3	3	
08.63	2	--				(.6Zn I 8R 3)
09.29	--	2				(.3Mo -- 5)
09.95	3	--	10.01	3	2	
12.60	2	--	.60	3	2	
13.61	7	20	.63	4	5	
14.22	1	2	.31	1d	2	.20Pb 6R 5R
14.59	--	5h				.5Ag 2 6
16.61	2	--	.64	4	3	
20.97	--	1	.95	1	2	
22.75	5	20	.76	6	6	
26.97	1	4	.96	3	4	
35.79	1	5	.81	3	4	(.82Ru 4 3)
37.00	3	--	.00	4	3	
38.72	10	30	.72	6	6	
39.00	--	2h				
41.42	10	50	.43	6	6	
42.07	2	--				
42.76	3	--	.74	5	3	
47.31	8	30	.31	6	6	
49.16	--	4	.13	3	4	
50.33	--	2				
51.18	1	10				
52	--	--	.35	1	2	
52	--	--	.79	3	2	
57.50	2	4	.51	4	4	
57.85	2	6	.86	5	5	
61.89	4	12	.89	5	5	
65.98	2	6	.98	5	5	
68.28	2	--	.30	4	3	.26Cb 2 1
69.01	2	3	.02	5	4	
71.26	1	4	.22	3	4	
76.63	--	3	.60	2	3	
77.57	--	1	.59	2	3	
78.43	--	2	.38	1	2	
83.36	5	20	.41	5	6	
84.03	--	1				
85.23	1	5	.21	3	4	
87.22	--	3h				
88.35	1	--	.37	2	1	
96.18	2	--				
97.07	2	2	.09(Cb)	2	2	.07Cb 3 7
98.90	1	--				
2699.63	2	--				
2703.19	--	1	.17	1	2	
05.62	10	1	.64	6	5	
06.71	3	15	.72	6	5	
11.83	2	--				
12.43	5	10				.42Zr II --5
13	--	--	.50	½	1	(.50Mo 1 5)
13.84	3	--	.88	4	3	
18.51	2	5	.58	5	5	
18.57	5	--				
26.69	2	--				
27	--	--	.45	3	2	
29.10	2	--	.11	4	3	
30.71	2	--				

TABLE 1.—*Arc and spark spectra of hafnium*—Continued

λ I. A.	Intensity		λ Hansen and Werner	Intensity		Notes
	Arc	Spark		Arc	Spark	
30.84	4	--				
31.16	--	3	.13	1d	2	
33.00	--	3h				
35.12	--	1	.09	--	1	
37.82	3	--	.84	3	2	.83Fe 3 --
38.76	10	25	.77	5	6	
43.63	5	--	.64	4	3	
46.62	1	--				
51.81	5	15	.87	5	5	
53.61	--	8				
56.91	1	7	.95	3	4	
58.31	2	--				.31Ta 3 1
61.19	--	2				
61.62	8	1	.68	5	4	
62.69	2	--	.72	4	3	
64	--	--	.56	½	1	
66.96	4	--	.98	4	3	
70.42	2	5h	.47	4	4	
72.33	1	4	.36	3	4	
73.01	4	--	.01	3	3	
73.37	20	50	.42	6	6	
74.02	4	10	.07	5	4	
75.27	1	4	.28	4	3	
76.15	--	1				
79.36	8	1	.39	5	5	
83.68	3	--				
84	--	--	.50	½	1	
86.32	1	5	.33	3	4	
89.51	1	8				
2789.74	4	20				
2808.00	5	10	.02	5	5	
09	--	--	.61	1	1	.63Bi 8R 2
12	--	--	.33	2	2	
13.86	5	8	.88	4	4	
14.47	3	10	.48	4	4	
14.77	2	6	.81	3	3	
15.80	1	--				
16.07	--	3	.11	1	2	
17.68	5	--	.72	5	3	
18.93	3	--	.96	4d	3d	
19.75	5	--	.77	4	3	
20.23	20	50	.24 (Tl)	6	6	
22.67	10	25	.71	6	6	
29.33	2	5	.34	3	4	
33.29	7	1	.32	5	4	
34.12	3	--	.16	4	3	
41.49	2	--				
45.83	9	1	.81	5	5	
49.21	5	25	.20	5	5	
50.15	1	4	.13	3	3	
50.96	8	--	.94	4	3	
51.21	6	12	.24 (Tl)	5	4	
52.03	5	10				1.98 Zr II -- 6
56.96	--	1				
57.65	1	4	.67	4	4	
58.69	1	2	.71 (Mn)	1	2	
60.32	1	4	.34	1d	3	
60.56	5	--	.59	3	3	
61.01	10	20	.06 (Cb)	5	6	
61.69	15	30	.72	6	6	
63.33	3	--	.39	3	2	.32 Sn 8R 6R
64.58	--	1				
66.38	20	3	.38	6	6	
67.69	2	--	.79	1	2	
69.24	1	--				

TABLE 1.—*Arc and spark spectra of hafnium*—Continued

λ I. A.	Intensity		λ Hansen and Werner	Intensity		Notes
	Arc	Spark		Arc	Spark	
73.63	1	?	.66	3	2	.63 Rh 4 1
76.33	4	20	.37	5	5	
77.16	2	--				
79.11	1	4	.14	4	4	
85.47	1	4	.52	3	4	
87.13	6	1	.16	4	4	
87.54	3	--	.56 (Ti)	4	3	
89.01	--	1				
89.62	15	2	.65 (Mn)	5	5	
91.03	1	--				
92.55	2	--	.59	4	3	
94	--	--	.04	--	1	
94	--	--	.88	1	1	
98.26	25	3	.31	6	5	
2898.71	3	12	.79	5	4	
2904.42	20	3	.44	5	5	
04.50	--	3				
04.76	20	2	.84	5	5	
07.66	1	--				
09.91	4	5	.91(Ti)	5	5	
12	--	--	.79	1	1	
13.22	--	2	.19	½	1	
16.49	30	5	.55	6	5	
17.51	1	3				
18.58	12	2	.65	5	4	
19.59	10	20	.61	6	6	
24.61	5	1	.66(Zr)	3	3	.61 Zr 2 1
26.35	1	2	.46	1	3	
28.98	2	--				
29.63	8	10	.66	6	5	
29.90	8	1	.95	4	4	
35.37	1	--				
37.80	10	30				
40	--	--	.25	1	2	
40.77	25	4	.80	5	5	
43.70	1	--				
44.71	5	1	.73	4	4	
47.14	1	4	.16	3	4	
50.68	20	3	.72	5	5	
51.22	1	--				
51.90	1	--				
53.64	1	--				
54.21	15	2	.24	5	5	
58.02	7	1	.04	4	4	
60.83	1	5				
61.80	2	3	.82	4	4	
64.88	20	3	.86	5	5	
66.95	10	1				
67.24	2	10	.26(Ti)	3d	4	.22 Ti 8 2
67.86	1	--				
68.83	10	25	.87	6	5	
70.59	--	1h				
73.38	3	--	.42	--	3d	
74	--	--	.11(Cb)	2	3	.12 Cb 4 6
75	--	--	.38	1	1	
75.90	12	30	.91	5	6	
77.59	2	6	.61	4	4	
79.28	5	1	.26	5	4	
80.20	--	1				
80.82	15	2	.84	5	5	
82.73	5	1	.74	5	4	
84.06	2	--	.08	--	3	
90.83	--	2	.83	--	3	
2992.06	1	--	.01	--	1	
3000.10	6	10	.12	5	5	

TABLE 1.—*Arc and spark spectra of hafnium*—Continued

λ I. A.	Intensity		λ Hansen and Werner	Intensity		Notes			
	Arc	Spark		Arc	Spark				
01.85	--	2h	.85	1	2				
05.56	15	3							
11.25	1	4	.23	2	3				
12.19	--	1							
12.90	15	25	.89	6	6				
15.29	1	--				.25	Cb	1	--
15.92	1	1				.93	Fe	3	1
16.78	30d?	2	.77	6	5				
16.93	--	2							
17.36	1	--							
18.32	15	2	.30	5	5				
20.54	20	3							
22.14	--	2h	.06	--	2				
24.61	2	--							
24.78	2	6	.73	--	4	.75	Cb	3	4
25.29	4	8	.34	--	4				
31.17	10	25	.16	5	6				
34.54	1	--	.56	2	1				
42.09	1	--							
46.03	2	5	.05	4	4				
49.30	2	--							
50.76	10	2	.76	5	4				
54.52	2	3	.50	4	3				
55.43	1	5	.47	4	3				
57.02	20	3	.04	5	5				
63.77	4	1				.82	Cb	2	3
64.68	2	8							
67.41	10	2	.39	6	5				
69.21	3	--	.18	3	3	.22	Ta	5	1
70.01	--	1							
70.47	1	--							
72.88	30	4	.94 (Ti)	6	5				
74.09	4	1	.11	3	3				
74.78	7	1	.81	4	4				
75.30	2	--				.25	Cb	2	2
75.94	2	--							
76.88	2	--	.88	2	3d				
80.63	3	20							
80.84	10	--	.77	6	6				
83.66	--	2h							
91.37	1	--							
91.78	--	2	.75	1	2				
92.25	2	5	.25	4	4				
96.76	6	1	.77	5	4				
3098.59	1	--							
3100.78	2	--	.77	--	1				
01.38	8	15	.42	6	6				
02.14	1	--							
02.34	1	--	.47	--	1	(.30	VII	10	10R)
03.69	2	--							
05.65	1	--							
06.01	2	1							
09.11	15	40	.14	6	6				
12.18	1	1							
14.80	1	--	.86	--	1				
16.94	1	4	.98	3	4				
19.97	4	--	.97	4	4				
22.55	1	--							
23.95	1	--	.90	1	1				
26.27	1	2	.31	2d	3				
26.65	1	--				.67	Cu	6	2
28.75	3	--	.75	3	3				
29.59	2	--							
31.81	12	2	.82	--	5				
33.10	--	1							

TABLE 1.—*Arc and spark spectra of hafnium*—Continued

λ I. A.	Intensity		λ Hansen and Werner	Intensity		Notes			
	Arc	Spark		Arc	Spark				
34.72	25	40	.77	6	6				
37.52	3	--	.55	3	3				
39.67	3	5	.69	3	4				
40.77	3	5	.78	3	4				
45.33	10	8	.33	5	6	.38	Cb	4	8
48.41	5	1	.46	4	4				
51.63	4	--	.65	4	3				
52.96	2	--							
56.68	10	1	.64	5	5				
59.83	10	1	.82	5	5				
61.55	1	--							
62.57	20	?	.59 (Ti)	5	6	.57	TiII	9	6
62.62	?	10							
65.73	2	--							
68.39	10	1							
72.94	15	2	.93	5	6				
74	--	--	.92	1	1				
76.86	10	20	.86	6	6				
78.43	2	--							
79.63	2	--	.48	1	2d				
81.02	5	--	.02	4	4				
81.13	4	--							
81.77	--	1h							
89.63	4	--	.69	4	4				
93.53	10	15	.50	5	5				
94.20	15	25	.20	6	6				
95.63	1	3	.62	2	2	(.61	Y II	8	10)
3196.92	5	--				.94	Fe	4	2
3200.00	3	7	.02 (Ti)	4	5				
02.16	1	2	.16	1	2				
03.68	1	4	.73	3	4				
06.11	7	1	.18	5	4				
06.77	1	2	.70	--	2				
10.97	4	1							
13.71	2	--							
17.30	5	4	.17	5	5				
18.20	--	3							
20.66	3	10	.61	4	5				
25.04	1	2				.03	Ni I	5R	2
27.00	1	2	6.97	2	3	(6.99	Co	6R	--)
27.87	2	--							
30.07	3	--	.10	3	2				
33.24	1	--							
33.80	1	1							
39.41	3	--							
43.00	1	3							
43.36	3	--	.40	4	2				
49.53	5	--	.52	4	3	.49	Cb	3	1
53.70	15	25	.70	6	6				
54.06	2	--				.05	Cb	3	6
54.86	2	--							
55.29	6	8	.30	5	6				
61.90	2	--							
62.47	3	--	.55	3	3				
65.29	2	--							
65.65	1	--				(.65	La II	6	4)
67.01	2	--				.03	Cb	2	1
67.17	3	--	.14	5	3				
73.66	1	2							
80	?Ag	?Ag	.02	5	5				
83.40	--	2	.42	5	3	.43	Cb	3	6
89.75	1	2	.73	1	1				
91.04	4	1	.05	4	3	.04	Cb	2	2
94.69	--	2h	.59	--	1				
3298.94	2	--	.96	3	2				

TABLE 1.—*Arc and spark spectra of hafnium*—Continued

λ I. A.	Intensity		λ Hansen and Werner	Intensity		Notes			
	Arc	Spark		Arc	Spark				
3306.12	6	--							
09.20	3	--	.26	4	3d				
10.27	8	2	.25	5	4				
10.85	1	3	.92	1	3d				
12.87	15	3	.86	6	6				
14.03	--	1							
16.18	3	--							
17	--	--	.21	½	1	.19	Cu	5	2
17.99	5	6	.97 (Ti)	5	6	8.02	Ti II	5	5
18.28	1	--							
23.36	1	5h		½	2				
24.18	--	2	.18	½	2				
27.82	2h	--							
28.21	4	5	.18	5d	5				
31.87	2	--							
32.73	20	2	.74	6	6				
33.51	--	1h							
52.06	10	20	.03 (Ti)	6	6				
53.03	1	--							
56.78	3	--							
58.30	--	4h							
58.95	8	1	.92	5	3				
60.06	8	1	.08	4	3				
66.68	3	--	.71	4	2				
70.70	--	2h							
78.93	4	--	.88	4	3				
84.15	--	3	.17	1d	3d				
84.70	1	3	.67	5	4	.66	Cb	2	1
86	?Ag	?Ag	.10	4	4				
89.83	10	15	.78	5	5				
92.81	3	--							
94.99	3	8	5.00	3	4	.96	Cb	1	1
95.90	1	--							
97.26	4	--							
97.60	4	--	.50	4d	3d				
3399.80	30	40	.80	6	6				
3400.21	3	--							
02.51	3	--	.44 (Ti)	4	3				
07.13	2	--							
07.76	2	4	.77	4	4				
08.72	1	--				.66	Cb	3	4
10.18	5	15	.17 (Zr)	5	6				
12.38	2	--	.35	3	1				
13.74	1	3	.78	5	3				
17.35	5	--	.36	5	3	(.35	Ru	10R	3)
19.18	8	1	.19	5	4				
28.36	7	4	.39	5	5				
34.88	2	--				(.90	Rh	10R	10)
38.43	4	--							
40.88	2	--							
41.84	2	--	.87	3	2				
48.30	1	--							
52.31	2	--				.33	Cb	2	2
62.65	3	3	.68	4	4	.62	Cb	2	1
67.56	3	--	.61	3	2				
69.21	2	1							
72.38	20	2	.40	5	5				
75.85	--	2							
78.93	3	9				(.91	Rh	10R	10)
79.28	9	10	.22	6	6				
81.87	1	--							
84.71	2	--							
87.57	2	2	.57	½d	3				
95.75	5	5	.77 (Ti)	5	5				
95.93	1	3							

TABLE 1.—*Arc and spark spectra of hafnium*—Continued

λ I. A.	Intensity		λ Hansen and Werner	Intensity		Notes
	Arc	Spark		Arc	Spark	
97.16	5	1				
97.49	15	2	.44	5	5	
3498.99	2	--				
3501.95	3	--				
03	--	--	.59	3	3	
05.23	20	40	.22	6	6	
06	--	--	.84	3	3	
11.88	1	3	.76	½	1d	
13.28	4	--	.28	3	3	
18.75	2	4	.74	3	3	
21.57	2	--	.57	2	2	(.57 CoI 5R 5)
23.02	15	1	2.99	5	5	
25.55	2	--				
26.87	1	--				(.85 CoI 9R 6)
30.87	2	--				
31.23	2	--	.21	2	2	
34	--	--	.49	3	2	
35.54	10	20	.51	5	5	
36.62	10	1	.59	4	4	
48.81	4	1	.80	3	3	
52.70	10	15	.67	5	6	
53.04	1	--				
54.00	3	--				
58.48	2	--				
61.65	20	25	.65	6	6	
64.31	3	--	.29	3d	3d	
65.32	2	--				
67.36	5	--	.37	3	4	
69.03	20	30	.04	5½	6	
79.91	2	--				
80.45	--	2				
83.27	2	--				
97.42	3	5	.43	4½	5	
97.50	3	--				
99.17	--	3h	.13	2	3	
3599.87	7	1	.88 (Zr)	4½	4	.89 Zr 3 6
3600.04	--	3h				
09.12	1	--				
15.05	3	--				
16.89	10	2	.87	5½	6	
17.70	2	--	.69	3	3	.66 Cb 2
20.04	2	--	19.99	3	3	
22.46	1	2	.43	2	3	
24.00	3	5				
27.83	2	--	.80	3	2	(.81 CoI 8R 4)
30.86	6	2	.85	4	4	
32.69	2	--	.68	2	2	
33.20	2	3	.15	--	3	
37.59	2	--	.60	3	3	
44.35	15	20	.31	6	6	
45	--	--	.80	1	1	
48.35	1	3	.33	3	3	
49.09	6	1	.08	4½	4½	
50.53	2	--	.49	3	3	
51.85	5	1	.80	4	4	(.83 ScII 10 10)
54.26	5nl	--	.22 B. H.?	3d	2d	
55.65	1+p	--				
56.64	--	2				
59.03	1	3	.00	2	3	
61.05	3	8	.04	4	4½	
61.74	--	1	.69	1	1	
64.65	3+p	--	.56	2	3	
65.36	4	10	.30	4½	5	
66.77	--	3d	.74	2	3	
68.20	2	--				

TABLE 1.—*Arc and spark spectra of hafnium*—Continued

λ I. A.	Intensity		λ Hansen and Werner	Intensity		Notes
	Arc	Spark		Arc	Spark	
72.28	8	2	.27	4	4	
75.74	9	2	.75	5	5	
78.06	--	3				
81.41	2	3	.37	3	3	
82.25	30?	?Ag	.24	6	6	.23 Fe 6 3
96.52	6	1	.50	4	4	
98.39	3	7	.34	2	2	
3699.73	7	15	.71	5	5	
3701.15	8	25	.14	5	6	
02.36	--	2				
04.92	2	--				
05.41	3	10	.40	4	4½	
07.36	2	--				
08	--	--	.87	2	2	(.83 Co 6 4)
17.80	15	3	.82	5	5	
18.83	--	2				.81 Zr 3 3
19.27	15	25	.30	6	6	
21.51	3	--				.50 Cb 2 1
22.65	--	2				
26.49	4	--	.50	3	3	
29.10	4	--				
33.78	10	2	.82	4	4	
37.88	4	10	.85	3	4	
39.02	3	1	.06	2	3	
41.96	--	2h				
44.98	3	10	.98	3	3	
46.80	9	2	.81	4	4	
47.48	3	4	.51	3	3	
53.21	4	1				.19 Cb 3 1
58.05	--	3				
62.51	2	20				
64.53	3	--				
66.12	1	--				
66.92	4	25				
68.25	5	1				
70.64	--	2h				
71.35	2	4				
72.86	--	1				
73.12	2	--				.18 Cb 2
77.64	30	4	.74	5	5	
80.09	2	3				
82.43	2	--				
82.78	3	5				
85.46	25	3	.40	5	5	
87.38	2	--				
88.22	2nl?	--				
93.37	20	20	.35	5	5	
97.95	2	8				
98.67	3	--				
3799.52	--	2				
3800.39	15	5	.40	4	4	
04.16	2	--				
04.52	3	1				
06.07	4	25				
11.76	5	1				
16.08	2	--				
17.20	4	12	.05	2	3	
19.36	2	--				
19.93	--	2h				
20.74	15	3				
23.54	1	4h				
29.67	3	1				.67 Mn 3 3
30.01	7	2				
31.12	2d	--				
33.67	2	--				

TABLE 1.—*Arc and spark spectra of hafnium*—Continued

λ I. A.	Intensity		λ Hansen and Werner	Intensity		Notes			
	Arc	Spark		Arc	Spark				
38.37	1	2							
40.03	1d?	--							
49.17	10	2							
49.52	3	15							
50.34	1	--							
54.34	1+p?	--							
58.30	12	2				(.30	Co	6	3)
60.91	3	1							
64.75	2	10							
67.31	2	7							
72.54	4	8							
77.11	3	20							
79.26	1d?	--							
80.81	12	10	.79	3	3				
82.24	--	2h				.3	L	--	2
82.52	3	--							
83.13	2	--							
83.77	3	6							
85.67	2	--				.72	Cb	4	3
89.24	5	--							
89.33	4	--	.32	3	4				
92.49	2	--	.46	2	3				
95.	--	--	.63	2	1	.66	FeI	5	3
96.77	1+p	--							
3899.93	12	2	.93	4	5				
3900.66	1	10				.88	AlII	--	10
02	--	--	.91 (Fe)	4d	4	.95	FeI	7	5
06.91	2	--	.88	3	3				
09.18	3	--	.19	3	3d				
12	--	--	.51	1d	1				
17.47	2	6	.43	4	4				
18.10	15	10	.07	6	6				
23.91	6	10	.91	5	5				
26.45	3	1	.41	3	3	.46	Mn	3	4
27.58	4	1	.58	2	4				
29.24	1	2				.30	Cb	3	1
31.36	8	2	.34	3	4				
31.75	2+p	--	.79	2	2				
32.40	2	3							
35.64	3	6	.68	3	3				
38	--	--	.41	1d	2				
39.04	3	--	.01	3	3				
41	--	--	.18	1	1				
43.06	2	--							
45.37	--	5h	.32	2	2				
46.03	--	3h							
48.09	1p?	--							
49.48	1p?	--	.48	1	2				
50.79	3	1	.77	3	4				
51.81	15	2	.81	5	5				
64.95	3	7	.96	3	4				
67.25	1	--							
68.01	4	1	.04	2	2				
70.06	10nl	--	.10 B. H.	4	3				
75.15	--	2							
79.40	1	12	.36	3	4				
84.03	1	4	.03	3	4				
84.85	--	3				(.86	Ru	8	4)
88.23	1	--				.15	Cb	2	2
96.80	1	3	.78	2	3				
3998.50	1	4							
4002.50	2p?	--							
03	--	--	.78	2	2				
07.36	1p?	6	.36	2	3				
08.47	--	4	.46	2	3				

TABLE 1.—*Arc and spark spectra of hafnium*—Continued

λ I. A.	Intensity		λ Hansen and Werner	Intensity		Notes			
	Arc	Spark		Arc	Spark				
09.78	2p?	--							
11	--	--	.80	2	2d				
11.94	1p?	--							
14.21	1p?	--							
20.25	2	2	.28	3	3				
22.84	2p?	--							
29.16	3	4	.19	3	3				
32.27	4	1	.20	4	4				
33.88	--	3	.88	1	2d				
44.38	3	1	.39	3	3				
46.75	1p?	--							
47.96	2	15	.98	3	4				
49.44	2	6	.45	3	3				
49.74	2	--	.76	1	1	.75	Cb	2	1
50.68	1	3	.63	3	3d				
50.88	2	--	.91	3	3				
53.25	1	--							
53.64	1	--							
57.42	2	--	46	3	2				
62.84	15	2	.86	4½	5				
64	--	--	.79	2	2				
66.23	8	1	.21	4	4				
67.84	5	1	.82	2	3				
80.44	10	10	.46	5	5				
83.36	10	2	.35	4	4				
87.96	1	--							
93.17	40	25	.18	6	6				
95.50	1	--				(.49	V	7	5)
4098.00	1p?	--							
[1] 4100.93	20ml	2				.90	Cb	30	10
04.23	3	1	.26	2	3				
06.56	4	1							
13.58	4	6	.54	4	4½				
15.89	1p?	--							
18.60	3	1							
18.91	2	--							
23.51	--	5							
25.10	--	3							
27.78	4	12	.76	4½	5				
36.38	2dp?	--	.37	2d	3d				
38.68	--	2							
41.83	--	3							
45.76	3	1	.76	3	4	(.76	Ru	6	4)
50.16	1p?	--							
51.49	1p?	--							
54.12	2p?	--							
56.12	2	1							
56.74	--	2							
58.90	2	10	.88	3	4				
62.40	4	15	.35	4	4				
62.68	3	--							
63.42	--	2							
70.41	2	1							
70.90	3	1							
74.33	30	3	.33	4½	5	.35	Cb	2	1
75.78	1p?	--							
77.50	3	15	.48	3	4	(.52	Y	10	10)
79.56	--	6							
87.67	2p?	4							
88.23	3	--							
4193.12	2p?	--							
4201.52	5	1				.54	Cb	4	2
06.57	5	20	.56	4½	5½				
09.71	5	2	.71	3	3				
21.75	1	--							

[1] Hf band head coincident with Cb impurity line.

TABLE 1.—*Arc and spark spectra of hafnium*—Continued

λ I. A.	Intensity		λ Hansen and Werner	Intensity		Notes			
	Arc	Spark		Arc	Spark				
28.08	7	1	.03	3	3				
31.19	1	--							
32.46	6	20	.39	4½	6				
45.15	5	1							
45.83	3	6	.84	3	4				
49.33	5	9	.32	4½	4½				
52.05	25nl	--	.02 B. H.	4	4				
53.59	5nl?	--							
60.96	4	2	1.02	3	4				
62.72	1	3	.72	3	3				
63.41	7	2	.42	4	4				
68.10	--	3							
69.66	1	6	.68	4	4				
70.59	2	1							
72.84	7	15	.84	4½	5				
83.45	2p?	--							
84.73	2p?	--							
94.77	20	3				0.79	Zr	6	2
4296.41	4	--	.42	3	3				
4303.60	3p?	1	.61	3	3	(.61	Nd	10	10)
04.41	3p?	1							
18.13	8	2	.17	4	4				
20.67	6	10	.67	4½	5				
21.36	1p?	10							
22	--	--	.67	1	2				
26.24	3d?	--							
30.27	8	2	.32	4½	4½				
34.64	3	8	.65	3	4½				
35.13	2	1	.15	2	3				
36.65	10	40	.71	5	6				
49.73	4	--	.78	3	3				
50.50	8	25	.53	4	6				
51.15	3	--							
52.56	3	--	.60	3	3				
53.32	3	--	.38	3	3d				
56.29	25	3	.33	5	6				
56.98	3	--							
65.37	4	--	.38	3	3				
67.89	8	6	.92	4	5				
79.13	3d	--	.19	2	2d				
85.52	--	2	.47	1	2				
90.70	1+p	--							
91.26	1	--							
92.69	2	--				.73	Cb	3	
4395.01	3c	--							
4408.82	6nl	--	.86	3	3				
15	--	--	.06	--	2				
16	--	--	.15	2	2				
17.35	8	10	.35 (Tl)	4½	6				
17.90	8	1	.86	3	4				
18.25	4	--							
22.24	2	--	.25	2	2				
22.75	6	30	.71	4	5				
30.63	1	--	.57	1	1	.62	Fe	4	--
32.93	2d	--	.95	1	2d				
34.52	3c	--							
38.02	10	2	.04 (Zr)	4	4				
43.07	4	2							
52.70	--	5							
52.97	4	--	.96	3	3				
57.35	15	2				(.36	Mo	7	3)
61.17	12	2							
66.38	3	8	.39	3	3				
73	--	--	.05	1	--				
83.29	--	2							

TABLE 1.—*Arc and spark spectra of hafnium*—Continued

λ I. A.	Intensity		λ Hansen and Werner	Intensity		Notes			
	Arc	Spark		Arc	Spark				
86.12	6	8	.15	4½	4½				
86.64	--	6							
90.59	1	6	.61	2	3				
4499.65	4	1	.65	2	3				
4518.30	5	1	.31	3	3				
19.01	--	4							
20.59	4	--	.60	2	3				
24.72	2	8	.66	--	3	.74	Sn	6	10
33.18	12	6	.15 (Tl)	5	5				
35.36	2	7	.32	2	3				
39.74	1	1							
40.92	20	3	.88	4	4				
41.29	4	6	.28	1	3				
41.70	4	--	.73	1	1				
43.01	2	--	.00	2	2				
44.02	7	1	.00	3	4				
46.83	10	1	.96	2	2d	.83	Cb	10	4
47	--	--	.76	--	2				
50.14	2	--							
53.27	2	--							
53.78	6	--				.83	Cb	3	--
58.94	1d	--							
62	--	--	.70	3	3d				
65.94	25	3	.93	5	5				
70.70	1	10	.62	2	3				
73.79	4	6	.78	4	4				
86.25	3	3	.24	--	3				
97.93	4	1	.94	3	3				
98.86	50	4	.86	6	6				
4590.46	2	10				.45	Cb	1	2
4602.71	4+p	3							
05.78	5	4	.76	3	4				
08.10	10	2	.10	4	4				
13.72	3	10?	.71	3	3				
14.20	3	--							
19.52	2	--	.46	2	2	.51	Ta	4	2
20.87	30	3	.85	6	5				
22.71	8	15	.70	4½	5				
28.19	2	--							
30.62	5	?							
40.13	3	4							
42.25	7	--	.25	4	3				
47.45	1	--				.44	Fe	4	2
48.32	2	--	.35	--	2d				
50.58	3	--	.62	2	3d				
52.25	2	--	.09	2d	3d				
55.19	40	3	.19	6	5				
59.20	2	2	.29	--	2				
60.21	1	--							
64.13	20	25	.14	5½	5½				
69.22	2	--	.25	2	2				
70.91	2	--	.94	--	2				
82.66	1?	4							
83.94	3	--							
86.38	2	--							
88.39	6	1							
95.98	1	--							
99.01	15	2	.02	4	4½				
4699.72	4	8	.70	3	4				
4703.11	10nl	--							
03.61	1+p	3							
08.86	2	--	.85	3	3				
12.20	1+p	--							
14.98	--	2							
19.10	8	8				.11	Zr	6	5

TABLE 1.—*Arc and spark spectra of hafnium*—Continued

λ I. A.	Intensity		λ Hansen and Werner	Intensity		Notes			
	Arc	Spark		Arc	Spark				
21.70	5	1	0.74	3	3				
29.10	1p?	--							
31.36	4	0							
35.67	5c	--	.62	3	3d				
37.66	2po	--							
38.13	2	--							
38.59	8	1	.61	3	3				
39.82	3	--							
46.72	1	--							
51.53	1d	--							
57.61	6	1	.60	3	3				
60.58	1	5	.53	2	3				
65.77	1	5	.80	2	3				
66.51	15	2	.51	4	4½				
69.36	2	--							
73.72	10	2	.73	4	4				
74.90	5	1	.90	3	3				
77.20	2	--	.16	1	2d				
82.75	40	3	.77	4	5				
87.33	1	--							
90.72	5	8	.72	3	4½				
4795.96	2	--	.98	2	2				
4800.50	70	8	.51	6	6				
07.14	3	4	.14	2	3				
09.18	2	3	.24	2	2				
11.14	3	1	.14	2	3				
13	--	--	.86	1	2				
17.22	5	12	.20	3	4½				
18.84	15	2	.86	4	4				
20.29	--	2							
34.20	10	1	.20	4½	3				
37.24	20	2	.26	5	5				
43.99	3	4	4.00	3	3				
47.44	2	--							
48.45	3	6	.50	2	3				
50.58	5	--	.64	3	3				
58.41	8	1	.45	3	4				
59.23	30	2	.26	4½	5½				
60	--	--	.60	1	1				
61.49	2	--	.54	2	1				
63.27	20	2	.31	4	5				
65.41	2	5th	.46	2	3				
72.94	5	1	.97	3	3				
77.58	20	2	.61	4½	5				
78.15	3	--	.16 (Ca)	3	3	.17	Ca	10	8
85.73	1	2							
86.32	2c	--							
88.07	2c	--							
89.57	2	--				.61	Cb		2
89.89	2	--	.70	2d	1d				
94.46	1	2							
4896.32	3	--	.36	3	3				
4903.04	2	--	.02	2d	3	(.04	Ru	15	3)
04.49	5	10	.44	3	4	∫.49	Zr	3	
						\.49	Cb	5	
06.33	3c	--	.29	1d	1d				
07.28	2c	--	.20	2d	1				
10.09	3	--	.05	2	2				
10.93	3	--							
15.28	5	--	.24	4	3				
20.96	2	4	.88	2	2	(.97	La	8	5)
26.14	2c	--							
26.95	2	2							
28.37	1	4							
33	--	--	.88	1to	4				
34.44	9	10	.34	4½	4½				

TABLE 1.—*Arc and spark spectra of hafnium*—Continued

λ I. A.	Intensity		λ Hansen and Werner	Intensity		Notes			
	Arc	Spark		Arc	Spark				
38.32	1	2							
43.40	1	--							
45.36	4	3	.32	4	3				
47	--	--	.34	2	1				
48.94	8	1							
62.37	5	1							
65.35	2d	--	.30	2	2				
69	--	--	.26	2	1				
69.87	1	--							
75.25	25	3	.22	6	5				
76	--	--	.94	2	2				
84.75	1	2	.68	2	2				
92.36	2d	--	.28	3	2				
4999.68	5	5	.61 (Ti)	5	4				
5000.54	2	--	.58	2	2				
03.39	1d	--							
05.12	1	--							
12.19	1	--							
18.20	20	2	.14	6	4½				
21.11	4	--	.09	3	2				
21.75	4	--							
23.07	4	--							
25.91	2	--	.80	2	2				
34.33	2	4							
34.90	3	--							
37.33	1	--	.32	2	1d				
37.78	1	--							
40.21	1	--							
40.82	15	30	.79	6	6				
45	--	--	.28	1	1				
47.45	15	5	.43	5	4				
51.32	3	--	.31	2	1				
57.93	2	6							
58.16	2	5	.09	3	2				
60.58	1	--							
63	--	--	.12	1	--				
69.80	2	--							
71.21	2	6	.18	2	1				
72.29	1	--							
74.71	20nl	--	.71 B. H.	3	3				
75.91	4	10	.90	2	2	.96	Cb	4	
79.63	8	30	.57 B. H.?	3	3d				
80.44	1	6							
90	--	--	.86	2					
93.88	5	--	.84 B. H.	4	2				
5098	--	--	.20 B. H.?	1					
5100.67	3	--	.68	2					
01.68	2	--	.64	2					
06.	--	--	.55	2					
09.66	2	--							
10.58	--	5							
11.33	1p?	--	.28	1					
12.13	6	1							
13.57	4	--							
14	--	--	.36	1		.37	Pd	8	--
18.46	2	--							
19.78	1p?	--							
28.52	4	12	.50	4	2d				
28.93	--	1							
31	--	--	.56	1d					
33.87	2p?	--							
36.19	1	--							
47.57	1	--							
53.12	3	--	.16	2	1				
54.64	2d	--							

TABLE 1.—*Arc and spark spectra of hafnium*—Continued

λ I. A.	Intensity		λ Hansen and Werner	Intensity		Notes
	Arc	Spark		Arc	Spark	
56.05	--	4				
57.96	12	10				
61.57	1	--				
62.06	1	--				
64.43	4c	--				
64.55	1	6				
66.38	2	--				
67.42	3	--				.44 Cb 1
70.18	10	5	.23	4½	2	
73.16	1	--				.15 Mo 9 2
76.09	1p?	--	.17	1		
81.86	25	10	.93	6	3	
82.87	1c	--				
84.29	2	--				
86.84	4	--				
87.73	4	15	.76	4	2	
94.55	1	3	.57	2		
5199.54	1	--				
5200.87	2	--				
05.10	1	--				
08	--	--	.86	3		.90 Pd 10
22.46	1	--				
35.12	2	--				
40.40	1	--				
43.99	15	2	.97	5½	2	
44.68	2	--	.60	3		
47.10	6	?	.07	4	2	
47.14	?	30				
54.49	2	--	.38	2d		
55.44	1	--				
58.75	2	--	.75	2		
60.43	4	15	.41	4	2	
64.95	6	20	.92	4½	3	
69.92	1	--				
75.04	7	1	.05	4	1	.02 Ta 5
76.36	--	1				
84.60	1	--	.63	1		
86.09	4	--	.10	3		
89.96	--	5	.94	1		
90.23	1	--				
90.80	2	--	.79	1		
92.78	2	--	.77	2d		
94.87	12	2				
98.06	10	30	.05	6	3	
5299.84	2	6	.86	2d		
5304.19	2	--	.18	2		
07.82	4	--	.83 (Zr)	3		
09.68	6	1	.67 (Zr)	4	1	
11.60	10	25	.55	6	4	
24.25	3	6	.29 (Fe)	4	2	
46.29	3	15	.31	3	2	
48.39	2	5	.45	3	1	
54.73	12	2	.75	6	2	
58.33	2	--	.35	2		
60.75	2h	--				
61.33	--	1e	.42	1		
68.50	1	--	.56	1		
71.12	2	--	.03	1d		
71.78	1	2				
73.86	15	3	.89	6	3	
83.04	3	--	.07	2		
89.33	6	1	.40	4½	1	
91.35	2	5	.33	2d	1	
94.89	2	--				
5398.64	1	--	.71	1d		

TABLE 1.—*Arc and spark spectra of hafnium*—Continued

λ I. A.	Intensity		λ Hansen and Werner	Intensity		Notes
	Arc	Spark		Arc	Spark	
5402.50	3	--				.53 Ta 5 3
04.47	4	--	.47	4	1	
11.25	1	--				
24.00	3	--	3.99 (Fe)	3	1	
28.30	1	--				
30.05	--	2e				
35.78	3	--	.79	2		
38.74	5	--	.78	4½	2	
44.06	3	10	.05	4	2	
52.92	8	2	.90	5½	2	
63.36	?	10?	.33	6	3	
93.22	--	3e				
5497.30	3	--	.26	3	1	
5503.28	1	--	.18	1		
10.12	3	--	.12	3		
10.44	3	--	.42	3	2	
15.00	--	1e				
17.33	1	--				
18.47	1	--				
20.00	1	--				
22.55	1	--				
24.35	5	15	.39	4	3	
24.96	1	--	.92	1		(.93 Co 7)
30.29	2	--	.30	2		
38.02	4	1	.09	4d	1	
38.26	3	--				
38.59	2	--				
41.91	1	1	.95	1		
47.83	--	1e				
50.60	30	5	.60	6	4	
52.12	40	5	.12	6	4	
75.86	6	5	.87	4½	2	
5590.70	--	1e	.75	2	1	(.73 Co 8 1)
5600.77	2	--	.82	2		
13.27	10	3	.31	5½	3	
14.01	3	--	3.99	3		
28.27	2	--	.21	2		.24 Cb 3
31.34	--	2e				
33.48	1	--				
36.61	--	1e				
44.69	1	--	.52	1		(.69 Y 4 1)
50.83	3	--	.74	3	1	
54.64	4	--	.56	3	1	
60.40	--	1e				
62.08	2	--	.08 (Ti)	2		
63.01	1	--	2.97	1		
64.33	--	1e				
68.72	1	1				
73.58	1	5	.60	1	1	
89.77	--	1e				
5698.04	10nl	--	.10 B. H.	4	2	
5702.09	1	--				
13.28	4	1	.28	4	2	
19.18	40	10	.22	6	4	
20.14	3nl	--	.14 B. H.	3		
34.54	3	--	.61	3	1	
42.52	2	--	.65	1d	1	
48.72	4	1	.73	3	2	
52.53	--	2e				
56.78	1p?	--				
61.14	1p?	--				
62.02	1p?	--				
65.38	2	--	.33	2d	2d	
65.57	1p?	--				
65.99	2	--	.98	2		

TABLE 1.—*Arc and spark spectra of hafnium*—Continued

λ I. A.	Intensity		λ Hansen and Werner	Intensity		Notes
	Arc	Spark		Arc	Spark	
67.19	3	10	.18	3	2	
88.08	2	--	.13	1		
96	--	--	.28	1		
5799.78	2	--	.72	1		
5801.71	2	4				
02.90	1	--				
07.17	1	--	.19	1		(.18 V 5 2)
08.42	2	--	.39	1		
09.51	3	5	.52	3		
11.26	1	--	.26	1		
17.47	3	--	.45	2	1	
38.87	2	--	.89	2		
42.23	5	15	.24	4½	1	
45.87	4	--	.88	3		
47.77	3	--	.76	2		
49.70	3	--				(.73 Mo 8 5)
58.35	2	--				
83.66	3	--	.66	3	1	
86.32	1	--	.30	1		
87.44	1	--				
90.45	8	--	.50	4		
96.61	2	--				
5898.24	--	1c				
5902.94	15	3	.93	6	3	
26.47	2	--	.52	2		
33.69	6	1	.74	4	3	
38.12	1	--				
69.40	1	2				
74.28	10	2	.31	4½	3	
74.72	2	--				
78.66	6	1	.67 (Ti)	4	2	
86.62	1	--	.49	1d	1d	.62 Cb 2
92.96	2	--	.99	2	1	
5994.59	1	--				
6016.79	4	1	.78 (Mn)	3	2	
21.14	3nl	--				
27.57	2	5				
31.94	[1] a. c.	a. e.				
	--	2				
41.46	--	3				
43.19	2c	--	.22	3d	1	
48.00	--	3				
54.17	2	--	.09	2d	1	
93.15	--	2				(.14 Co 6 2)
97.47	--	2				
6098.67	5	1	.67	4½	2	.70 Ti 5 3
6118.16	2	--	.20	2	1	
35.10	1	5	.13	1		
56.28	--	2d?				
58.74	--	2				
60.70	--	2				.7 L — 1
85.13	5	6	.13	5		
6192.50	1	2	.46	1		
6202.85	--	1	.78	1		
06.96	--	2				
09.42	1	1?	.45	2		
10.70	3	4	.72	3		
11	--	--	.92	1		
16.82	1	3	.78	3		
22.80	1	4				
29.65	--	2				

[1] a. c.=arc center; a. e.=arc electrode.

TABLE 1.—*Arc and spark spectra of hafnium*—Continued

λ I. A.	Intensity		λ Hansen and Werner	Intensity		Notes
	Arc	Spark		Arc	Spark	
30.84	2	15				
38.58	3	4	.49	3		
48.96	5	20	.90	4		
57.00	2	6				
58.81	2	4				
71.09	--	3				
79.85	2	15				
91.48	1	2d?				
6299.54	2	5				
6306.19	1	5				
08.67	1	2				
10.75	1	2				
11.85	3	6	.76	2		
13.46	2	3				
15.94	1	5				
18.33	3	5	.36	1		
28.86	1	2				
34.55	1	2				
37.76	--	1				
38.10	4	7	.14	3		
40.71	1	2				
43.76	--	4				
47.62	1	2				
49.86	1	1				
57.36	1	2				
59.83	1	2				
74.60	1	2				
76.20	1	3				
80.19	3	6				
83.75	1	2				
86.23	15	20	.34	5		
88.20	1	2				
88.91	1	2				
90.30	1	2				
6391.00	1	2				
6409.52	3	5	.54	2		
29.49	1	2				
31	--	--	.8	2		
44.98	1	2				
48.43	1	2				
49	--	--	.9	2		.81 Ca 5 3
55.87	1	4				
56.97	4	8	7.0	2		
62.31	1	4				
71	--	--	.5	1		.68 Ca 5 5
73.92	2	6				
78	--	--	.7	1		
82.57	1	2				
86	--	--	.5	2		
6494.60	1	3				
6511.63	--	4				
12.63	--	6				
23.94	1	2				
26.22	1	4				
31.68	1	5				
36.56	1	2				
37.06	1	2				
41.01	1	2	.2	1		
42.81	1	6				
46.02	1	2				
48.25	1	3				
50.02	1	3				
52.92	1	2				
55.98	1	2				
56.50	4	8	.6	2		

TABLE 1.—*Arc and spark spectra of hafnium*—Continued

λ I. A.	Intensity		λ Hansen and Werner	Intensity		Notes
	Arc	Spark		Arc	Spark	
57.00	1	1				
57.93	3	15	8.0	3		
65.77	--	3				
67.41	2	12	.5	2		
81.15	1	1				
84.55	2	10	.6	1		
87.23	5	10	.2	4		
6590.77	--	2				
6605.91	--	1				
09.22	--	4				
16.14	1	2				
24	--	--	.4	2		
28	--	--	.1	1d		
31	--	--	.5	1d		
35.38	1	2				
44.60	10	40	.6	6		
47.05	5	20	.0	4		
56	--	--	.7	2d		
59.40	1	3	.5	2d		
60.84	2h	10hAg?				
65.08	--	1				
69.31	1	2				
71.29	1	2				
84.48	--	1				
91	--	--	.0	2		
91.67	1	2				
6693.49	--	1				
6708.33	--	2				
09.41	1	6				
13.48	4	8	.5	4		
16.00	1	3				
34	--	--	.7	2		
47	--	--	.6	3		
54.62	5	15	.6	5		
69.95	2	4				
73.07	1	3				
6789.27	10	20	.3	6		
6803	--	--	.0	1		
18.94	20	40	9.0	6		
26.56	2	5	.6	3		
33.77	1	2				
36	--	--	.4	1		
50.07	1	4	49.9	1		
55.29	1	4				
57.00	1	2				
58.70	3	15	.6	3		
6874.95	1	2d				
6906	--	--	.3	1		
11.40	3	10	.3	3		
26.19	1	3				
35.17	1	3	.2	1		
37	--	--	.1	1		
65.80	1	3				.85 L 1
70.44	--	2				
76.18	--	1				
79.59	1	4	.6	2		
80.90	3	25	.8	4		
81.60	1	2				
6997.81	--	3				
7010.68	--	2				
16.99	--	2				
19.25	--	2				
21.21	--	3				
30.32	2	10	.3	2		
35.13	1	2				

TABLE 1.—*Arc and spark spectra of hafnium*—Continued

λ I. A.	Intensity		λ Hansen and Werner	Intensity		Notes
	Arc	Spark		Arc	Spark	
52.62	--	1				
54.06	--	2				(.05 Co 8 ...)
61.88	--	2				
62.87	1	3				
63.83	8	20	.7	5		
7094.40	1	3				
7100.54	1	3				
15.65	--	1				
19.52	3	10	.5	2		
31.81	30	50	.8	6		
7164.54	--	2				
7237.10	20	40	.2	5		
40.87	15	30	.9	5		
62.62	1					
77.68	2	3				
7278.76	--	1				
7320.05	3	5				
21.76	1	2				
28.61	1	2				
46.82	3?	--				
56.10	2					
65.28	2					
90.70	1	2				
7398.99	--	1				
7409.38	1h					.35 Ni 9
23.69	1	3				
37.56	1	4				
42.33	1	3				
63.86	2					
7484.56	1					
7556.37	2					
62.93	8					
64.22	2					
76.95	2					
7592.96	2					
7605.78	1					
08.59	2					
24.40	30					
7645.64	2					
7708.36	2					
40.17	10					
43.58	1					
57.87	1					.8 Rb 6
7790.90	5					.91 Mn 2
7814.55	3					
7845.35	20					
7920.71	8					
38.06	2					
71.56	1					
76.84	1					
86.91	1					
7994.73	20					
8010.58	2					
46.03	3					
56.52	4					
59.10	3					
8080.32	4					
8143.60	1					
73.89	5					
74.89	1					
93.74	1					
8194.78	8					
8204.58	20					
16.32	3					
36.15	2					

TABLE 1.—*Arc and spark spectra of halfnium*—Continued

λ I. A.	Intensity		λ Hansen and Werner	Intensity		Notes
	Arc	Spark		Arc	Spark	
44.37	1					
48.81	3					
8276.95	20					
8338.12	2					
44.25	8					
61.78	4					
82.98	2					
84.94	1					
8399.97	1					
8451.73	1					
54.11	1					
60.01	10					
75.35	1					
8497.49	1					
8508.11	1					
46.48	20					
69.0	3d					
84.12	5h					
8592.23	1					
8603.24	2					
29.43	1					
40.06	15					
58.41	1d					
61.88	2					
8673.90	1					
8711.24	7					
8715.62	2					
8825.30	1					
8836.16	3					
9004.73	3					
9182.07	2					
9193.23	1					
9250.27	3					

[18] Hansen and Werner, see reference 4. Hevesy, see reference 5.

[19] Exner and Haschek, Die Spektren der Elemente bei Normalen Druck, **II**, p. 341; 1911; and **III**, p. 334; 1912.

[20] Kiess, B. S. Sci. Papers (548), **22**, p. 47; 1927; and unpublished data.

[21] Bachem, Diss. Bonn; 1910.

[22] Vahle, Zeitschr. Wiss. Phot., **18**, p. 84; 1918.

IV. DISCUSSION

1. COMPARISON WITH ZIRCONIUM SPECTRA

The statement has frequently been made that all zirconium minerals contain appreciable amounts of hafnium and that consequently all the samples of zirconium salts and metals which have been used heretofore for the description of zirconium spectra contained hafnium as an unrecognized impurity.[18] The truth of this statement is attested by Table 2 in which faint lines observed in zirconium spectra by various observers are identified with the stronger lines of hafnium as determined in the present investigation. Comparison is made with the measurements of zirconium spectra by Exner and Haschek,[19] by Kiess,[20] by Bachem,[21] and by Vahle.[22] In addition to proving that strong hafnium lines have been observed

faintly in zirconium spectra this comparison supports, in general, my differentiation of arc and spark lines, and gives furthermore an indication of the accuracy of my wave-length values.

Practically all of the stronger lines of hafnium not obscured by true zirconium lines are to be found in the zirconium lists of Exner and Haschek, and, in general, my spark lines appear most prominently in their spark spectrum table, while my arc lines have a tendency to show only in their arc spectrum table, except in the region of wave lengths greater than 3400 A where it appears that their arc exposures were relatively much weaker than their spark exposures.

Kiess, before publishing, compared his zirconium measurements with Hansen and Werner's hafnium list and with a portion of mine which was completed a year ago, and was thus able to remove most of the hafnium lines as impurities. The data presented in Table 2 are mainly from his unexpurgated lists which cover 2200 A to 6100 A in the spark and 4900 A to 9300 A in the arc spectrum.

Bachem and Vahle each measured the arc spectrum of zirconium with a large concave diffraction grating and each strove to obtain values so that the probable errors would be less than 0.01 A. As mentioned above, the values by Bachem in certain spectral regions have errors of scale several times this amount, and the values in Table 2 have, therefore, been corrected to the scale of Vahle's observations. The agreement between these accurately measured faint lines in their zirconium spectra and the stronger lines in my hafnium list is remarkably good. The difference for 20 lines is 0.00 A, for 16 lines it is ±0.01 A, for 4 lines ±0.02 A, and for one line 0.03 A.

The + sign after an Exner and Haschek intensity number means "not sharp"; the notation s after Vahle's intensity number signifies "weak," and ss, "very weak."

TABLE 2.—*Hafnium lines observed in zirconium spectra*

Meggers			Exner and Haschek			Kiess			Bachem		Vahle	
	Intensity			Intensity			Intensity					
λ	Arc	Spark	λ	Arc	Spark	λ	Arc	Spark	λ	arc	λ	arc
2277.15	10	10	.19	--	1	.17		2	.165	1		
2310.21	--	10	--	--	--	.23		1				
13.42	1	30	.45	--	1	--		--				
19.06	1	8	--	--	--	.06		1				
22.46	10	15	.50	--	2	.47		2	.461	1		
36.47	1	50	.50	--	1+	.50		3				
47.45	8	25	.42	--	1	.45		1				
51.22	10	30	.20	--	1	.21		2				
55.49	--	20		--	--	.50		1				
77.57	--	20		--	--	.61		1				
80.29	5	10	.3	--	1+	.31		1				
83.55	1	30	.54	--	1	.56		2				
93.36	5	10	.3	--	1+			--				
2393.83	10	20	.82	--	1			--	.824	1		
2405.43	10	25	.43	--	1			--				

TABLE 2.—*Hafnium lines observed in zirconium spectra*

Meggers			Exner and Haschek			Kiess			Bachem		Vahle	
λ	Intensity		λ	Intensity		λ	Intensity		λ	arc	λ	arc
	Arc	Spark		Arc	Spark		Arc	Spark				
10.13	8	15	.13	--	1	.14		1				
17.69	8	15	.70	--	1	.68		1				
33.56	5	15	.55	--	1	.56		1				
47.25	10	20	.22	--	1	.24		1				
60.50	15	40	.53	--	1	.47		1				
64.19	20	75	.22	--	1	.15		1				
69.18	8	20	.22	--	1+			--				
2495.17	1	80		--	--	.12		1				
2512.68	15	30	.72	--	1	.65		1				
13.02	25	50	.06	--	1	.01		1				
15.16	--	30		--	--	.14		1				
16.88	25	100	.91	--	1	.86		1	.866	1		
31.20	10	25		--	--	.20		1				
51.40	10	50	.41	--	1	.39		1				
73.92	8	40	.94	--	1			--				
76.84	7	20		--	--	.84		1				
2582.51	5	15		--	--	.51		1				
2606.38	8	20	.34	--	1	.38		1				
07.04	10	30	6.99	--	1			--				
13.61	7	20	.61	--	1			--				
22.75	5	20	.76	--	1	.75		1				
38.72	10	30	.68	--	1	.70		1	.720	1	.718	1ss
41.42	10	50	.38	--	2	.40		2	.408	1		
47.31	8	30	.24	--	2	.29		1	.284	1		
61.89	4	12	.88	--	1	.95		1				
65.98	2	6		--	--	6.01		1				
2683.36	5	20	.36	--	1	.36		1				
2738.76	10	25	.74	--	1	.76		1	.759	1		
73.37	20	50	.37	--	1	.35		3	.362	1	.360	1s
89.51	1	8		--	--	.47		1				
2789.74	4	20	.75	--	1	.73		1				
2814.47	3	10		--	--	.45		1				
20.23	20	50	.22	1	1	.22		2			.232	1ss
22.67	10	25	.68	--	1			--				
49.21	5	25	.19	--	1+	.17		1				
61.01	10	20	.0	--	1+			--	.013	1		
61.69	15	30	.72	1	1	.68		2	.700	1	.707	1s
66.38	20	3	.39	1	--			--	.378	1	.378	1s
76.33	4	20		--	--	.30		1				
98.26	25	3	.29	1	--			--			.259	1
2898.71	3	12	.74	--	1	.72		4ZrII	.712	2	.715	2
2904.42	20	3	.43	1	--			--	.409	1	.419	1
04.76	20	2	.79	1	--			--	.754	1	.762	1ss
16.49	30	5	.49	1	--			--	.479	1	.488	1
19.59	10	20		--	--	.56		1				
29.63	10	10	.59	1	--			--	.630	1	.617	1ss
29.90	8	1		--	--			--			.923	1s
37.80	10	30	.77	--	1			--				
40.77	25	4	.74	1	--			--	.755	1	.773	1ss
30.68	20	3	.68	1	--			--	.680	1		
54.21	15	2	.22	1	--			--				
64.88	20	3	.87	1	--			--	.873	1		
75.90	12	30	.88	1	1	.86		1				
2980.82	15	2	.85	1	--			--	.810	1		
3012.90	15	25	.89	1	--	.88		1				
16.78	30d?	2	.78	1+	--			--				
18.32	15	2	.28	1+	--			--				
50.76	10	2	.79	1	--			--				
57.02	20	3	.03	1	--			--				
64.68	2	8	.66	--	1			--				

TABLE 2.—*Hafnium lines observed in zirconium spectra*

Meggers			Exner and Hoschek			Kiess			Bachem		Vahle	
λ	Intensity		λ	Intensity		λ	Intensity		λ	arc	λ	arc
	Arc	Spark		Arc	Spark		Arc	Spark				
3072.88	30	4	.93	1	--			--			.881	1
3101.38	8	15		--	--	.36		1				
09.11	15	40	.14	1	1	.11		1				
34.72	25	40	.72	1	1	.72		1				
76.86	10	20	.87	--	1			--				
3194.20	15	25	.14	--	1	.20		1				
3220.66	3	10	.67	--	1			--				
53.70	15	25	.68	--	1	.68		1				
3255.29	6	8	.3	--	1+			--				
3312.87	15	3	.88	--	1			--				
32.73	20	2	.75	1	1			--				
52.06	10	20	.07	--	1	.02		1				
89.83	10	15	.81	--	1			--				
3399.80	30	40	.80	1	2	.80		2	.776	2		
3472.38	20	2	.38	--	1			--				
3505.23	20	40		--	--			--	.227	1		
35.54	10	20	.52	--	2			--				
36.62	10	1	.6	--	1+			--				
52.70	10	15	.76	--	1			--				
61.65	20	25	.66	--	2	.66		1				
3569.03	20	30	.03	--	1	.05		1				
3616.89	10	2	.87	--	1			--				
44.35	15	20	.39	--	2	.36		1				
65.36	4	10	.36	--	1			--				
75.74	9	2	.75	--	1			--				
3699.73	7	15	.75	--	1			--				
3701.15	8	25	.15	--	2	.15		1				
05.41	3	8	.43	--	1			--				
17.80	15	3	.79	--	1			--				
19.27	15	25	.30	--	1	.28		1				
33.78	10	2	.78	--	1			--				
44.98	3	10	5.01	--	1			--				
62.51	2	20	.55	--	1			--			.511	1s
66.93	4	25		--	--			--			.952	1ss
77.64	30	4	.67	--	1			--				
3793.37	20	20	.38	--	2			--				
3806.07	4	25		--	--	.06		1				
3809.93	12	2	.93	--	1							
3918.10	15	10	.10	--	1							
23.91	6	10	.90	--	2							
31.36	8	2	.40	--	1+							
51.81	15	2	.81	--	1							
64.95	3	7	.92	--	1							
79.40	1	12	.35	--	1+							
84.03	1	4	.00	--	1							
3996.80	1	3	.83	--	1							
4047.96	2	15	8.00	--	1+							
80.44	10	10	.49	--	1							
4093.17	40	25	.17	1	2				.157	1	.162	1ss
4158.90	2	10	.94	--	1							
62.40	4	15	.44	--	1							
74.33	30	3	.40	--	1							
4177.50	3	15	.59	--	1+							
4232.46	6	20	.48	--	1							
49.33	5	9	.39	--	1+							
4272.84	7	15	.91	--	1							
4320.67	6	10	.7	--	1+							
34.64	3	8	.7	--	1+							
36.55	10	40	.70	--	1+							
50.50	8	25	.54	--	1							

TABLE 2.—*Hafnium lines observed in zirconium spectra*—Continued

Meggers			Exner and Haschek			Kiess			Bachem	Vahle
λ	Intensity		λ	Intensity		λ	Intensity		λ arc	λ arc
	Arc	Spark		Arc	Spark		Arc	Spark		
4367.89	8	6	.9	--	1+					
4417.35	8	10	.4	--	2+					
22.75	6	30	.80	--	1					
4438.02	10	2	.04	3	2					
4533.18	12	6	.2	--	1+					
70.70	1	10	.7	--	1+					
4598.86	50	4	.82	1+	--					
4622.71	8	15	.72	--	1					
4640.13	3	4	.13	2	1					
4782.75	40	3	.68	1	--					
4800.50	70	8	.57	1+	--					
7131.81	30					.84	3			
7237.10	20					.08	3			
7240.87	15					.88	3			
7562.93	8					.94	1			
7624.40	30					.48	2			
7740.17	10					.13	2			
7845.35	20					.34	2			
7994.73	20					.75	1			
8460.01	10					.04	1			
8546.48	20					.48	1			

2. COMPARISON WITH SOLAR SPECTRUM

It appears that a considerable number of the stronger lines of hafnium in Table 1 are identifiable with faint Fraunhofer lines in the sun's spectrum. Unfortunately, no comparisons can be made in the region short of 3000 A where many of the strongest hafnium lines occur, and in the spectrum above 3000 A recognition of certain hafnium lines in the sun is prevented by approximate coincidences with strong lines of iron, cobalt, nickel, titanium, chromium, calcium, etc. The best coincidences are displayed in Table 3 in which Rowland's [23] wave lengths of Fraunhofer lines and the corrected international values appear in column 1, Rowland's intensities in column 2, followed by my hafnium wave lengths and intensities in columns 3 and 4. A question mark in the last column indicates that the identification is doubtful, either on account of discordant wave length or intensity. The latter applies especially to arc lines. Since the strongest are not recorded in the sun the coincidence of weaker arc lines with Fraunhofer lines is probably accidental. Coincidences occur, for the most part, only with the faintest lines observable in the solar spectrum, OOO or OOOO on Rowland's scale of intensities. Occasional coincidences with intensity 1 lines are probably accidental or blends. This appearance of hafnium in the solar vapors might have been deduced from the behavior of its chemical analogues, titanium and zirconium. The former is rather conspicuous in the

[23] Rowland, Solar Spectrum Wave Lengths; 1896.

solar spectrum while the latter is much less prominent, and hafnium being still heavier could be expected to be represented only by the faintest lines, if at all. In each case the lines from ionized atoms are stronger on the average than those from neutral atoms.

TABLE 3.—*Identification of hafnium lines in the solar spectrum*

Sun {R I. A.	Intensity	Hf I. A.	Intensity			Sun {R I. A.	Intensity	Hf I. A.	Intensity		
			Arc	Spark					Arc	Spark	
3057.117	OON	3057.02	20	3	?	3733.910	OO	3733.78	10	2	?
.011						.770					
3131.920	OOO	3131.81	12	2	?	3738.026	OO	3737.88	4	10	
.814						7.886					
3134.830	OO	3134.72	25	40		3877.232	OO	3877.11	3	20	
.724						.092					
3159.945	OON	3159.83	10	1	?	3900.797	OOO	3900.66	1	10	
.837						.657					
3176.946	OOO	3176.86	10	20		3924.065	OOO	3923.91	6	10	
.836						3.925					
3193.661	OOON	3193.53	10	15		4080.588	OO	4080.44	10	10	
.543						.433					
3194.346	OO	3194.20	15	25		4083.515	OOO	4083.36	10	2	?
.228						.360					
3253.841	OOOO	3253.70	15	25		4174.479	OO	4174.33	30	3	?
.715						.316					
3255.413	OOO	3255.29	6	8		4206.735	1	4206.57	5	20	?
.287						.575					
3332.850	OOOO	3332.73	20	2	?	4232.618	OO	4232.46	6	20	
.724						.459					
3389.960	OOOO	3389.83	10	15		4336.774	OON	4336.65	10	40	?
.820						.612					
3399.942	ON	3399.80	30	40							
.802						4418.044	OOO	4417.90	8	1	?
						7.883					
3505.371	OOOO	3505.23	20	40		4422.872	OOO	4422.75	6	30	?
.230						.711					
3535.660	OOOO	3535.54	10	20							
.519						4438.192	OO	4438.02	10	2	?
3561.796	OOOO	3561.65	20	25		.029					
.655						4599.618	OOOO	4599.46	2	10	
						.444					
3617.016	OOOON	3616.89	10	2	?						
6.876						4773.900	OOOO	4773.72	10	2	?
3644.455	OOOON	3644.35	15	20	?	.716					
.315						5576.079	OOOO	5575.86	6	5	?
3661.176	OOON	3661.05	3	8		5.862					
.036											
3699.877	OOO	3699.73	7	15							
.737											
3705.561	OON	3705.41	3	10							
.421											
3719.405	OOOO	3719.27	15	25							
.265											

3. PERSISTENT LINES OF HAFNIUM

The preceding identifications of hafnium lines in zirconium spectra, and in the solar spectrum, perhaps, give some indication as to which hafnium lines are sensitive in revealing the element as a spectroscopic impurity. From the above tables a dozen arc lines and the same number of spark lines have been selected as representative of the persistent lines of hafnium. They are collected in Table 4. The *raie ultime* can not be established with certainty, but it appears very probable that 4093.17 A plays this rôle for neutral hafnium

atoms and 2773.37 A for ionized atoms. An attempt to establish the persistent lines of hafnium has been made by Petersen,[24] who examined the arc spectra of zirconium ores and oxides in a limited spectral range (2500 A to 3500 A). He found the lines at 2773.37 A, 2866.38 A, and 2919.59 A to be most persistent, while 2516.88 A, 2887.13 A, 2898.26 A, 2904.42 A, 2964.88 A, and 3194.20 A were slightly less persistent. While some of these lines are true spark lines, others are undoubtedly arc lines. The spark line 2773.37 A was selected as the most persistent. It is of interest to note that the line at 4093.17 A is the only hafnium line identifiable with lines observed 30 years ago in the arc spectrum of zirconium by Rowland and Harrison.[25] They reported a line of intensity 2 at 4093.16 A. The fact that this line is not recorded in the solar spectrum makes the recognition of neutral hafnium in the sun very doubtful.

TABLE 4.—*Persistent lines in hafnium spectra*

λ	Hf I intensity		λ	Hf II intensity	
	Arc	Spark		Arc	Spark
2898.26	25	3	2512.68	15	30
2904.42	20	3	2513.02	25	50
2904.76	20	2	2516.88	25	100
2916.49	30	5	2773.37	20	50
2940.77	25	4	2820.23	20	50
2950.68	20	3	3134.72	25	40
2964.88	20	3	3194.20	15	25
3072.88	30	4	3399.80	30	40
3332.73	20	2	3505.23	20	40
3777.64	30	4	3561.65	20	25
4093.17	40	25	3569.03	20	30
4174.33	30	3	3719.27	15	25

A very excellent method of arriving at the true *raie ultime* of a spectrum is through an analysis of the structure of the spectrum and classification of its lines. No spectral regularities have been announced for hafnium spectra, but such are now being sought in a list of vacuum wave numbers derived from the wave lengths in Table 1.

In conclusion, the author wishes to express his appreciation for the assistance in thousands of wave-length calculations carefully performed by Bourdon Scribner in this laboratory.

WASHINGTON, March 21, 1928.

[24] Petersen, Nature, **119**, p. 352; 1927.
[25] Rowland and Harrison, Astrophys. J., **7**, p. 373; 1898.

TESTS OF THE EFFECT OF BRACKETS IN REINFORCED CONCRETE RIGID FRAMES

By F. E. Richart

ABSTRACT

This paper contains results of analyses and tests of rigid frames of reinforced concrete with and without enlargements (termed "brackets") at the intersection of the horizontal top member with the vertical legs. All the frames tested were of inverted U form hinged at the lower end of the vertical legs. All had a span of 14 feet and a height of 7 feet; the length of the bracket used varied from 0 to 42 inches with different frames. It is shown that the relations between moments and size of brackets, which are determined exactly only by tedious and long-drawn-out computations, may be expressed by a simple empirical equation with an accuracy sufficient for many cases met with in practice. The application of formulas derived for the freely supported frames to the case of inverted U frames with legs fixed at the bottom or of closed frames is also made possible by showing that the vertical distance from the horizontal member to the point of inflection of the leg may be substituted for the total height of the freely supported U frame with nearly correct results. An empirical expression for the moment of inertia for use in determining the distribution of moments (but not for use in computing stress) has been developed which should assist greatly in preliminary or even final design of a frame. Throughout the paper comparisons of the test results with the simplified equation have been shown. In general, it appears that the use of properly designed brackets should result in economy of design.

CONTENTS

	Page
I. Introduction	190
1. Preliminary	190
2. Nature of investigation	191
II. Analytical treatment	191
1. Analysis of the effect of brackets	190
2. Effect of brackets with different loadings	200
3. Effect of brackets in various types of frames	201
III. Test specimens and apparatus	205
1. Description of test specimens	205
2. Materials and making of specimens	209
3. Testing apparatus	211
IV. Test data and discussion of results	213
1. Procedure and phenomena of tests	213
2. Thrusts and moments	216
3. Flexural stresses and deformations	218
4. Shearing stresses	223
5. Moment of inertia	226
6. Deflections	230
7. Conclusions	233
V. Appendix I	236
Test data and sketches of frames	236
VI. Appendix II	251
Supplementary tests of paper models	251

I. INTRODUCTION

1. PRELIMINARY

This paper is based upon the results of one of a number of investigations conducted in 1918 by the concrete ship section of the Emergency Fleet Corporation in developing the design and construction of reinforced concrete ships. The immediate object of the investigation described herein was to determine the effect produced upon the distribution of bending moments in a transverse ship frame by using brackets or haunches at the inside corners of the frame. The results of the investigation have a wider significance, however, as a contribution to present knowledge of the behavior of framed structures under stress, and their principal value doubtless lies in their application to the general field of reinforced concrete construction.

In recent years considerable attention has been paid to methods of analysis of rigidly connected frames, and this theoretical treatment has been supplemented by a comparatively few tests of reinforced concrete bents. However, there is little information available as to the correct analysis of frames with haunches or brackets at the intersections of members and apparently no test data bearing upon this form of construction. A well-known method of analysis has been used here, and although its application requires a number of assumptions it seems to give satisfactory results.

The value of definite knowledge regarding the effect of brackets on stress distribution follows from the fact that through their use the bending moment at any section may be made to vary considerably, and that the material used in brackets is placed where it can resist the increased bending moments which the brackets attract to the corners of the frame. Properly designed brackets will produce a considerable economy of weight.

The tests were made in 1918 at the John Fritz Civil Engineering Laboratory, Lehigh University, as a part of the structural laboratory investigation initiated by R. J. Wig, head of the concrete ship section, Emergency Fleet Corporation. This work was under the direction of W. A. Slater, engineer physicist of the National Bureau of Standards, to whom acknowledgment is made for his hearty support and generous assistance throughout the investigation and the preparation of this paper. Acknowledgments for assistance in the planning and performance of the tests are also due to G. A. Maney, designing engineer in the concrete ship section, and to Maj. W. M. Wilson and Maj. A. R. Lord, successively in charge of the laboratory for the Emergency Fleet Corporation. R. L. Brown, of the Engineering Experiment Station, University of Illinois, assisted in the supplementary tests of paper models described in Appendix II.

2. NATURE OF INVESTIGATION

An important use of brackets in ship construction is at the corners of transverse frames. Since a sharp corner at the intersection of horizontal and vertical members produces a section of highly concentrated fiber stress combined with a large negative bending moment, a bracket is used primarily to reduce the compressive stress at this place. In addition, since, in all types of statically indeterminate frames, the distribution of bending moments depends upon the relative stiffness of the members or parts of which the structure is composed, the bracket produces two other effects—(1) it affects the distribution of moments throughout the frame because of the local variation in stiffness that it produces, and (2) it affects the magnitude of the negative moment as well as the distribution of moments because it changes the shape of the axis of the members at the corners of the frame. The effect of this change in shape is sometimes regarded as a shortening of the span of the members in which the brackets are used.

In choosing the type of specimen for these tests the object was to secure a frame similar in form and loading to a ship frame and of fairly large size. A rectangular two-legged bent was chosen as approximating, in the inverted position, the lower part of a transverse ship frame. The columns were made hinged at the base in order to simplify the interpretation of the results. The brackets used were similar to those used in ship design.

In testing, all specimens were loaded to failure and observations of deformation and deflection were made at regular increments of load. The experimental data have been compared with analytical deductions. and, in general, a satisfactory agreement has been found.

II. ANALYTICAL TREATMENT

1. ANALYSIS OF THE EFFECT OF BRACKETS

Mathematical analyses of rigidly connected frames are usually based upon the assumption that the members of the frame are uniform in section throughout their length, and there is little information on the proper way of analyzing frames in which abrupt changes in cross section occur. However, in the analysis which follows, it was considered sufficiently accurate for frames containing brackets to sketch in the approximate axis of the frame (a line midway between the tension and compression faces) and to consider as fully effective the depth of the cross section measured normal to this axis. A semigraphical method often used in arch analysis was then applied to the frame.

In the analysis of the two-hinged frame of Figure 1, which shows one of the types tested, the outline of the frame was first drawn to

scale and the axis divided into a number of sections approximately equal in length. The length of a section was denoted by ds, the depth of cross section by d, and the vertical distance of the centroid of the section above the hinges by y. Values of ds, d, and y were scaled from the drawing where necessary for each section of the frame. Values of d were used to calculate the moment of inertia, I, which, for reasons to be discussed in Section IV, was considered to vary as $d^{5/2}$. Letting M represent the bending moment at the centroid of a section due to vertical loads and reactions only, the following general formula [1] for the horizontal reaction of a two-hinged

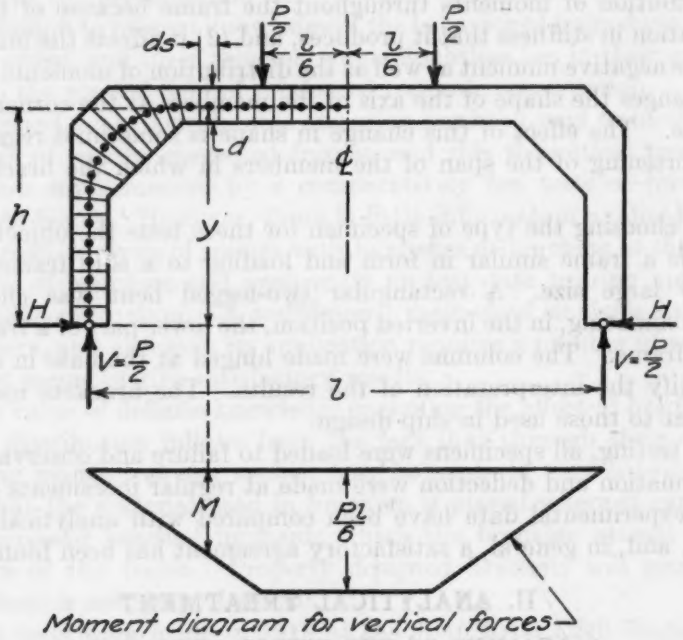

FIG. 1.—*Outline drawing used in analysis of frame*

arch was applied:

$$H=\frac{\Sigma My\frac{ds}{I}}{\Sigma y^2\frac{ds}{I}} \tag{1}$$

From the conditions for static equilibrium of the frame the value of the moment at mid span M_c for one-third-point loading was found to be

$$M_c=\frac{Pl}{6}-Hh \tag{2}$$

[1] For derivation of this formula see Johnson, Bryan, and Turneaure, "Modern Framed Structures," Pt. II, pp. 138 and 158. In this derivation the effect of deformations due to internal shearing and direct stresses are neglected. While these effects are usually negligible, they may be included in equation (1) by measuring y to a point other than the centroid of each section. Such points may be determined by use of the theory of the ellipse of elasticity.

Substituting values of H from equation (1) in equation (2), values of M_c were obtained and for convenience have been expressed in terms of the maximum moment, $\frac{Pl}{6}$, for a simple beam loaded as the top member was loaded. The latter quantity was used for the reason that it simplifies the application of values of M_c to designing.

To illustrate the relations expressed by equation (2), let it be assumed that the value of M_c is known for the rectangular frame of Figure 2 (*a*). Since the horizontal member is a straight beam, the numerical sum of the maximum negative and maximum positive moments is equal to $\frac{Pl}{6}$, and the trapezoid $ABCD$ represents the moment diagram for a single beam. Hence, laying off M_c fixes the

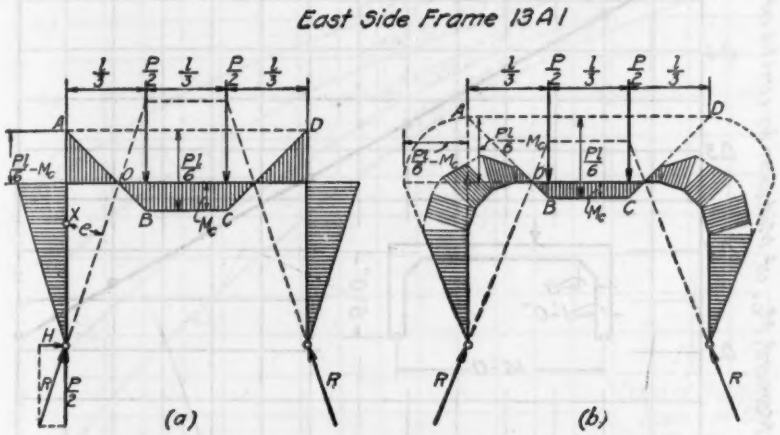

FIG. 2.—*Relations between moments and reactions in frames*

value of the negative moments at the corners, and the entire moment diagram for the frame is easily drawn. It is further evident that if R is the resultant of the horizontal and vertical reactions at the base, the moment about any point, x, lying in the axis of the frame and to the left of B is Re. This relation is particularly useful in treating a frame having brackets in which the axes of the horizontal and vertical members do not meet at right angles, as in Figure 2 (*b*). Here the top member is not straight and the numerical sum of the maximum positive and the maximum negative moments is not equal to $\frac{Pl}{6}$. However, if the simple beam moment diagram $ABCD$ and the known moment M_c be laid off, the moment diagram for the horizontal and vertical portions of the frame will be determined, and the point of inflection, O, will be located as shown in Figure 2 (*b*).

Figure 3 shows the results of analyses made by use of equation (1) for the purpose of designing test specimens. Values of the bending

moment at mid span are plotted as ordinates against horizontal lengths of brackets as abscissas. All the brackets were assumed in the computations to make an angle of 45° with the horizontal. The points representing the calculated moments are seen to lie nearly on a straight line. The variation in moment at mid span is due almost entirely to the variation in stiffness produced by varying the length of the bracket. It is rather surprising, however, that the moment should vary so nearly as a linear function of the bracket length, and hence of the clear span for these particular frames. From the difficulty of analyzing such a frame a straight-line relation would not be expected to obtain, and it is evident that the line does

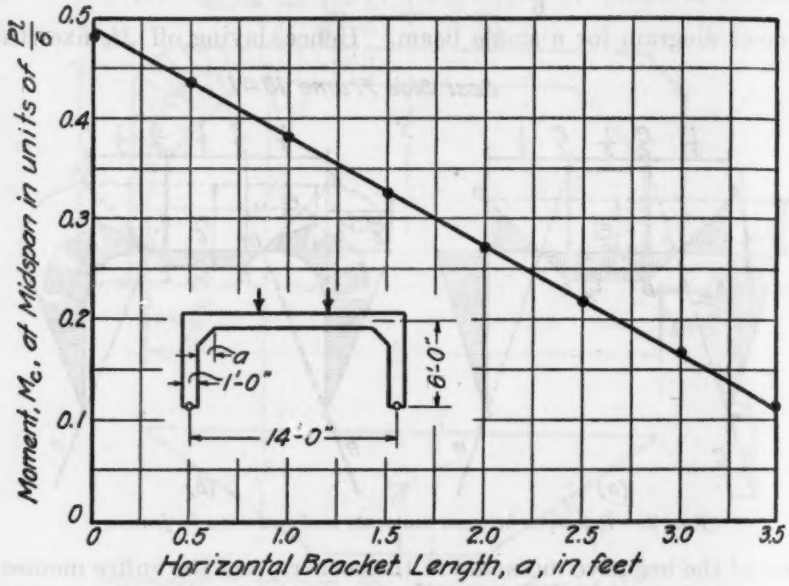

FIG. 3.—*Relations between calculated moments and size of brackets*

not apply exactly at the two extremities of the diagram where the bracket is either very small or very large.

To determine whether similar curves may be drawn for frames of other proportions, further calculations have been made. Figure 4 indicates the relative effectiveness of brackets when used in frames having different ratios of height to span. It is seen that the use of a given bracket has the greatest effect in changing the value of the moment at mid span when the ratio of height to span of the frame is small. This is apparently due to the fact that as the ratio of height to span decreases the bracket occupies a larger portion of the region of high negative moment. The principle involved here is sufficiently important to warrant further elaboration. For illustration, if in any frame the moment of inertia for a short portion of length be varied, there will result a change in the bending moment at all points in the

frame. This change will be approximately proportional to the original bending moment at the section where the variation in moment of inertia is introduced. It will be seen, therefore, that an increase in the moment of inertia, such as that produced by a bracket or haunch, will be most effective if made where the original bending moment is largest. Referring again to Figure 4, when the ratio of height to span is 1.0, the negative moment at the corner of a frame without brackets is $0.40\frac{Pl}{6}$, and a 24-inch bracket reduces the moment at mid span only 20 per cent. On the other hand, when the

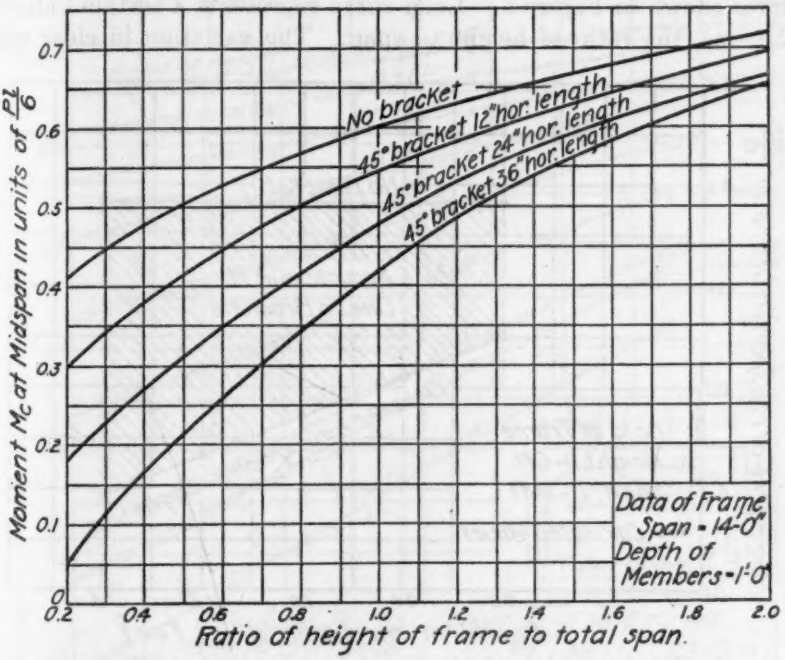

FIG. 4.—*Calculated effect of bracket with varying proportions of frame*

ratio of height to span is 0.3, the negative moment at the corner of the frame without brackets is $0.56\frac{Pl}{6}$, and the 24-inch bracket reduces the moment at mid span by 51 per cent. Hence, for brackets to be most effective both in changing moment distribution and in reducing stresses[2] they must be used at points of high bending moments.

Another series of calculations was made to investigate the effect of slenderness of members on the effectiveness of haunches. For two frames which are alike, except that one had depths of members

[2] Wherever in this paper the word "stress" is used it designates the internal force per unit of area. This usage is consistent with the recommendations of Committee E-1 of the American Society for Testing Materials. See Proceedings A. S. T. M., **23**, Pt. I, p. 937; 1923; also **25**, Pt. I, p. 879; 1925.

and lengths of brackets greater than the other by a fixed percentage, Figure 5 shows that the effectiveness of the brackets in reducing the moment at mid span is less with the smaller than with the greater depth of member. This might be expected because the lighter frame is stiffened along a smaller portion of its length than the heavier one, and because the axis of the lighter frame at the corner lies farther from the resultant reaction than that of the heavier one. The information of Figures 4 and 5 has been replotted, using values of the moment at mid span, M_c, as ordinates and the ratio of the clear span to the total span, s/l $(=m)$, as abscissas, producing the curves shown in Figure 6. Each curve represents a certain value of h/l $(=n)$, the ratio of height to span. The variation in clear span

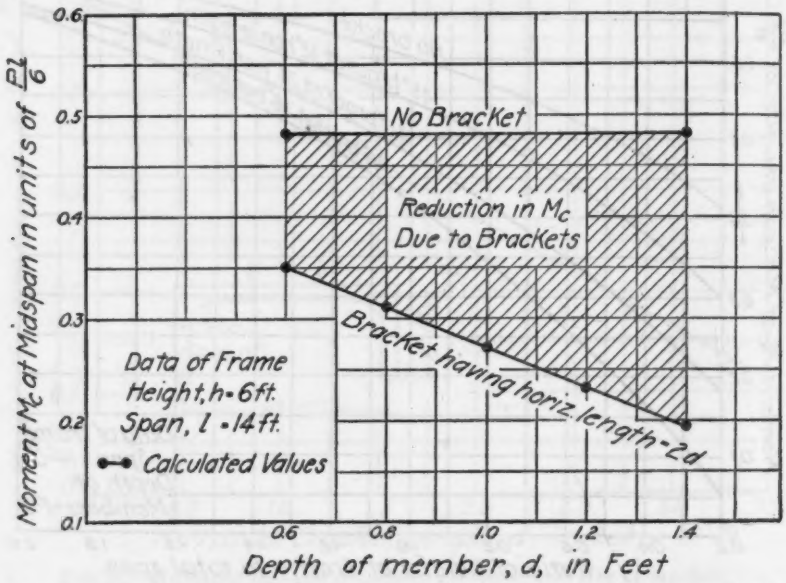

FIG. 5.—*Relation between slenderness of frame and calculated reduction in moment due to bracket*

indicated in this diagram is obtained by varying both the size of the brackets and the slenderness of the members of the frame.

Figure 6 indicates that the moment at mid span varies very nearly as a linear function of the clear span, or distance between bracket edges, for frames of the proportions shown. That is, just as in the case of the curve of Figure 3, here a series of straight lines seem to fit the several groups of calculated points fairly well, the divergence from the linear relation being shown mainly at the extremities of the lines by the dotted curves. The solid straight line represents the range of values ordinarily encountered in the use of brackets; with brackets so small that the ratio s/l becomes 0.9 or more further analysis and supporting test data are needed to determine the exact effect upon the moment distribution.

It is significant that for the ratios of depth to span of members to be found in practice the moment M_c is not greatly affected by a variation in slenderness of members as long as the clear span is not changed. This indicates that the clear span is the variable of major importance. The effect of a variation in slenderness is still less with higher values of n than that shown with values of n equal to 0.25 and 3/7.

It is thought that an equation representing the curves of Figure 6 may be found useful. Such an equation must naturally reduce to

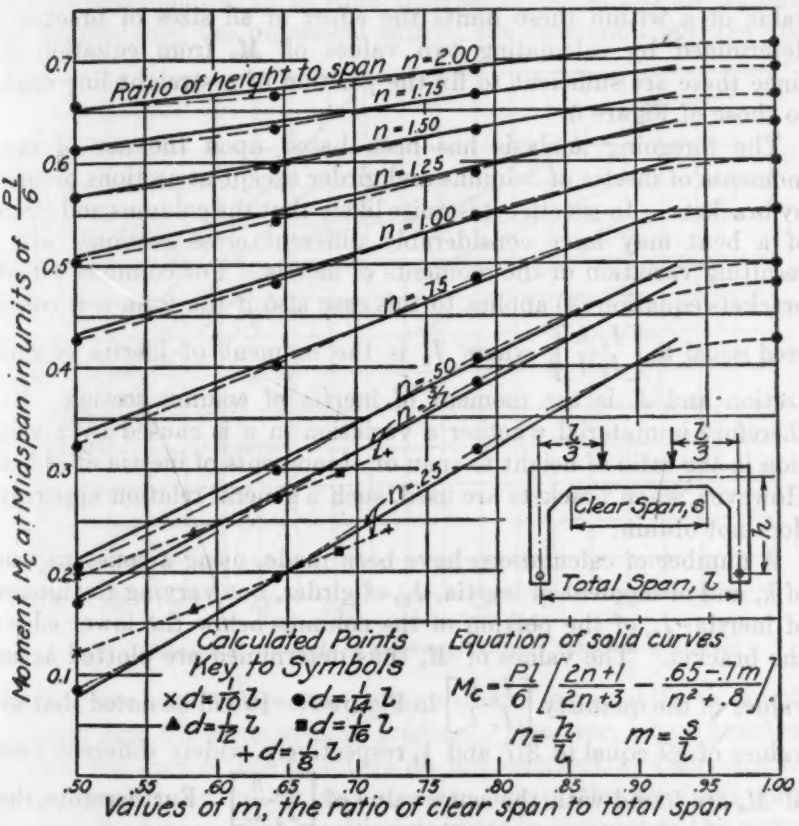

FIG. 6.—*Effect of length of clear span upon moment at mid span*

the ordinary equation for rectangular frames when no brackets are used. If n represents the ratio h/l, the moment at mid span, due to a total load P applied in equal parts at the one-third points of the span of a frame without brackets, is expressed by the equation [3]

$$M_c = \frac{Pl}{6}\left[\frac{2n+1}{2n+3}\right] \qquad (3)$$

[3] For demonstration leading to this equation see Bull. 108, Eng. Expt. Sta., University of Illinois, p. 58; 1918.

For frames with brackets [4] it is found that letting $m=s/l$, the ratio of clear span to total span, the straight portions of the curves of Figure 6 may all be expressed by the equation

$$M_c=\frac{Pl}{6}\left[\frac{2n+1}{2n+3}-\frac{0.65-0.7m}{n^2+0.8}\right] \quad (4)$$

This is an empirical equation fitted to the results of semigraphical analyses and hence has a theoretical basis. Its use, however, should be limited to values of m between 0.5 and 0.93 and to values of n between 0.3 and 2.0. It may be noted that for any particular value of n within these limits the effect of all sizes of brackets is determined by calculating two values of M_c from equation (4), since these are sufficient to fix the position of a straight line similar to those of Figure 6.

The foregoing analysis has been based upon the use of equal moments of inertia of columns and girder except at sections occupied by brackets. In practice it is quite likely that the columns and girders of a bent may have considerably different cross sections, with a resulting variation in the moments of inertia. For columns without brackets equation (3) applies to this case also if the term n is considered equal to $\left[\frac{I_g}{I_c}\cdot\frac{h}{l}\right]$, where I_g is the moment of inertia of girder section and I_c is the moment of inertia of column section. It is therefore immaterial whether a variation in n is caused by a variation in the ratio of height to span or of moments of inertia or of both. However, when brackets are used, such a general relation apparently does not obtain.

A number of calculations have been made, using a constant value of h, and of moment of inertia, I_g, of girder, but varying the moment of inertia, I_c, of the portion of the columns below the lower edge of the bracket. The values of M_c thus determined are plotted against values of the quantity $\left[\frac{I_g}{I_c}\cdot\frac{h}{l}\right]$ in Figure 7. It will be noted that with values of h/l equal to 3/7 and 1, respectively, widely different values of M_c are found with the same value of $\left[\frac{I_g}{I_c}\cdot\frac{h}{l}\right]$. Furthermore, these values do not compare at all closely with the moments obtained by assuming $\left[\frac{I_g}{I_c}\cdot\frac{h}{l}\right]$ equal to n in equation (4). It seems unwarranted,

[4] A method of analyzing frames similar to these is given by E. Björnstad in "Die Berechnung von Steifrahmen nebst anderen statisch unbestimmten Systemen." Berlin, 1909. One equation is used for frames both with and without brackets by proper choice of the terms corresponding to n—that is, the members which contain brackets are considered replaced by "equivalent" members of constant cross section throughout. The section of the equivalent member from which n is calculated obviously varies with the size of bracket. This treatment of the subject from a purely theoretical viewpoint neglects the change in shape of the axis of a frame containing brackets. Further, the assumption is made that for a haunch which varies uniformly in depth the moment of inertia also varies as a linear function between the two extremities of the haunch. The results obtained are stated to be approximate.

therefore, to attempt to use equation (4) to investigate frames in which the moments of inertia of the girder is not equal to that of the columns. Figure 7 indicates the general range of values of moments to be obtained in most cases of this sort; frames of other proportions may be analyzed by the application of equation (1).

It has been shown that the moment at mid span decreases with the increase in stiffness at the corners of the frame produced by the use of brackets. If the corners of a rectangular frame could be stiffened without the use of brackets, a decrease in moment at mid span would be accompanied by an equal increase in moment at the corners, since in this case the numerical sum of the maximum positive and

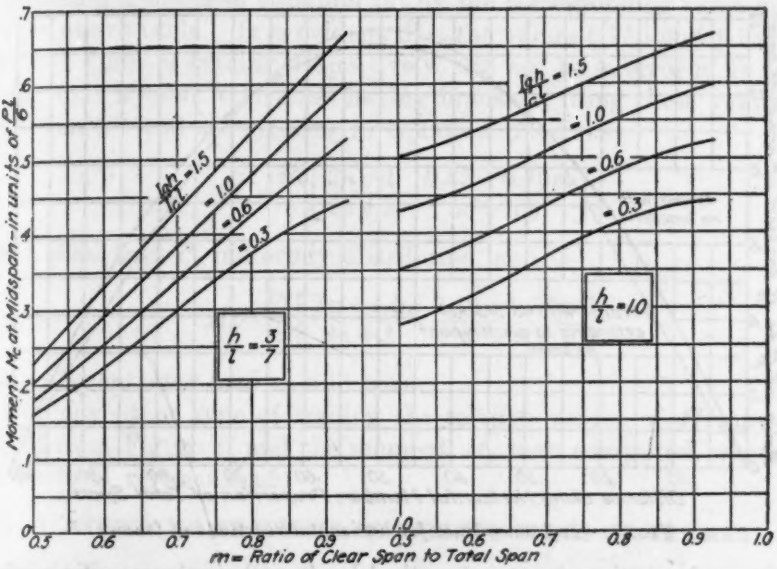

FIG. 7.—*Calculated moments in frames of varying moments of inertia*

negative moments is equal to the maximum moment for a simple beam carrying the same vertical loading. However, where brackets are used the axes of the members do not intersect at right angles, but approach more nearly the pressure line of the resultant force acting on the hinge. The resulting decrease in moment at the corner due to this variation in shape of specimens with brackets approximately offsets the increase in moment at the corner due to the variation in stiffness of the different parts of the frame. Hence, the negative moments in the different types of frame are nearly equal in magnitude for a given load, as will be noted later from the results of tests.

2. EFFECT OF BRACKETS WITH DIFFERENT LOADINGS

Equation (4) has been developed for the special case of third-point loading which was used in the test frames. This form of loading is frequently used in tests because it is easy to apply and produces a moment diagram somewhat similar to that due to a uniformly distributed load. A study of the effect of other loadings shows that equation (4) may be adapted to a form which gives the effect of brackets for such cases.

Influence lines for the horizontal reactions of a two-hinged frame under vertical loads are shown in Figure 8.[5] That is, the ordinate of any point on the influence line represents the relative value of the

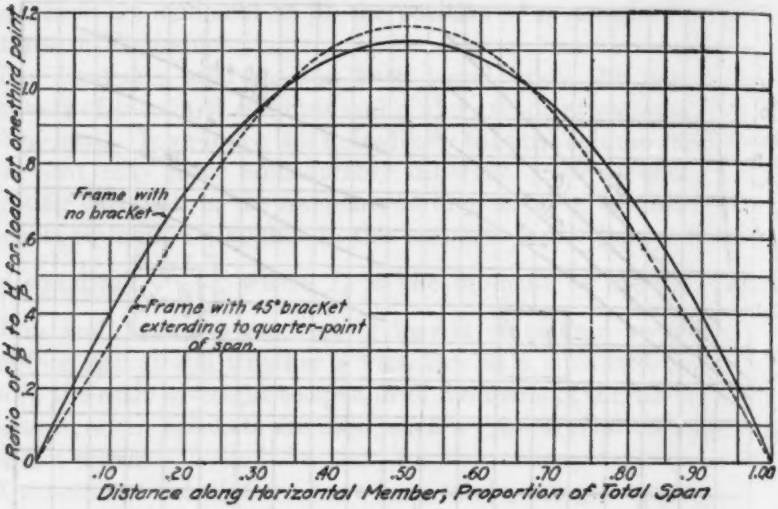

FIG. 8.—*Influence lines for horizontal reactions of frames*

horizontal reaction due to a vertical load at the corresponding point on the span. These relative values are independent of the ratio of height to span of the frame. From these curves it is found that certain common types of loading (with equal total loads) produce the following relative values of the horizontal reaction, H, considering the reaction due to one-third point loading as unity.

[5] The construction of these influence lines is based upon the following theory: With a frame of the type used in this investigation suppose outward thrusts to be applied at the hinges, causing the top member to deflect downward. From Maxwell's theorem of reciprocal displacements it is known that the elastic curve of the top member of this frame is an influence line for the horizontal reactions of a similar frame loaded with vertical loads on the top member and having the hinges at the base held stationary. Figure 8 was, therefore, obtained by computing the shape of the elastic curves of two extreme forms of top member—one having no bracket and one having large 45° brackets extending to the quarter points of the span. It is to be noted that these curves give only relative (not absolute) values of the horizontal reaction, and that the curves can not be used to compare values of the reactions for the two types of frame. However, relative values are sufficient to compare loads at different points on the same frame, which is the purpose of this diagram.

Frame having—	Third point loads	Uniform load	Concentrated center load
No bracket	$H=1.00$	$H=0.750$	$H=1.125$
Large bracket	$H=1.00$	$H=.720$	$H=1.167$

From equations (2) and (4), for the third-point loading,

$$H=\frac{Pl}{6h}\left[\frac{2}{2n+3}+\frac{0.65-0.7m}{n^2+0.8}\right] \tag{5}$$

An expression for the value of H for a frame under uniform load or a concentrated center load may be obtained by multiplying the right-hand member of equation (5) by the corresponding value given in the above table. It is evident that the values 0.750 and 1.125 for the two kinds of loading, respectively, will not be in error more than 4 per cent if used for frames having brackets; using these values in equation (5) and substituting in equation (2) gives

$$M_c=\frac{Pl}{8}\left[\frac{2n+1}{2n+3}-\frac{0.65-0.70m}{n^2+0.8}\right] \tag{6}$$

for a total load P, uniformly distributed, and

$$M_c=\frac{Pl}{4}\left[\frac{2n+1.5}{2n+3}-\frac{0.49-0.53m}{n^2+0.8}\right] \tag{7}$$

for a concentrated load at mid span.

For any other type of loading the relative values of H may be found from Figure 8, and the moment M_c then computed, where P is the total vertical load.

3. EFFECT OF BRACKETS IN VARIOUS TYPES OF FRAMES

While the results of the foregoing analyses may be found useful in the design of two-hinged frames, the question immediately arises as to what quantitative application may be made to other kinds of frames. For example, brackets may well be used in the closed rectangular frame, in the two-legged frame with column bases fixed, in building or viaduct frames and similar structures. In the absence of test data theoretical analyses have been made for two types of frame, and it appears that an application of equation (4) may be made to these cases. In these analyses also the moment of inertia was assumed to vary as $d^{5/2}$.

The frames analyzed are the closed rectangular or quadrangular frame, in which the columns are assumed to be rigidly attached at the bases to a horizontal member of equal section, and the two-legged frame with the columns fixed at the bases. Each of these frames has points of contraflexure in the columns at a distance h_o

equal to two-thirds h or more from the top of the frame. The portion of the frame above these points of contraflexure may be considered as a two-hinged frame in which the bases have been allowed to move apart a small amount. Such an outward movement tends to increase the moment at mid span in a two-hinged frame.

The analysis of these frames has been made by use of the general theory of indeterminate structures used in Section II, 1.[6] The span and depth of members used were the same as those used in the test specimens, while the height and clear span of the frames were varied. Figure 9 shows values of the calculated moment at mid span for

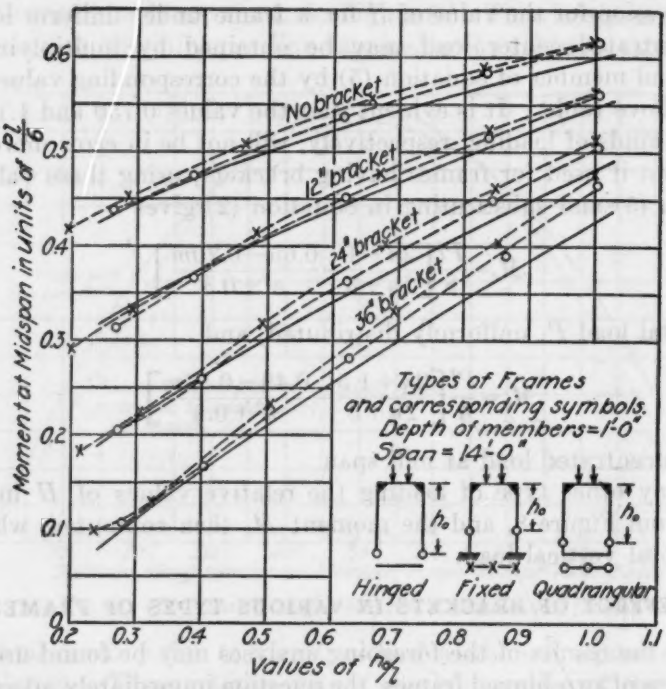

FIG. 9.—*Moments at mid span for frames of different types and proportions*

varying proportions of these frames and compares them with values for the two-hinged frame. It is seen that for frames having the same distance, h_o, from the top to the point of contraflexure, the moments M_c are very nearly the same. The values for the fixed-base and quadrangular frames are slightly higher than for the two-hinged frame because the columns at the point of contraflexure have deflected outward slightly. However, if the value of h_o has been determined it appears that these frames may all be treated as two-hinged frames by use of equation (4) without appreciable error. For determining h_o for frames of different proportions, Figure 10 may be used.

[6] See Johnson, Bryan, and Turneaure, Modern Framed Structures, Pt. II, p. 386.

The procedure in determining the effect of certain brackets in a quadrangular or a "fixed-base" frame may be summed up as follows: Knowing the proportions of the frame, the position of the points of contraflexure may be determined from the curves of Figure 10. Placing the value of $\frac{h_o}{l}$ equal to n in equation (4) gives the value of M_c, the moment at mid span of the top member. The moments at all other parts of the frame may be found from the equations of statics. While the value of M_c may be slightly inexact, the error is small.

The curves of Figure 10 giving the position of the points of contraflexure are applicable for any loading on the top member that is symmetrical about the center line of the frame. Hence, if uniform

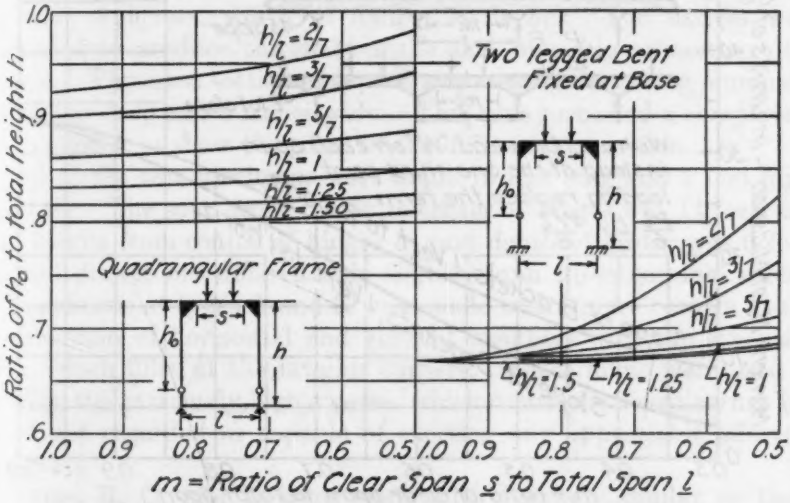

FIG. 10.—*Distance h_o from top of frame to point of contraflexure*

or concentrated loads are used, the procedure is the same except that equations (6) or (7) must be used to determine the value of M_c.

One or two other types of rigidly connected structures may be mentioned. For example, the continuous beam of three spans, with loads on the middle span only, may be treated as a two-legged frame with the columns swung up into the horizontal position. While certain features of the rectangular frame, such as column action, curved beam action, and direct compression due to horizontal thrust, are absent in the continuous beam, brackets used at the supports will occupy the same region of bending moment in the beam as in the frame. Hence, equation (4) will give substantially correct results when used with this special case of a continuous beam.

Another very common form of continuous beam is one having a large number of spans of identical dimensions and with all spans

subjected to equal loads. To illustrate the effect of brackets used at the supports in such a beam, two numerical cases have been analyzed by the method explained at the beginning of Section II, 3. In one case brackets with a 45° or 1 to 1 slope were used at both sides of each support; in the other case brackets having a 2 to 1 slope (making an angle of 26° 32′ with the horizontal) were used. The depth of the beam was one-tenth of the span. Figure 11 shows values of the moment at mid span, due to one-third point loading, for various values of the ratio of clear span to total span. Denoting this ratio by m, it is found that approximate formulas for the moment at mid span are:

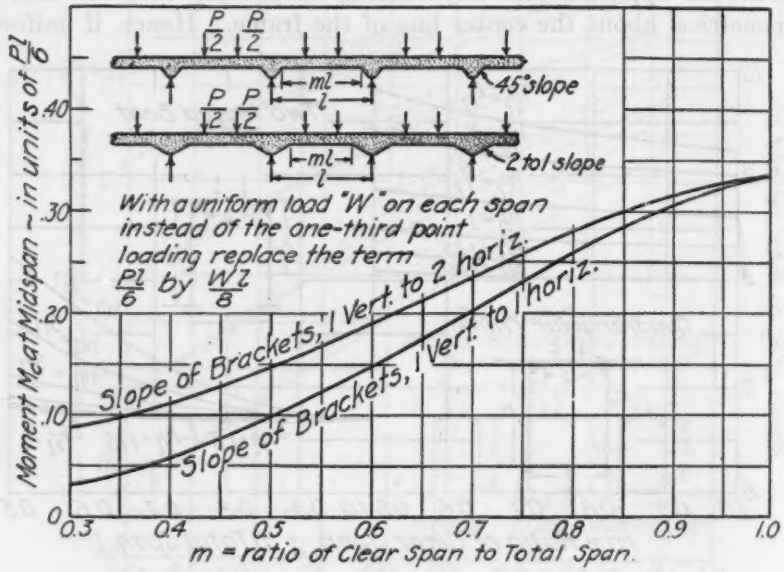

FIG. 11.—*Moments at mid span of continuous beams with brackets*

$$M_c = \frac{Pl}{6}\,\frac{(4m-1)}{9} \tag{8}$$

For brackets with 2 to 1 slope

$$M_c = \frac{Pl}{6}\,\frac{(m)}{3} \tag{9}$$

The moment over the supports in either case is

$$M_s = -\frac{Pl}{6} + M_c \tag{10}$$

Equations (8), (9), and (10) may be applied to the case of a uniformly distributed load W on each span by replacing the quantity $\frac{Pl}{6}$ by $\frac{Wl}{8}$. These equations should not be used for values of m smaller than those shown in Figure 11.

The diagram shows clearly that with very large brackets, corresponding to small values of m, the bracket carries nearly all of the load directly to the support, acting as a very stiff cantilever. The positive moment at mid span accordingly becomes very small.

III. TEST SPECIMENS AND APPARATUS

1. DESCRIPTION OF TEST SPECIMENS

Test specimens of five types were used—two specimens each of types A, B, C, and D, and one of type E. All were two-legged frames with the columns hinged at the bases. The details of these specimens are indicated in Figures 12 to 14. The cross sections of types A, B, C, and D were of T shape, having the following nominal dimensions: Depth, 12 inches; thickness of flange, 3 inches; width of web, 8 inches; width of flange, 30 inches. The flanges were intended to produce the effect of the shell of a ship adjacent to the frame. The cross section of type E was rectangular, being nominally 12 inches deep and 8 inches wide. This type furnished a comparison with type A to show the effect of the difference in section.

All of the test specimens were made 15 feet long and 7 feet high, over all. The span from center to center of hinges was 14 feet, and the height from center of hinges to mid depth of girder was 6 feet. Actual dimensions differed only slightly from these nominal values.

Specimens of types A and E were made with square corners at the intersection of horizontal and vertical members with the exception of a 2-inch fillet at the interior corners. These fillets were used to modify the extremely high stresses which occur at a sharp corner but were not regarded as capable of exerting any appreciable effect as brackets.

Types B, C, and D were made with brackets similar to those actually used in concrete-ship construction. Type B had 45° brackets, 12 inches in horizontal length; the exterior corners were given a 45° chamfer equal in size to the bracket, making the depth of cross section normal to the face of the bracket about 17 inches. Type C was similar to type B, but had a bracket 24 inches in horizontal length, making the depth of cross section at the corner approximately 25 inches. Type D was modified from type C by filling in the angles between the bracket and the main members with two supplementary haunches, so that the inside line of the frame approached the outline of a curved soffit.

The hinge detail at the base of each column was provided by casting in place a steel shoe formed of ¾-inch bearing plates and lugs with a 3-inch pinhole at each side of the column connected by a 3-inch pipe sleeve 28½ inches long. A 2$\frac{15}{16}$-inch steel pin passing through the pinholes and pipe sleeves engaged similar plates on the test base and formed a simple hinge.

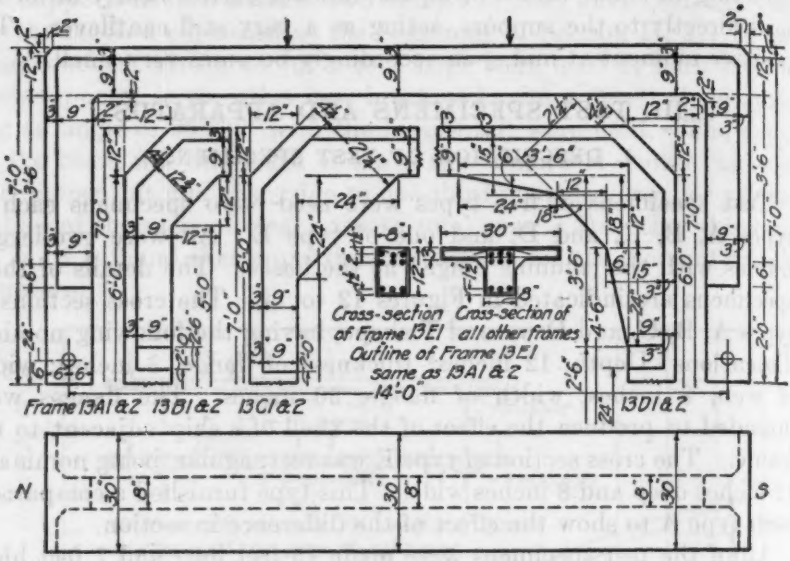
Cross-section of Frame 13E1
Outline of Frame 13E1 same as 13A1 & 2
Cross-section of all other frames
14'-0"
Frame 13A1 & 2 13B1 & 2 13C1 & 2
13D1 & 2
N
S

DESIGN DIMENSIONS OF FRAMES

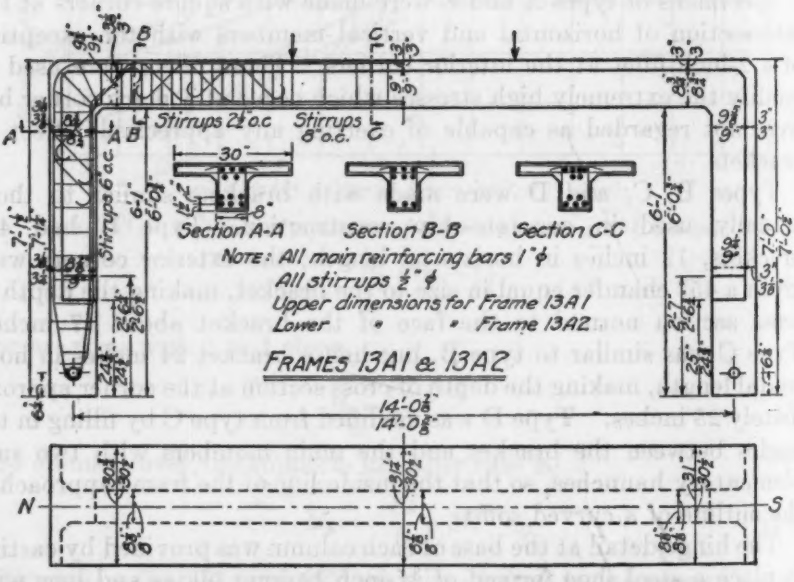

FIG. 12.—*Design dimensions of test specimens and details of test specimens 13A1 and 13A2*

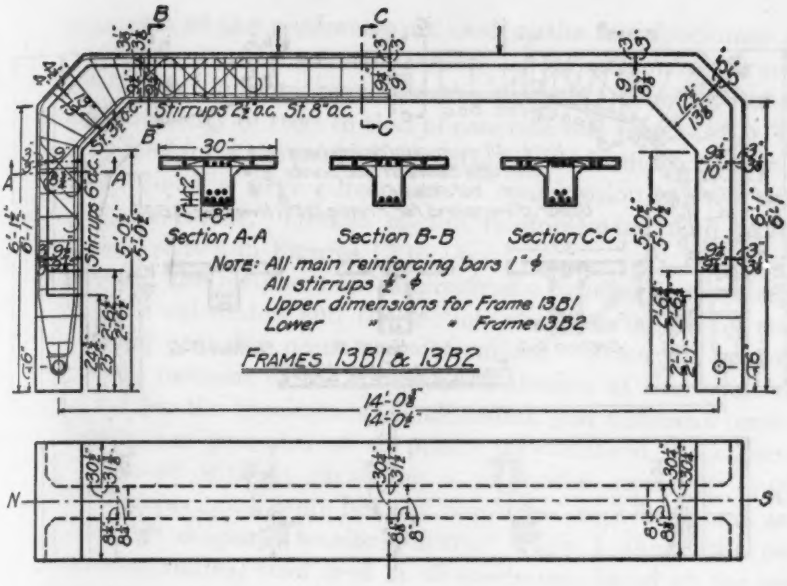

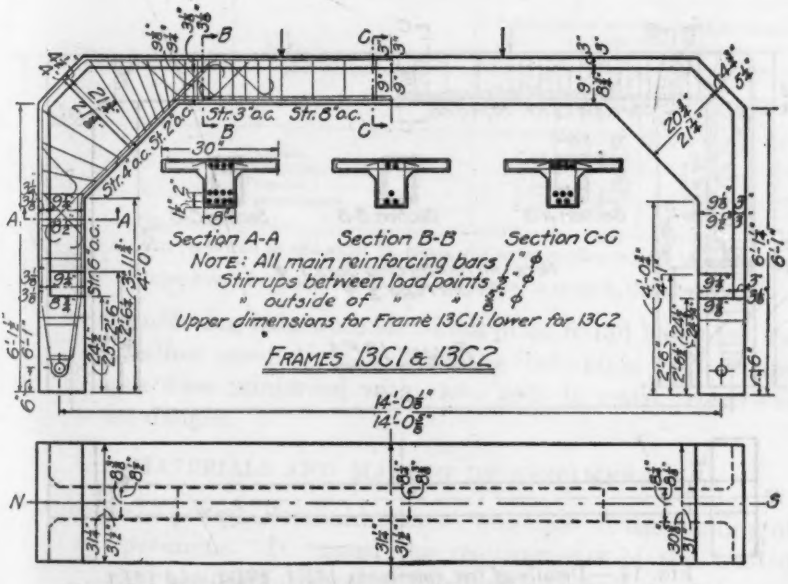

FIG. 13.—*Details of test specimens 13B1, 13B2, 13C1, and 13C2*

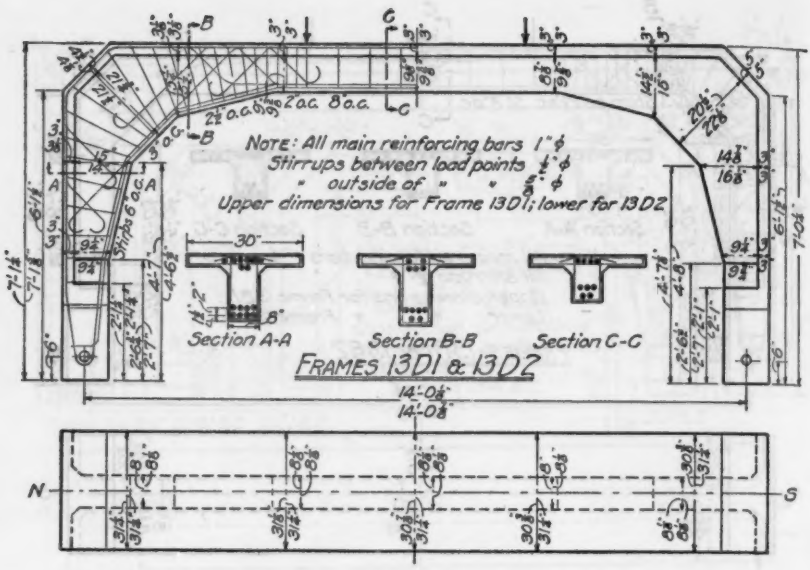

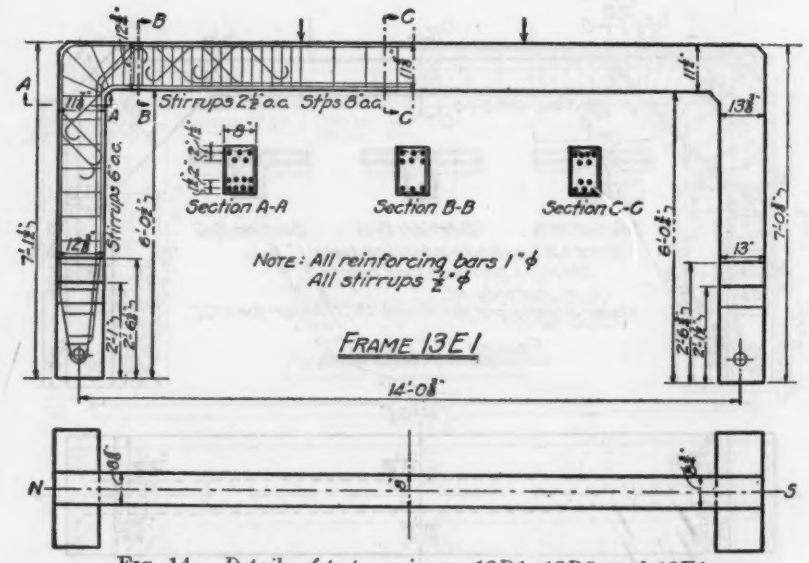

FIG. 14.—*Details of test specimens 13D1, 13D2, and 13E1*

In the design of the reinforcement used in the test specimens the working stresses assumed were 16,000 lbs./in.^{2} for tension in the steel, and 1,500 lbs./in.^{2} for compression in the concrete. The ratio of the modulus of elasticity of steel to that of concrete was taken as 8. The design provided for a reversal of the direction of loading, so that all sections contained a large percentage of compression as well as of tension reinforcement. Details of the reinforcement used in the specimens are shown in Figures 12 to 14.

In designing the members the approximate bending and resisting moments were calculated and the section at which failure by compression would probably occur was determined. From the approximate resisting moment of the compressive stresses at this point the working load for the specimen was calculated, and sufficient tension reinforcement was provided at all points to withstand the external bending moment without exceeding a computed stress of 16,000 lbs./in.^{2} The specimens were heavily reinforced with bent bars and stirrups against diagonal tension failure. Table 1 shows the percentage of longitudinal steel used in all specimens, based on the area of cross section exclusive of flanges.

TABLE 1.—*Percentage of longitudinal reinforcement*

Location of section	Stress in reinforcement (downward loads)	Percentage of reinforcement for specimens Nos.[1]—			
		13A1–2 13E1–	13B1–2	13C1–2	13D1–2
Center of girder	Tension	4.67	4.67	4.67	4.67
	Compression	5.61	7.48	3.74	3.74
Corner of frame [2]	Tension	4.67	3.79	2.05	2.05
	Compression	5.61	4.41	2.46	2.46

[1] This investigation was performed as test series 13; hence, the series number is used as a part of all specimen numbers.
[2] Vertical section for types A and E; section normal to face of bracket in types B, C, and D.

The main reinforcing bars were all 1-inch plain round bars, and the stirrups were either one-half or five-eighths inch plain round bars. The tee flanges were reinforced with cross rods to resist transverse bending in the flanges.

2. MATERIALS AND MAKING OF SPECIMENS

(*a*) CEMENT.—Lehigh Portland cement was used in the making of all the test specimens. It passed the requirements of the United States Government specifications for Portland cement.[7]

(*b*) AGGREGATE.—The sand and gravel were obtained from local deposits at South Bethlehem, Pa. The material was siliceous, clean, and gritty. It was carefully separated by screening into three sizes—(1) Fine sand consisting of grains smaller than one-eighth inch in

[7] Circular of the Bureau of Standards, No. 33; third edition; Jan. 18, 1917.

diameter, (2) coarse sand falling between one-eighth and one-fourth inch in diameter, and (3) gravel exceeding one-fourth inch but less than one-half inch in diameter. The separation of the sand into fine and coarse grades was introduced to avoid the lack of uniformity in the concrete mixture which would result from segregation of sizes in the bin.

(*c*) STEEL.—The reinforcing bars were rolled from rejected shrapnel steel billets of high yield point. The physical properties of this steel are shown in Table 2. Each value in the table is the average of two tests.

TABLE 2.—*Physical properties of reinforcing steel*

Diameter of bar (inches)	Yield point	Ultimate tensile strength	Elongation in 8 inches	Reduction in area
	Lbs./in.²	*Lbs./in.²*	*Per cent*	*Per cent*
½	63, 800	104, 400	16. 6	27. 5
⅝	66, 070	108, 440	18. 0	42. 2
1	55, 800	91, 420	20. 5	38. 2

(*d*) CONCRETE.—The concrete used was mixed in the proportions 1 : 1 : 1 by volume. The unit quantity of sand consisted of 0.8 part fine sand and 0.2 part coarse sand. In preparation for mixing the concrete each kind of aggregate was thoroughly mixed by shoveling, and determinations of the moisture content were made upon samples taken at random. Enough water was added when the concrete was mixed to make the total water 13 per cent of the combined weight of the dry materials, thus producing a rather stiff mixture, considerably drier than is generally used in reinforced concrete construction work.

Six 6 by 12 inch cylinders were made with each test specimen and were stored with the specimen until they were tested. Three cylinders in each lot were tested at the age of 7 days and the remaining three at the age of 40 days, which was the approximate age of the frames when tested. The average compressive strength of the concrete is given in Table 3. The average initial modulus of elasticity of the concrete in the frames was assumed to be 3,750,000 lbs./in.^{2}; this value was found from a large number of compression tests of concrete cylinders having identical proportions and materials but made in connection with other investigations at the laboratory. The stress-strain curves for these cylinder tests were closer to straight lines than is usually expected with concrete.

TABLE 3.—*Compressive strength of concrete*

[Each value represents the average strength of three 6 by 12 inch cylinders]

Made with specimen number	Compressive strength at age of 7 days	Compressive strength at age of 40 days	Made with specimen number	Compressive strength at age of 7 days	Compressive strength at age of 40 days
	Lbs./in.²	*Lbs./in.²*		*Lbs./in.²*	*Lbs./in.²*
13A1	2,220	3,110	13D1	2,870	4,420
13A2	2,975	3,765	13D2	3,075	5,860
13B1	2,880	4,260	13E1	2,815	4,995
13B2	2,535	3,665			
13C1	2,775	4,505	Average	2,785	4,290
13C2	2,900	4,040			

(*e*) MAKING OF SPECIMENS.—One wooden form was used for all test specimens, and the inside corners of the form were designed to provide for the variation in shape of the brackets. The inner surfaces of the forms were well oiled. In order to insure plumbing of the specimen and proper alignment of the hinges in the columns of the test specimens, the form was erected in position on the large concrete base used in making the load test, with the steel shoes and hinge pins in position. The reinforcing bars were bent as required, in an Olsen cold-bend testing machine and were wired in place after being set in the form. Concrete was dumped from the mixer into a tight wooden box, carried to the form by a traveling crane, and shoveled into the form. A considerable amount of tamping and rapping was required to get the concrete into place, especially at the corners of the frame. The forms were stripped when the concrete was about 24 hours old, and the specimen was lifted off the test base and transferred to another place in the laboratory. Wet burlap was kept wrapped around the specimens up to the time of testing.

3. TESTING APPARATUS

A heavy concrete test base was made especially for this investigation. A general view of the base with a specimen in position for testing is shown in Figure 16. The base was 22 feet long, 5½ feet high and 2½ feet wide, and was reinforced to withstand a reversal both of vertical loads and horizontal thrusts. A vertical steel link at one end allowed for a practically frictionless horizontal movement at the bottom of one leg of the specimen under test. A 60-ton hydraulic jack acting against this link was arranged to produce a horizontal reaction through the axis of the hinge and either to maintain a fixed distance between the two hinges or to move the hinge in or out any desired amount. Such movement was measured by means of a screw micrometer bar.

Downward loads were applied on the top of all specimens at two points 2 feet 4 inches on each side of mid span. The distance between the load points was one-third of the nominal span from center to

center of hinges. The diagram of Figure 15 shows the arrangement for applying and measuring loads and reactions. The vertical loads were produced by two 100-ton hydraulic jacks acting downward on a steel box girder which transmitted the pressure through a heavy knife-edge casting and a roller to the specimen. Steel plates embedded in plaster of Paris were used to distribute the bearing pressure over the concrete. The upward reaction of the jacks was exerted against built-up steel sections connected by six tie rods to other steel sections beneath the test base.

Two strain gauges were used in the tests, one of 4 inch gauge length for measuring deformations of concrete and one of 8 inch gauge

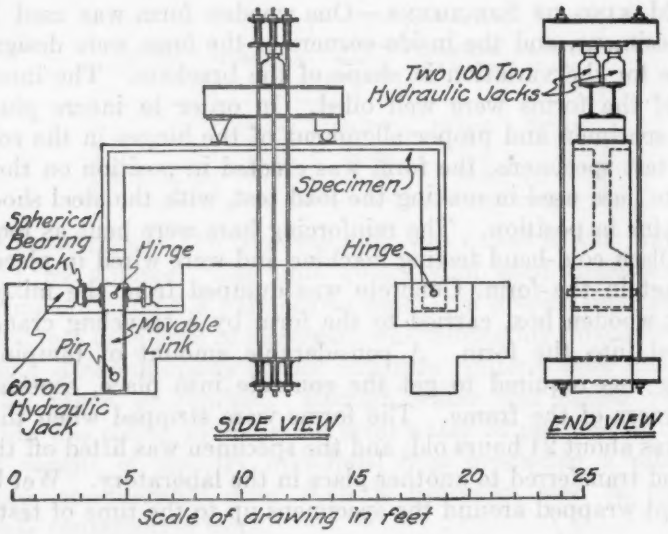

FIG. 15.—*General arrangement of test apparatus*

length for measuring deformations in the reinforcement. A continuous row of gauge lines was located on the reinforcement along the length of the outer face of the specimen, and a similar row was laid off along the inner face. Deformations of the concrete were also measured on several gauge lines along the sides of the brackets.

Deflections were measured at points 1 foot apart on the horizontal member and on the two columns. A black linen thread was stretched at constant tension between points at the two ends, at mid depth of the girder. Similar threads were hung as plumb lines along the sides of the columns. Movement of the specimen with reference to the thread was observed by means of paper scales pasted to small mirrors and attached to the specimen. Readings, which were taken by lining up one edge of the thread with its reflection in the mirror, could be duplicated within 0.01 inch.

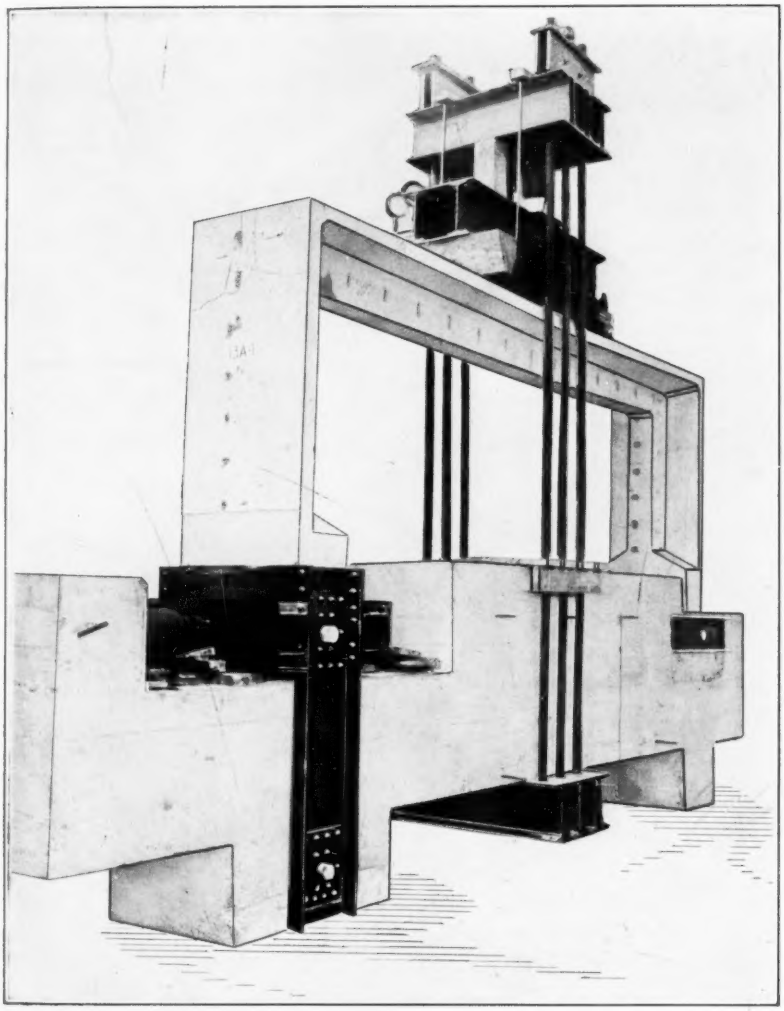

FIG. 16.—*General arrangement of test apparatus*

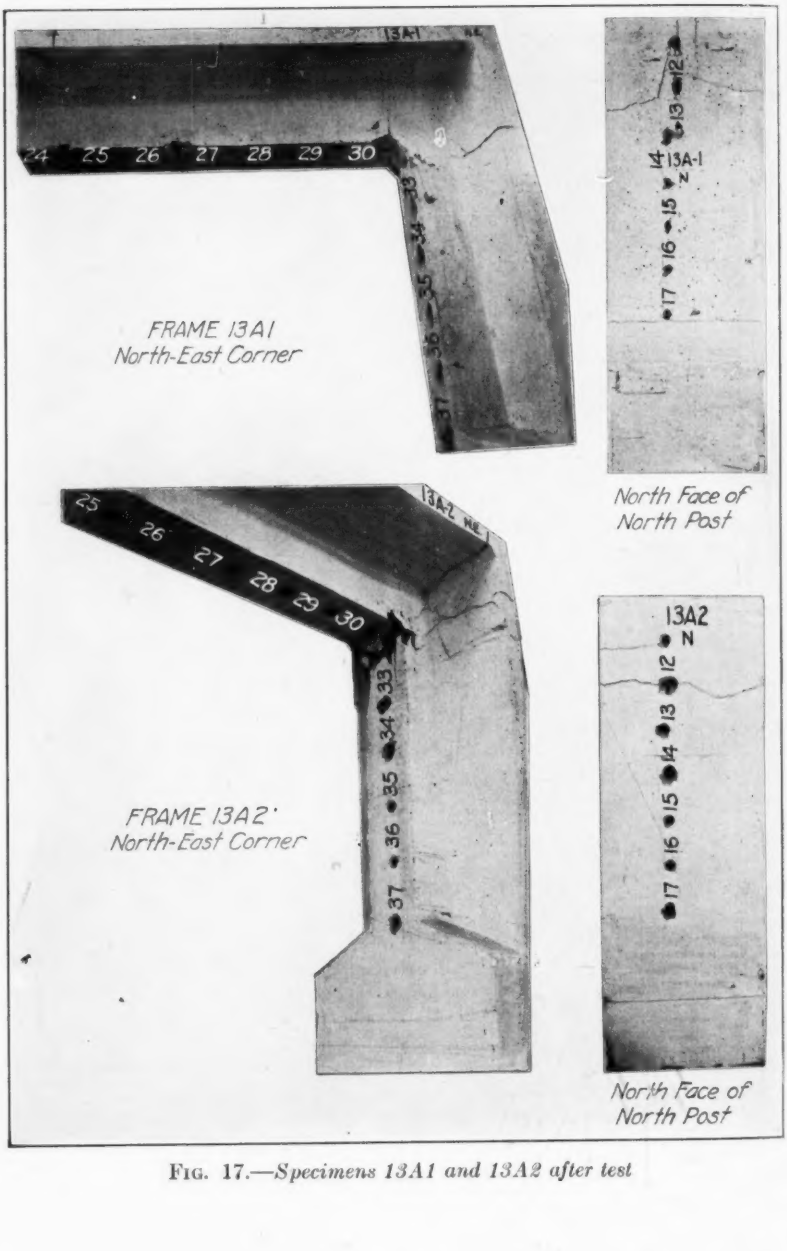

FIG. 17.—*Specimens 13A1 and 13A2 after test*

IV. TEST DATA AND DISCUSSION OF RESULTS

1. PROCEDURE AND PHENOMENA OF TESTS

In general, downward loads were applied to the test specimens in increments of 30,000 pounds, with the hinges at the bases of the columns held in a stationary position. Zero readings were taken with no downward load except that of the loading rig, which weighed about 3,000 pounds, and with just enough horizontal pressure applied at the hinges to tighten up all movable parts of the hinge apparatus.

The effect of a reversal of stress was obtained in the testing of each specimen in the following manner: After readings of deformation and deflection had been taken under a load of 90,000 pounds all downward load was released. The movable hinged end of the specimen was then pushed inward an amount sufficient to produce maximum deformation readings at critical sections as great as those observed under the 90,000-pound vertical load. Following readings under this condition of loading and still without applying any vertical loads, the horizontal jack was swung around to act on the inside of the hinge, and the movable end of the column was thrust outward until stresses were again produced which were comparable to those observed under the 90,000-pound load. The change in distance between hinges was measured in both cases. With the horizontal jack swung back to the outside of the frame and the distance between hinges brought back to its original amount, vertical loading was resumed on the top of the frame. Complete readings of deformation and deflection were taken at a load of 120,000 pounds, and at increments of 30,000 pounds up to the maximum load. Final readings were taken in each case after the maximum load was applied, in order to obtain information on the manner of failure. Figures 17 to 21 show views of the different specimens after failure had taken place. The following paragraphs give a short description of the principal phenomena of the tests.

Specimen 13A1.—Loads were applied as described in Section IV, 1. Numerous cracks were observed under the 60,000 and 90,000 pound loads. After application of end thrusts inward and outward with top load released the movable hinge did not return entirely to its original position but was pushed back into place with little effort. Failure occurred at a maximum load of 120,000 pounds with noticeable crushing and spalling at the north inside corner. This spalling was apparently due largely to slipping of bars at the inside face of the column near the corner. There was also apparent slipping of tension bars near mid span. Tension cracks were numerous in the middle portion of the frame, also across the tee flanges on both vertical and horizontal members near both corners.

Specimen 13A2.—A number of tension cracks appeared near mid span at the 30,000 pound load. Cracks also appeared across the

tee flanges about 15 inches from each corner on both horizontal and vertical members. At loads of 60,000 and 90,000 pounds several more cracks opened in the same regions. With inward thrusts several new cracks opened in the top face of the girder within the middle half of the span. With outward thrusts tension cracks were opened at the inside corners of the frame. Failure occurred under vertical load through crushing at the north inside corner and by yielding of the steel in tension at the outside of the same corner. While the tension failure may have occurred first, the yield point was exceeded in the compression reinforcement at the corner, and also in the tension reinforcement under the load points. There were pronounced radial cracks around both corners of the frame. Maximum load, 119,000 pounds.

Specimen 13B1.—Failure began with crushing of the concrete at the north inside corner at the intersection of bracket and girder. After this corner had yielded somewhat a large number of diagonal cracks appeared between the bracket and load point. Cracks were not large at other parts of the frame. Horizontal cracks in the tee flange at the north end of the girder indicated that the flange was shearing loose from the web at failure. Large tension cracks were observed on the top face of the girder at the north end. Some crushing occurred at the top of the south bracket and at the bottom of the north bracket. Maximum load, 152,000 pounds.

Specimen 13B2.—At a load of 30,000 pounds there were a few straight tension cracks on the lower side of the girder. With a load of 60,000 pounds, a number of cracks opened on the outside faces of the columns and on the top face of the girder near the ends. With inward thrusts, a few additional cracks appeared in the top face of the girder, one being between the load points. With outward thrusts, a few cracks opened at the junctions of girder and brackets. At a load of 120,000 pounds pronounced diagonal tension cracks developed in the web of the girder, running outward from the load points at an angle of about 45°. The maximum load was reached at 138,000 pounds. Failure came when the yield point of the steel was reached in the outside face of the south column and at mid span. At about the same time crushing occurred at the junction of the north column and bracket, and the concrete spalled off considerably. There was a slight indication of crushing at the south end, near the junction of the column and bracket.

Specimen 13C1.—Several cracks opened near mid span at a load of 30,000 pounds. At a load of 60,000 pounds cracks opened at about mid height of the outside faces of both columns. With inward thrusts, cracks opened in the outside face of the columns, and one or two opened at each end on the top of the girder. With outward thrusts, cracks opened in the upper part of each bracket and ran down

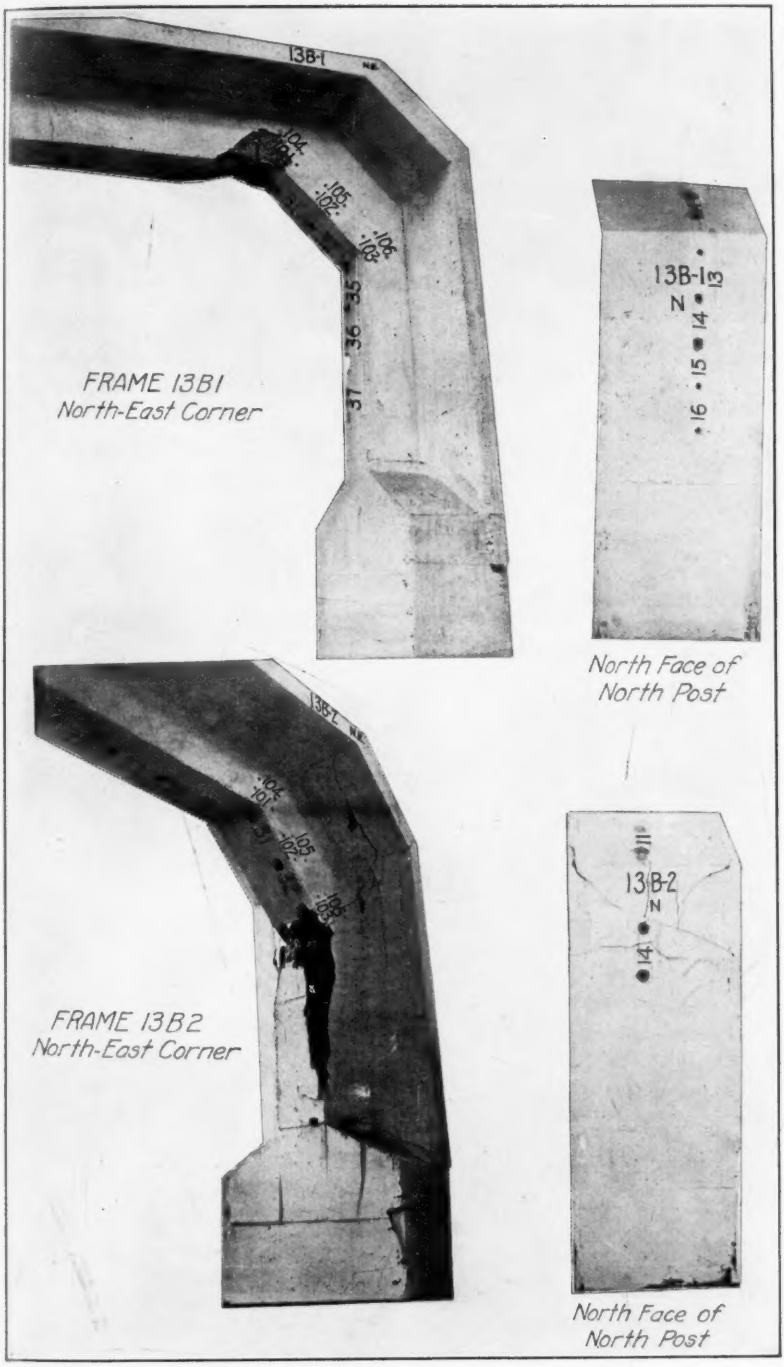

FIG. 18.—*Specimens 13B1 and 13B2 after test*

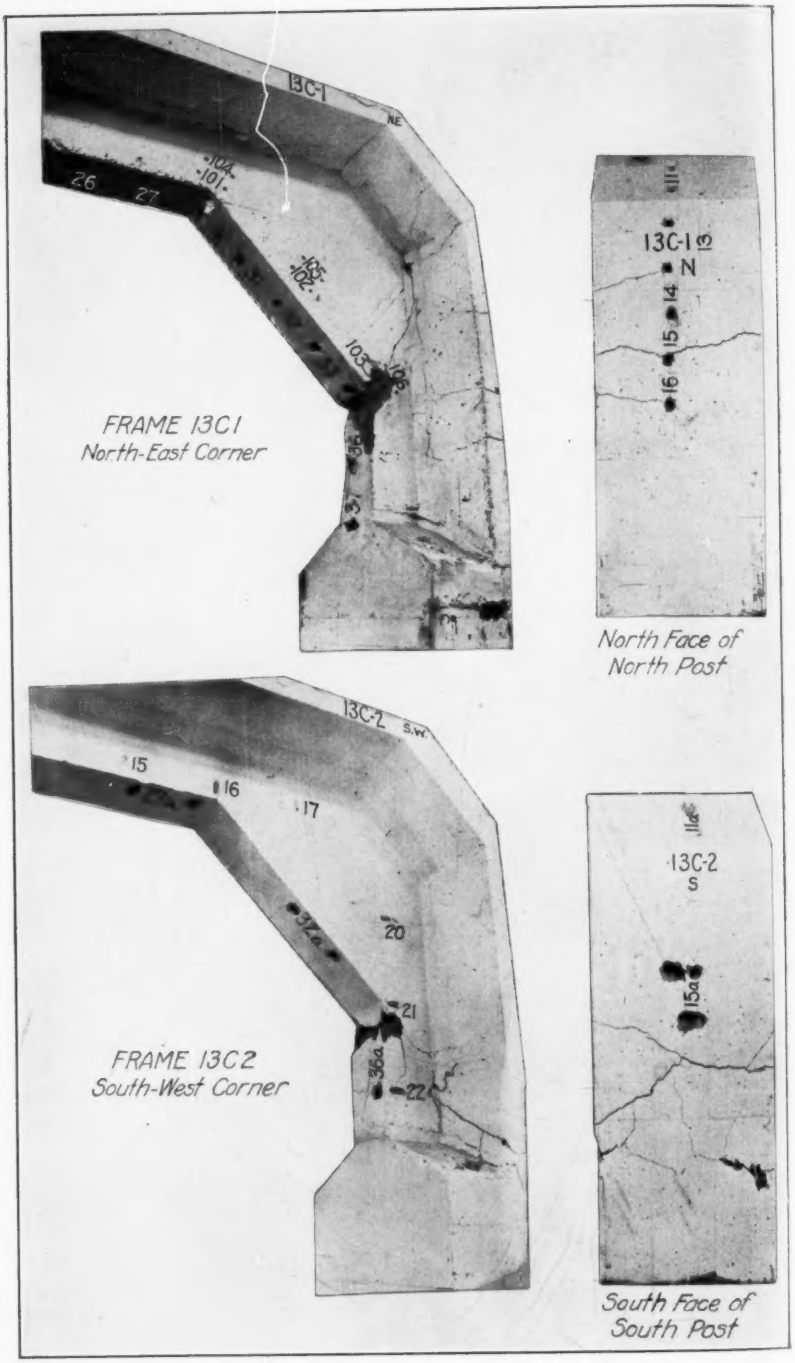

FIG. 19.—*Specimens 13C1 and 13C2 after test*

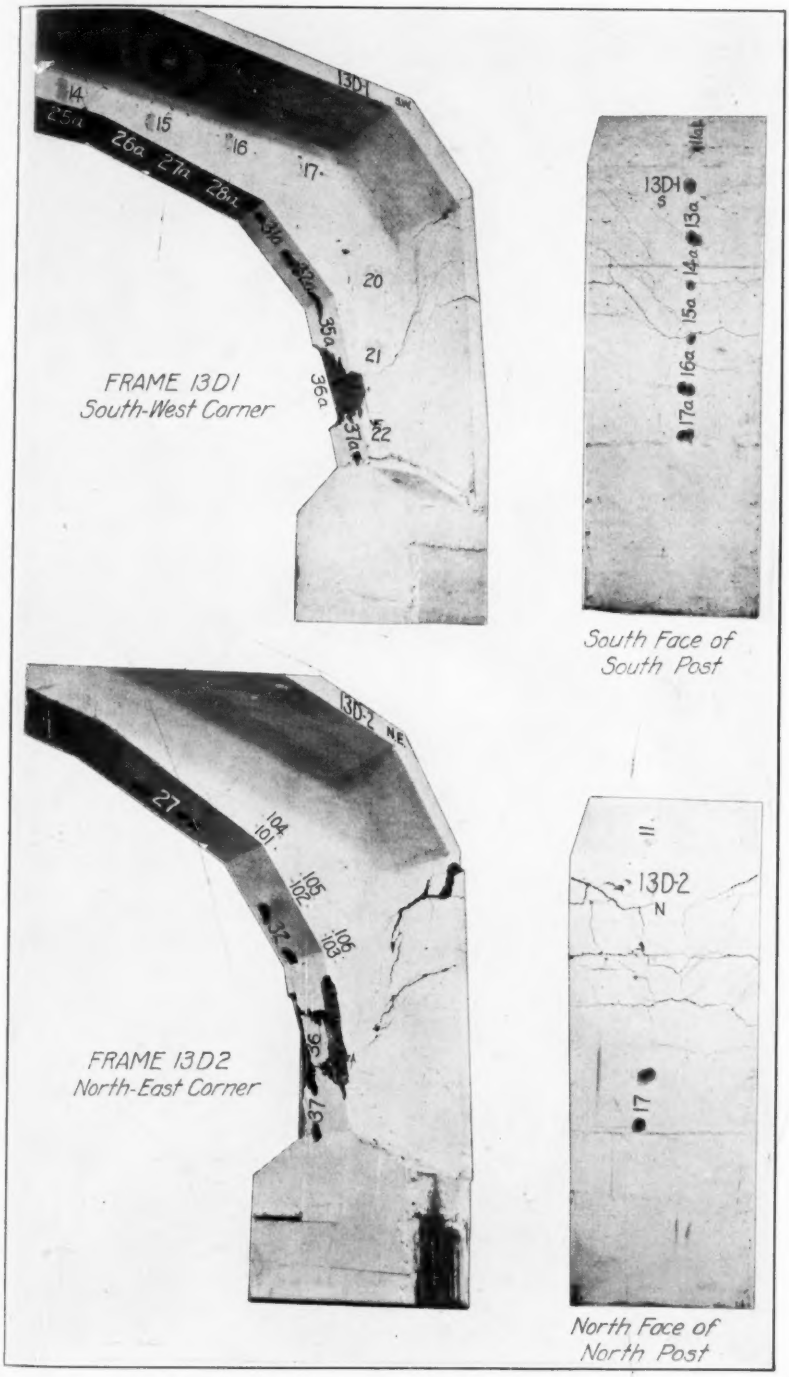

FIG. 20.—*Specimens 13D1 and 13D2 after test*

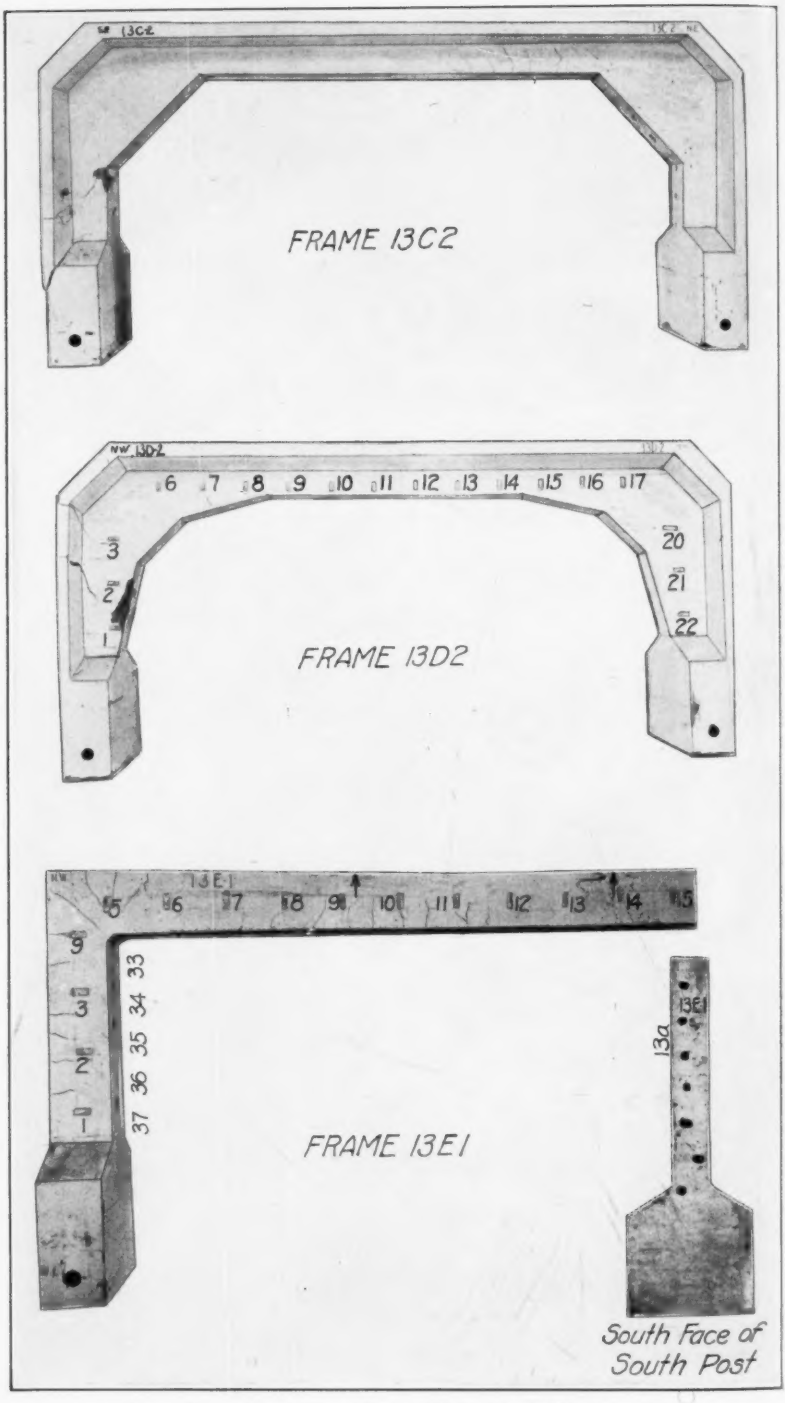

FIG. 21.—*Specimens 13C2, 13D2, and 13E1 after test*

at about 45° with the horizontal, parallel to the face of the bracket. Cracks of this type were produced in all frames with this kind of loading and were at right angles to those produced by inward thrusts. At loads of 120,000 and 150,000 pounds cracks began to run through from the outer face of each column downward diagonally across the webs toward the inside face at the junction of bracket and column. At the maximum load of 182,000 pounds crushing occurred at the bottom of the north bracket. Large cracks opened in the outside face opposite the crushed area, and the yield point of the tension steel was passed here and at mid span.

Specimen 13C2.—A few cracks were observed near mid span at a load of 30,000 pounds, and others opened across the outer face of each column at the loads of 60,000 and 90,000 pounds. Several cracks opened in the upper face of the girder when inward thrusts were applied alone. With outward thrusts the cracks were similar to those found in specimen 13C1. At a load of 120,000 pounds large cracks opened in the outside faces of columns. This specimen was weakened by the accidental omission of two of the four longitudinal reinforcing bars in the outer face of each column. Due to this, failure occurred in the outside face of the south column, opposite the bottom of the bracket where crushing failure rapidly followed. The maximum load was 148,000 pounds.

Specimen 13D1.—A few cracks were observed near mid span at the load of 30,000 pounds, and others opened across the outer faces of both columns at loads of 60,000 and 90,000 pounds. Several cracks opened in the upper face of the girder when inward thrusts were applied and under outward thrusts a large tension crack opened just outside of the south load point. At later loads this crack gave the impression of impending diagonal tension failure; however, failure did not occur in this part of the frame. At a load of 180,000 pounds large cracks appeared at both ends at the top of the vertical faces of the columns. The maximum load was 208,500 pounds. Failure occurred when the yield point of the reinforcement was reached simultaneously in compression on the inside face and in tension on the outside face of the south column at about mid height. The concrete crushed over a considerable area in the locality of the failure.

Specimen 13D2.—A few cracks were observed on the outer faces of the columns near the corners and near mid span at the 60,000-pound load. With inward thrusts, several cracks opened on the top face of the girder. With outward thrusts, cracks on the tension side of the girder were opened. Under the 180,000-pound load larger cracks appeared across the face of the north column, and failure occurred by yielding of the reinforcement of the north column in tension about 3 feet from the top and by crushing on the inside of the column below the junction of the bracket and the lower haunch.

A number of diagonal cracks ran between the sections of tension and crushing failures. Maximum load, 232,000 pounds.

Specimen 13E1.—In this specimen of rectangular cross section the reinforcement was crowded together closely and was probably not as nearly in its designed position as in the other specimens. At a load of 30,000 pounds there were a large number of cracks near mid span, around the corners of the frame, and across the outside faces of the columns. At 60,000-pound load several diagonal cracks had opened between the south load point and the end of the girder. At the maximum load of 77,000 pounds the top of the specimen began to crush just inside the south load point. The crushing extended from the edge of the bearing plate for a distance of several inches. Large tension cracks formed under the south load point and at the south corner. It was noticeable that a large number of tension cracks developed around the corners of the frame, radiating toward the inside corner as a center. These cracks extended to within 3 inches of the inside or compression face.

Values of the ultimate loads and other information regarding the tests are given in Table 4.

TABLE 4.—*Results of tests*

Specimen number	Age	Ultimate load	Manner of failure
	Days	*Pounds*	
13A1	43	120,000	Bond at outside of north corner, followed by crushing at inside of corner; tension at middle between load points.
13A2	39	119,000	Compression at inside of north corner; tension at outside of corner and at middle between load points.
Average	41	119,500	
13B1	42	152,000	Compression at top of north bracket; some shearing between the flange and web at north corner.
13B2	40	138,000	Tension at middle of top member and at outside of north corner on column; followed by crushing at bottom of north bracket; shearing between tee and web at corner.
Average	41	145,000	
13C1	39	182,000	Compression at bottom of north bracket; tension at outside of north bracket and in top member between load points.
13C2	41	148,000	Tension at south end in outside face at bottom of bracket, followed by crushing on inside at bottom of bracket; this specimen was weakened by the accidental omission of two of the reinforcing bars in the outside face of each column, where failure occurred.
Average	40	165,000	
13D1	40	208,500	Compression at south end at middle of lower haunches and tension in outside face of column at bottom of bracket.
13D2	41	232,000	Compression at north end at bottom of lower haunch, tension at outside face at bottom of bracket, and in top member between load points.
Average	41	220,250	
13E1	41	77,000	Compression just inside of south load point.

2. THRUSTS AND MOMENTS

The ratio of the end thrusts to the downward load for the tests of frames with hinges held stationary was calculated from the gauge readings of the hydraulic jacks. This ratio, in general, seemed about constant for each specimen until near the maximum load, when it

decreased considerably. The variation could probably be ascribed to a decrease in the moment of inertia of section at points of high stress. Obviously at stresses near the ultimate strength less elasticity of action would be expected than at lower loads.

Table 5 presents (*a*) ratios of horizontal thrust to total vertical load (average for all but ultimate loads), (*b*) average actual bending moments calculated from the measured vertical loads and horizontal thrusts, and (*c*) bending moments determined by the analytical method described in Section II, 1, on the assumptions that the moment of inertia varied throughout all specimens—first, as the cube of the depth of section and, second, as the 5/2 power of the depth of section. A fair agreement between calculated moments and the average of observed moments is seen, but the variation of individual values from the averages is large.

TABLE 5.—*Comparison of observed and calculated moments*

Specimen number	$\frac{H}{P}$ average of test	Ratio of bending moment to $\frac{Pl}{6}$					
		From test—		Calculated ($I = Qd^3$)—		Calculated $I = Qd^{5/2}$—	
		At mid span	At corner	At mid span	At corner	At mid span	At corner
13A1	0.168	0.568	0.432				
13A2	.202	.480	.520				
Average	.185	.524	.476	0.481	0.519	0.481	0.519
13B1	.200	.486	.426				
13B2	.236	.392	.520				
Average	.218	.439	.473	.370	.524	.379	.517
13C1	.241	.380	.438				
13C2	.305	.215	.602				
Average	.273	.297	.520	.258	.536	.271	.526
13D1	.312	.198	.574				
13D2	.352	.095	.674				
Average	.332	.146	.624	.186	.590	.203	.577
13E1	.218	.440	.560	.481	.519	.481	.519

Values of the bending moment at mid span, taken from the third and seventh columns of Table 5, are plotted in Figure 22 as ordinates against horizontal lengths of bracket as abscissas. Since the frames of type D had a haunch different in shape from those of the other frames, it was found convenient to reduce it to an equivalent length of 45° bracket. From calculations it was found that the haunch of type D would produce the same moment at mid span as a 45° bracket 32 inches in horizontal length. The points in Figure 22 which represent average bending moments as determined by test are seen to agree fairly well with the calculated bending moments based on

equation (1). Considering the variable nature of the materials, the difference in details of design and dimensions, and the various possible sources of error in observations, considerable differences between calculated moments and the moments determined from the measured strain in individual specimens are to be expected.

The variation of the bending moment throughout the frames may be seen in Figure 23, which shows graphically the relative magnitude of the actual bending moments and their distribution in the different types of frame as determined by the tests. This variation is due to two distinct factors—variation in stiffness and variation in the shape of the axis of the frame—as noted in Section II, 1. It is seen that while the moment at mid span varies with the size of the brackets,

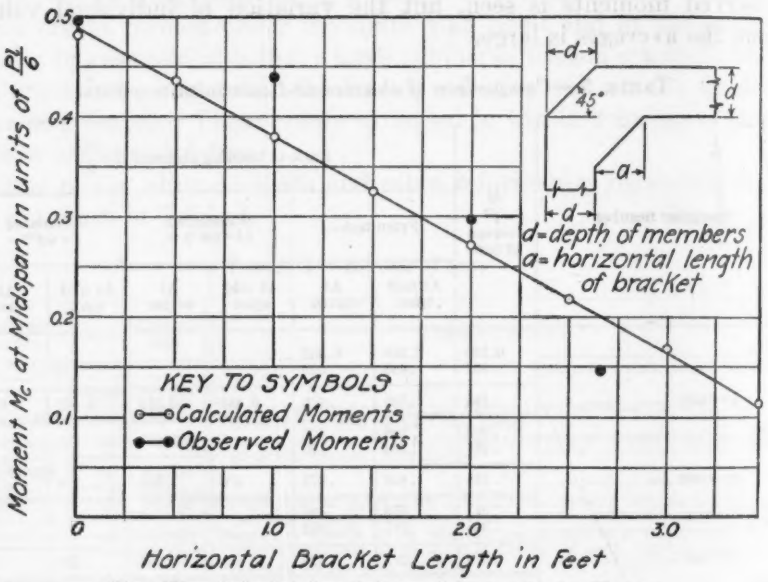

FIG. 22.—*Calculated and observed moments at mid span*

the moment at the corner of the frame is about the same in all types of frame.

3. FLEXURAL STRESSES AND DEFORMATIONS

Tabulated strain gauge data from the tests of all frames are given in Appendix I, which also contains diagrams showing the positions of all gauge lines for measurement of deformations and deflections and shows the positions with respect to these gauge lines of cracks and crushed areas observed at the maximum loads.

Stresses in the steel reinforcing bars as determined from strain gauge measurements are shown graphically in Figures 24 to 26. The stresses were measured on the reinforcing bars which were within the concrete 1½ to 3 inches from the surface. The points where a line

lying about 2 inches (to proper scale) within the frame intersects the lines radiating from the axis of the frame indicate the positions of the centers of the gauge lines in which the strains were measured, and the distance from the axis along the radiating line indicates the intensity of the stress. Within straight portions of the frame the solid lines connecting the stress at successive gauge lines give a stress graph which indicates roughly the probable values of the stress at points intermediate between gauge lines. At angles in a frame the stress can not be so interpolated with even approximately correct results. Light broken lines are used to connect the points wherever

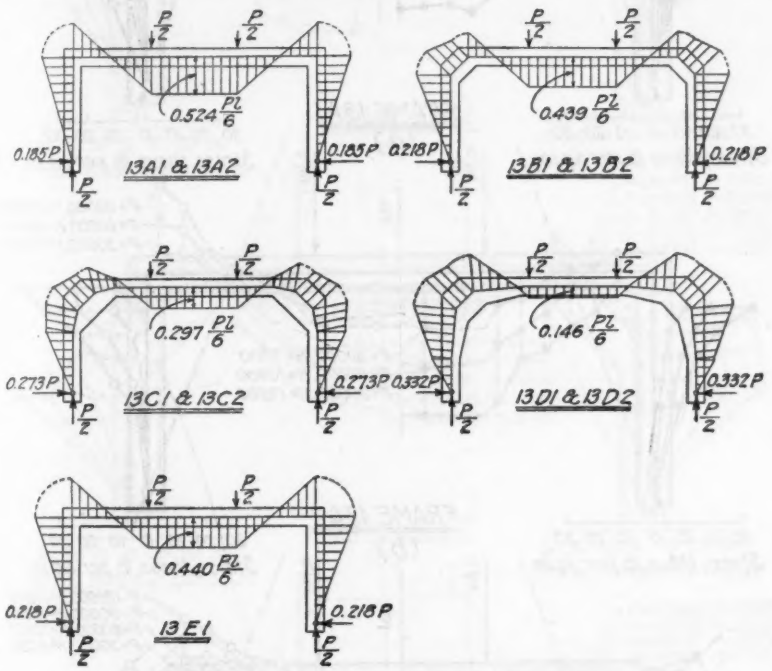

FIG. 23.—*Relative moments in frames*

a direct interpolation of this kind is not permissible. While the stresses shown represent combined flexural and direct stresses, the latter (which were compression for all cases of downward loading) were comparatively small and did not exceed 7 per cent of the total maximum stress in the extreme case of the frames of type D. For the other frames the direct stresses are much less, and, hence, do not have an appreciable influence upon the total stresses measured.

The calculation of stresses in the concrete and steel of these frames is quite laborious, due to the many changes in cross section and reinforcement and the variation in the bending moment. A sufficient number of calculations have been made, however, to show a

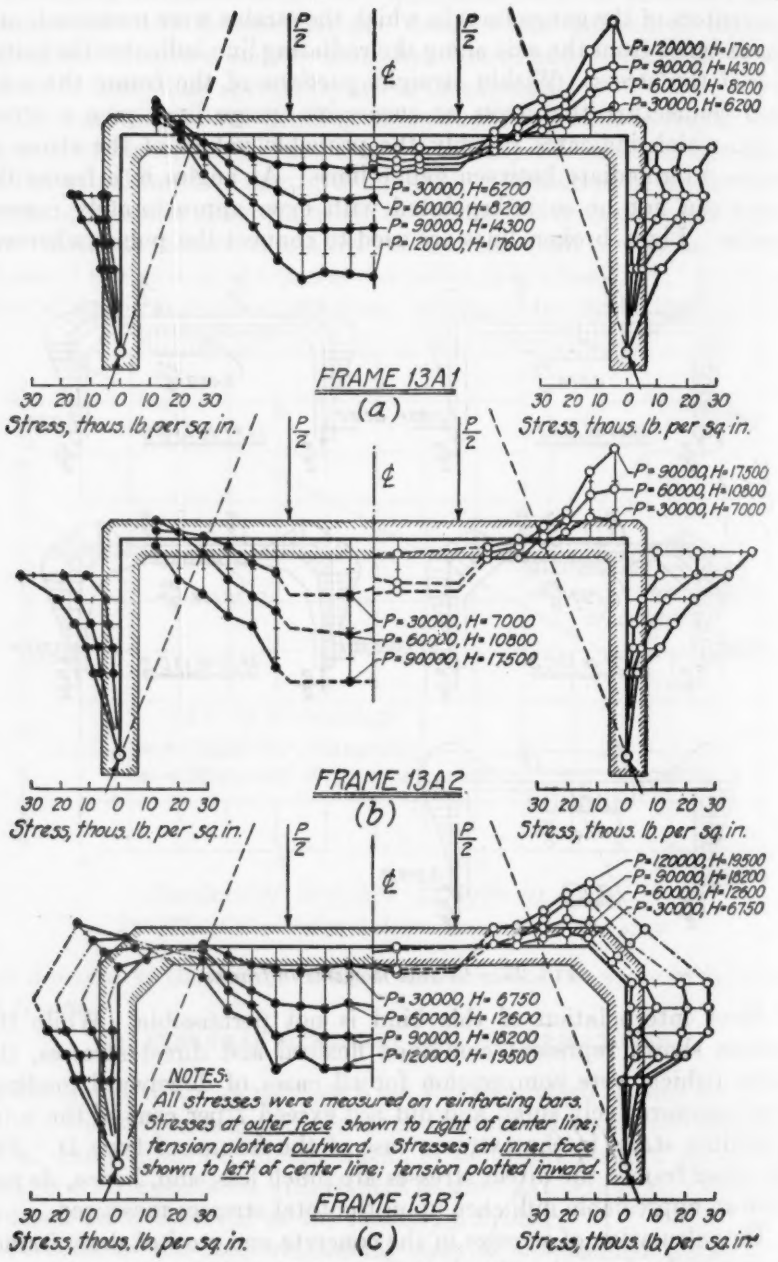

FIG. 24.—*Observed stresses in specimens 13A1, 13A2, and 13B1*

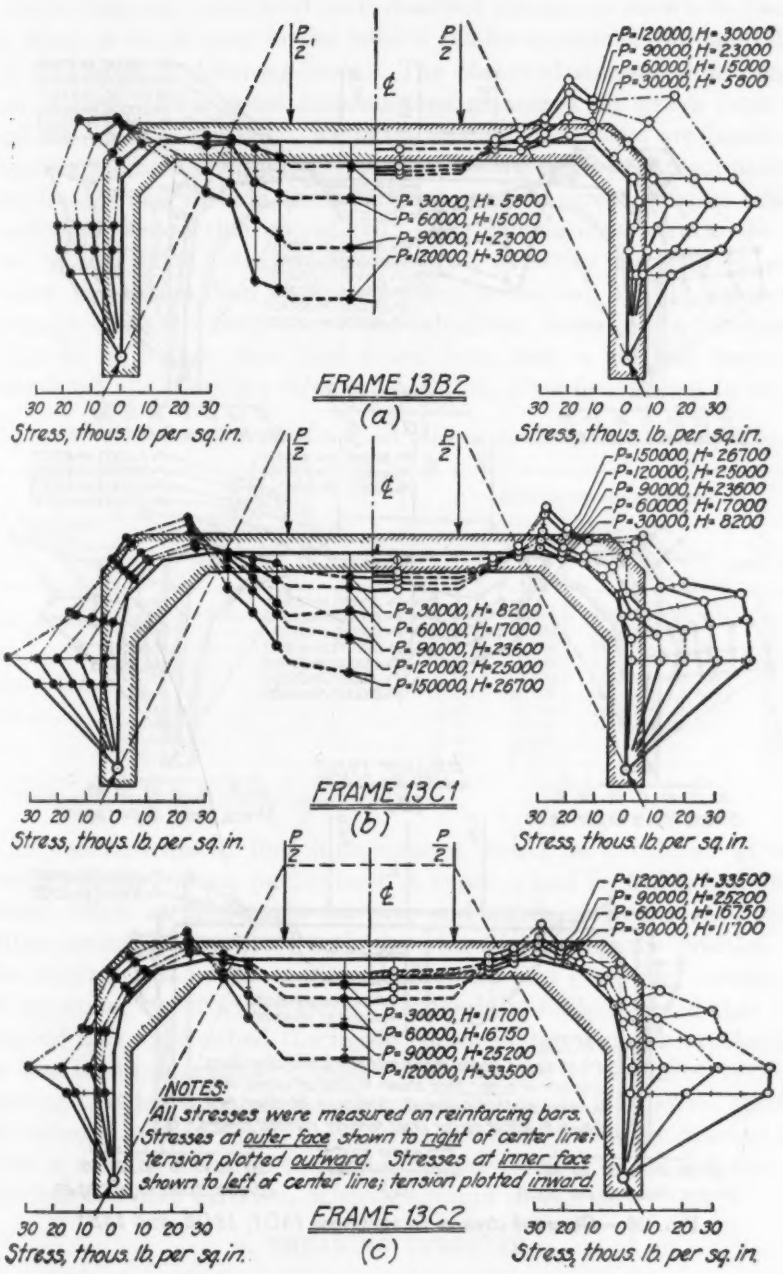

FIG. 25.—*Observed stresses in specimens 13B2, 13C1, and 13C2*

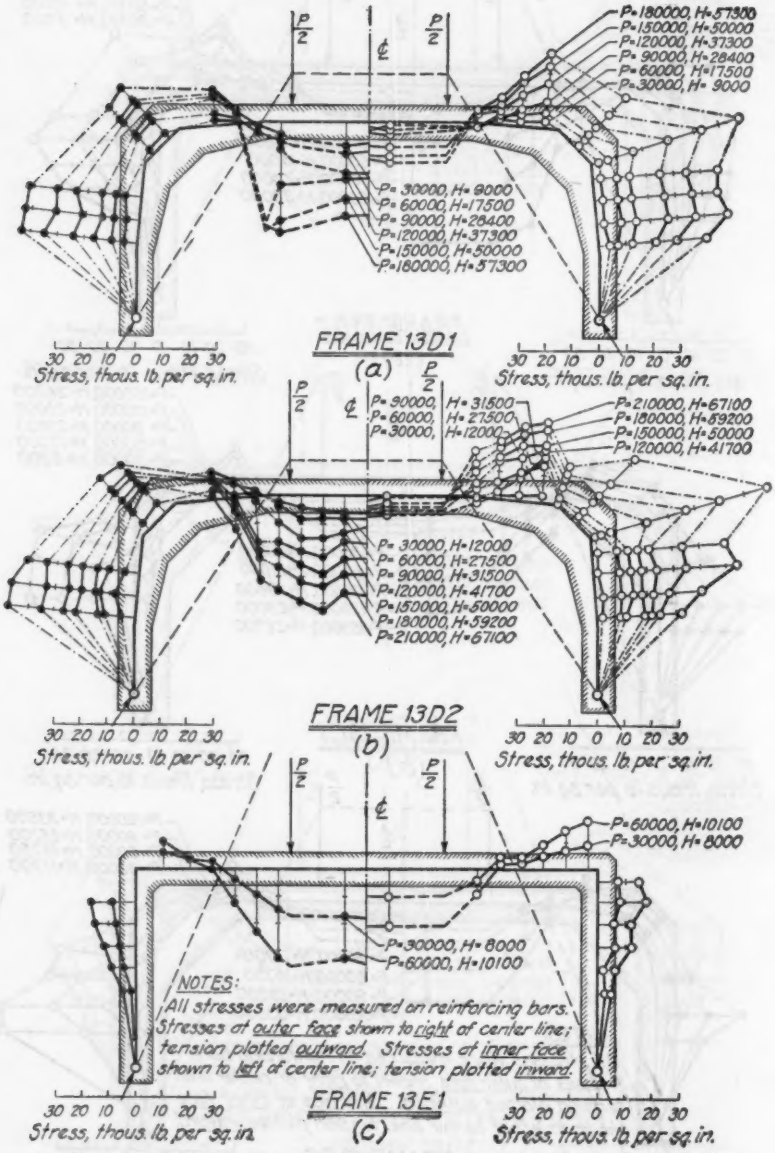

FIG. 26.—*Observed stresses in speimens 13D1, 13D2, and 13E1*

fair agreement with the results of the tests. An example of the comparison between calculated and observed stresses is shown in Table 6, which gives stresses in the tension reinforcement at mid span due to a number of different loads. The observed stresses were determined from the average deformations measured on gauge lines 22 and 22a of each specimen, while the calculated stresses are based on bending moments computed from the known loads and reactions on the frames and include the small compressive direct stresses which existed at the section considered. The calculations were made on the conventional "straight-line theory" of stress distribution and follow the assumption that no tension is carried by the concrete. In most cases the table shows the calculated stress in the reinforcement to be higher than that found from test, a relation between calculated and observed stresses which has often been found to exist.

TABLE 6.—*Comparison of calculated and observed tensile stresses in reinforcement*

Specimen number	Stress	Load on specimen (pounds)				
		30,000	60,000	90,000	120,000	Maximum load
13A1	Calculated	11,500	32,000	42,300	61,400	61,400
	Observed	12,000	21,800	31,600	(1)	(1)
13B1	Calculated	10,000	22,000	34,500	55,900	60,400
	Observed	7,100	19,600	30,000	40,100	44,500
13C1	Calculated	7,100	13,000	23,600	45,500	46,500
	Observed	3,600	13,700	21,700	31,000	(1)
13D1	Calculated	5,300	11,700	12,900	18,500	50,000
	Observed	7,500	11,000	18,200	20,200	58,200
13E1	Calculated	8,600	32,400			42,900
	Observed	18,100	34,900			47,800

[1] Yield point of steel, 55,000 to 60,000 lbs./in.²

It was anticipated that high stresses would be developed at the corners of the frames, particularly in types A and E, which had only 2-inch fillets at the inside corners, and strain measurements were taken around the corners with the idea of locating the position of the neutral axis. The readings taken did not give very complete information, but it was evident from the information gained that the neutral axis approached the inside corner of the frame very closely, so that high compressive stresses were produced by the usual vertical loading. It is evident that such concentrations of fiber stress should be reduced, and it would seem advisable that a fillet or bracket be used in a sharp corner of this kind. A curved fillet or bracket should produce the best variation of stress around the corner.

4. SHEARING STRESSES

In all cases the frames were highly reinforced against diagonal tension by the use of U stirrups and bent-up longitudinal bars. The ends of stirrups were hooked, being bent out into the flange of

the T sections and bent inward in the rectangular sections. The bent-up bars were also anchored by semicircular hooks having a radius of four diameters of bar.

The effectiveness of the web reinforcement was demonstrated by the fact that none of the frames failed by diagonal tension, and that diagonal cracks were, in general, quite small. Knowing this, the shearing unit stresses which were developed seemed quite noteworthy, inasmuch as they are considerably higher than have been

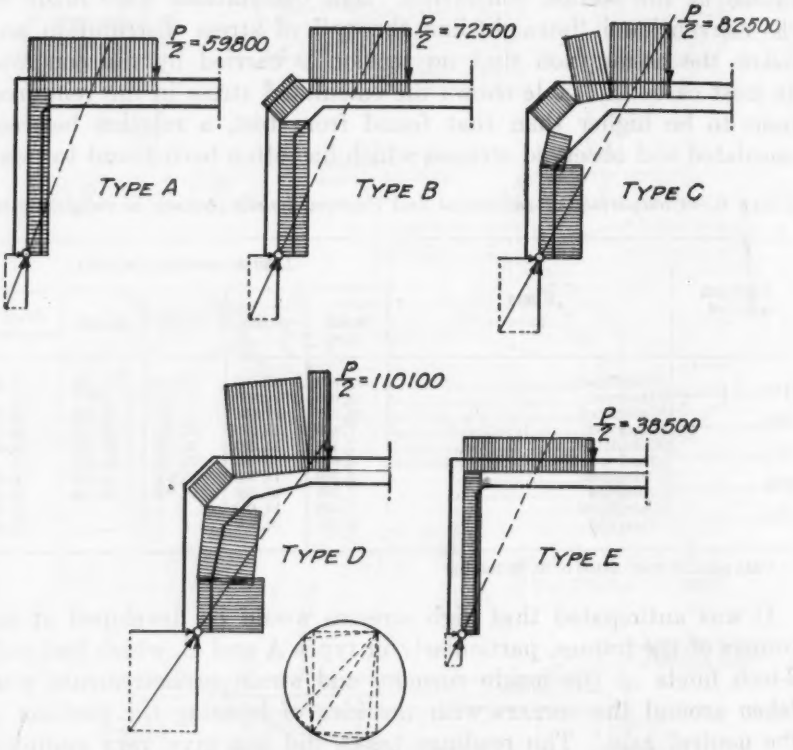

FIG. 27.—*Shear diagrams for frames at maximum load*

found in any tests outside the investigations of the concrete ship section.[8]

Shear diagrams for the different frames at maximum load are shown in Figure 27, and Table 7 gives values of the shearing stresses developed, as calculated at sections of maximum shear just outside the load points. The diagrams show the direction of the axis in each portion of the frame. The total shear at any section in this figure is the component, at right angles to the axis of the frame, of the reaction shown at the lower end of the left end post. The shear-

[8] Slater, Lord, and Zipprodt, Shear Tests of Reinforced Concrete Beams, B. S. Tech. Paper No. 314; 1926.

ing stress, v, equals $\frac{V}{bjd}$, in which V is the total shear, b is the width of the stem of the beam or end post, jd is the distance from the center of the tensile to the center of the compressive bending stresses, and d is the depth of the member. Specimens 13A1 to 13D2, inclusive, were of T section, having a flange 30 inches wide and 3 inches thick, and the value of j used was 0.88. Specimen 13E1 was of rectangular section, and the value of j used was 0.83. A comparison is also made in the table between the shearing stress and the compressive strength of the concrete as determined from tests of 6 by 12 inch cylinders made and tested with the frames.

TABLE 7.—*Maximum observed shearing stresses in frames*

[No failures occurred by diagonal tension]

Specimen number	Maximum vertical shear	Width of section, b	Depth of section, d	$b\,j\,d$	Shearing unit stress v	Cylinder strength f'_c	Ratio $\frac{v}{f'_c}$
	Pounds	*Inches*	*Inches*	*Square inches*	*Lbs./in.²*	*Lbs./in.²*	
13A1	60,000	8.12	9.75	69.7	860	3,110	0.28
13A2	59,500	8.00	9.75	68.6	865	3,765	.23
13B1	76,000	8.12	10.00	71.5	1,060	4,260	.25
13B2	69,000	8.00	9.75	68.6	1,005	3,665	.27
13C1	91,000	8.25	9.75	70.8	1,285	4,505	.29
13C2	74,000	8.27	9.75	71.8	1,030	4,040	.26
13D1	104,200	8.12	9.87	70.6	1,475	4,420	.33
13D2	116,000	8.12	10.12	72.3	1,605	5,860	.27
13E1	38,500	8.00	8.92	59.2	650	4,995	.13

Since there were no failures by diagonal tension, and no strain measurements were taken on the stirrups, there is nothing to show how high a shearing stress could have been developed. The shearing stresses were accompanied by a small, direct compression which balanced a little of the stress on the tension side of the frames and may have reduced somewhat the tendency to diagonal tension failure; still, there were generally fine vertical tension cracks present just outside the load points at very low loads. It does not seem likely that the direct compression produced any considerable increase in the resistance to diagonal tension.

Due to the fact that the positive and negative moments in continuous frames may be equalized by the judicious use of haunches, the magnitude of the moments is usually comparatively small; conversely, in such frames the shearing stresses will be correspondingly large. Hence, it is of considerable value to find that safe shearing strengths may be obtained which are much greater than those commonly allowed in building practice. This is clearly dependent, however, upon the use of a sufficient amount of web reinforcement, properly distributed and anchored, and upon proper anchorage of the longitudinal reinforcement.

5. MOMENT OF INERTIA

In Section II, 1, it was stated that in computing I for the purpose of determining the probable moment distribution in a frame I was assumed to vary as $d^{5/2}$. A study of the variation in I with d and with the increase of load is here made with the purpose of deriving a simple empirical expression for I which, without taking into account small variations in cross section and reinforcement, will indicate the proportional variations in I throughout the frame with sufficient accuracy to justify its use in determining moment distribution in the structure.

The distribution of statically indeterminate bending stresses is governed by the relative stiffness of the various parts of the structure. The stiffness of a member in flexure is usually measured by two quantities; I, the moment of inertia, a function of the size and shape of the cross section, and E, the modulus of elasticity, a physical property of the material. However, in a composite member of steel and concrete, the latter of which is so deficient in tensile strength, the modulus of elasticity, the tensile resisting moment of the concrete, the position of the neutral axis, and, consequently, the moment of inertia about the neutral axis vary with the stress in the member. A large reduction in I occurs when the concrete fails on the tension side of the member, and a further reduction takes place in E and I as the concrete fails to take compressive stress in proportion to its deformation. Throughout this variation in stress distribution for the concrete part of the member the neutral axis changes and this, in turn, slightly affects the moment of inertia of both the concrete and steel areas.

Aside from the question of the effect of stress, the variation in the moment of inertia with the shape of the cross section of a member must be considered. For rectangular areas of width b and depth d, containing equal percentages of reinforcement similarly placed, I varies as bd^3. If such areas contain not equal percentages, but equal areas, A, of steel similarly placed, I varies with powers of d, which lie between 2 and 3. Similarly for a T-beam of constant flange width, constant thickness, and constant area of reinforcement, but varying depth, I varies according to powers of d, which lie between 2 and 3. For a given member, however, the exponent may vary considerably between these limits.

In calculating I for a section of a reinforced concrete beam, especially when combined flexure and direct stress are encountered, a clear distinction must be made between the center of gravity and the axis of zero stress usually termed the neutral axis. One method of calculation (commonly termed the method of transformed sections) is to consider that the effective area of a section consists of the uncracked portion of concrete and an imaginary concrete area which has the same resistance to bending and to direct forces as the rein-

forcement. Bending moments and moments of inertia of the section are calculated about an axis through the center of gravity of this effective area.

However, the resultant stress at any point in the section will not, in general, be proportional to the distance from an axis through the center of gravity of this section. If there were no direct stresses present, the neutral axis (the axis of zero stress) would pass through the center of gravity of the effective area. The effect of a direct stress is to make the resultant stress at any point greater or less than the stresses due to flexure alone, and thus to shift the axis of zero stress. The resultant stress will then be proportional to the distance from the neutral axis rather than from the gravity axis.

Moments of inertia calculated, by the method described, from the nominal dimensions of the cross section of the test specimens are shown by the broken lines in Figure 28. A section 10.5 inches in effective depth and having 4.75 per cent of steel in both tension and compression was assumed. Using a modulus of rupture of 450 lbs./in.^{2} for this concrete and a value of n equal to 8, the section that may be assumed to be intact at different stages of loading was determined. The discontinuity of the broken line is a recognition of the sudden decrease which should occur in the moment of inertia with the formation of cracks.

As a method of determining the value of the product EI from test data, use was made of the well-known flexure formula $M=\frac{SI}{c}$. This may be written in the form $I=\frac{Mc}{Ee}$, in which e is the unit deformation and c is the distance from the neutral axis to the point where e is measured. Values of M, c, e, and d were obtained from the test data. The sections considered were on members having tension and compression faces parallel, or inclined to each other not more than 14°, as in the case of the tapered haunches of frames 13D, 1 and 2. The effect of this slight amount of taper was neglected and d was measured in all cases on a section normal to the axis of the frame (a line between tension and compression faces). From the measured values of d and the strains on tension and compression gauge lines at a given cross section the position of the neutral axis and the value of c were calculated. For convenience, E has been considered as having a constant value of 3,750,000 lbs./in.^{2}, which was the initial modulus of elasticity for this concrete, and all variation in the quantity EI is included in the single quantity I. Figure 28 shows the variation in I at different values of the compressive stress, f_c, in the concrete as determined from sections approximately 10.5 inches in effective depth.[9] The wide divergence of points shown

[9] A somewhat similar variation in the moment of inertia of a reinforced concrete beam is described by Dr. P. von Emperger in an article "Die Wahre Grosze des Tragheitsmoments im Eisenbetonbalken," Beton und Eisen, June 5, 1916.

may be attributed to errors of observation in M, c, and e to a considerable variation from the nominal depth of 10.5 inches, to the variation from the design dimensions of the section, to the difference in the steel area used in different specimens, to lack of proportionality between stress and distance from the neutral axis, and to the formation of cracks.

Until the concrete in the tension surface begins to crack, I should be expected to remain approximately constant. For Figure 28 the computed value of I with the concrete intact is 3,450 in.^{4}, and this value has been used in the graphs of that figure for all stresses below 500 lbs./in.^{2}

The tension failure of the concrete began generally when the compressive stress was about 500 lbs./in.^{2}, and after this the moment of

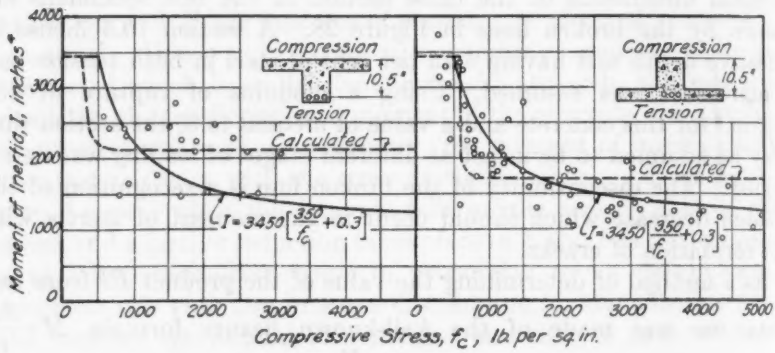

FIG. 28.—*Variation in I with compressive stress*

inertia decreased rapidly. The average values of the experimental data are represented roughly by the hyperbola

$$I=3{,}450\left(\frac{350}{f_c}+0.3\right).$$

Further values of I were computed from the test data for members of various depths and for loads giving several different ranges of computed compressive stresses and have been plotted in Figure 29 as ordinates against depths of section as abscissas. From the average curves drawn for each range of compressive stress, I is found to vary approximately as $d^{5/2}$. Hence, each curve represents an equation of the form $I=Qd^{5/2}$. The values of Q are found from Figure 29 to decrease as the values of f_c become larger, in the same general way as was shown by the values of I in Figure 28. This indicates that for a section in which a crack has formed the extent of the crack is a function of the compressive stress, f_c. The following general expression for the relation between moment of inertia and the compressive stress has been found to fit the curves of Figure 29.

$$I = 9.6d^{2.5}\left(\frac{350}{f_c} + 0.3\right) \tag{11}$$

It is assumed that the cracks began to form when the compressive stress was approximately 500 lbs./in.^{2}; before the formation of cracks, the value of f_c in equation (11) may be taken at 500, which modifies equation (11) to

$$I = 9.6d^{2.5} \tag{12}$$

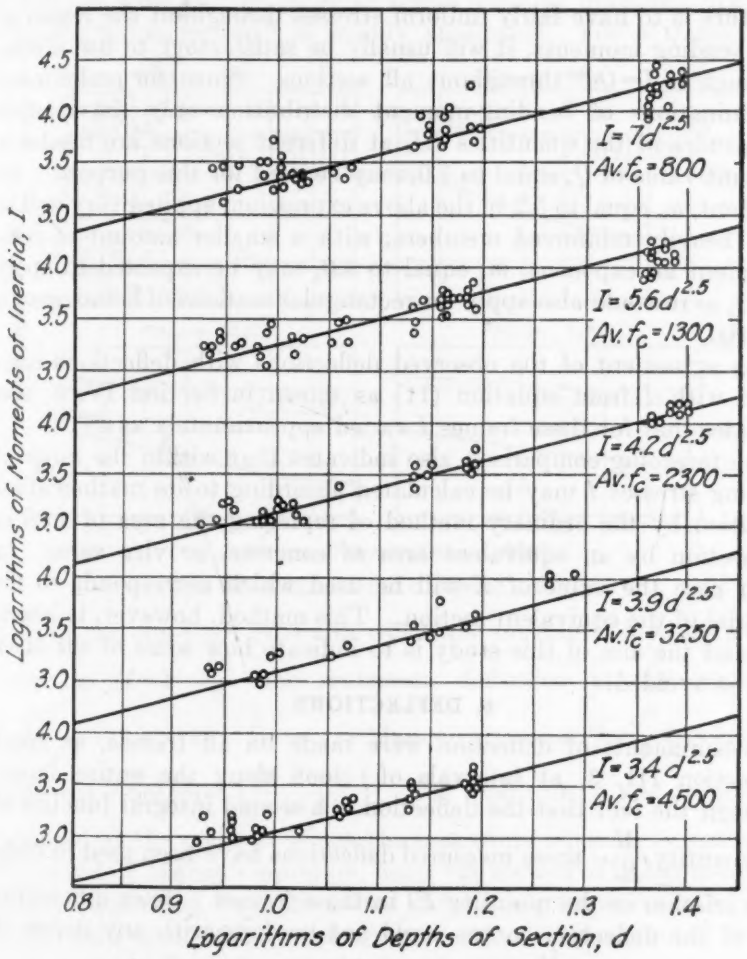

FIG. 29.—*Variation in I with depth of member.*

Equation (11) shows that at a compressive stress of 1,500 lbs./in.^{2} in the concrete, the value of I is only about half as great as it was before the tensile strength of the concrete was lost. Hence, in analyzing a structure especially for stresses above ordinary working stresses, the use of the assumption that I varies throughout directly as some power of the depth of members is not exactly logical and will

give too high a value of I at points of high stress. This is confirmed by specimens of the types B and C. Equations (11) and (12) can not be expected to apply to members in which the shape of cross section, percentage of reinforcement, or quality of concrete varied greatly from those used in these tests. It is believed, however, that these equations show the general way in which the moment of inertia varies in a reinforced conrete member. For a preliminary determination of the distribution of moment in design, especially if the structure is to have fairly uniform stresses throughout the region of high bending moments, it will usually be satisfactory to use a relation such as $I=Qd^m$ throughout all sections. Since for preliminary determinations of bending-moment distribution only the relative magnitudes of the quantities EI, at different sections are needed a constant value of Q, equal to 1.0, may be used for this purpose. An exponent, m, equal to 5/2 in the above expression, applied very well to these heavily reinforced members; with a smaller amount of reinforcement an exponent, m, equal to 3.0, may be expected to apply better, as it would also apply for rectangular sections of homogeneous material.

The agreement of the observed deflections with deflections computed with I from equation (11) as shown in Section IV, 6, also indicates that for these frames I varied approximately as $d^{5/2}$.

The foregoing comparison also indicates that within the range of working stresses I may be calculated according to its mathematical definition by the ordinary method of replacing the area of steel in the section by an equivalent area of concrete, or vice versa. In either case the value of E will be used which corresponds to the material of the equivalent section. This method, however, is laborious, and the aim of this study is to indicate how some of the labor may be avoided.

6. DEFLECTIONS

Measurements of deflection were made on all frames, as noted in Section III, 3, at intervals of 1 foot along the entire frame. Through the fact that the deflection is a second integral function of the quantity $\frac{M}{EI}$, these measured deflections have been used to study the variation in the quantity EI in these frames. Since differentiation of the deflection curves could not be done with any degree of accuracy, the exact $\frac{M}{EI}$ diagram corresponding to a given elastic curve was not found; however, the reverse operation was performed. Knowing values of M from the observed loads and reactions and assuming certain values of EI, elastic curves were obtained by two successive graphical integrations of the $\frac{M}{EI}$ curves, and these curves were then compared with the experimental curves.

Figure 30 shows values of the observed and computed deflections, as well as the $\frac{M}{EI}$ diagrams upon which the latter were based, for frames of types A, B, C, and D, at a load of 60,000 pounds. In calculating values of EI, the quantity E was assumed constant and equal to 3,750,000 lbs./in.^{2}, and the value of I was computed by use of equation (11). A good agreement is seen between the calculated and observed deflections.

For use with any rectangular frame without brackets, Maney's equation for deflection[10] is readily applicable. For a frame with

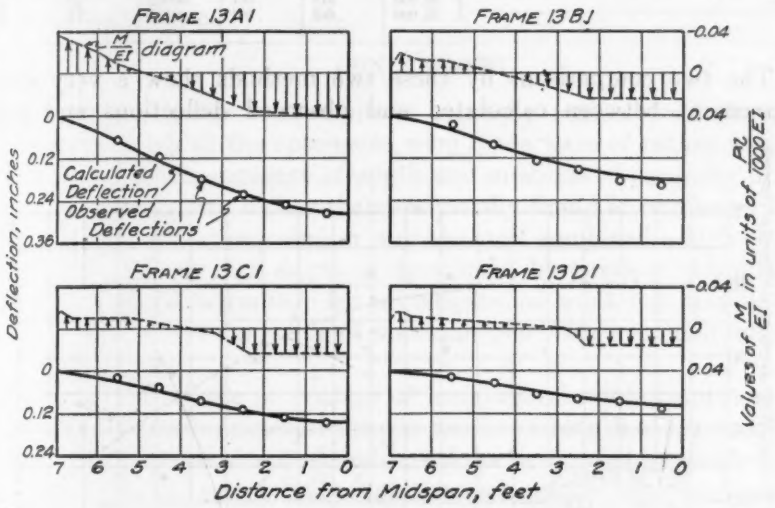

FIG. 30.—*Calculated and observed deflections*

loads at the one-third points in which the maximum moment at the center is $M=k'\frac{Pl}{6}$, the maximum deflection at the center is $\frac{Pl^3}{1{,}296\ EI}(27\,k'-4)$. Hence, in Maney's equation, $f=\frac{cl^2}{d}(e_s+e_c)$, the coefficient c becomes $\left(\frac{27\,k'-4}{216\,k'}\right)$. The quantities e_s and e_c must be measured at the point at which the maximum moment is measured. By the aid of Maney's equation, using the measured deformations in the steel and using for d the actual distance center to center of reinforcing bars upon which readings were taken, the computed deflections shown in Table 8 were obtained.

[10] "Relation between deformation and deflection in reinforced concrete beams," by G. A. Maney, Proc. A. S. T. M., Technical Papers, 14, p. 310; 1914.

TABLE 8.—*Calculated and observed deflections at mid span*

Specimen number	Load	k'	c	(e_s+e_c)	Calculated deflection $\left[c\frac{P}{d}(e_s+e_c)\right]$	Observed deflection
	Pounds				*Inches*	*Inches*
13A1	30,000	0.466	0.085	0.00052	0.14	0.14
	60,000	.648	.097	.00099	.31	.28
	90,000	.590	.094	.00138	.42	.42
13A2	30,000	.400	.079	.00074	.18	.16
	60,000	.536	.090	.00139	.39	.39
	90,000	.500	.088	.00219	.60	.68
13E1	30,000	.314	.067	.00093	.23	.26
	60,000	.560	.091	.00186	.61	.55

The two comparisons by these two methods show a very close agreement between calculated and observed deflections and give

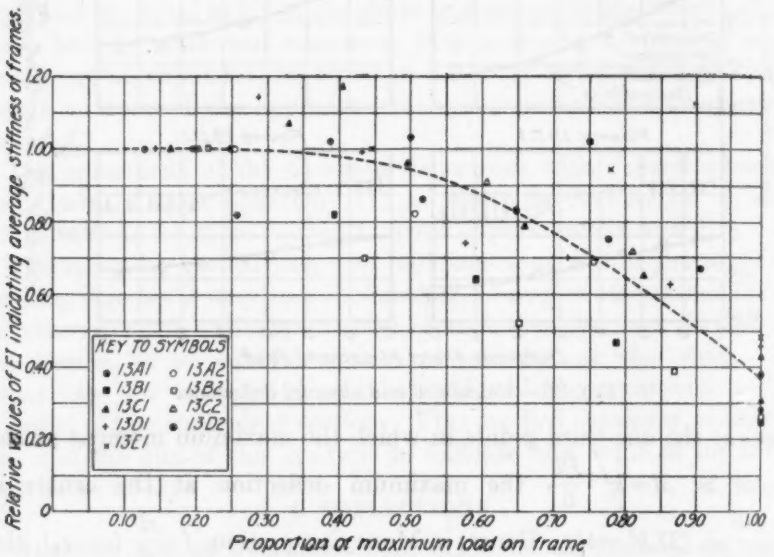

FIG. 31.—*Decrease in stiffness with increasing loads on frames*

further evidence that theoretical relations which were derived for elastic structures also hold true for these frames.

Further use has been made of the measured deflections in studying the variation in stiffness of each frame as a whole during the application of the test loads. In a homogeneous beam within the elastic limit of the material the quantity EI is constant and is proportional to the ratio of load to deflection, P/f. In these test specimens the ratio P/f varied, and, hence, the variation in EI, which is proportional to P/f, may be calculated from measured values of P/f. On this basis Figure 31 has been constructed, using a relative value of P/f equal to unity for the 30,000-pound load on each frame. The value

of f used in each case was the average of measurements on deflection points 10, 11, 12, and 13, near mid span. While the decrease in stiffness with increasing load indicated in Figure 31 is similar to that shown by Figure 28, it must be remembered that in the former the deflections are influenced by the stiffness of all sections of the frame. While the various parts of the frame are subject to widely differing intensities of stress, the sections most highly stressed have the greatest influence upon the deflections at mid span. The decrease in stiffness under increasing load, as shown by both deflection and deformation readings, seems to be a typical phenomenon of reinforced concrete members.

7. CONCLUSIONS

In analyzing the test results it must be remembered that the materials of which the specimens were made were of rather unusual quality. The compressive strength and modulus of elasticity of the concrete were much higher than are usually found in reinforced concrete construction; in a similar way the steel combined a high elastic limit with a fairly high degree of ductility. Materials of this quality were of especial advantage for investigational work but may not be considered as representative of materials generally available for construction work.

The use of a large percentage of longitudinal reinforcement made it possible to utilize much of the compressive strength of the concrete, while the large amount of web reinforcement used permitted the development of exceptionally high shearing stresses without diagonal tension failures.

Certain definite effects have been determined from the use of brackets in the particular test pieces described herein, but more tests are necessary before any broad generalization can be made concerning the effectiveness that a bracket will have in different types and shapes of frames. A number of tentative conclusions, however, may be formulated.

1. From an analysis of the test results it appears that the reinforced concrete frame can be treated with a fair degree of accuracy by analytical methods similar to those used in arch analysis. A study has been made as to the validity of some of the assumptions usually employed in such an analysis.

2. For the purpose of determining the distribution of bending moments, it seems to be sufficiently correct to consider the entire section of a specimen as effective, even at points of sudden change of shape. The effect of such a change in shape upon the stress in the member is a matter which needs further experimental investigation.

3. In the analysis of statically indeterminate frames the modulus of elasticity of the material and the moment of inertia of the cross

section are quantities of primary importance. Within the range of working stresses, the value of the product EI as determined from a large number of test readings agreed closely with the value of EI as computed by the common method of replacing the steel area by an equivalent concrete area and neglecting the tension area of the concrete if cracks have formed. At higher stresses the tests indicate a decrease in the value of EI, resulting in a relative loss of rigidity at points thus stressed. This might produce a slight readjustment of the moment distribution, and some leeway should be allowed in the design of the structure to accommodate such an occurrence. It is to be noted, however, that if the structure can be designed so as to develop nearly uniform stresses throughout, the relative rigidity of different portions will change but little with increasing loads.

4. Fairly consistent quantitative information as to the variation in EI has been obtained from the tests of the different specimens. The value of EI appeared to vary about as the 5/2 power of the depth of the section. After the concrete began to fail in tension the value of EI gradually decreased, in the manner indicated by equation (11).

The assumption that EI can be expressed by a simple equation, $EI=Qd^m$ is evidently not correct, but will usually be satisfactory for preliminary designs. An exponent m equal to 5/2 in the above expression applied very well to these highly reinforced members; with a smaller amount of reinforcement an exponent m equal to 3 may be expected to apply, as it would also for rectangular sections of a homogeneous material. For determining bending moment distribution the relative magnitudes only of the quantities EI at different sections are needed, so that the magnitude of the coefficient Q is immaterial for such calculations.

5. Calculated deflections of the test specimens based on values of moment of inertia from equation (11) agree very well with measured deflections, and also with deflections calculated by use of Maney's equation. This is significant as showing a fairly consistent agreement among the various results of the test.

6. From calculations, the basis of which is confirmed by the tests, it is found that the effect of brackets on the bending moments in a frame may be expressed as a function of the clear span (from edge to edge of brackets), of the ratio of height to span of frame, and of the given loading. The importance of the various factors is indicated in equation (4).

7. The effect of brackets is sometimes considered as a shortening of the span of the loaded member; that is, the bracket is considered a part of the end support, and thus the center of bearing is brought out from the center line of the column. It has been found that this shortening of the span is not constant for a given bracket, but also varies with the ratio of height to span of the frame. For the frames tested, the total span may be considered as reduced by about two-

thirds of the horizontal length of the bracket at each end. While the total moment has been reduced in this way, its distribution between positive and negative sections has varied. The proportional amount of negative moment increased considerably as the size of bracket increased. Hence, while the decrease in total moment was in effect a shortening of the span, this viewpoint does not lead to logical conclusions, since the negative moment actually increased as the span was shortened.

8. The use of 45° brackets in these tests is not intended to imply that this shape is the most effective. For any given frame and loading, the most desirable shape of bracket may be determined. The general rule should be kept in mind that the bending moment diagram for a frame of uniform section is an approximate influence line for the effectiveness of brackets or haunches; that is, an ordinate at any point of this diagram represents the relative usefulness of an increase in section at that point.

9. While brackets will usually have rectilinear outlines, it is evident that the brackets of specimen 13D1 and 13D2, which approached a curved form, had certain advantages. This shape of bracket was very effective in reducing the moment at mid span, and it also produced a fairly uniform distribution of stress throughout. The result was that these frames withstood a much greater load than any frames of the other types.

10. Brackets should not be used for the purpose of reducing stresses, without also determining what effect they will produce upon moment distribution. A large bracket may produce a high moment at a section where it would not occur without the bracket and where the member consequently is not reinforced sufficiently. For example, it is seen from the test of specimen 13D1 that while the bracket was deep enough to provide for the large moment at the corner it caused failure to occur at the weaker section at mid height of the column.

11. The results of these tests confirm the theoretical deduction that brackets can be used to effect a considerable saving of material and of dead weight in a structure. The bracket eliminates the high local stress found at the sharp corners of a frame; it produces a more uniform variation in stress along the frame, thus minimizing the tendency for the formation of cracks; and it reduces bond and shearing stresses at the corners of the frame. Further, by the careful choice of the brackets the bending moments may be varied considerably, and thus a proper balance may be secured between the stresses in regions of positive and negative moments.

The desirable features mentioned apply to all forms of continuous beam and frame construction. In reinforced concrete work the forming of brackets and haunches is comparatively easy, and in important structures the saving of material should considerably overbalance the extra cost of construction.

APPENDIX I

TEST DATA AND SKETCHES OF FRAMES

A summary of deformations, deflections, loads, and reactions observed in the tests is given in Table 9. The table includes all original data of the tests except the stresses shown in Figures 24 to 26.

Following Table 9, detailed sketches showing the position of all strain gauge lines and deflection points, as well as the position of cracks at failure, are given in Figures 32 to 40. It will be noted that strain-gauge points on the steel are marked by solid circles, those on concrete by open circles, and deflection points by open triangles. The gauge lines are numbered to correspond with the data of Table 9. It is felt that the crack drawings furnish considerable information regarding the behavior of the frames under load.

TABLE 9.—*Data of tests*

[Loads are recorded in pounds, deflections or movements in inches, unit stresses in thousands of pounds per square inch, and unit deformations in thousandths of an inch per inch. The + sign indicates tensile stress or deformation and upward or outward deflection and the − sign indicates the opposite]

FRAME NO. 13A1

Observation	Load on frame (pounds)					Base moved outward
	30,000	30,000	60,000	90,000	120,000	
End thrust.....pounds..	6,200	6,200	8,200	14,300	17,600	5,500
End movement.....inch..	−.01	0	+.01	−.04	−.01	+1.64
Unit deformation on gauge line—						
101	−.04	+.04	−.04	−.11	−.89	.....
102	−.07	−.06	−.15	−.24	−.02	.26
103	−.15	−.15	−.22	−.13	−.63	.52
104	+.07	+.13	+.26	+.69	.....	2.03
105	+.15	−.04	−.02	−.04	.....	+.11
106	+.11	−.04	0	+.26	+.94	+1.26
Deflection on point—						
D1.....inch..	+.01	−.01	+.02	+.01	−.44	+.47
D2.....do....	+.01	0	+.03	+.04	−.22	+.32
D3.....do....	+.01	+.01	+.03	+.03	−.02	+.17
D4.....do....	0	+.01	+.01	+.02	+.06	+.04
D5.....do....	0	0	0	−.01	−.05	−.04
D6.....do....	−.03	−.02	−.07	−.10	−.43	−.10
D7.....do....	−.07	−.07	−.13	−.19	−.83	−.14
D8.....do....	−.09	−.09	−.18	−.27	−1.20	−.18
D9.....do....	−.11	−.12	−.22	−.34	−1.20	−.20
D10.....do....	−.13	−.14	−.26	−.39	−1.86	−.22
D11.....do....	−.15	−.15	−.28	−.42	−2.07	−.24
D12.....do....	−.13	−.14	−.28	−.42	−2.13	−.23
D13.....do....	−.13	−.14	−.26	−.40	−2.10	−.23
D14.....do....	−.11	−.12	−.23	−.36	−1.81	−.20
D15.....do....	−.09	−.10	−.19	−.27	−1.37	−.17
D16.....do....	−.06	−.07	−.12	−.18	−.93	−.13
D17.....do....	−.05	−.04	−.07	−.10	−.52	−.10
D18.....do....	−.01	−.01	−.02	−.02	−.10	−.04
D19.....do....	+.01	0	+.01	+.01	+.08	+.03
D20.....do....	+.01	+.01	+.03	+.04	+.28	+.13
D21.....do....	+.02	+.03	+.04	+.04	+.44	+.25
D22.....do....	+.01	+.01	+.03	+.03	+.57	+.36

TABLE 9.—*Data of tests*—Continued

FRAME NO. 13A2

Observation		Load on frame (pounds)				Base moved outward
		30,000	60,000	90,000	119,000	
End thrust	pounds	7,000	10,800	17,500	17,700	4,800
End movement	inches	+0.02	+0.01	+0.01	+0.03	+1.66
Unit deformation on gauge line—						
101		−.07	−.17	−.46		+.66
102		−.20	−.53	−.85		+1.22
103		−.30	−.77	−1.66		+.68
104		0	−.09	−.15	−2.52	+3.19
105		+.06	+.46	+1.18	+4.50	+1.16
106		−.20	−.28	−.35		+2.71
Deflection on point—						
D1	inches	0	+.01	−.03	−.84	+.34
D2	do	+.01	0	0	−.47	+.25
D3	do	+.02	+.03	+.04	−.10	+.12
D4	do	+.01	+.02	+.04	+.13	+.03
D5	do	−.01	−.02	−.03		−.03
D6	do	−.04	−.09	−.16	−.51	−.10
D7	do	−.07	−.17	−.30	−.98	−.14
D8	do	−.11	−.25	−.45	−1.47	−.21
D9	do	−.13	−.32	−.58	−1.93	−.25
D10	do	−.15	−.37	−.66	−2.27	−.27
D11	do	−.16	−.39	−.68	−2.47	−.28
D12	do	−.16	−.38	−.68	−2.52	−.28
D13	do	−.14	−.35	−.63	−2.34	−.26
D14	do	−.13	−.31	−.56	−2.00	−.24
D15	do	−.10	−.24	−.44	−1.55	−.20
D16	do	−.06	−.16	−.30	−1.07	−.14
D17	do	−.04	−.09	−.17	−.61	−.10
D18	do	0	−.02	−.03	−.13	−.03
D19	do	+.01	+.02	+.03	+1.0	+.03
D20	do	+.01	+.03	+.06	+.40	+.14
D21	do	+.02	+.04	+.10	+.68	+.29
D22	do	+.02	+.04	+.10	+.96	+.43

TABLE 9.—*Data of tests*—Continued

FRAME NO. 13B1

Observation	Load on frame (pounds)					Base moved outward
	30,000	60,000	90,000	120,000	152,000	
End thrust ..... pounds	6,750	12,600	18,200	19,500	26,700	9,100
End movement ..... inches	+0.02	+0.02	+0.02	+0.06	−0.01	+1.81
Unit stress on gauge line—						
35	−.4	−6.8	−1.6		−3.2	+8.6
32	−3.4	−10.5	−15.4	−23.3	−28.5	−3.8
28	−1.1	+3.0	+4.5	+10.5		+19.9
22	+9.0	+20.6	+30.0	+40.1	+34.9	+15.4
22a	+5.3	+18.7	+29.9	+40.1	+54.4	+13.9
23a	+7.1	+20.3	+29.6	+40.9	+43.1	+15.4
24a	+8.6	+19.9	+26.6	+36.0	+34.5	+14.6
25a	+6.7	+18.4	+29.8	+40.9	+58.1	+16.1
26a	+6.4	+14.2	+19.1	+24.4	+24.4	+17.6
Unit deformation on gauge line—						
101	−.17	−.39	−.40	−1.47		
102	−.13	−.30	−.52	−.99	−1.03	−.24
103	−.18	−.39	−.74	−1.05	−.90	+1.79
104	−.09	−.30	−.13	−.20		+1.25
105	−.18	−.41	−.53	−.81	−.74	−.22
106	−.04	−.28	−.15	−.24	+.40	−.18
Deflection on point—						
D1 ..... inches	+.02	+.03	+.03	+.04	−.35	+.46
D2 ..... do	+.04	+.03	+.05	+.06	−.21	+.30
D3 ..... do	+.01	+.02	+.04	+.06		+.13
D4 ..... do	−.01	0	0	+.01	−.04	+.02
D5 ..... do	0	−.01	−.01	−.01	+.01	−.02
D6 ..... do	−.02	−.04	−.06	−.10		−.18
D7 ..... do	−.04	−.03	−.15	−.25		−.23
D8 ..... do	−.05	−.13	−.23	−.40	−1.30	−.27
D9 ..... do	−.06	−.16	−.32	−.57	−1.67	−.32
D10 ..... do	−.08	−.19	−.37	−.66	−1.73	−.35
D11 ..... do	−.08	−.20	−.39	−.69	−1.67	−.36
D12 ..... do	−.08	−.20	−.39	−.68	−1.56	−.35
D1[illegible] ..... do	−.08	−.19	−.37	−.66	−1.53	−.34
D1[illegible] ..... do	−.05	−.15	−.30	−.56	−1.21	−.27
D15 ..... do	−.05	−.13	−.24	−.43	−.90	−.25
D16 ..... do	−.04	−.08	−.15	−.26	−.56	−.21
D17 ..... do	−.02	−.04	−.06			−.14
D18 ..... do	0	0	0	−.01	−.01	−.02
D19 ..... do	0	0	0	0	+.02	+.01
D20 ..... do	+.02	+.03	+.06	+.08	+.20	+.13
D21 ..... do	+.02	+.05	+.07	+.10	+.33	+.25
D22 ..... do	+.03	+.05	+.07	+.11	+.44	+.34

TABLE 9.—*Data of tests*—Continued

FRAME NO. 13B2

Observation	Load on frame (pounds)					Base moved outward
	30,000	60,000	90,000	120,000	138,000	
End thrust.....pounds..	5,800	15,000	23,000	30,000	31,500	8,300
End movement.....inches..	+0.04	+0.04	+0.05	+0.08	+0.07	+1.65
Unit deformation on gauge line—						
101	+.03	−.23	−.40	−.70	−1.40	+6.56
102	−.03	−.40	−.55	−.63	−.65	−.30
103	−.45	−.63	−1.03	−1.03	−2.05	+6.90
104	+.03	+.03	+.03	+.68	−.68	+1.70
105	−.55	−.18	−.30	−.80	−.95	−.45
106	+.70	+.73	+.73	+1.05	+3.60	+2.25
Deflections on point—						
D1.....inches..	+.01	+.01	+.02	+.03	+.35	+.43
D2.....do....	+.01	+.02	+.04	+.07	.....	+.28
D3.....do....	+.01	+.03	+.06	+.09	.....	+.14
D6.....do....	−.01	−.04	−.07	−.12	−.30	−.13
D7.....do....	−.03	−.09	−.18	−.30	−.65	−.19
D8.....do....	−.05	−.14	−.28	−.49	−1.00	−.24
D9.....do....	−.07	−.20	−.39	−.69	−1.36	−.29
D10.....do....	−.08	−.23	−.45	−.79	−1.58	−.32
D11.....do....	−.08	−.24	−.48	−.84	−1.74	−.33
D12.....do....	−.08	−.24	−.49	−.83	−1.80	−.32
D13.....do....	−.09	−.24	−.47	−.82	−1.73	−.32
D14.....do....	−.07	−.21	−.42	−.74	−1.49	−.30
D15.....do....	−.05	−.16	−.32	−.57	−1.17	−.25
D16.....do....	−.03	−.10	−.19	−.30	−.74	−.18
D17.....do....	−.02	−.05	−.09	−.16	−.37	−.13
D20.....do....	+.01	+.04	+.06	+.11	+.32	+.11
D21.....do....	+.02	+.05	+.08	+.15	+.53	+.21
D22.....do....	+.03	+.05	+.08	+.16	+.72	+.31

FRAME NO. 13C1

Observation	Load on frame (pounds)						Base moved outward
	30,000	60,000	90,000	120,000	150,000	182,000	
End thrust.....pounds..	8,200	17,000	23,600	25,000	26,700	48,000	8,200
End movement.....inches..	+0.02	+0.02	+0.02	+0.02	0	−0.03	+1.79
Unit deformation on gauge line—							
101	−.48	−.54	−.81	−.95	−1.27	−1.23	.....
102	−.05	+.14	−.09	−.18	−.16	−.53	+.02
103	−.22	−.48	−.54	−.95	−1.03	.....	+.46
104	−.03	−.11	−.20	0	−.36	−.36	+5.7
105	−.16	−.01	−.14	−.18	−.11	−.66	+.04
106	−.01	0	0	+.24	+.73	−.64	+.39
Deflection on point—							
D1.....inches..	+.03	+.05	+.08	+.11	+.22	.....	+.43
D2.....do....	+.02	+.04	+.07	+.11	+.21	.....	+.28
D3.....do....	+.01	+.02	+.04	+.07	+.12	+.31	+.16
D6.....do....	−.03	−.03	−.04	−.07	−.11	−.30	−.15
D7.....do....	−.02	−.05	−.08	−.13	−.22	−.58	−.28
D8.....do....	−.04	−.09	−.14	−.23	−.36	−.89	−.34
D9.....do....	−.04	−.11	−.21	−.32	−.49	−1.18	−.37
D10.....do....	−.08	−.14	−.24	−.38	−.58	−1.40	−.40
D11.....do....	−.08	−.15	−.25	−.40	−.61	−1.51	−.41
D12.....do....	−.08	−.15	−.26	−.41	−.62	−1.55	−.42
D13.....do....	−.07	−.14	−.24	−.39	−.58	−1.47	−.40
D14.....do....	−.05	−.11	−.19	−.31	−.46	−1.26	−.37
D15.....do....	−.05	−.09	−.15	−.24	−.37	−.97	−.35
D16.....do....	−.02	−.05	−.08	−.14	−.22	−.63	−.28
D17.....do....	−.02	−.01	−.05	−.07	−.11	−.33	−.15
D20.....do....	0	+.02	+.04	+.05	+.09	+.30	+.13
D21.....do....	+.02	+.05	+.08	+.12	+.18	+.64	+.28
D22.....do....	+.02	+.05	+.08	+.12	+.21	+.81	+.41

TABLE 9.—*Data of tests*—Continued

FRAME NO. 13C2

Observation	Load on frame (pounds)					Base moved outward
	30,000	60,000	90,000	120,000	148,000	
End thrust.....pounds..	11,700	16,750	25,200	33,500	30,500	13,700
End movement.....inches..	+0.02	+0.03	+0.04	+0.03	+0.03	+1.88
Unit deformation on gauge line—						
101	−.35	−.35	−.75	−.67	−.90	
102	0	−.32	−.37	−.02	−.05	+.22
103	−.20	−.50	−.75	−.25	−.25	+.63
104	−.10	−.12	−.40	+.52		
105	+.07	−.17	−.40	−.12	−.28	−.12
106	+.05	−.15	−.20	+.52		+.38
Deflection on point—						
D1.....inches..	+.01	+.04	+.09	+.13	+.53	+.48
D2.....do....	+.01	+.04	+.08	+.16	+.40	+.32
D3.....do....	+.01	+.02	+.06	+.10	+.24	+.16
D6.....do....	−.01	−.02	−.05	−.08	−.20	−.13
D7.....do....	−.02	−.04	−.09	−.16	−.40	−.27
D8.....do....	−.04	−.08	−.15	−.27	−.61	−.32
D9.....do....	−.07	−.12	−.24	−.40	−.86	−.37
D10.....do....	−.08	−.14	−.27	−.46	−.95	−.40
D11.....do....	−.09	−.15	−.29	−.48	−1.00	−.42
D12.....do....	−.09	−.16	−.29	−.49	−1.02	−.42
D13.....do....	−.08	−.14	−.27	−.46	−.97	−.42
D14.....do....	−.07	−.12	−.23	−.41	−.89	−.39
D15.....do....	−.04	−.08	−.16	−.29	−.65	−.36
D16.....do....	−.03	−.06	−.10	−.18		−.32
D17.....do....	−.02	−.03	−.06	−.09	−.24	−.18
D20.....do....	+.01	+.03	+.04	+.08	+.21	+.16

FRAME NO. 13D1

Observation	Load on frame (pounds)							Base moved outward
	30,000	60,000	90,000	120,000	150,000	180,000	208,500	
End thrust.....pounds..	9,000	17,500	28,400	37,300	50,000	57,300	58,500	17,500
End movement.....inches..	+0.01	+0.03	+0.04	+0.07	+0.08	+0.05	+0.06	+2.04
Unit deformation on gauge line—								
101	−.02	−.31	−.49	−.81	−1.04	−1.60	−1.78	+2.01
102	−.05	−.13	−.29	−.49	−.49	−.42	+.79	+.16
103	−.14	−.20	−.36	−.18	−.33	−.44	−.51	+.38
104	−.01	−.05	−.20	0	−.14	−.46	−.62	+2.28
105	−.14	−.18	−.35	−.36	−.42	−.53	−.62	+.16
106	−.09	−.16	−.23	−.23	−.22	−.22	−.31	+.12
Deflection on point—								
D1.....inches..	+.02	+.04	+.06	+.09	+.12	+.15	+.34	+.44
D2.....do....	+.01	+.03	+.05	+.08	+.11	+.14	+.28	+.30
D3.....do....	+.01	+.02	+.03	+.05	+.06	+.09	+.16	+.16
D6.....do....	−.01	−.02	−.04	−.06	−.07	−.15	−.13	−.13
D7.....do....	−.02	−.04	−.07	−.11	−.15	−.19	−.33	−.28
D8.....do....	−.04	−.07	−.11	−.18	−.24	−.31	−.53	−.39
D9.....do....	−.05	−.08	−.16	−.25	−.34	−.44	−.73	−.47
D10.....do....	−.06	−.10	−.18	−.30	−.40	−.53	−.86	−.53
D11.....do....	−.06	−.11	−.19	−.32	−.44	−.57	−.93	−.54
D12.....do....	−.07	−.12	−.20	−.34	−.45	−.59	−.97	−.58
D13.....do....	−.06	−.10	−.18	−.33	−.44	−.57	−.94	−.56
D14.....do....	−.05	−.09	−.16	−.30	−.39	−.50	−.81	−.54
D15.....do....	−.03	−.07	−.12	−.22	−.27	−.35	−.59	−.47
D16.....do....	−.03	−.04	−.07	−.12	−.16	−.20	−.36	−.53
D17.....do....	−.01	−.02	−.03	−.06	−.07	−.09	−.17	−.18
D20.....do....	+.01	+.02	+.03	+.06	+.07	+.08	+.17	+.17
D21.....do....	+.01	+.02	+.06	+.09	+.11	+.13	+.30	+.32
D22.....do....	+.03	+.05	+.06	+.10	+.12	+.13	+.23	+.49

TABLE 9.—*Data of tests*—Continued

FRAME NO. 13D2

Observation	Load on frame (pounds)								Base moved outward
	30,000	60,000	90,000	120,000	150,000	180,000	210,000	232,000	
End thrust.....pounds..	12,000	27,500	31,500	41,700	50,000	59,200	67,100	66,300	16,800
End movement.....inches..	+0.02	+0.02	+0.02	+0.05	+0.06	+0.06	+0.07	+0.08	+1.74
Unit deformation on gauge line—									
101	−.25	−.44	−.52	−.61	−.81	−.94	−1.28	−1.54	−1.39
102	−.05	−.24	−.31	−.44	−.59	−.66	−.72	−.93	+.04
103	−.18	−.35	−.37	−.70	−.81	−1.18	−1.18	−1.18	+.13
104	−.12	−.20	−.17	−.40	−.40	−.54	−.63	−.81	+.15
105	−.20	−.20	−.26	−.40	−.37	−.31	−.35	−.72	+.04
106	−.10	−.15	−.18	−.26	−.24	−.28	−.24	−.40	+.09
Deflection on point—									
D1.....inches..	+.02	+.04	+.04	+.05	+.08	+.10	+.14	.....	+.38
D2.....do....	+.01	+.03	+.04	+.05	+.08	+.11	+.14	+.45	+.26
D3.....do....	+.01	+.02	+.03	+.04	+.06	+.08	+.10	+.27	+.14
D6.....do....	−.01	−.01	−.02	−.03	−.05	−.06	−.09	−.21	−.12
D7.....do....	−.03	−.05	−.06	−.09	−.12	−.16	−.21	−.46	−.25
D8.....do....	−.03	−.08	−.09	−.13	−.21	−.27	−.36	.....	−.35
D9.....do....	−.05	−.12	−.14	−.23	−.30	−.39	−.53	−1.05	−.42
D10.....do....	−.07	−.15	−.18	−.28	−.36	−.47	−.62	−1.22	−.47
D11.....do....	−.06	−.15	−.18	−.29	−.38	−.50	−.66	−1.32	−.47
D12.....do....	−.07	−.16	−.19	−.30	−.39	−.51	−.68	−1.36	−.50
D13.....do....	−.05	−.15	−.18	−.29	−.38	−.47	−.65	−1.33	−.48
D14.....do....	−.05	−.13	−.15	−.25	−.34	−.44	−.58	−1.18	−.44
D15.....do....	−.03	−.08	−.10	−.17	−.23	−.30	−.41	−.88	−.37
D16.....do....	−.03	−.06	−.07	−.12	−.15	−.19	−.26	−.57	−.29
D17.....do....	−.02	−.04	−.04	−.06	−.07	−.10	−.13	−.30	−.16
D20.....do....	+.01	+.03	+.03	+.05	+.07	+.08	+.11	+.23	+.14
D21.....do....	+.02	+.04	+.06	+.08	+.10	+.13	+.18	+.43	+.27
D22.....do....	+.02	+.05	+.06	+.09	+.12	+.15	+.20	+.57	+.40

FRAME NO. 13E1

Observation	Load on frame (pounds)		
	30,000	60,000	77,000
End thrust.....pounds..	8,000	10,100	14,500
End movement.....inches..	0.06	0.05	0.05
Unit deformation on gauge line—			
101	−.22	−.37	−.64
102	−.44	−.92	−1.60
103	−.28	−.39	−.53
104	−.05	−.13	−.09
105	−.02	+.97	+2.39
106	−.09	+.02	.....
Deflection on point—			
D1.....inches..	+.04	+.09	+.31
D2.....do....	+.05	+.09	+.26
D3.....do....	+.03	+.07	+.18
D4.....do....	+.02	+.04	+.10
D5.....do....	−.01	−.03	−.08
D6.....do....	−.07	−.14	−.31
D7.....do....	−.12	−.25	−.55
D8.....do....	−.17	−.35	−.79
D9.....do....	−.21	−.45	−1.02
D10.....do....	−.25	−.52	−1.15
D11.....do....	−.26	−.55	−1.36
D12.....do....	−.26	−.55	−1.46
D13.....do....	−.24	−.52	−1.43
D14.....do....	−.22	−.46	−1.23
D15.....do....	−.17	−.35	−.88
D16.....do....	−.12	−.25	−.57
D17.....do....	−.06	−.13	−.27
D18.....do....	−.01	−.02	−.01
D19.....do....	+.02	+.02	+.01
D20.....do....	+.03	+.04	−.03
D21.....do....	+.06	+.06	−.07
D22.....do....	+.07	+.06	−.14

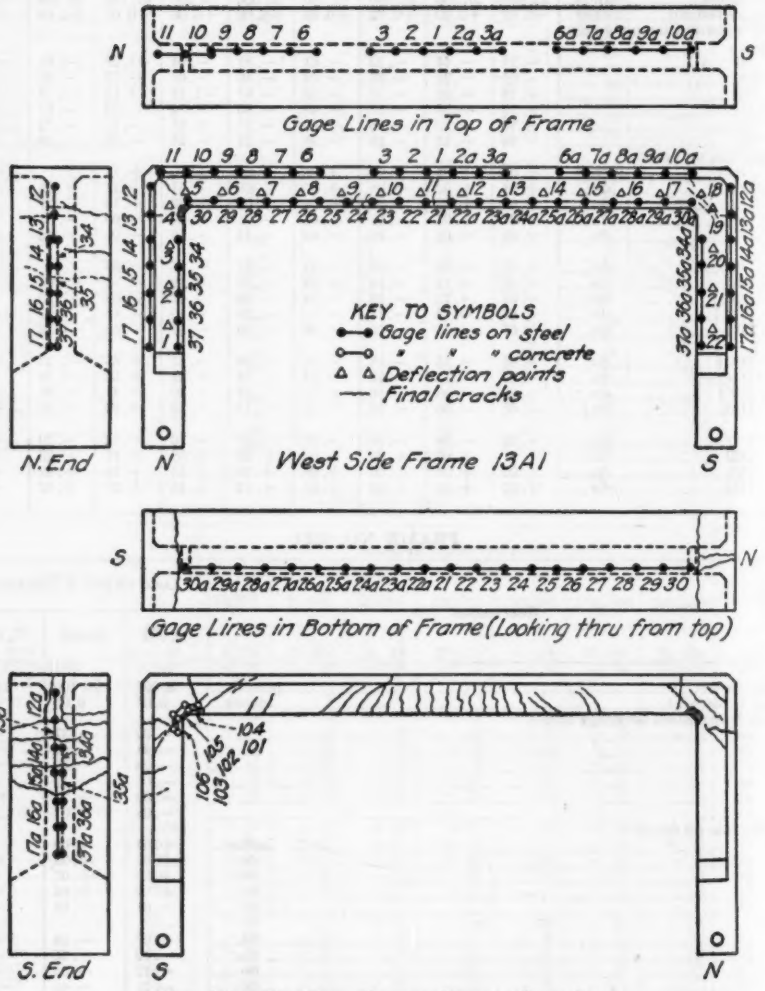

FIG. 32.—*Position of gauge lines and cracks*

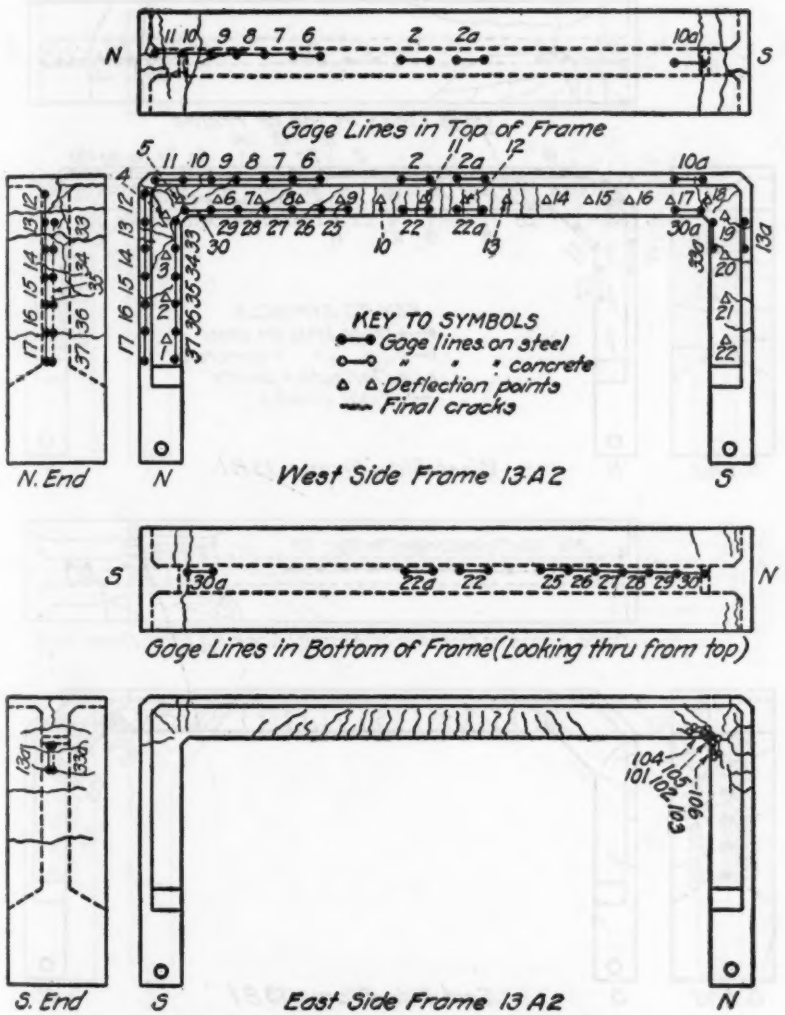
Gage Lines in Top of Frame
KEY TO SYMBOLS
Gage lines on steel
" " " concrete
Deflection points
Final cracks
N. End
West Side Frame 13 A 2
Gage Lines in Bottom of Frame (Looking thru from top)
S. End
East Side Frame 13 A 2

FIG. 33.—*Position of gauge lines and cracks*

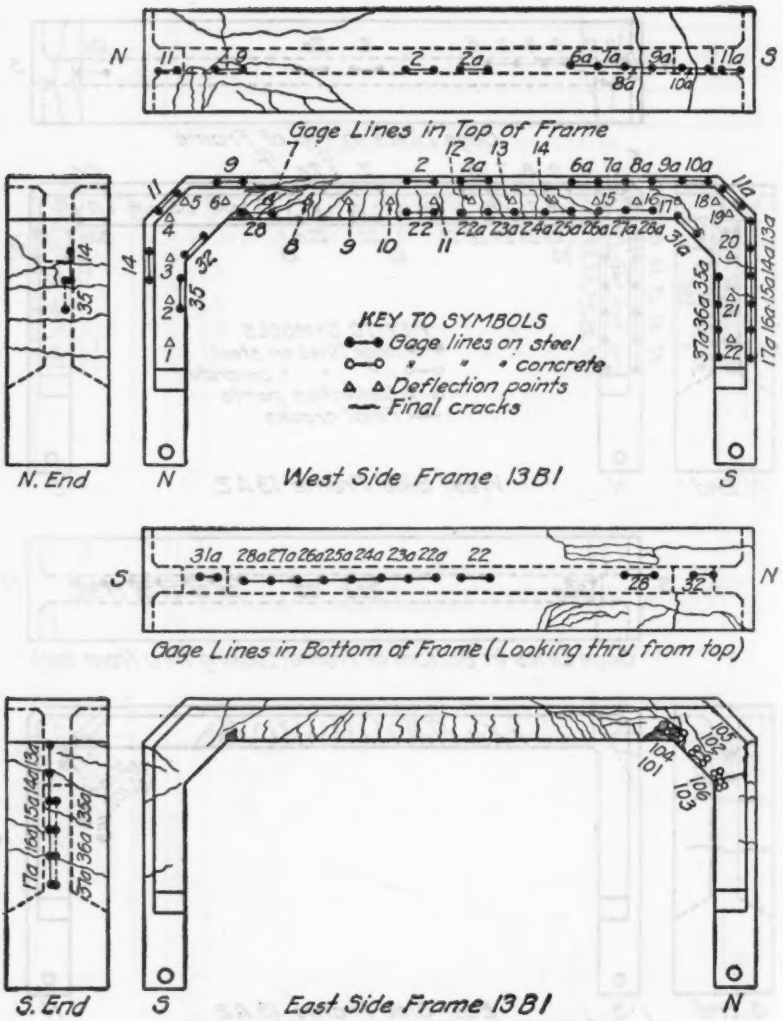

FIG. 34.—*Position of gauge lines and cracks*

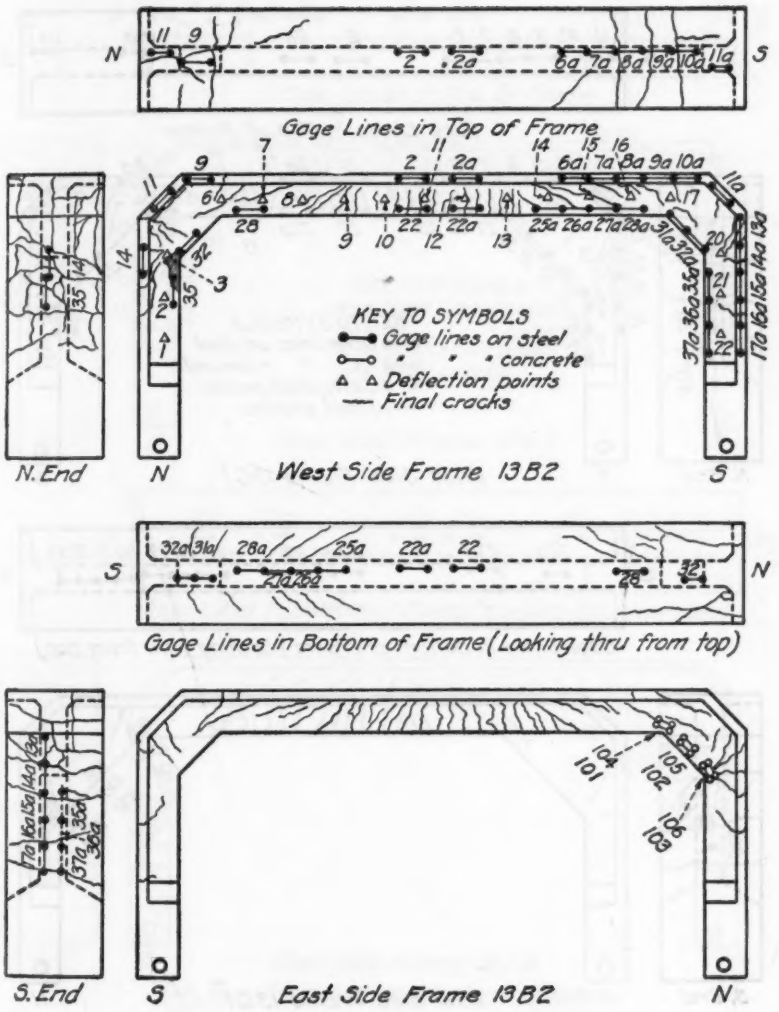

FIG. 35.—*Position of gauge lines and cracks*

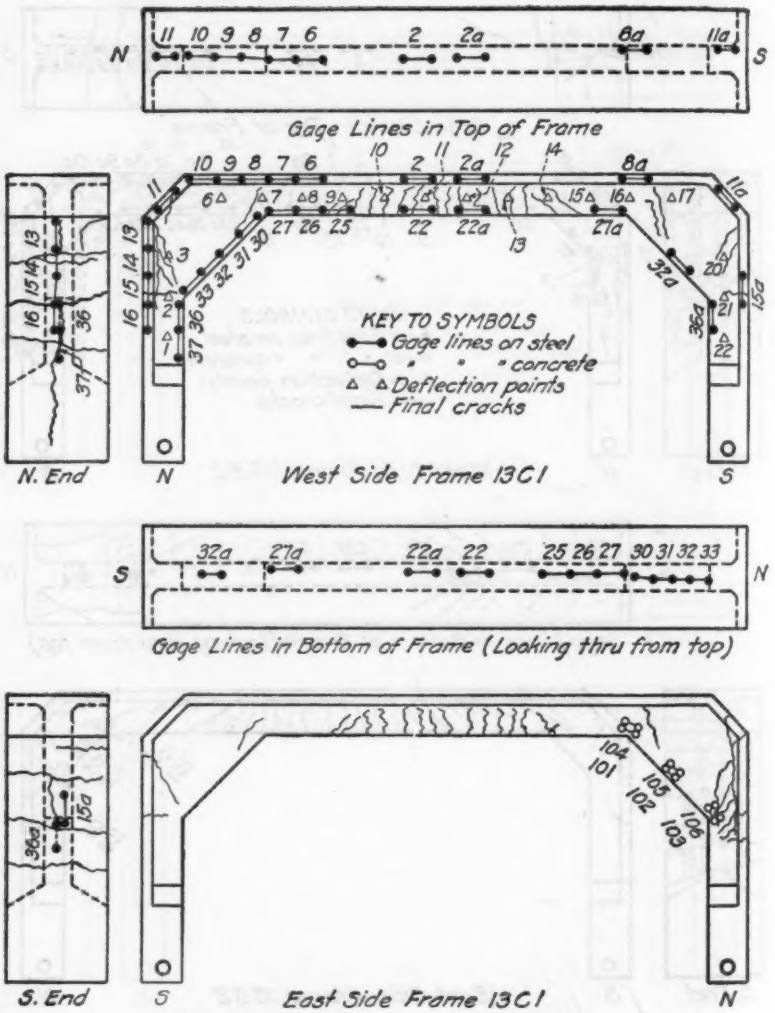
N
11 10 9 8 7 6 2 2a 8a 11a
S
Gage Lines in Top of Frame
KEY TO SYMBOLS
Gage lines on steel
" " " concrete
Deflection points
Final cracks
N. End
N
West Side Frame 13C1
S
32a 27a 22a 22 25 26 27 30 31 32 33
Gage Lines in Bottom of Frame (Looking thru from top)
S. End
East Side Frame 13C1

FIG. 36.—*Position of gauge lines and cracks*

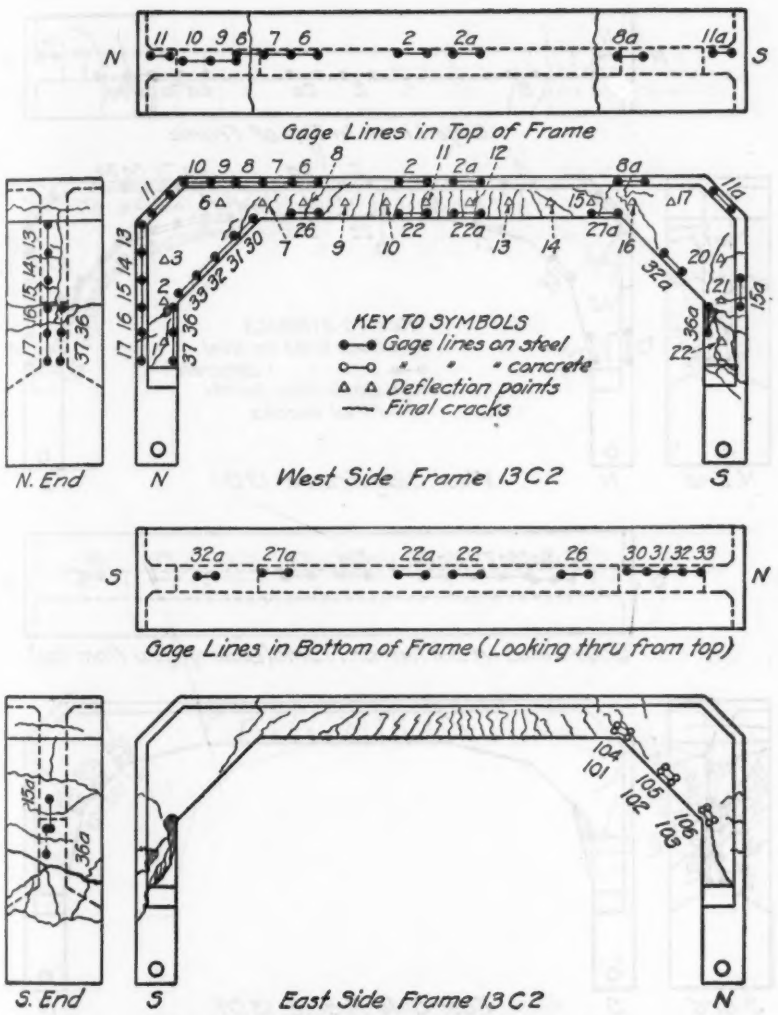

FIG. 37.—*Position of gauge lines and cracks*

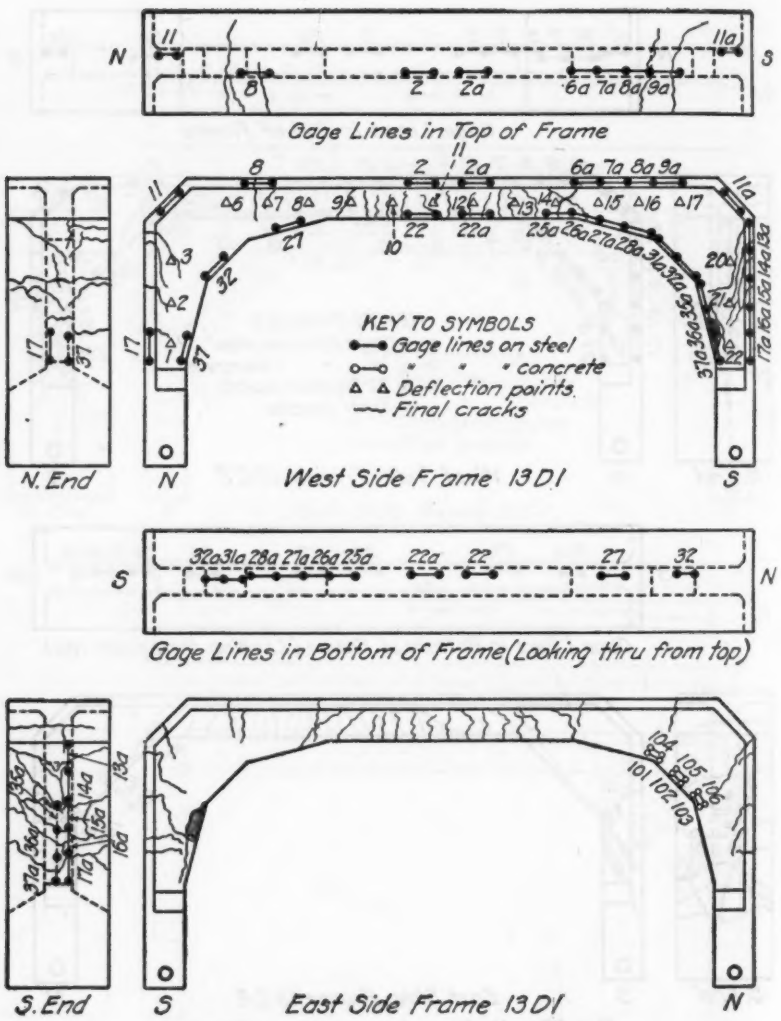
Gage Lines in Top of Frame
KEY TO SYMBOLS
Gage lines on steel
" " " concrete
Deflection points.
Final cracks
N. End
West Side Frame 13 D1
Gage Lines in Bottom of Frame (Looking thru from top)
S. End
East Side Frame 13 D1

FIG. 38.—*Position of gauge lines and cracks*

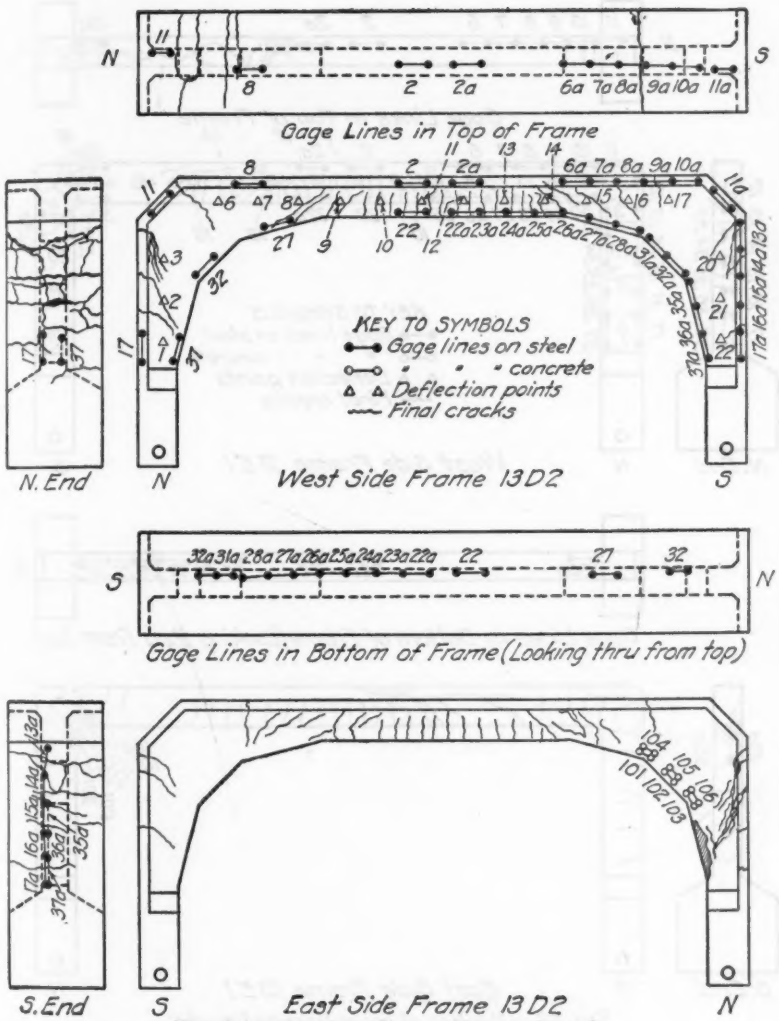

FIG. 39.—*Position of gauge lines and cracks*

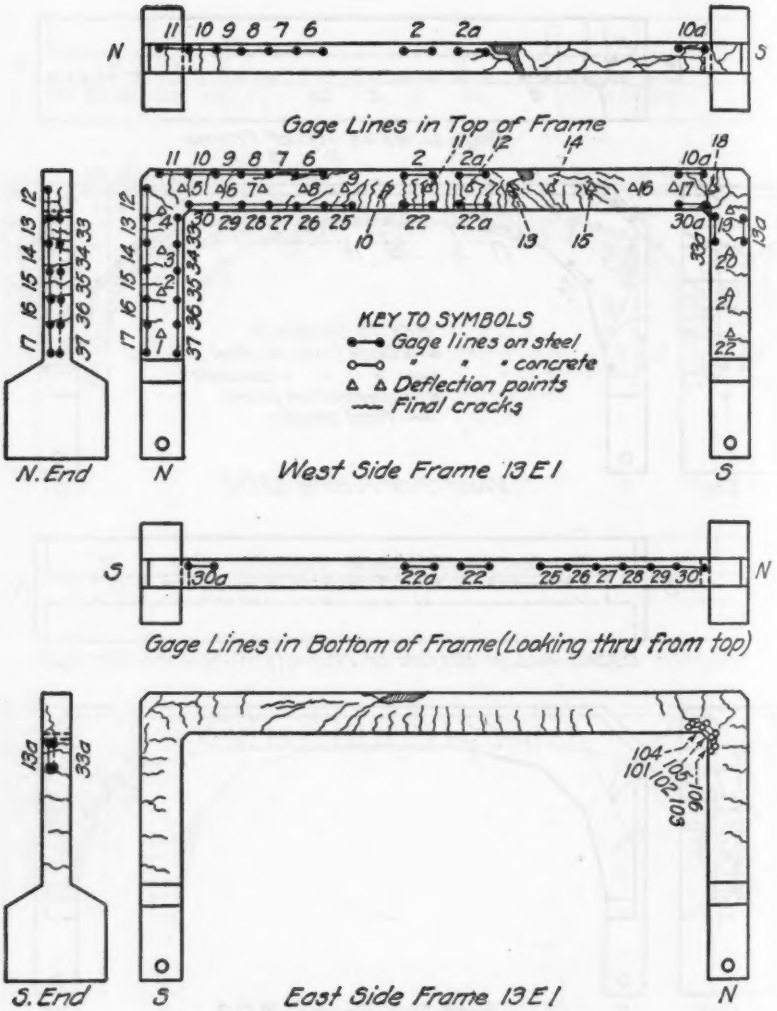
Gage Lines in Top of Frame
KEY TO SYMBOLS
Gage lines on steel
concrete
Deflection points
Final cracks
N. End
West Side Frame 13 E 1
Gage Lines in Bottom of Frame (Looking thru from top)
S. End
East Side Frame 13 E 1

FIG. 40.—*Position of gauge lines and cracks*

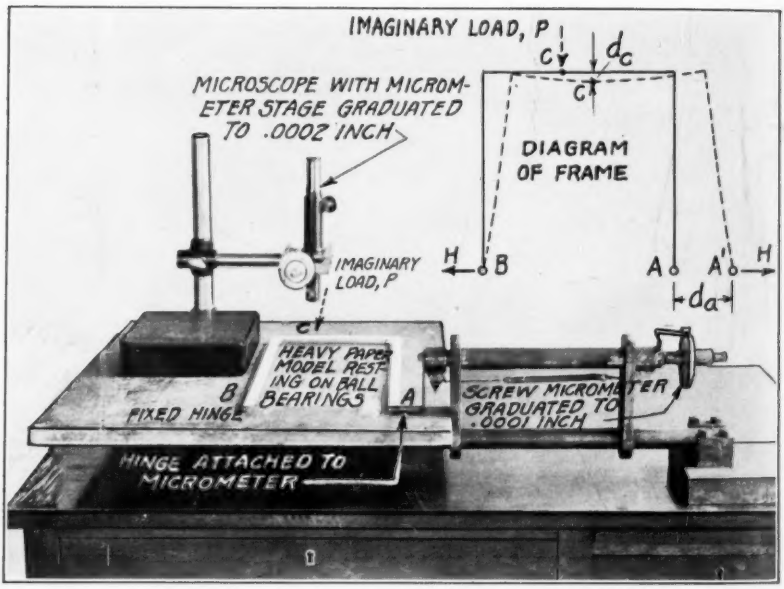

FIG. 41.—*Arrangement of apparatus for testing paper models*

APPENDIX II

SUPPLEMENTARY TESTS OF PAPER MODELS

For comparison with the foregoing analysis and tests a series of tests of paper models has been made by a method [11] devised by Prof. G. E. Beggs, of Princeton University. The tests were made with the assistance of R. L. Brown, of the engineering experiment station, University of Illinois.

By the Beggs method the reactions and moments in indeterminate frames are determined by measuring certain deflections or displacements of a paper or cardboard model of the frame. The theory involved in the tests of models is not new, being based upon Maxwell's well-known "Theorem of reciprocal displacements." The novel feature is the use of small models of paper or other isotropic material and the measurement of deflections by means of microscopes and micrometer gauges. The theory and procedure in the tests may be described with reference to Figure 41, which shows the arrangement of apparatus which was utilized for the purpose. The model of the frame to be tested was placed on a horizontal surface and supported on ball bearings to reduce friction. The hinge B was held stationary by means of a needle, while the hinge A was attached by means of another needle to the screw micrometer D. In forming the hinge between paper and needle, care was taken to make the fit loose enough to obviate high frictional resistance to turning but not loose enough to allow play in the hinge.

To find the horizontal reaction H at A and B, due to a load P acting at the point C, the procedure was to move the hinge A to the right a distance d_a by means of the micrometer D, and with the microscope to read the movement d_c of the point C in the direction of the imaginary load P (which was taken in this case to be at right angles to the direction BA). By the application of Maxwell's theorem the ratio $\frac{d_c}{d_a}=\frac{H}{P}$, or the horizontal reaction $H=P\frac{d_c}{d_a}$. In practice it was found advisable to repeat the operation, moving the hinge A to the left of its initial position and measuring d_c and to use the numerical average of several sets of observations taken in opposite directions in calculating the value of H.

The paper models tested were of types A, B, C, and D, as described in Section III, 1, except that eight different heights of each type of frame were used. To eliminate differences in the quality of the paper of the models, all were made from one sheet of paper, the frame of

[11] An accurate mechanical solution of statically indeterminate structures by use of paper models and special gauges, by G. E. Beggs, Proc. Am. Concrete Inst.; 1922.

type D being first cut out and tested without damaging it, the brackets then cut down to the form of type C and later of types B and A. The paper showed some variability in stiffness, and the values recorded were the average of a number of observations. The values of H/P, the ratio of horizontal reaction to vertical load applied at the one-third points of the top member of the bent, are plotted in Figure 42 for the four types of frame. For comparison, values of H/P have been calculated from equation (5), assuming the haunch of type D to be equivalent to a 45° bracket 4/3 as long as that of type C, and are also plotted in Figure 42. The agreement in the results obtained

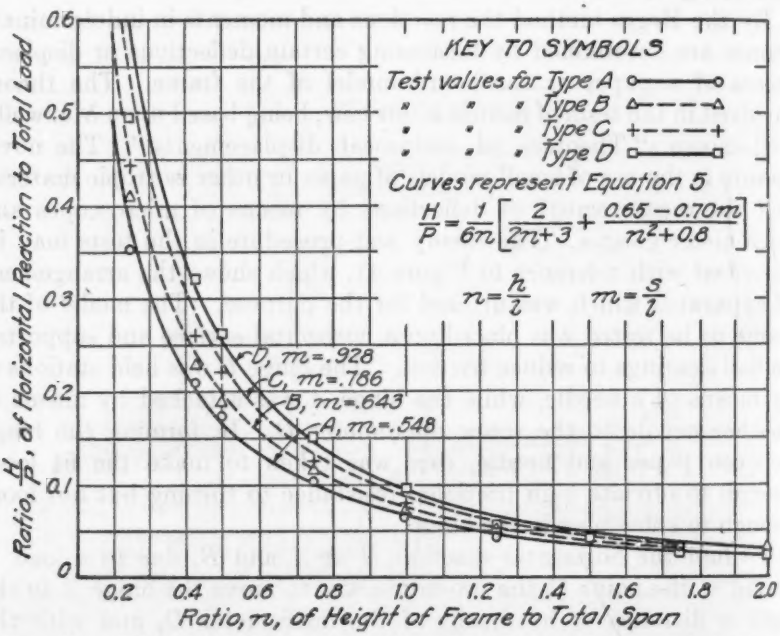
KEY TO SYMBOLS
Test values for Type A
" " " Type B
" " " Type C
" " " Type D
Curves represent Equation 5
$\frac{H}{P}=\frac{1}{6n}\left[\frac{2}{2n+3}+\frac{0.65-0.70m}{n^2+0.8}\right]$
$n=\frac{h}{l}$ $m=\frac{s}{l}$
D, m=.928
C, m=.786
B, m=.643
A, m=.548
Ratio, $\frac{H}{P}$, of Horizontal Reaction to Total Load
Ratio, n, of Height of Frame to Total Span
0 0.1 0.2 0.3 0.4 0.5 0.6
0.2 0.4 0.6 0.8 1.0 1.2 1.4 1.6 1.8 2.0

FIG. 42.—*Values of H/P from tests of paper models and from calculations*

by the two methods is very close and may be considered a satisfactory verification of equations (4) and (5).

Another use has been made of the models in determining relative deflections at various points on the top member of the frame. Figure 43 shows relative deflections of the top members of the models of types A, B, and C. These curves are, in effect, influence lines [12] for the horizontal reactions of the frame with a vertical load on the top member. It should be noted, however, that the purpose of these curves, which are similar to those of Figure 8, is to compare values of H/P with the loads at different points on the same frame and not to compare values between different types of frame. It is found that the horizontal reactions with loads at mid span and at the one-third

[12] See footnote 5, p. 200.

points are in the ratios of 1.15, 1.16, and 1.17, for types A, B, and C, respectively; with uniform loads and one-third point loads the reactions are in the ratios 0.75, 0.73, and 0.71 for the three frames, respectively. Comparing these ratios with those calculated in section 4, where for type A the ratio between the reactions for loads at mid span and at one-third points was taken at 1.125, and the ratio for uniform load and one-third point load was taken at 0.75, the agreement is seen to be very close and the correctness of the basis of equations (6) and (7) is thus substantiated.

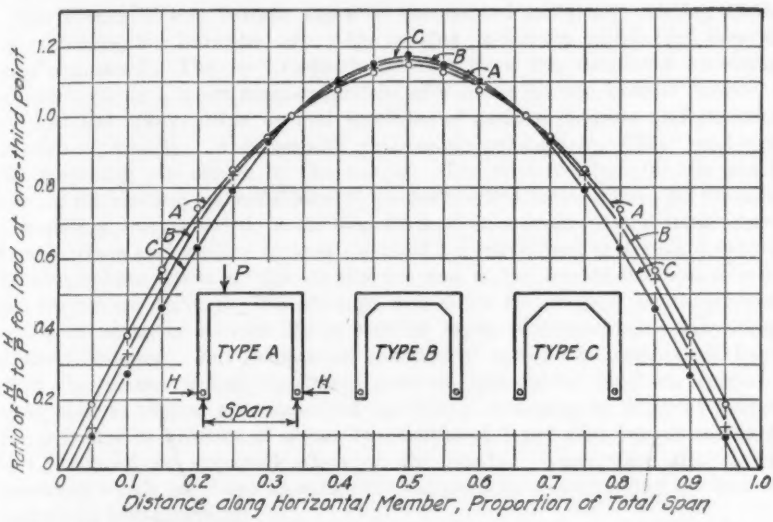

FIG. 43.—*Influence lines for horizontal reactions of frames of Types A, B, and C*

In conclusion it may be said that the tests on paper models gave results which were remarkably close to those found by analysis. However, individual observations varied considerably from the mean value found, and it was necessary to take a number of readings to eliminate errors of observation and manipulation. Further, preliminary tests with these models indicated that some grades of paper are not isotropic or are not uniform in certain properties, so that considerable care must be used in the selection of the material if such tests are to be used for scientific work.

WASHINGTON, April 4, 1928.

ACCELERATED LABORATORY CORROSION TEST METHODS FOR ZINC-COATED STEEL

By Edward C. Groesbeck and William A. Tucker

ABSTRACT

The merits of two certain types of accelerated laboratory testing methods for evaluating the indicated life of the coating on hot-dip zinc-coated sheet steel were compared. The two methods studied were the simulated atmospheric corrosion, using a moist gaseous mixture of sulphur dioxide, carbon dioxide, and air, and the spray, using normal solutions of sodium chloride and ammonium chloride separately. A consistent relationship between the "life" and weight of the coating was shown by the results. The time required for the breaking down of the coating was considerably less for the first method than for the second. The coating was corroded, in the first method, in a progressive manner over the entire surface and similar to that reported for galvanized materials corroded in the atmosphere under service conditions, and in the second method, in a local and capricious manner. No attempt was made to interpret the experimental results in terms of service life in various types of atmospheres prevailing in different climates. Any satisfactory attempt at such an evaluation will have to await the results of long-time field tests on zinc-coated products carried out under several typical atmospherical conditions obtaining at different locations. The presence or absence of about two-tenths of 1 per cent copper in the steel base produced no apparent effect on the results. Tests were also made on specimens which had been annealed for the purpose of converting the zinc coating into an iron-zinc alloy.

CONTENTS

	Page
I. Introduction	256
II. Previous work	258
1. Simulated atmospheric corrosion method	258
2. Spray test method	263
III. Materials and experimental methods	264
1. Materials	264
2. Experimental methods	268
(*a*) Simulated atmospheric corrosion test	268
(*b*) Spray tests	272
IV. Experimental results	273
V. Discussion of results	280
1. Simulated atmospheric corrosion test	280
2. Spray tests	287
(*a*) Sodium chloride	287
(*b*) Ammonium chloride	290
VI. Summary and conclusions	292

I. INTRODUCTION

A reliable means of forecasting the probable life under severe atmospheric conditions of "galvanized" materials is much to be desired, since these materials (amounting to about 1,350,000 tons in 1926) constitute a very considerable proportion of the annual production in the United States of iron and steel products to which a metallic protective coating of one kind or another has been applied for the purpose of prolonging their useful life by postponing as long as possible the inevitable corroding away of the underlying iron or steel. (The term "galvanized" used throughout this paper refers to material zinc coated by any process, other than that in which electrodeposition is employed for the coating operation. Immersion in a bath of molten zinc—that is, the hot-dip process—is the most common.) Of course, field tests carried out on specimens of galvanized materials exposed to conditions as similar to those obtaining in actual service as practicable should furnish the desired information, but much time (probably several years) must elapse between the start of the test and the appearance of the first definite signs of failure of the protective coating. This is particularly true when the field test is carried out in a locality where the prevailing atmospheric conditions are not of a markedly corrosive nature, and also when specimens with relatively heavy zinc coatings are included in the test. A laboratory test method so devised that it would furnish results which will serve as a reliable index of the behavior obtaining under actual service conditions and, indeed, yield information similar to that produced by the field tests, but in a very much shorter time, should be of much value to the industry. In such an accelerated test, one or more of the important controlling factors present in service conditions must be exaggerated in order that the corroding effect may be made to proceed at a more rapid rate.

It is apparently only within the last few years that any definite efforts have been made to develop such an "accelerated test" of metallic coatings for the sole purpose of ascertaining the probable life of the coating. The so-called "stripping tests" are not to be included in this category, since the main objects of these tests are to give the total amount of the zinc coating present on a surface and to reveal the presence of thin spots in the coating. Another type of laboratory testing which should not be classed with these "life tests" is that designed to bring out any defects present in the coating, such as pinholes and other forms of discontinuity in the covering qualities of the coating, particularly of the electroplated kind.

The following report gives the results of experiments undertaken to test, on a comparative basis, two certain types of laboratory testing methods for determining the "life" of the coating on "hot-dip"

galvanized sheets with the object of determining their value as an "accelerated test." One type is known as the "simulated atmospheric corrosion test," wherein the specimens are exposed to a muggy, acidic atmosphere corresponding in nature, although much more concentrated in acid content, to that often prevailing in certain industrial districts, as, for example, Pittsburgh, Pa. The results of such a test would, of course, not be comparable to those obtaining in another and less corrosive type of atmosphere but could be taken as a measure of the life of the coatings under the severest service conditions galvanized products would ordinarily be subjected to. The measures for the other types of atmospheric conditions might be expected to bear ratios to this measure as obtained above. These ratios would have to be determined by experiment or by the results of long-time field tests carried out under a set of different typical atmospheric conditions. The other type of testing method tried is based on the well-known salt spray test. The essential value of this method would seem to lie in the use of a corroding solution, which, when atomized within the chamber containing the test specimens, would be expected to remove the zinc coating in a progressive and more or less even manner within a reasonable period of time. The two corroding solutions tried out in this investigation were normal solutions of sodium chloride and ammonium chloride.

Two classes of hot-dip galvanized sheet material were used for the experimental work, namely, copper-bearing and noncopper-bearing sheet steel or iron, for the purpose of determining whether or not the presence of copper, totaling about two-tenths of 1 per cent, in the steel base, in addition to the small amount usually present in non-copper-bearing steel, would exert any clearly defined influence on the resistance to accelerated attack of the zinc coating. The galvanized sheet material was mostly of 22 and 28 gauge, and the weights of zinc coating ranged from about 0.75 to 2.5 ounces of zinc per square foot of sheet. A few test specimens, which had been heat treated after the galvanizing process with the object of obtaining a larger proportion of, and a more evenly distributed, iron-zinc alloy in the coatings, were also included in the tests.

All references to weight of zinc coating expressed throughout this paper are in the terms of the weight, in ounces, of the coating per square foot of sheet (that is, the coating on both faces of the sheet), unless otherwise stated.

II. PREVIOUS WORK

1. SIMULATED ATMOSPHERIC CORROSION METHOD

The fact that the zinc coating of a galvanized article is very slowly attacked during exposure to a normal, relatively uncontaminated atmosphere is a matter of common knowledge. The surface of the coating reacts with the oxygen and carbon dioxide of the atmosphere in the presence of moisture. This reaction leads to the formation of a very thin adherent film of basic zinc carbonate or a mixture of zinc carbonate and zinc oxide which is apparently quite resistant to ordinary weathering effects. This protective film is subjected to the eroding effects of wind and rain and may possibly be affected by temperature changes in so far as the differential expansion of the metal coating and the overlying adherent film leads to the cracking of the latter. The eroding effect of the wind and rain will, of course, depend largely upon the amount and nature of the dust suspended in the atmosphere. Furthermore, the dust in the atmosphere of seacoastal, desert, and industrial regions contains appreciable proportions of sodium chloride, alkalies, and sulphur compounds present in the cinder or ash particles, respectively, and, therefore, should exert, in the presence of moisture, a corroding influence, As the film deteriorates and wears away, it is replaced by a new one. This building up and breaking down of the protective film constitutes a continuous process, which may be an extremely slow one in a region where a quite pure and dry atmosphere prevails, until the zinc coating is entirely consumed at some points.

In certain regions, such as large cities and industrial centers, there are present in the atmosphere appreciable amounts of carbonic acid, sulphur dioxide, and sulphurous acid (and even sulphuric acid in much smaller quantities), more noticeably so where foggy or misty weather prevails and also during the winter months when the coal consumption is necessarily greater. Because of their relatively high solubility, the zinc sulphates and sulphites forming in the protective film by the reaction with the acid-laden atmosphere would tend to break the film up and lay bare the underlying zinc coating to the corrosive influences of the atmosphere. It is within the bounds of reason to expect that the corroding away of the zinc coating would thus be accelerated.

The presence of a continuous zinc coating is, of course, assumed in the above discussion of the corroding effects, and, hence, any consideration of electrochemical reactions between the coating and base metal has no place in this stage of corrosive attack.

Galvanized materials are known to have a much shorter life in a highly corrosive atmosphere, such as that prevailing in the Pittsburgh, Pa., district, than those in the relatively very pure atmosphere

of a country district, which may be even only 100 miles distant. Even though no numerical data as to the comparative life of zinc coatings in various atmospheres appear to have been published, the following estimate by Hubbell and Finkeldey [1] may be mentioned as a matter of interest:

TABLE 1.—*Estimated life of galvanized products in several types of atmosphere*

Class of material	Type of atmosphere			
	Rural	Seacoast	Semi-industrial	Heavy industrial
	Years	*Years*	*Years*	*Years*
Commercial rolled zinc sheet or strip 0.020 inch thick	50–75	50	20–30	10–15
Galvanized product 1.25 ounce coating/sq. ft. of surface	30–35	20–25	15–20	8–10
Galvanized product 1.0 oz./sq. ft. of surface	20–25	15	10–15	6–8
Galvanized product 0.6 oz./sq. ft. of surface	8–10	5–8	5	3–5
Galvanized product 0.2 to 0.3 oz./sq. ft. of surface	3–4	2–3	1–2	1

The types of failure produced in galvanized materials by exposure to severely corroding atmospheres have been observed to be quite similar in appearance to those obtained by long exposures to less corrosive atmospheres.

It is only natural that there should have arisen, in connection with the search for laboratory methods of determining the comparative life of galvanized products, the idea of developing a simulated atmospheric corrosion test method, in which the proportions of the corrosive elements present in the atmosphere are accentuated with the sole object of shortening in a large degree the time required for the zinc coating to be corroded away. Szirmay published in 1905 [2] an account of some tests made to determine the relative resistance of iron and steel wires, zinc coated by the electroplating and "hot-dip" galvanizing processes, by exposing them to a gaseous mixture of air, CO_2, and SO_2 over moderately heated water. The wire specimens were kept in a bell jar, which was placed in a basin partly filled with water, and the two gases were passed into the bell jar in the proportions of 12 per cent SO_2 and 15 per cent CO_2 in the resulting mixture. Heyn and Bauer [3] later employed a similar method in carrying out some tests on the relative resistance to corrosion of the zinc coating on electroplated and hot-galvanized pipes. A few years ago the New Jersey Zinc Co. developed a "plant-size" testing apparatus designed for testing comparatively large sized specimens of galvanized sheets and other products.[4] This apparatus was essentially a

[1] Hubbell, J. P., and Finkeldey, W. H., Trans. Amer. Inst. Chem. Engrs., 18, p. 51; 1926.

[2] Szirmay, I., "Testing the corrodibility of zinc-coated iron and steel wire, including barbed wire," Zeit. Elektrochem., 11, p. 333; 1905.

[3] Heyn, E., and Bauer, O., "Corrosion tests of galvanized tubes," Mitt. Kgl. Materialprüfungsamt, 30, p. 101; 1912.

[4] Rawdon, H. S., Krynitsky, A. I., and Finkeldey, W. H., "Types of apparatus used in testing the corrodibility of metals," Proc. Amer. Soc. Test. Matls., 24, pt. 2, p. 731; 1924.

rectangular-shaped, lead-lined wooden tank with a lead-lined cover fitting into a troughlike arrangement on the sides, which when filled with water served as a water seal during operation. The tank was filled to a certain height with water, which was heated by electric heaters placed at the bottom. A mixture of 100 parts air, 5 parts CO_2, and 1 part SO_2, the proportions being controlled by flow meters, was passed into the tank at one end and just above the water level, along over the water surface and under a false bottom to the opposite end, and thence upward into the specimen chamber above the false bottom. The proportions used in this air-gas mixture were arbitrarily chosen, as they were found in some preliminary tests to produce a failure of the zinc coating within a reasonable length of time (a slight modification of these proportions was adopted subsequently, namely, 94 parts air instead of 100). The air-gas mixture was admitted at the rate of approximately 6.4 liters per minute, and it became warmed and then saturated with water vapor as it passed through the lower part of the tank. The temperature of the water was thermostatically regulated so as to give a temperature of 55° C. (131° F.) in the atmosphere within the specimen chamber. An exhaust pipe, large enough to prevent the building up of pressure in the air-gas mixture within the tank during operation, was provided in the upper part of the tank. The test was carried out in three steps: (1) Exposure to the warm, moist gaseous mixture for 10 hours; (2) thorough washing of the specimens with water, furnished by a sprinkling system which was placed below the top edges of the tank, for 2 hours (this was intended to imitate the washing action of rain, which would remove more or less completely the corrosion products from the surface); and (3) drying of the specimens by exposure to the ordinary surrounding atmosphere (with the tank cover removed) at room temperature for 12 hours—here the zinc coating should have the opportunity to renew its protective film which had been removed or damaged during the preceding exposure to the corroding conditions. These three steps constituted a cycle, and the number of cycles required to produce a definite rusting of the base metal was taken as a measure of the life of the protective coating, or, in other words, an indirect measure of the ability of the coating to withstand atmospheric corrosion.

It must be admitted that this form of test by no means constitutes an atmospheric corrosion test in the true sense of the word, but it does produce types of failure in the zinc coating which are similar to those occurring under actual conditions of atmospheric corrosion (at least, so far as can be judged by surface appearance), and with the added advantage of requiring very much less time to attain these results. According to Finkeldey,[5] the progressive changes in the

[5] See discussion on p. 757 of reference cited in footnote 4, p. 259.

appearance of galvanized sheet specimens carrying light and heavy coatings of zinc, as revealed in test by the New Jersey Zinc Co.'s simulated atmospheric corrosion test method, is about as follows: After the first or second cycle the coating loses its metallic luster and becomes covered with a light gray-colored protective film; after additional cycles the spangles gradually disappear, and then dark-colored spots begin to appear on the surface of the specimen. After a few more cycles the entire surface of the specimen assumes a dark color. This change in color from light to dark gray is ascribed to the removal of the zinc layer and the consequent laying bare of the iron-zinc alloy layer overlying the iron base. Exposure to several additional cycles will remove this alloy layer, and the iron base thus laid bare will start rusting. There is a very close resemblance between the appearance of the coating on specimens during the progress of the accelerated test and that of the coating on ordinary galvanized iron as it fails in the atmosphere; the revealing of the dark-colored alloy layer is the principal characteristic feature of this similarity. It has been repeatedly observed that, with heavily coated galvanized iron, a larger number of cycles is required to bring out the first spots of the dark-colored alloy layer than in the case of the lightly coated material. When exposed to the atmosphere these two classes of galvanized iron have been observed to show the same characteristic difference of performance. To put it in another way, the length of time required for the dark spots to show up on the galvanized material when exposed to atmospheric conditions should constitute a good index of the relative thickness, at the thinnest point, of the zinc coating overlying the iron-zinc alloy layer. However, no information has been forthcoming as to the relative rates of corrosion in the atmosphere of the zinc and zinc-iron alloy layers; it is to be expected that these rates would probably vary with the composition and thickness of the two layers.

The only experimental data obtained by this simulated atmospheric corrosion method that has been published to date are those reported by the New Jersey Zinc Co.'s research laboratory [6] for a number of special steel specimens, coated with zinc by several processes and with lead by the metal spray process, in connection with a series of short-time tests undertaken by several laboratories in cooperation with Subcommittee VII of Committee A-5, American Society for Testing Materials.

At a little later date, and apparently independently, Fowle [7] developed a simulated atmospheric corrosion test method and apparatus somewhat similar, in general details, to that worked out by the

[6] Report of Subcommittee VII on Accelerated tests. Proc. Amer. Soc. Test. Matls., **26**, Pt. I, p. 147; 1926.

[7] Fowle, F. F., "Accelerated corrosion tests on bare overhead electrical conductors," Proc. Amer. Soc. Test. Matls., **25**, Pt. II, p. 137; 1925.

New Jersey Zinc Co., but primarily for testing uninsulated overhead electrical conductors. The essential difference was that instead of the SO_2 gas-CO_2 gas-air mixture dilute bituminous coal smoke, which was generated outside of the test box, was employed to produce in a more moderate degree the simulation of the corroding influence of outside atmospheres prevailing in city and industrial regions.

The chemical action of the smoke in both gaseous and finely divided solid form upon the protective coating should, in the presence of moisture, be of an acidic nature and, therefore, be similar, though different in degree, to that of the gaseous mixture employed in the other method. The materials under test—namely, copper, aluminum, iron, steel, copper-clad steel, and galvanized iron and steel in wire and strand form—were exposed repeatedly to the simulated weathering effects in cycles of short duration. Each cycle lasted 8 hours and was divided into four periods—(1) warm moist air, 1.5 hours; (2) air charged with bituminous coal smoke, 3 hours; (3) fine water spray, 0.5 hour; and (4) warm dry air, 3 hours. The first period was intended to simulate a normal atmospheric condition which prevails during much of the time, the second and third periods introduced the chief corroding agents (the water spray to simulate the action of rain), and the fourth period to secure thorough drying of the specimens and the box following the water-spraying operation. The repetition of cycles was maintained continuously day and night, excepting Sundays, holidays, and occasional interruptions. A gentle circulation of air and smoke, maintained by an exhaust fan placed at one end of the test box, was directed up and down along the length of the box by means of transversely placed baffle plates. The coal-smoke atmosphere was found by analysis, made on two different occasions, to contain from 5.1 to 8.6 per cent CO_2 and, as determined at the center of the box, 86 parts, by volume, of sulphuric acid per million parts, by volume, of total gas. The temperature in the box obtaining under the different conditions of the test ranged from 14 to 42° C. (57 to 108° F.). The specimens, which were initially about 14 feet long and placed along the length of the test box, were taken out and examined at intervals. The specimens of galvanized iron and steel were reported as having shown a progressive change of appearance similar to that described by Finkeldey, as noted above.

A laboratory test apparatus, designed on similar general principles as that of the New Jersey Zinc Co., but differing mainly in constructional details, was developed at this bureau.[8] A description of this apparatus, which was subsequently modified in several constructional details, and the results of a program of tests carried out with this apparatus on several types of "hot-dip" galvanized sheet-steel material are given in the following sections.

[8] See footnote 4, p. 259.

Speaking in a larger sense, we must accept the truth that the varying nature of climatic conditions, both regional and seasonal, should render the formulation of a simulated atmospheric corrosion testing method which would be universally adaptable to all types of atmospheric corrosion an extremely difficult, if not impossible, matter. However, it seems possible that, if we should take the measure given by the simulated atmospheric corrosion test as being representative of the severest corroding set of conditions likely to be found in the atmosphere, we could apply, for any definite kind and weight of zinc coating, a ratio of this measure to each of the various types of atmospheric conditions of a less corrosive nature. Such ratios could probably be best determined, on a practical basis, by the results of field tests carried out at various localities where different and distinct types of atmospheric conditions prevail. Considerable lengths of time would necessarily elapse before the results of such field tests could be made available, particularly those tests carried out in localities where the corroding conditions are not severe.

The American Society for Testing Materials, through Subcommittee VIII of its Committee A–5, has had in progress during the past two years at five localities an extensive program of field tests undertaken on a series of galvanized and other metallic-coated products.[9] These localities were selected as being representative of the following five types of atmospheric conditions: Severe industrial, moderate industrial, rural, foggy seacoast, and tropical seacoast. The results of these field tests, when they are completed, should be of great value in determining the ratios between the different types of atmospheric exposure. The principle of applying ratios, for each kind and weight of zinc coating, would, of course, be only an approximation but should, however, serve as a reliable index of the probable service behavior of the material that could be obtained on a laboratory basis and within a reasonable period of time.

2. SPRAY-TEST METHOD

The first application of the spray method type to the testing of metallic protective coatings appears to have been made some 20 years ago.[10] This method of testing has been described in detail in several subsequent publications [11] in connection with its use for testing different metals in various corrodents.

The essential feature of this test consists in exposing the test specimens to the corrodent in the form of a very fine spray or mist

[9] Report of Subcommittee VIII on Field tests of metallic coatings, Proc. Amer. Soc. Test. Matls., **27**, Pt. I, p. 191; 1927.

[10] Capp, J. A., "A rational test for metallic coatings," Proc. Am. Soc. Test. Matls., **14**, Pt. II, p. 474; 1914.

[11] (*a*) Finn, A. N., "Method of making the salt-spray test," Proc. Amer. Soc. Test. Matls., **18**, Pt. I, p. 237; 1918. (*b*) B. S. Circular No. 80, 2d ed.; 1922. (*c*) See footnote 4, p. 259. (*d*) Rawdon, H. S., and Groesbeck, E. C., B. S. Tech. Paper No. 367, The Effect of the Testing Method on the Determination of Corrosion-Resistance; 1928. (*e*) Whitman, W. G., and Chappell, E. L., "Corrosion of steels in the atmosphere," Ind. Eng. Chem., **18**, p. 533; 1926. This form of apparatus is different from that described in the above references and was developed for testing bare-steel specimens by exposing them to intermittent spraying with water, in connection with life tests carried out on the same steel materials in the atmosphere at different localities.

and noting the length of time required for the metallic coating on the specimen to break down. The specimens are placed in a suitable box, and the mist is produced within the covered box by atomizing the solution with compressed air under moderate pressure, care being taken to prevent, by means of baffle plates, the direct impinging of the sprayed stream on the specimens. In general, the mist would be expected to condense and collect over the surface of the specimen as a very thin liquid film, but actually a coalescing of the liquid into easily visible aggregates occurs at more or less favorable locations on the surface during the course of the exposure.

III. MATERIALS AND EXPERIMENTAL METHODS

1. MATERIALS

Since a comparative study of the two types of laboratory corrosion testing methods, as used for determining the "life" of the zinc coating on galvanized iron or steel products, was the main object of this investigation, the materials used in this study were confined to iron and steel sheets of different gauges and with various weights of zinc coating applied by the hot-dip galvanizing process. These materials, which were made under commercial conditions, are listed in Table 2.

There were included in these materials two series of galvanized sheets, having the same gauges and weights of zinc coating, which had for the base metal ordinary noncopper-bearing open-hearth steel in one and copper-bearing steel with about 0.2 per cent copper in the other. This was done with the hope that if the presence of copper in the base metal in a greater amount than that usually present in ordinary commercial steels and irons, does exert any influence upon the "life" of the galvanized product, such effect would be manifested in the test results.

One 6 by 12 inch piece (152 by 305 mm) was cut from selected copper-bearing and noncopper-bearing galvanized sheets having 0.9, 1.5, and 2.5 ounces zinc coating, and the six pieces were annealed, at the New Jersey Zinc Co.'s research laboratory, in the air for one-half hour at 500° C. (932° F.) with the object of diffusing iron through the zinc coating and obtaining a larger proportion of the iron-zinc alloy in the coating. The annealed pieces were then cut into three 6 by 3¾ inch (152 by 95 mm) specimens for inclusion in the laboratory tests. The spangled surface of the zinc coating had been changed by the heat treatment to a smooth, fairly dark gray matte surface. Each piece gained in weight, as determined by weighing before and after the annealing treatment, by the same amount, namely, 0.014 oz./ft.^{2} of sheet (0.043 g/dm^2). A microscopic examination of the coating on these heat-treated pieces showed that it consisted mostly of the iron-zinc alloy, probably $FeZn_7$, with a narrow layer of the iron-zinc alloy, $FeZn_3$, next to the steel base.[12]

[12] Private communication from W. H. Finkeldey, formerly of the New Jersey Zinc Co.

TABLE 2.—*Sheet materials used in simulated atmospheric corrosion and spray tests*

TABLE 2.—*Sheet materials used in simulated atmospheric corrosion and spray tests*

Material No.	Source of material	Laboratory No.	Base metal	Nominal sheet gauge	Type of zinc coating	Weight of zinc coating in ounces per square foot of sheet, as determined by—				
						Weighing method [1]	Stripping test [2]			
						Average	Average	Maximum	Minimum	Maximum deviation from average
1	Maker A	SH 1	Noncopper-bearing steel	22	Hot-dip galvanized	0.83	0.88	0.96	0.80	0.08
2	do	SH 2	do	22	do	.87	.95	1.13	.89	.18
3	do	KH 1	Copper-bearing steel	22	do	.91	.94	.97	.89	.05
4	do	KH 2	do	22	do	.88	.90	.92	.87	.03
5	do	SE 1	Noncopper-bearing steel	22	do	1.26	1.28	1.43	1.18	.15
6	do	SE 2	do	22	do	1.17	1.26	1.35	1.18	.09
7	do	KE 1	Copper-bearing steel	22	do	1.19	1.26	1.40	1.18	.14
8	do	KE 2	do	22	do	1.18	1.24	1.32	1.10	.14
9	do	SC 1	Noncopper-bearing steel	22	do	1.54	1.63	1.87	1.48	.24
10	do	SC 2	do	22	do	1.57	1.63	1.73	1.42	.21
11	do	KC 1	Copper-bearing steel	22	do	1.50	1.88	2.84	1.45	.96
12	do	KC 2	do	22	do	1.46	1.30	1.47	.92	.38
13	do	SB 1	Noncopper-bearing steel	22	do	2.06	2.14	2.36	1.88	.26
14	do	SB 2	do	22	do	2.05	2.14	2.26	1.99	.14
15	do	KB 1	Copper-bearing steel	22	do	2.15	2.19	2.42	2.06	.22
16	do	KB 2	do	22	do	2.09	2.16	2.53	1.96	.38
17	do	SA 1	Noncopper-bearing steel	22	do	2.54	2.62	3.23	2.36	.61
18	do	SA 2	do	22	do	2.61	2.63	3.15	2.27	.53
19	do	KA 1	Copper-bearing steel	22	do	2.70	2.59	3.10	2.34	.50
20	do	KA 2	do	22	do	2.59	2.63	3.24	2.27	.61
21	do	SK 1	Noncopper-bearing steel	28	do	.83	.85	1.01	.79	.16
22	do	SK 2	do	28	do	.77	.80	.91	.73	.11
23	do	KK 1	Copper-bearing steel	28	do	.83	.92	1.04	.82	.12
24	do	KK 2	do	28	do	.85	.93	1.27	.79	.35

[1] These values were obtained by weighing the sheet before and after galvanizing. For Nos. 25 to 32, inclusive, the weights of coating were stamped on the sheets; it is presumed that these values were obtained by the weighing method, although no confirmatory statement to this effect had been received.

[2] Nine stripping-test determinations for each of the materials Nos. 1 to 32 and 43 to 47, inclusive (see foot-note 3 for Nos. 33 and 34), were made by the New Jersey Zinc Co.'s research laboratory. For these determinations a 2¼-inch square specimen was cut out in three locations at both ends and in the middle of the 28 by 108 inch sheet.

TABLE 2.—*Sheet materials used in simulated atmospheric corrosion and spray tests*—Continued

Material No.	Source of material	Laboratory No.	Base metal	Nominal sheet gauge	Type of zinc coating	Weight of zinc coating in ounces per square foot of sheet, as determined by—				
						Weighing method	Stripping test			
						Average	Average	Maximum	Minimum	Maximum deviation from average
25	Maker B	C 886	Open-hearth iron	20	Hot-dip galvanized	1.22	1.18	1.42	1.06	0.24
26	do	C 887	do	20	do	1.26	1.24	1.59	1.04	.35
27	do	C 880	do	20	do	1.52	1.59	1.81	1.18	.41
28	do	C 881	do	20	do	1.41	1.59	1.93	1.25	.34
29	do	C 882	do	20	do	2.02	2.12	2.34	1.61	.51
30	do	C 883	do	20	do	2.13	2.14	2.45	1.70	.44
31	do	C 884	do	20	do	2.44	2.41	3.00	1.83	.59
32	do	C 885	do	20	do	2.59	2.42	2.70	2.23	.28
33	Maker A	24	Steel	24	Hot-dip gray galvanized		[3] 1.51	1.61	1.43	.10
34	do	30	do	30	do		[3] 2.12	2.14	2.10	.02
35	Maker C	S8SL		22	Lead-coated [4]					
36	do	S8SG		22	Commercially heat-treated [5]					
37	Maker A	SH 2B	Noncopper-bearing steel	22	Hot-dip galvanized heat-treated [6]					
38	do	KH 2B	Copper-bearing steel	22	do. [6]					
39	do	SC 1B	Noncopper-bearing steel	22	do. [6]					
40	do	KC 1B	Copper-bearing steel	22	do. [6]					
41	do	SA 1B	Noncopper-bearing steel	22	do. [6]					
42	do	KA 1B	Copper-bearing steel	22	do. [6]					
43	do	X 1	Steel	26	Hot-dip galvanized-blistered coating		1.17	1.81	.91	.64
44	do	X 2	do	26	do		1.38	2.08	1.02	.70
45	do	X 4	do	30	Hot-dip galvanized-hard sheet, stringy coating.		1.65	2.29	1.29	.64
46	do	X 5	do	30	Hot-dip galvanized-irregular gray		1.60	2.24	1.21	.64
47	do	X 3	do	14	Hot-dip galvanized gray		2.34	2.54	2.05	.29

[3] Three stripping-test determinations of each of these two materials were made at this bureau. The 2¼-inch square specimens were cut at random from two 30-inch square sheets.

[4] A miscroscopic examination of a cross section of the coated sheet revealed the presence of a thin layer lying between the base metal and the lead coat. The exact nature of this layer was not determined, but it appears probable that the sheet had been galvanized before the lead coating was applied, since the underlying surface laid bare by the blistering of the lead coat was gray in color and did not show any formation of iron rust for awhile afterwards while in test.

[5] This term is applied to a patented process where the hot-dipped zinc-coated material, particularly "unwiped" wire, is given a heat treatment immediately following the passage through the molten-zinc bath, for the purpose of making the zinc coating more uniformly distributed, increasing the proportion of the iron in the coating, and improving the bending qualities of the treated material. This process has also been successfully applied to sheets.

[6] A piece 6 by 12 inches was cut from each of material Nos. 2, 4, 9, 11, 17, and 19, and the 6 pieces were sent to the New Jersey Zinc Co.'s research laboratory, where they were annealed at 500° C. for one-half hour. After their return, they were cut up into 6 by 3¾ inch specimens for inclusion in the laboratory corrosion tests.

There were also included in these tests, as a matter of information to this bureau, specimens cut from 20-inch (508 mm) square lead-coated and "commercially heat-treated" sheets, products in process of commercial development which were received from a manufacturer for this purpose.

The specimens cut from all the materials, excepting the heat-treated ones just mentioned above, were 4 inches (102 mm) square. A 1/8-inch (3 mm) diameter hole was drilled at the middle of and close to one edge of the specimens for suspending on glass hooks in the spray tests. A large portion of the specimens used in the simulated atmospheric corrosion tests had this hole, even though it was not needed. At the outset of the tests, a number of specimens were coated along the edges for a width of about three-sixteenths inch (5 mm) with one or two applications of bitumastic enamel, care being taken to include the suspension hole well within the coated area, in order that no galvanic action would occur between the zinc coating and the steel body at the cut edge. The coated specimens were kept in an electric oven at about 50° C. (122° F.) for a few hours to harden the enamel coating. This coating was found to be unsatisfactory, as it blistered and flaked off badly during the early stages of the tests. Asphalt varnish was substituted with somewhat more satisfactory results, the coating being air-dried rather than oven-dried and with two or three applications. This coating usually remained quite adherent and continuous for a fairly large number of cycles. No attempt was made to recoat the specimens during the progress of the test, as the coating on the edges of the specimens appeared to be quite intact, and any rusting that may have occurred along the edges did not interfere with the results observed on the faces of the specimens. After the experimental work described in this paper had been completed, some tests were made with vulcalock rubber cement and with a mixture of this cement and aluminum powder for coating the cut edges of galvanized sheets. It had been found at this bureau recently that, when applied as a protective coating to metal surfaces, the latter showed very satisfactory protective qualities, and the former but a short-lived resistance, during long-continued exposures in a laboratory weathering test, wherein the specimens were subjected to repeated cycles of exposure to (*a*) a vigorous water spray, (*b*) the rays of a carbon arc light, (*c*) a freezing temperature, and (*d*) an ozonized atmosphere. When applied as a thin, smooth covering along the edges of the galvanized sheet specimens, these two types of coating were found to stand up very well, especially the rubber cement alone, in the simulated atmospheric corrosion, sodium chloride spray, and ammonium chloride spray tests. Both showed good adherence and no signs of cracking or peeling off at the stage where the asphalt-varnish coating on other specimens included in the test had already blistered and flaked off to a large extent.

2. EXPERIMENTAL METHODS

(a) SIMULATED ATMOSPHERIC CORROSION TEST

This test was carried out in 24-hour cycles, each cycle consisting of three stages:

1. Exposure to a muggy, corroding atmosphere, consisting by volume or 94 parts air, 5 parts carbon dioxide gas, and 1 part sulphur dioxide gas and saturated with water vapor, for five hours.

2. Exposure to a water spray for one hour, wherein the corrosion products formed were washed off in a manner similar to the action of the rain.

3. Drying period of 18 hours, during which the specimens became thoroughly dried by exposure to the room atmosphere of the laboratory, and the rebuilding of the protective film on the zinc coating destroyed in the first stage was thus promoted.

The cycles were continued until the failure of the zinc coating on one face, and on both faces in most cases, of the specimens was clearly manifested by the formation of red-brown colored rust at the point where the steel or iron base was laid bare. The lengths of time for the first two stages were arbitrarily chosen, although in the same ratio as in the New Jersey Zinc Co. tests, in order that these stages could be carried out to completion within the limits of the working-day. Oftentimes one and even several days elapsed between successive cycles, so the length of exposure of the specimens to the room atmosphere varied, but probably little or no marked change in the surface conditions of the specimens occurred in the interval between the 18-hour drying period and the start of the next cycle.

The apparatus employed in this work is shown in Figures 1, 2, and 3. The test was carried out in two wooden containers, *K*, one of which served as the "tank" and the other as the cover to the tank by being placed on top and in an inverted position. The containers were of cypress wood and of a variety which may be found in most any household-furnishings store. Their dimensions were 29½ inches (750 mm) in diameter at the open end, 27¼ inches (692 mm) in diameter at the closed end, and 14½ inches (368 mm) in height.

At the start of the first stage of the test, the tank was filled with hot water up to a definite height. Next, a circular false bottom, *F*, 26 inches (660 mm) in diameter and made from a board 1⅛ inches (29 mm) thick, was placed upon four 1¼-inch (32 mm) square wooden uprights, *U*, being at a short distance above the water level when in position. A glass tube, serving as a gas inlet, was then placed in position as indicated in Figure 2. The specimen holder, *SH*, which was in two separate parts, each consisting of four wooden semi-annular rings held in position by a wooden strip extending along at approximately the diameter of the rings (see fig. 3), was next laid on

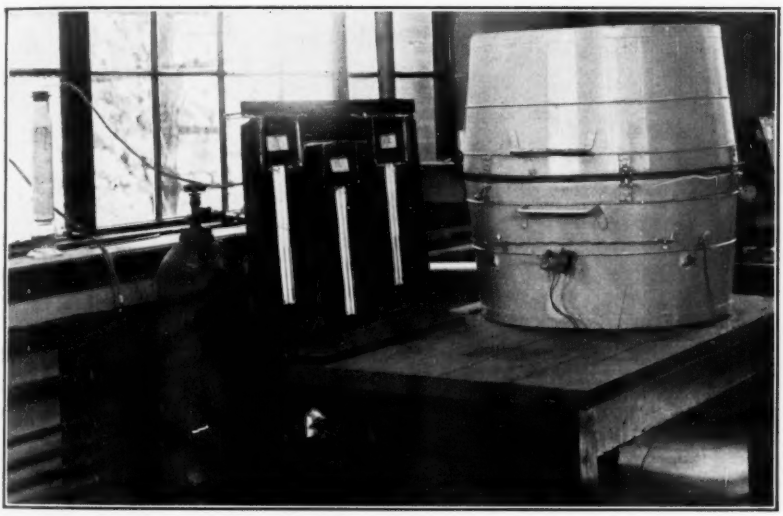

FIG. 1.—*Simulated atmospheric corrosion test apparatus, shown as assembled*

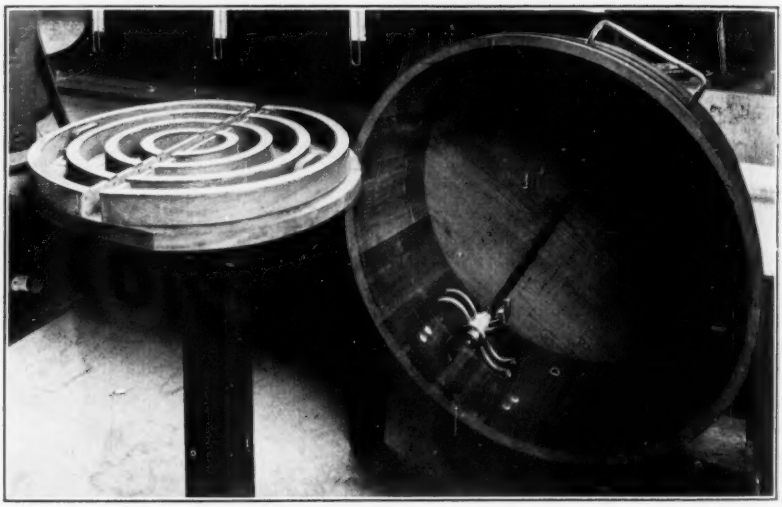

FIG. 3.—*Water-spraying arrangement and specimen racks for simulated atmospheric corrosion test apparatus*

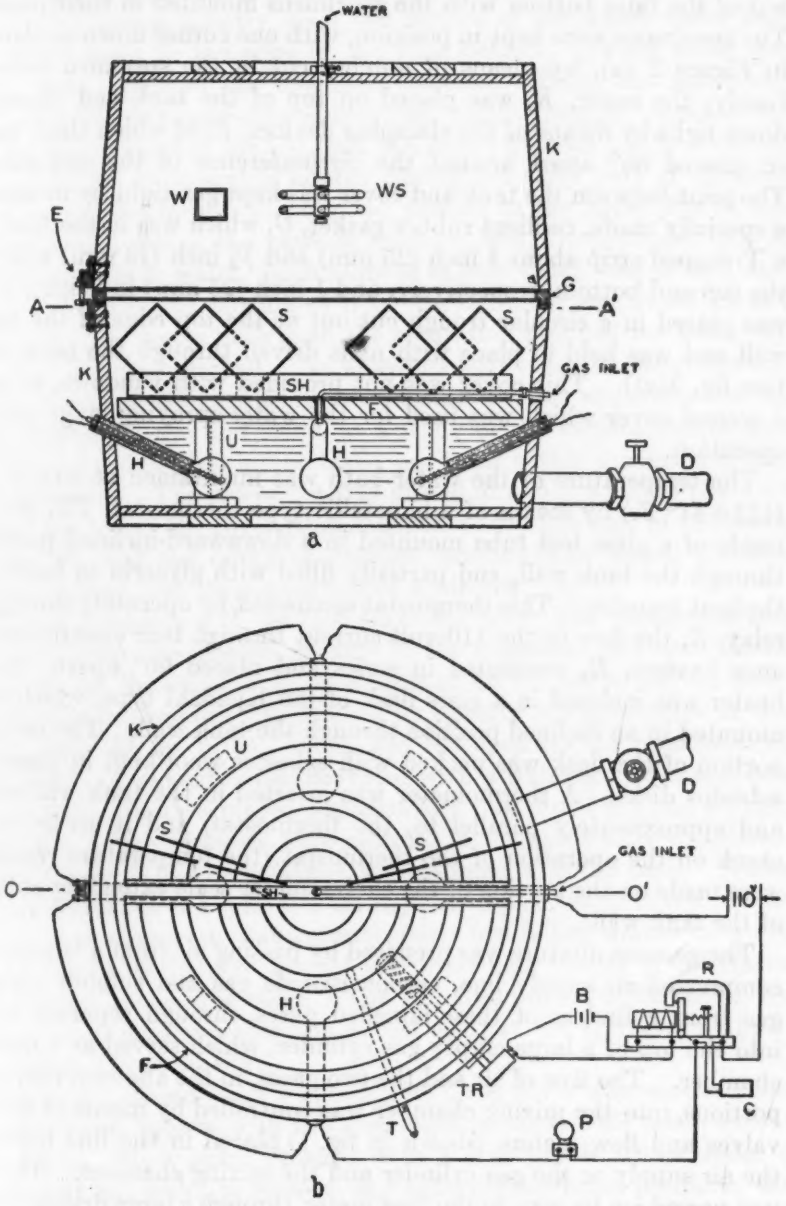

FIG. 2.—*Details of simulated atmospheric corrosion test apparatus*

a, vertical section at *O–O'*; the cover shown here was that used in the water-spraying stage of the operation; *b*, plan below horizontal plane *A–A'*: The wiring arrangement is shown at lower right; *WS*, water sprinkler; *W*, window; *S*, specimens; *SH*, specimen holder; *F*, false bottom; *H*, electrical heater; *D*, drain pipe; *U*, supports for false bottom and specimen holders; *T*, thermometer; *TR*, thermoregulator; *R*, relay; *P*, pilot light; *B*, battery; *C*, condenser; *K*, wooden container; *E*, clamping arrangement; *G*, rubber gasket

top of the false bottom with the specimens mounted in their places. The specimens were kept in position, with one corner down as shown in Figure 2 (*a*), by means of notches cut in the specimen holder. Lastly, the cover, *K*, was placed on top of the tank and clamped down tight by means of the clamping devices, *E*, of which there were six placed 60° apart around the circumference of the apparatus. The joint between the tank and cover was kept gas-tight by means of a specially made, resilient rubber gasket, *G*, which was in the form of a T-shaped strip about 1 inch (25 mm) and ½ inch (13 mm) wide at the top and bottom, respectively, and 1 inch (25 mm) in height, that was placed in a circular trough cut out at the top edge of the tank wall and was held in place with nails driven through the tank wall (see fig. 2(*a*)). This cover was not provided with windows, as was a second cover which was used for the water-spraying stage of the operation.

The temperature of the water bath was maintained at 50 ± 5° C. (122 ± 41° F.) by means of a bimetallic type thermostat, *TR*, placed inside of a glass test tube mounted in a downward-inclined position through the tank wall, and partially filled with glycerin to facilitate the heat transfer. This thermostat controlled, by operating through a relay, *R*, the flow of the 110-volt current through four electric resistance heaters, *H*, connected in series and placed 90° apart. Each heater was inclosed in a glass flask of the Kjeldahl type, which was mounted in an inclined position through the tank wall. The tubular portion of the flask was packed with asbestos wool kept in place by asbestos disks. A thermometer was inserted in the tank wall near, and approximately parallel to, the thermostat, and it served as a check on the operation of the thermostat (the temperature readings were made on the portion of the thermometer scale extending outside of the tank wall).

The gaseous mixture was prepared by passing air from a laboratory compressed-air supply line, carbon dioxide gas and sulphur dioxide gas from cylinders of these liquefied gases, through separate inlets into the top of a large empty gas cylinder, which served as a mixing chamber. The flow of air and the two gases, in the above-stated proportions, into the mixing chamber was controlled by means of needle valves and flow meters (shown in fig. 1) placed in the line between the air supply or the gas cylinder and the mixing chamber. The air was passed, on its way to the flow meter, through a large drying tower filled with soda lime to remove any carbon dioxide present. Concentrated sulpburic acid was used as the liquid in the flow meters. The resulting gaseous mixture was passed out through the bottom of the mixing chamber and into the testing apparatus. The terminus of

the gas-inlet tube on the tank was situated beneath the false bottom, as shown in Figure 2 (*a*), so that the incoming stream of gaseous mixture would come directly upon the surface of the warm water and spread radially to the edge of the false bottom, upward along the tank walls and into the specimen chamber. Thus, the specimens were exposed to a corroding atmosphere under "muggy" conditions.

The proportions of the CO_2 and SO_2 in the gaseous mixture would, of course, be considerably altered during the early part of the first stage, since the large volume of air present in the apparatus at the outset would dilute the gaseous mixture, and, furthermore, SO_2 is readily soluble in water, much more so in cold water than in hot, and thus a considerable portion of it in the incoming gas would be absorbed by the water bath until the saturation point of the water for SO_2 and CO_2 was reached. No attempts were made to determine the composition of the gaseous mixture inside the test apparatus during the progress of the first stage, as a study of the various details and refinements of the test methods did not come within the scope of this investigation. The gas outlet was placed at about 3 inches (76 mm) below the top of the cover (this is shown at the left edge of the cover in fig. 1), and the outgoing gaseous mixture was passed through rubber tubing into the air outside of a window.

At the completion of the first stage the cover was unclamped and removed after the gaseous mixture in the apparatus had been blown out through the exit tubing by a blast of air for about half an hour. The water in the tank was drained by opening the gate valve of the drain pipe (*D*, fig. 2 (*a*)), which was left open for the remainder of the cycle. A second cover, provided with a water sprinkler and two small glass windows placed diametrically opposite (*WS* and *W*, figs. 2 (*a*) and 3; the windows were inserted in the cover after the photograph for fig. 3 had been taken), was clamped onto the tank. Water was admitted to the sprinkler through the top of the sprinkler pipe at a rate slow enough so that a steady, fairly fast falling shower of water drops would be directed toward the underlying cluster of specimens throughout the second stage. The windows proved to be useful, for the pressure in the water line varied so that the sprinkler stopped functioning occasionally.

When the second stage was completed, the cover was removed and the specimen holders with the specimens in place were taken out of the tank. After being brushed with a stiff bristle brush under a stream of tap water to remove any adhering corrosion products, the specimens were put back in their places on the specimen holders, and the latter were either put back into the tank or placed on a near-by laboratory table for the third, or drying, stage.

109748°—28——3

(b) SPRAY TESTS

The apparatus employed in the spray tests is shown in Figure 4(*a*). The outside dimensions of the two Alberene stone boxes were 32 by 16½ by 12 inches (813 by 419 by 305 mm) in height, and the walls were 1¼ inches (32 mm) thick. A piece of plate glass served as the top cover, *D*, and permitted ready observation of the progress of the test. The specimens were suspended from glass rods, extending across inside the box, by means of glass hooks passing through a hole, ⅛-inch (3 mm) diameter, at the middle of one edge of the specimen (these details are not shown in Figure 4 (*a*). The corrodent was

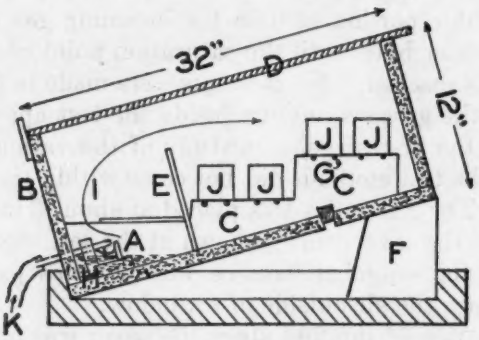

FIG. 4 (a).—*Details of spray box*

B, Alberene stone box; *A*, atomizer; *H*, corrosive solution; *K*, compressed air stream; *E*, baffle plates; *I*, course of spray; *D*, glass cover; *J*, specimens; *F*, support for box

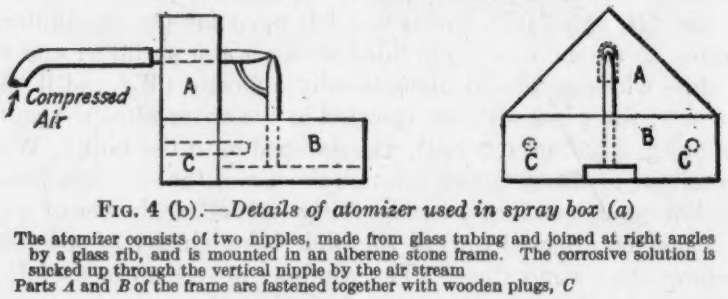

FIG. 4 (b).—*Details of atomizer used in spray box (a)*

The atomizer consists of two nipples, made from glass tubing and joined at right angles by a glass rib, and is mounted in an alberene stone frame. The corrosive solution is sucked up through the vertical nipple by the air stream
Parts *A* and *B* of the frame are fastened together with wooden plugs, *C*

atomized, by means of the device shown in Figure 4 (*b*), into a fog or fine mist which completely filled the specimen chamber. A stream of compressed air at 7 to 10 pounds pressure was used in atomizing the solution; the precaution was taken to remove any oil present by passing the air stream through a short length of a 2-inch diameter iron pipe filled with absorbent cotton. The baffle plates, *E*, served to protect the specimens from direct exposure to the stream of spray issuing from the atomizer and to swirling currents in the mist; the vertical baffle plate served also as a "dam" which prevented the condensed spray, containing the corrosion products from the specimens, from flowing back to the reservoir of solution, *H*. This res-

ervoir was at all times maintained at a level high enough for the efficient operation of the atomizer. The consumption of the corrodent amounted to about ½ liter per 24 hours.

Sodium chloride and ammonium chloride solutions of 1 *N* strength (containing 5.65 per cent NaCl and 5.35 per cent NH_4Cl by weight, respectively) were chosen for these spray tests, as they were of intermediate strength. The test with one solution was carried out in one box and that with the other simultaneously in another box. Both boxes were connected to the same air supply.

This form of test used with sodium chloride solution, usually a concentrated one (containing 20 per cent sodium chloride salt by weight), has been rather widely employed for testing all types of protective coatings, more particularly zinc coatings. It has been subjected to many criticisms, especially with respect to the lack of discrimination shown in bringing out thin spots in the coating and in the unsatisfactory differentiating between zinc coatings of generally similar nature and quality. It has, however, been considered useful by many in determining the relative value of coatings for marine or seacoastal exposure.

Farnsworth and Hocker [13] found in some tests, carried out by the intermittent-immersion method of testing, on iron specimens electroplated with zinc that a 2 per cent solution of ammonium chloride attacks and removes the zinc-corrosion products from the surface of the specimen without producing any or only a very slow action on the zinc metal, since the surface of the specimen and the salt solution remained clear of undissolved corrosion products. The addition of a small amount of an oxidizing agent to the salt solution produced a relatively more rapid action. They also noted that in a comparative test, carried out at 22°C. (72°F.) for 33½ hours, zinc continuously immersed in an aerated 2 per cent sodium chloride solution suffered a rate of attack, as determined by the rate of loss in weight, about one-third as fast as that in aerated ammonium chloride solution of the same strength. Results obtained at this bureau have shown that zinc on plated and "hot-dipped" sheets is not removed by immersion in a solution of salt (NaCl) nearly so rapidly as it is by a spray of the same solution.

IV. EXPERIMENTAL RESULTS

The results for the simulated atmospheric corrosion test are tabulated in Table 3 and summarized in Figure 5 (Tables 3 and 4 have been included in this paper for the benefit of those desiring to make a more detailed analysis of the test data). There are given in this table

[13] Farnsworth, F. F., and Hocker, C. D., "An intermittent-immersion test as an aid in evaluating zinc coats plated on iron and steel," Tr. Am. Electrochem. Soc., 45 p. 281; 1924.

the number of cycles, for both faces of each specimen, which were required to produce the first clearly defined indications that the coating had broken down as shown by the formation of a red-brown rust on the steel or iron base thus laid bare. In reaching the point of failure the second face of the specimen lagged behind the first face by one cycle in about 25 per cent of the cases and by two or more cycles in about 45 per cent of the cases. This is not surprising, for the thickness of the coating may not be quite the same on opposite surfaces of the sheet and even at different portions of the same surface. The

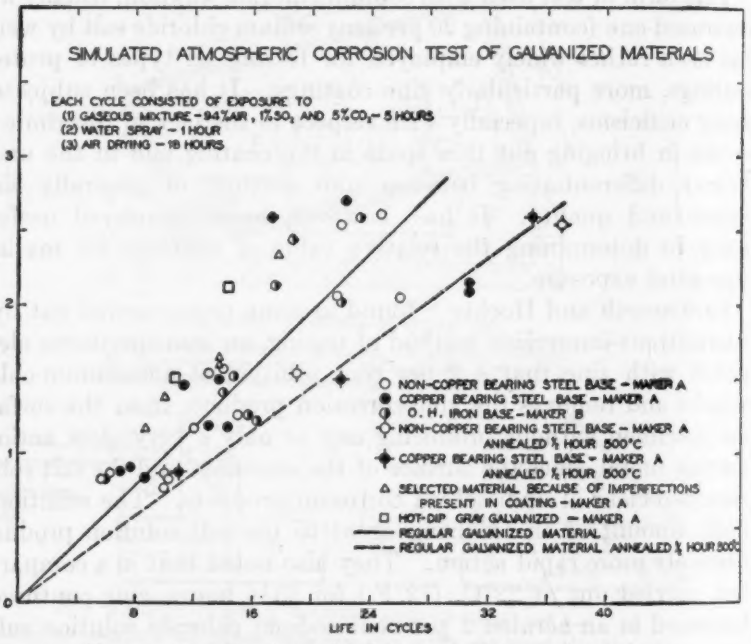
SIMULATED ATMOSPHERIC CORROSION TEST OF GALVANIZED MATERIALS
EACH CYCLE CONSISTED OF EXPOSURE TO
(1) GASEOUS MIXTURE - 94% AIR, 1% SO2 AND 5% CO2 - 5 HOURS
(2) WATER SPRAY - 1 HOUR
(3) AIR DRYING - 18 HOURS
WEIGHT OF COATING - OUNCES PER SQUARE FOOT OF SHEET
LIFE IN CYCLES
0
1
2
3
8
16
24
32
40
NON-COPPER BEARING STEEL BASE - MAKER A
COPPER BEARING STEEL BASE - MAKER A
O. H. IRON BASE - MAKER B
NON-COPPER BEARING STEEL BASE - MAKER A ANNEALED ½ HOUR 500°C
COPPER BEARING STEEL BASE - MAKER A ANNEALED ½ HOUR 500°C
SELECTED MATERIAL BECAUSE OF IMPERFECTIONS PRESENT IN COATING - MAKER A
HOT-DIP GRAY GALVANIZED - MAKER A
REGULAR GALVANIZED MATERIAL
REGULAR GALVANIZED MATERIAL ANNEALED ½ HOUR 500°C

FIG. 5.—*Results of simulated atmospheric corrosion tests*

Each point plotted in the diagram is the average value of three determinations

average values for the face (face No. 1) of the specimen, which first reached the failure point have been plotted in Figure 5 for the different test materials. Each point plotted represents the average of three determinations, which were made at the same time and under the same conditions. Although the plotted data show a considerable scattering, the solid line, which has been drawn in as nearly a mean position as practicable (with reference to all uncrossed circles), indicates the relation between the "life" of the coating, expressed in cycles, and the weight of the coating in oz./ft.^{2} of sheet; for example, a coating of 2.0 oz./ft.^{2} of sheet should require 20 or 21 cycles of exposure, under the conditions of the experiment, for the coating to break down.

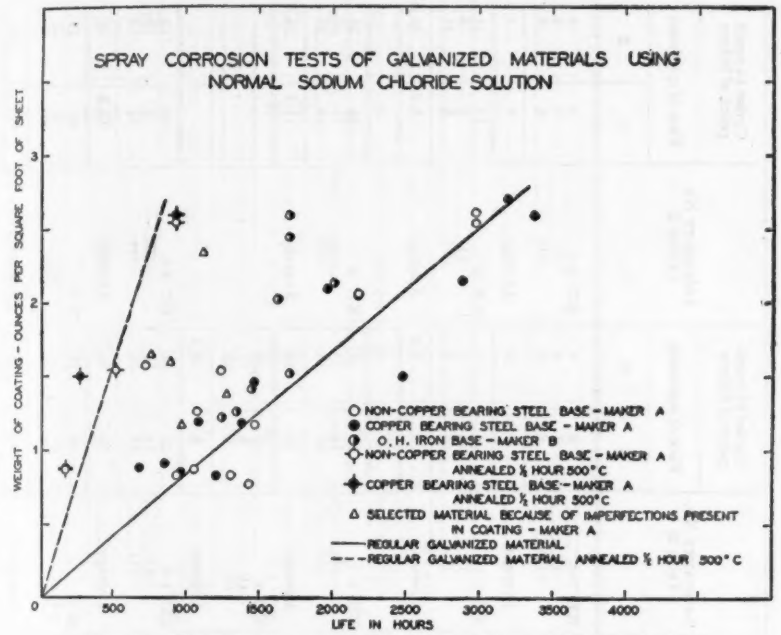
SPRAY CORROSION TESTS OF GALVANIZED MATERIALS USING
NORMAL SODIUM CHLORIDE SOLUTION
WEIGHT OF COATING - OUNCES PER SQUARE FOOT OF SHEET
LIFE IN HOURS
0
500
1000
1500
2000
2500
3000
3500
4000
1
2
3
NON-COPPER BEARING STEEL BASE - MAKER A
COPPER BEARING STEEL BASE - MAKER A
O. H. IRON BASE - MAKER B
NON-COPPER BEARING STEEL BASE - MAKER A ANNEALED ½ HOUR 500° C
COPPER BEARING STEEL BASE - MAKER A ANNEALED ½ HOUR 500° C
SELECTED MATERIAL BECAUSE OF IMPERFECTIONS PRESENT IN COATING - MAKER A
REGULAR GALVANIZED MATERIAL
REGULAR GALVANIZED MATERIAL ANNEALED ½ HOUR 500° C

FIG. 6.—*Results of spray tests with N sodium chloride solution*
Each point plotted in the diagram is the average value of three determinations

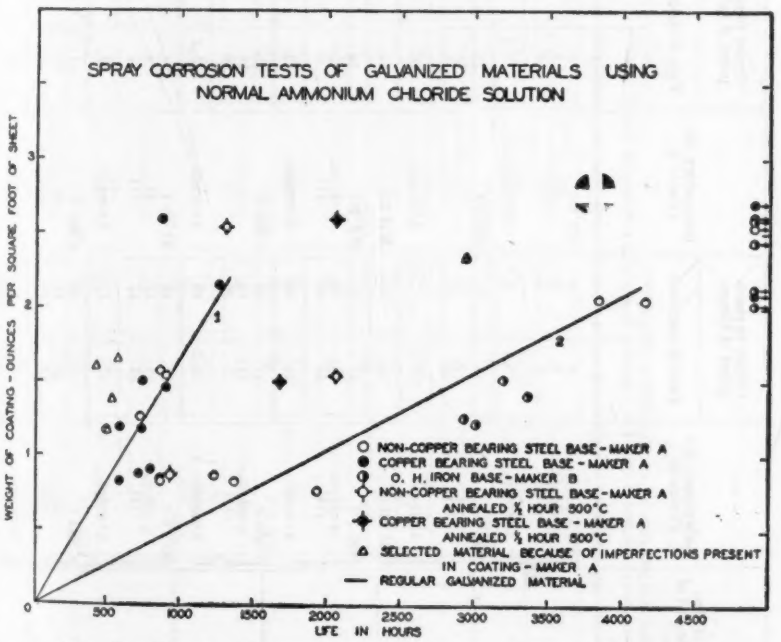

FIG. 7.—*Results of spray tests with N ammonium chloride solution*
Each point plotted in the diagram is the average value of three determinations. The results represented by curves 2 and 1 were influenced by the fact that the simulated atmospheric corrosion test was run, and was not run, respectively, simultaneously with and in close proximity to the spray test

TABLE 3.—*Results of simulated atmospheric corrosion test*

Weight of zinc coating (oz./ft.² of sheet)	Laboratory No. (Table 2)	Cycles to reach point of failure		Laboratory No. (Table 2)	Cycles to reach point of failure		Laboratory No. (Table 2)	Cycles to reach point of failure		Laboratory No. (Table 2)	Cycles to reach point of failure	
		Face of specimen			Face of specimen			Face of specimen			Face of specimen	
		1	2		1	2		1	2		1	2
0.75–1.0	SH 1–1	6	[1] 8	SH 2–1	7	9	KH 1–1	8	8	KH 2–1	8	8
	–11	6	6	–11	5	5	–11	7	8	–11	7	8
	–111	5	6	–111	7	9	–111	8	8	–111	6	6
	Average	5.7	6.7	Average	6.3	7.7	Average	7.7	8	Average	7	7.3
	SK 1–1	11	11	SK 2–1	11	11	KK 1–1	8	8	KK 2–1	12	14
	–11	10	10	–11	11	12	–11	6	8	–11	6	9
	–111	10	10	–111	8	9	–111	4	9	–111	8	11
	Average	10.3	10.3	Average	10	10.7	Average	6	8.3	Average	8.7	11.3
	SH 2B	10	13	KH 2B	11	11						
	SE 1–1	15	15	SE 2–1	12	14	KE 1–1	13	13	KE 2–1	14	14
	–11	15	15	–11	15	15	–11	13	13	–11	15	15
	–111	15	15	–111	9	10	–111	13	13	–111	14	15
	Average	15	15	Average	12	13	Average	13	13	Average	14.3	14.7
1.25	C886–1	17	19	C887–1	15	18	X 1–1	9	10			
	–11	17	19	–11	16	24	–11	8	11			
	–111	15	19	–111	16	18	–111	9	10			
	Average	16.3	19	Average	15.7	20	Average	8.7	10.3			
	SC 1–1	13	18	SC 2–1	14	16	KC 1–1	13	13	KC 2–1	10	12
	–11	13	17	–11	14	18	–11	14	15	–11	12	12
	–111	13	17	–111	14	17	–111	14	16	–111	12	12
	Average	13	17.3	Average	14	17	Average	13.7	14.7	Average	11.3	12
1.5	C880–1	15	18	C881–1	13	[1] 21	24–1	10	12	X 2–1	10	11
	–11	13	16	–11	15	17	–11	12	15	–11	9	12
	–111	16	18	–111	14	16	–111	10	12	–111	11	13
	Average	14.7	17.3	Average	14	18	Average	10.7	13	Average	10	12

1.5	X4-1	14	15	X 5-1	12	13	SC 1B	19	22	KC 1B	22	(3)
	-11	14	14	-11	13	14						
	-111	13	15	-111	16	17						
	Average	13.7	14.7	Average	13.7	14.7						
2.0	SB 1-1	26	27	SB 2-1	27	27	KB 1-1	30	30	KB 2-1	34	37
	-11	22	24	-11	24	26	-11	31	34	-11	31	33
	-111	17	17	-111	27	28	-111	31	32	-111	27	30
	Average	21.7	22.7	Average	26	27	Average	30.7	32	Average	30.7	33.3
	C882-1	19	25	C883-1	20	21	30-1	13	18			
	-11	25	31	-11	15	20	-11	16	16			
	-111	22	23	-111	(2)	(2)	-111	14	16			
	Average	22	26.3	Average	17.5	20.5	Average	14.3	16.7			
2.5	SA 1-1	28	31	SA 2-1	24	38	KA 1-1	22	22	KA 2-1	16	23
	-11	20	23	-11	26	[1] 42	-11	23	25	-11	18	19
	-111	18	27	-111	24	32	-111	22	27	-111	18	18
	Average	22	27	Average	24.7	37.3	Average	22.3	24.7	Average	17.3	20
	C884-1	20	30	C885-1	20	25	X 3-1	18	22			
	-11	17	23	-11	25	25	-11	18	20	SA 1B	37	37
	-111	19	24	-111	25	30	-111	17	17			
	Average	18.7	25.7	Average	23.3	26.7	Average	17.7	19.7			
	KA 2B	35	38									
Unknown	SSSG-1	1	1	SSSL-1	5	5						
	-11	1	2	-11	5	5						
	-111	1	1	-111	6	9						
	Average	1	1.3	Average	5.3	6.3						

[1] Estimated. The specimen was taken out of test in the previous cycle, but the appearance of the second face indicated that the failure point would probably have been reached in the next cycle.
[2] Specimen was taken out of test before the second face had reached the failure point.
[3] Specimen was lost before the conclusion of the test.

TABLE 4.—*Results of spray corrosion tests made with sodium chloride and ammonium chloride solutions of normal strength*

[The specimens were taken out of test at irregular intervals for inspection and the noting of the progress of corrosion. They were washed and brushed as free of corrosion products as possible before each inspection]

Weight of zinc coating (oz./ft.² of sheet)	Laboratory No. (Table 2)	Hours to reach point of failure on either face of specimen		Laboratory No. (Table 2)	Hours to reach point of failure on either face of specimen		Laboratory No. (Table 2)	Hours to reach point of failure on either face of specimen		Laboratory No. (Table 2)	Hours to reach point of failure on either face of specimen	
		NaCl	NH_4Cl		NaCl	NH_4Cl		NaCl	NH_4Cl		NaCl	NH_4Cl
	SH 1-1	1,185	1,190	SH 2-1	815	775	KH 1-1	885	675	KH 2-1	765	865
	-11	1,185	425	-11	1,185	995	-11	1,475	865	-11	765	425
	-111	1,555	995	-111	1,185	1,935	-111	520	865	-111	520	865
	Average	1,310	870	Average	1,060	1,235	Average	860	[1] 800	Average	685	[1] 720
0.75–1.0	SK 1-1	815	1,190	SK 2-1	1,185	1,935	KK 1-1	1,500	675	KK 2-1	765	865
	-11	815	1,935	-11	1,185	1,935	-11	640	425	-11	640	865
	-111	1,185	995	-111	1,935	1,935	-111	1,500	675	-111	1,500	865
	Average	940	1,375	Average	1,435	1,935	Average	1,210	[1] 590	Average	970	[1] 865
	SH 2B	170	935	KH 2B*	170	935						
	SE 1-1	1,475	675	SE 2-1	1,475	425	KE 1-1	885	425	KE 2-1	1,160	865
	-11	885	845	-11	1,475	630	-11	885	675	-11	1,500	675
	-111	885	675	-111	1,475	425	-111	1,500	675	-111	1,500	675
	Average	1,080	[1] 730	Average	1,475	[1] 495	Average	1,090	[1] 590	Average	1,385	[1] 740
1.25	C 886-1	1,250	2,930	C 887-1	1,550	2,930	X 1-1	1,160	425			
	-11	1,250	2,930	-11	1,250	2,930	-11	885	545			
	-111	1,250	3,175	-111	1,250	2,930	-111	885	545			
	Average	1,250	3,010	Average	1,350	2,930	Average	975	[1] 505			
	SC 1-1	765	990	SC 2-1	520	865	KC 1-1	3,060	990	KC 2-1	2,635	865
	-11	1,475	865	-11	765	865	-11	2,890	250	-11	885	990
	-111	1,475	865	-111	885	865	-111	1,500	990	-111	885	865
	Average	1,240	[1] 905	Average	725	[1] 865	Average	2,480	[1] 745	Average	1,470	[1] 905
1.5	C 880-1	1,550	3,195	C 881-1	1,550	3,195	X 2-1	1,475	630	X 4-1	765	545
	-11	1,790	3,195	-11	1,550	3,440	-11	1,475	425	-11	765	545
	-111	1,790	3,195	-111	1,250	3,440	-111	885	545	-111	765	630
	Average	1,710	3,195	Average	1,450	3,360	Average	1,280	[1] 535	Average	765	[1] 575

1.5	X 5-1	885	425	SC 1B	520	2,060	KC 1B	270	1,680			
	-11	640	425									
	-111	1,160	425									
	Average	895	[1] 425									
2.0	SB 1-1	2,180	3,845	SB 2-1	2,180	3,845	KB 1-1	2,890	865	KB 2-1	2,180	[2]
	-11	2,180	3,845	-11	2,180	4,790	-11	2,890	1,530	-11	2,180	[2]
	-111	2,180	3,845	-111	2,180	3,845	111	2,890	1,405	-111	1,555	4,065
	Average	2,180	3,845	Average	2,180	4,160	Average	2,890	[1] 1,265	Average	1,970	[2]
	C 882-1	1,790	4,145	C 883-1	2,015	[2]						
	-11	1,550	[2]	-11	2,015	4,145						
	-111	1,550	[2]	-111	2,015	[2]						
	Average	1,630	[2]	Average	2,015	[2]						
	SA 1-1	2,980	[2]	SA 2-1	2,980	[2]	KA 1-1	2,890	[2]	KA 2-1	3,625	1,215
	-11	2,980	[2]	-11	2,980	[2]	-11	3,825	[2]	-11	3,625	425
	-111	2,980	[2]	-111	2,980	[2]	-111	2,890	[2]	-111	2,890	990
	Average	2,980	[2]	Average	2,980	[2]	Average	3,200	[2]	Average	3,380	[1] 875
2.5	C 884-1	1,790	[2]	C 885-1	1,790	[2]	X 3-1	815	1,935			
	-11	1,790	[2]	-11	1,790	[2]	-11	1,935	3,440			
	-111	1,550	[2]	-111	1,550	[2]	-111	615	3,440	SA 1B	935	1,310
	Average	1,710	[2]	Average	1,710	[2]	Average	1,120	2,940			
	KA 2B	935	2,060									
Unknown	SSSG-1	700	700	SSSL-1	700	700						
	-11	700	700	-11	700	700						
	-111	700	700	-111	700	700						
	Average	700	700	Average	700	700						

[1] These specimens were put into the ammonium chloride spray test and had reached the failure point before the simulated atmospheric corrosion tests were started. The KA 1 specimens were put into test at the same time but did not reach the failure point for a long time afterwards.
[2] Over 5,000 hours.

The data for the heat-treated specimens (Nos. 37 to 42, Table 2) have been plotted as crossed circles. The dashed line drawn for these data clearly indicates the improvement in the "life" of the coating to be gained by the heat treatment, as compared with the solid line for the nonheat-treated material. The results for the test materials with imperfect coatings (Nos. 43 to 47, Table 2) have been plotted as triangles; the unfavorable effect of the imperfection in the coating upon the "life" of the coating appears to be borne out by the fact that all the results lie to the left of the general trend for the materials with normal coatings. The imperfections in the coating were blisters of varying length and width scattered over the surface of the sheet, very small spangles which were quite uniformly distributed over the surface ("gray galvanized"), spangles on the same surface which varied very markedly in size and distribution ("irregular gray"), and coatings of a stringy nature. Furthermore, the results for the two "gray-galvanized" materials (Nos. 33 and 34, Table 2, plotted as squares in fig. 5) also lie to the left, thus appearing to fall in the same category as the materials with imperfect coatings.

The results for the spray tests made with both sodium chloride and ammonium chloride solutions have been collected in Table 4, the data here included being only for the one face of the specimen which first reached the failure point. The positions of the specimens in the spray boxes were changed intermittently during test, and without regard to any clearly defined plan. No efforts were made to maintain the faces of the specimens in the same general direction with respect to exposure to the currents of mist. The simultaneous reaching of the failure point by both faces of the specimens was observed in only about 25 per cent of the cases. Since a prolonged period of time was required in these tests for the breaking down of the coating, many of the specimens were taken out of test before the second face of the specimen had reached the failure point. The plotted results (average of three determinations made at the same time and under the same conditions) for the sodium chloride and ammonium chloride spray tests are shown in Figures 6 and 7, respectively.

V. DISCUSSION OF RESULTS

1. SIMULATED ATMOSPHERIC CORROSION TEST

The results for the regular galvanized material, represented by the solid line in Figure 5, show a quite consistent trend in the relationship between the weight and the "life" of the coating, particularly in view of the probability that the actual weight of the coating on the individual specimens tested may have varied to an appreciable extent from the average weight of coating determined for the large sheet. An examination of the data in the last four

columns in Table 2 will indicate that such a variation occurs, and that the variation tends to be greater with the heavier coats. This is borne out by the greater scattering of the plotted data for the heavier coated materials shown in Figure 5. Furthermore, it has been stated in a handbook on the manufacture of steel products [14] that a variation of 0.35 ounce per square foot of sheet in a 2-ounce coat is considered as satisfactory in good commercial practice, even when the galvanizing operation is carried out mechanically.

The only known published data for hot-dip galvanized sheets tested by this form of testing method are those reported by Finkeldey in connection with some accelerated tests that were carried out by the American Society for Testing Materials through Subcommittee VII of its Committee A–5.[15] Since in these tests the exposure of the specimens to the corroding atmosphere and to the water spray during each 24-hour cycle was twice as long as in our tests, direct comparisons in the results of both tests could hardly be expected. One should rather look for a shorter "life" on the part of the coating exposed for a longer time per cycle to the corroding influences. In the three cases reported, the specimens, which had a coating of 4.36 and 5.20 ounces per squre foot of sheet (2.18 and 2.60 ounces per square foot of surface) showed a "life" of about 25 to 30 cycles. The extrapolation of the solid line in Figure 5 would indicate a "life" for a 5.0-ounce coating of about 50 cycles, which is about twice the number of cycles required under the above-mentioned more concentrated conditions. It might appear from this that approximately the same ratio holds between the length of exposure to the corroding conditions and the number of cycles required for the coating to reach the failure point; further data would be needed to establish this conclusion.

The results for the six specimens of regular galvanized materials, which were subjected to an annealing treatment for one-half hour at 500° C. for the purpose of converting, through diffusion, at least a considerable portion of the zinc coating into an iron-zinc alloy, were also quite consistent (crossed circles and dashed line in fig. 5). The employment of a relatively high temperature should increase the affinity between the iron of the base metal and the zinc in the coating and consequently the amount of the iron-zinc alloy formed.[16] This heat treatment appears to have prolonged somewhat the "life" of the coating, especially in the case of specimens with heavier zinc coatings. A possible explanation for this seems to be that, since the

[14] Camp and Francis, The Making, Shaping, and Treating of Steel, 4th ed., p. 970; 1925.

[15] See p. 145 of reference cited in footnote 6.

[16] The heat treatment of hot-dipped zinc coatings has been discussed by H. S. Rawdon in his book, Protective Metallic Coatings, American Chemical Society Monograph Series No. 40, Chemical Catalog Co. (Inc.); p. 97; 1928. Also see Figure 27 on p. 92, which gives a much clearer reproduction of the micrographs shown in Figures 7 to 10 of W. H. Finkeldey's paper, "Microstructure of zinc coatings," Proc. Am. Soc. Test. Mat., 26, Pt. II, p. 308; 1926.

amount of zinc metal in the outer portions of the coating was evidently reduced, the corrosive attack produced by the corrodent in question on the iron-zinc alloy as a whole proceeded at a slower rate than would have been the case if portions of an overlying zinc metal layer were present whereby the general corrosive attack would have been accelerated by the reaction between the anodic zinc layer and the cathodic iron-zinc alloy layer. This accelerative effect should be the more marked as the weight of the zinc coating increases and the coating tends to become more uneven in thickness. The corroding away of the zinc metal layer down to the underlying iron-zinc alloy layer should occur at a considerably earlier stage along the relatively much thinner portions, as at the boundaries of the spangles and between the fernlike ribs of the rosette-shaped spangles, than elsewhere.

With the materials having a lower grade of coating, such as gray-galvanized, blistered coatings, etc. (see Nos. 33, 34, and 43 to 47, inclusive, Table 2), the results, which have been plotted in Figure 5 as triangles and squares, show a decided trend toward a shorter "life." The less satisfactory nature of the coating appears to be thus confirmed.

A record was kept of the progressive changes in the surface appearance of the coating for the various specimens in the course of test. The general type of progressive changes was found to be much the same as that outlined by Finkeldey. (See Sec. II, p. 258.) Figures 9, 10, 11, 13, and 15 show several characteristic types of the progressive corroding away of the zinc coating, and Figures 8, 12, 14, and 16, for purposes of comparison, the original appearance of the materials having the lightest and heaviest hot-dip galvanized coatings, "gray-galvanized" coating, and lead coating. In all cases, the hot-dip galvanized specimens began to lose their metallic luster in the first cycle. Dark-colored (dark gray or blue black) patches began to appear at the thinnest portions of the coating after, on an average, about 2 or 3 cycles for the lightest coatings (0.75 to 1.25 ounces) and about 10 cycles for the heaviest coatings (2.5 ounces). These patches generally started along the boundaries of the grains or spangles (figs. 17, 18, and 19) and extended out in an irregular manner. These dark-colored areas (*B* in figs. 9, 10, 11, and 13) were the portions of the outer iron-zinc alloy (presumably $FeZn_7$) which had been laid bare by the removal of the overlying layer of zinc metal. Next, after an additional number of cycles, there appeared in one or more places in the dark-colored patches light areas with a metallic luster (*C*), which were portions of the subjacent iron-zinc layer (probably $FeZn_3$). Shortly before and coincident with their appearance there was present on the surface of the specimen, in conjunction with their locations, a yellow-colored film

FIG. 8.—*Appearance of an 0.9-ounce coating in the "as received" condition. (Material No. 4, Table 2.)* × ¾

This coat had a smooth surface with no ridges between the adjacent spangles standing out in relief

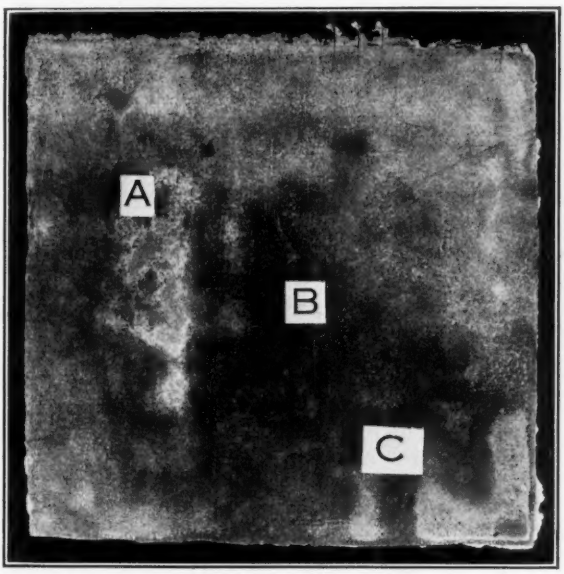

FIG. 9.—*Change in appearance of an 0.8-ounce coating after 11 cycles' exposure in the simulated atmospheric corrosion test. (Material No. 21, specimen SK1–111, Table 2.)* × ¾

A, relics of zinc metal layer; *B*, outer iron-zinc alloy layer; *C*, inner iron-zinc alloy layer; the dark patch shown in the lower right corner of the L-shaped area is red-brown iron rust.

UNIV OF MICH

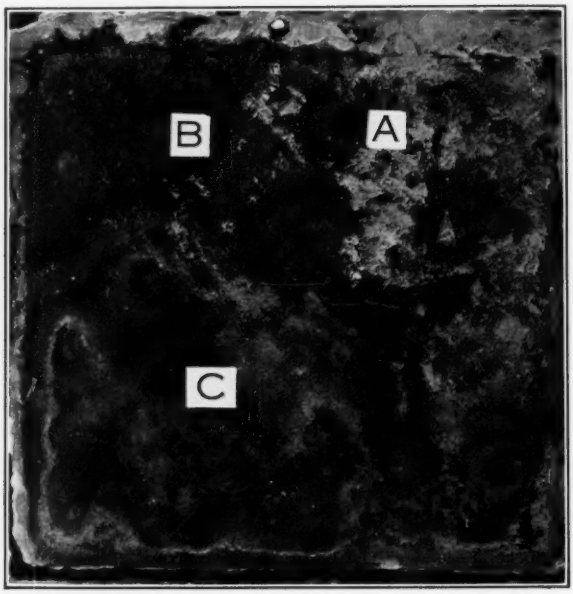

FIG. 10.—*Change in appearance of a 2.2-ounce coating after 34 cycles' exposure in the simulated atmospheric corrosion test. (Material No. 15, specimen KB1–11, Table 2.)* × ¾

A, relics of zinc metal layer; *B*, outer iron-zinc alloy layer; *C*, inner iron-zinc alloy layer; the dark patches shown scattered through this area are red-brown iron rust

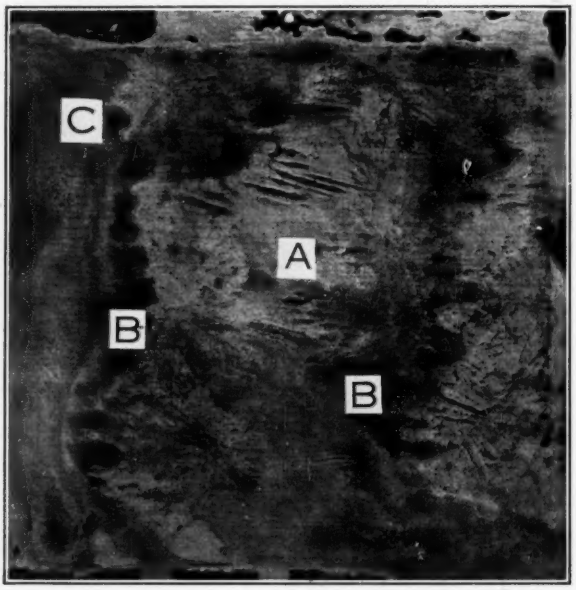

FIG. 11.—*Change in appearance of a 2.1-ounce coating after 23 cycles' exposure in the simulated atmospheric corrosion test. (Material No. 30, specimen 883–11, Table 2.)* × ¾

A, relics of zinc metal layer; *B*, outer iron-zinc alloy layer; *C*, inner iron-zinc alloy layer; the dark patch shown at the lower end of this elongated area is red-brown iron rust

FIG. 12.—*Appearance of a 2.6-ounce coating in the "as received" condition. (Material No. 18, Table 2.)* × ¾

Various portions of the surface, as along the boundaries between the spangles and also alongside some of the dendritic branches of the spangle, stood out in decided relief and the corroding through of the zinc metal layer usually occurred first at these places where the coating was thinnest. In the center of the two large adjacent spangles may be seen "chain conveyor marks." Several materials having these marks, which were generally not deep-seated, showed no tendency for the failure point to occur first at these points

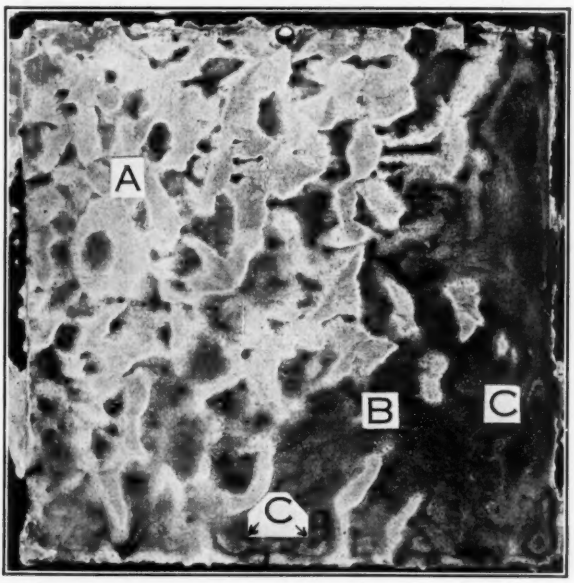

FIG. 13.—*Change in appearance of a 2.7-ounce coating after 27 cycles' exposure in the simulated atmospheric corrosion test. (Material No. 19, specimen KA1–11, Table 2.)* × ¾

A, relics of the zinc metal layer; *B*, outer iron-zinc alloy layer; *C*, inner iron-zinc alloy layer; the darker portions of these areas are red-brown iron rust

UNIV OF MICH

FIG. 14.—*Appearance of a specimen of lead-coated material in the "as received" condition. (Material No. 35, Table 2.)* × ¾

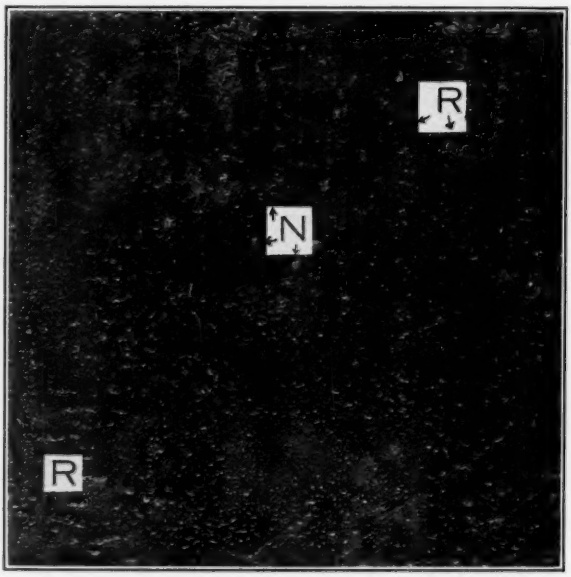

FIG. 15.—*Change in appearance of a specimen of lead-coated material after 55 cycles' exposure in the simulated atmospheric corrosion test. (Material No. 35, specimen SSSL–1, Table 2.)* × ¾

The lead coat is badly roughened and many blisters have formed (compare with fig. 14). The underlying surface at some of the blisters is strongly rusted (*R*) while that at some of the other blisters show a gray-colored, matte appearance (*N*). This specimen had reached the "failure point" after 5 cycles, exposure

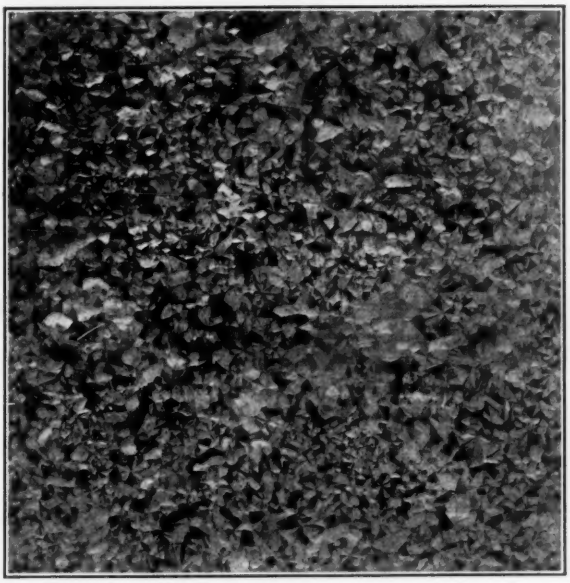

FIG. 16.—*Appearance of a "gray galvanized" coating in the "as received" condition (1.6-ounce coating; material No. 46, Table 2.)* × ¾

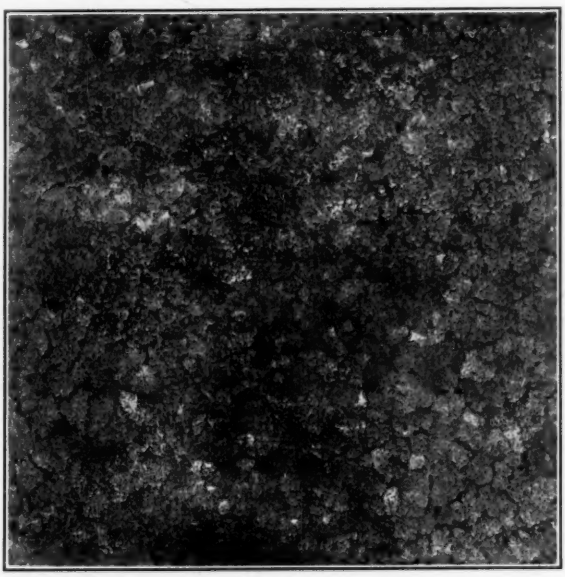

FIG. 17.—*Change in appearance of the "gray galvanized" coating after 5 cycles' exposure in the simulated atmospheric corrosion test (1.6-ounce coating; material No. 46, specimen X5–1, Table 2.)* × *1*

The corroding away of the "gray galvanized" coat has started along the grain boundaries

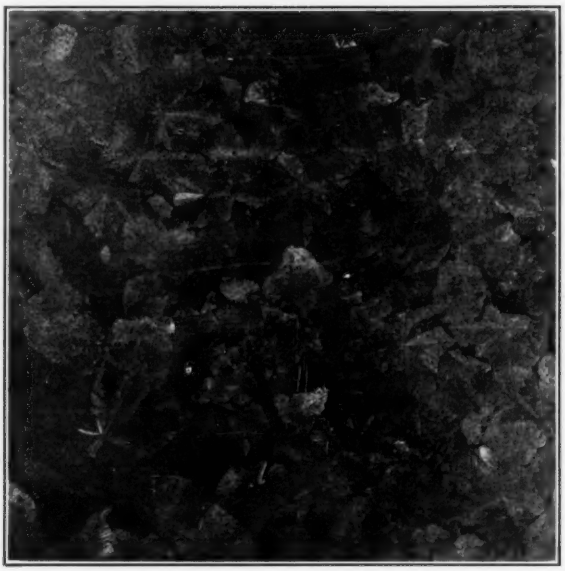

FIG. 18.—*Change in appearance of a 1.7-ounce coating after 5 cycles' exposure in the simulated atmospheric corrosion test (Material No. 45, specimen X4-1, Table 2.)* × 1

The corroding away of the coating has started along the grain boundaries

FIG. 19.—*Change in appearance of a 2.7-ounce coating after 5 cycles' exposure in the simulated atmospheric corrosion test. (Material No. 19, specimen KA1–11, Table 2.)* × 1

The corroding away of the coating is starting at the junctions between the adjoining grains

(a corrosion product containing both zinc and iron) which was easily brushed off during the cleaning operation following the water-spraying stage of the cycle. In the following cycles this inner iron-zinc alloy layer gave way, usually along the central portions of the exposed surface, to the underlying base metal, whose presence was made evident by the formation, at these points, of red-brown iron rust. The first definite appearance of this rust constituted the

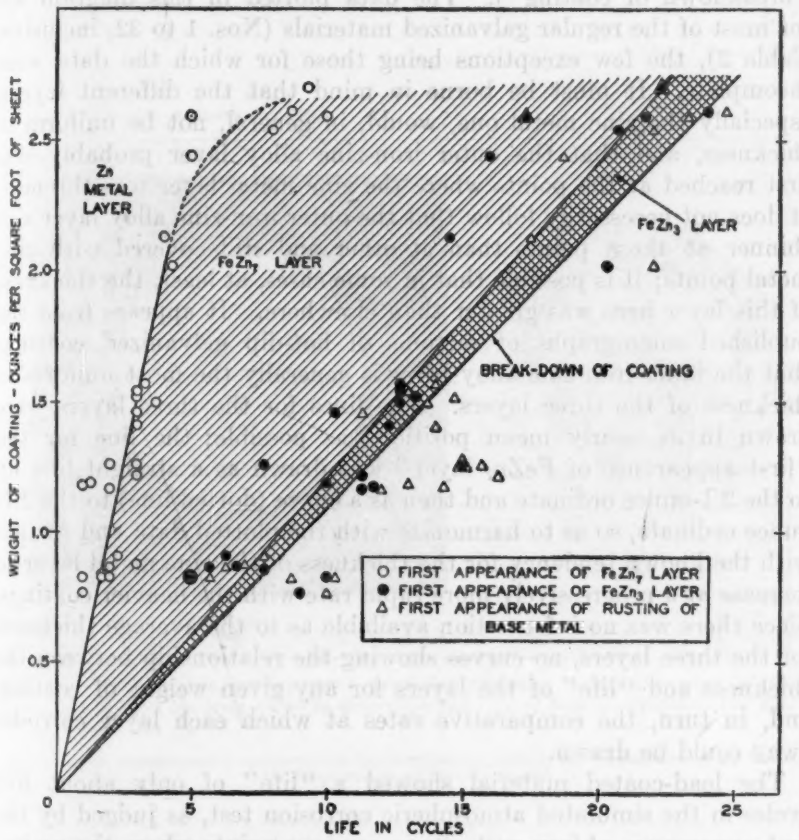

FIG. 20.—*"Life" of the three layers constituting hot-dip zinc coatings, as determined by the first appearance of the inner two layers and base metal in the simulated atmospheric corrosion test*

Each point plotted in this diagram is the average of three determinations

"failure-point" in these tests. The rusted areas are clearly indicated in Figures 9, 10, 11, and 13, as dark patches lying within the lighter areas designated by *C*. With the heavier-coated materials, there was, oftentimes, a considerable portion of the zinc-metal layer, *A*, which remained quite intact while the corrosion of the other portion of the surface had proceeded to the outer and inner iron-zinc alloy layers and to the base metal. (See fig. 13.) There were also cases

noted, as illustrated by Figure 11, where the zinc coating at different portions of the surface was distinctly irregular in thickness.

Figure 20 shows the "life" of the three components of the zinc coating, as judged by the time from the start of the tests, expressed in cycles, required for the first appearance of the outer iron-zinc alloy ($FeZn_7$), the inner iron-zinc alloy ($FeZn_3$), and the red-brown iron rust due to the corroding of the base metal (designated as the "breakdown of coating"). The data plotted in this diagram are for most of the regular galvanized materials (Nos. 1 to 32, inclusive, Table 2), the few exceptions being those for which the data were incomplete. It must be borne in mind that the different layers, especially the zinc metal one, would, in general, not be uniform in thickness, and that the outer iron-zinc alloy layer probably was first reached at the points where the zinc metal layer was thinnest. It does not necessarily follow that the outer iron-zinc alloy layer was thinner at these points than at other and still covered with zinc metal points; it is possible that in some cases, at least, the thickness of this layer here was greater than elsewhere. It appears from the published micrographs of sections of hot-dip galvanized coatings that the inner iron-zinc alloy layer is generally the most uniform in thickness of the three layers. The lines for the three layers were drawn in as nearly mean positions as possible; the line for the "first appearance of $FeZn_7$ layer" was drawn as a straight line up to the 2.1-ounce ordinate and then as a curve (dotted line) to the 2.7-ounce ordinate, so as to harmonize with the plotted data and further with the known tendency for the thickness of the zinc metal layer to increase at a progressively more rapid rate with the heavier coatings, Since there was no information available as to the average thickness for the three layers, no curves showing the relationship between the thickness and "life" of the layers for any given weight of coating. and, in turn, the comparative rates at which each layer corrodes away could be drawn.

The lead-coated material showed a "life" of only about five cycles in the simulated atmospheric corrosion test, as judged by the first appearance of iron rust at one or more points where the underlying metal had been laid bare by comparatively very small-sized blisters that had formed in the lead coating. The "breaking down" of the lead coating started with the formation, in the second or third cycle, of blisters in the coating, followed first by the appearance in or around the blisters of a yellow-colored rust ascribed to the corroding of the iron-zinc alloy in a thin zinc coating which must have been present between the lead coating and the steel base, and finally by the presence within the blistered area of red-brown rust produced by the corroding of the steel base. The lead coating itself remained uncorroded, yet the very fact that, under the conditions of the test,

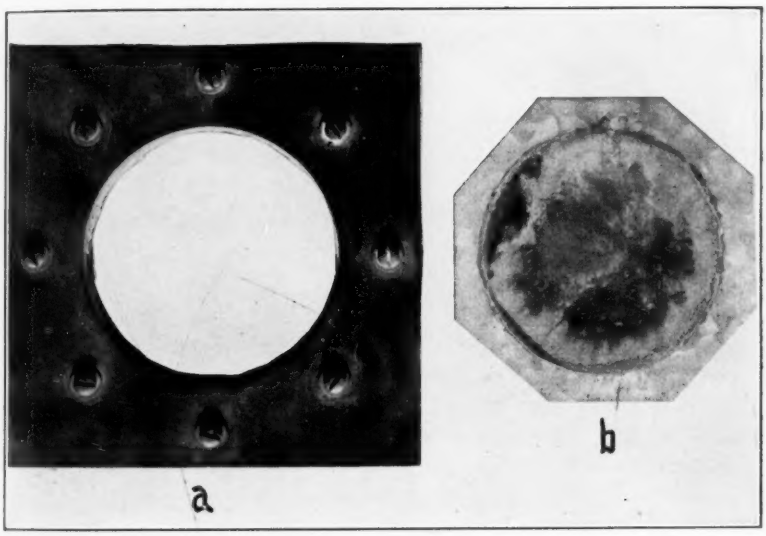

FIG. 21.—*Clamping arrangement used for exposing a definite area of the specimen in the tests made to determine the rate of loss in weight of the zinc coating.* × ½

a, clamping arrangement; *b*, specimen; the dark areas shown inside of the circular area on the face of the specimen are red-brown iron rust

it showed a tendency to blister lessened its value as a protective coating, at least in the case of thin coatings. The formation of blisters, simultaneous with that of very small moundlike protuberances in the intervening portions of the lead coating, increased in extent with the time of exposure. After a sufficiently long exposure the lead coating assumed a generally roughened and unsightly appearance, with small rusted areas scattered here and there. Figure 15 shows the appearance, after 55 cycles exposure, of one of the three specimens which were kept in test for many additional cycles after the "failure point" had been reached with the object of observing the progressive development of the roughened surface. Here the lead coating appears badly roughened (compare with fig. 14) and with blisters formed in many places. The underlying metal left bare by some of these blisters was strongly rusted, while that at other places showed a gray, mattelike appearance quite free from rust. The behavior manifested during this long exposure confirmed the conclusion that the lead-coated material had been galvanized before the lead coating was applied, and that the latter shows a distinct tendency to separate from the underlying zinc coating as corrosion progresses. Furthermore, it is apparent that the simulated atmospheric corrosion test serves admirably to show the presence of "pinholes" in lead coatings.

It was of interest to know whether or not the corroding away of the zinc coating was maintained at any definite rate for all the cycles up to the point of failure, and this rate was independent of the initial weight of coating. Some tests were carried out in an attempt to determine this point experimentally. Specimens of selected materials were mounted in hard-rubber clamps provided with a circular hole having an area of 3 square inches (1,935 mm^2). Figure 21 shows one of these clamps and also one of the specimens used in these tests. The specimen was clamped between two sheets of soft rubber, each being about one-sixteenth inch (2 mm) thick and having the same size hole as that in the mount, inside of the mount. Care was taken with the aid of reference marks to place the specimen back in the same position, with respect to the edge of the hole, for each succeeding cycle in order that the area on both surfaces of the specimen exposed in the series of cycles remained always the same during test. The clamps with the specimens mounted therein were placed in a vertical position on the specimen holder in the test apparatus (*SH*, fig. 2(*a*)). There were included with the series of coated specimens two specimens of commercially pure sheet zinc, 4 inches (102 mm) square and 0.017 inch (0.4 mm) thick. A typical analysis of this zinc material was as follows: Pb, 0.19 per cent; Cd, 0.38 per cent; Fe, 0.02 per cent; Cu, not detected; and Zn, 99.41 per cent (by difference). The results of two series of tests, the second one being carried out as a matter of checking up the first one, are given in Table 5. The losses in weight

for the individual zinc-coated and zinc-metal specimens were found to vary in an irregular manner from cycle to cycle between the limits given in the sixth and seventh columns of Table 5. The variations lay within the range, 0.013 to 0.033 oz./ft.^{2} of sheet in 93 per cent of the cases for the first series and 0.018 to 0.055 oz./ft.^{2} of sheet in 91 per cent of the cases for the second series. However, in both series of tests, the average loss in weight per cycle (fifth column, Table 5) for the zinc-coated specimens approached a quite definite value, which was independent of the initial weight of coating. These average values were in good agreement with those for the zinc metal specimens. Furthermore, the ratio of the initial weight of coating to the total loss in weight (last column, Table 5) approached a constant value, which was independent of the initial weight of coating. In comparing the results of the first series with those of the second series, these average values differ rather markedly. The only explanation offered to account for the greater losses in weight in the second series is that the concentration of the corroding gases may possibly have been allowed to run at a little higher level than in the first series. It is of interest to note that the loss in weight suffered by most of the coated specimens in both series was greater in the first cycle than in the subsequent cycles.

TABLE 5.—*Results of tests made to show the rate at which the zinc coating lost in weight in the simulated atmospheric corrosion test*

FIRST SERIES

Laboratory No. (Table 2)	Weight of zinc coating (W), as determined by weighing method	Tested to point of failure							Ratio weight of coating to total loss in weight
		Number of cycles	Total loss in weight of specimen (TL)	Average loss in weight of specimen per cycle	Loss in weight in any cycle		Deviation from average loss in weight		
					Maximum	Minimum	Maximum	Minimum	
	Oz./ft.^{2} of sheet		*Oz./ft.^{2} of sheet*	*Oz./ft.^{2} of sheet*	*Oz./ft.^{2} of sheet*	*Oz./ft.^{2} of sheet*	*Per cent*	*Per cent*	W/TL
SH 1	0.83	5	0.1029	0.0206	[1] 0.0308	0.0155	49.5	24.8	8.0
KH 1	.91	5	.1049	.0210	[1] .0300	.0137	42.9	34.8	8.7
KE 1	1.19	8	.1507	.0188	[1] .0308	.0135	63.8	28.2	7.9
KC 1	1.50	10	.2081	.0208	[1] .0282	.0148	35.6	28.8	7.2
KB 1	2.15	13	.2968	.0228	[2] .0476	.0140	108.8	38.6	7.2
KA 1	2.70	16	.3242	.0203	[2] .0346	.0104	70.4	48.8	8.3
Average				.0207					7.9
Zinc No. 1		16	.3421	.0214	[3] .0310	.0112	44.9	47.7	
Zinc No. 2		16	.3646	.0228	[3] .0386	.0135	69.3	40.8	

SECOND SERIES

SH 1	0.83	4	0.1199	0.0300	[1] 0.0581	0.0165	93.7	45.0	6.9
KH 1	.91	5	.1404	.0281	[1] .0546	.0163	94.3	42.0	6.5
KE 1	1.19	7	.1967	.0281	[1] .0557	.0070	98.2	75.1	6.0
KC 1	1.50	7	.2016	.0288	[1] .0528	.0186	83.3	35.4	7.4
KB 1	2.15	12	.3655	.0305	[1] .0570	.0180	86.9	41.0	5.9
KA 1	2.70	17	.5053	.0297	[1] .0478	.0165	60.9	44.4	5.3
Average				.0292					6.3
Zinc No. 1		17	.4709	.0277	[1] .0397	.0164	43.3	40.8	
Zinc No. 2		17	.4595	.0270	.0354	.0181	31.1	33.0	

[1] In first cycle. For zinc No. 2 in the second series, the maximum loss in the first cycle was not much less (0.0328) than the value given. [2] In twelfth cycle. [3] In seventh cycle.

In order to note what effect, if any, the presence of copper in the steel base of hot-dip galvanized sheets would have on the nature of the iron rust formed by prolonged exposure to the conditions of the simulated atmospheric corrosion test, as compared with the known strong adherence of the rust films formed on copper-bearing steel in ordinary atmospheric corrosion, three pairs of copper-bearing and noncopper-bearing steel specimens having zinc coatings of 0.8 to 0.9, 1.5, and 2.5 ounces. (Nos. 1, 3, 9, 11, 17, and 19, Table 2) were kept in test for 71 cycles. These specimens were not brushed or cleaned in any manner between cycles and, in fact, were left entirely undisturbed throughout the course of test. The zinc coating had disappeared more or less completely long before the completion of the test. The coat of iron rust thus formed on both the copper-bearing and noncopper-bearing steel specimens appeared to be very similar in nature; that is, it was loosely adherent and similar in texture and color. A typical appearance of the rust coat thus formed on these two classes of sheet material is shown in Figure 22; the rust coat had reached the peeling-off stage when these photographs were taken about eight months after the completion of the test. It is clear that no distinction between the rust coat formed by the two classes of base metal was offered by the conditions of this type of corrosive atmosphere.

2. SPRAY TESTS

(a) SODIUM CHLORIDE

The results obtained follow a quite consistent trend, as shown in Figure 6, and it might appear that this testing method would serve satisfactorily for the determination of the "life" of the galvanized coating. However, a serious drawback is the prolonged time of exposure to the sodium chloride spray required for the specimens to reach the failure point, which is characterized by the formation of red-brown iron rust at the points where the coating has broken down. With a sodium chloride solution of normal strength, approximately 1,000 hours (42 days) for the lightest weight coatings (0.75 to 1 ounce) and 3,000 hours (125 days) for the heaviest coatings (2.5 ounces) were required to reach the failure point. Another and an important disadvantage is the localized nature of the breakdown of the coating, a further discussion of which will be made in a later paragraph.

It will be noted, in reference to Figure 6, that, with the exception of the results for the annealed specimens, similar characteristics in the results obtained hold true for this diagram as for the simulated atmospheric corrosion test (fig. 5); that is, there was an appreciable scattering of the plotted data for the regular galvanized materials along the solid line, which was drawn in as nearly a mean position as practicable. Also, the data for the materials with imperfect coatings (plotted as triangles) lay decidedly to the left of the solid line. On the other

hand, the results for the annealed specimens were on the side of the solid line reverse to that in the simulated atmospheric corrosion test. They showed a much shorter life than the regular, nonannealed galvanized material. A probable reason for this more rapid corrosive action is that a greater electrolytic action is set up by sodium chloride solution with the iron-zinc alloy than with zinc metal. The lead-coated and "galvannealed" specimens (Nos. 35 and 36, Table 2) showed a comparatively short life, namely, 700 hours—a result which approached, approximately, those for the annealed specimens. Since the hot-dip "gray-galvanized" materials (Nos. 33 and 34, Table 2) were received at a time when the spray tests were well along toward completion and the regular hot-dip galvanized material with a similar weight of coating had required a long exposure to reach the failure point, it was considered not worth while to include these materials in the spray tests.

The corroding of the zinc coating occurred in an entirely different manner from that in the simulated atmospheric corrosion test. Here the breakdown of the coating was confined within those portions of the surface of the specimen which had been attacked. There were three distinct types of surface attack: (*a*) Formation of streaks, extending from the upper to the lower edge of the specimen produced by the downward flow of condensed spray which had collected along the top edge or at the point where the glass suspension hook entered the hole; (*b*) a general corroding of the surface that extended over a part or the whole of the face of the specimen and which was produced by a condensation of the spray in the form of small drops distributed over the area in question and somewhat after the manner of dew; and (*c*) formation of isolated areas at points on the surface where local conditions favored the collection of condensed spray and the consequent corrosion of the underlying coating. The first type was the one met with in most all cases, and the streak extending along the central part from the suspension hole was usually much further developed than the other streaks present on either side of the central streak.

In the light of the experimental results obtained in this work, a different method of supporting the specimens in a vertical position in the spray box, whereby the amount of condensed spray flowing downward from the upper edge could be minimized as much as possible, would have been more desirable than the method of suspending the specimens on glass hooks. Such a method could consist of placing the bottom edge of the specimens within grooves of a bottom support in such a manner that no accumulation of condensed spray would tend to form at the points of contact, which should be well below the upper edge of the enamel border. The specimens

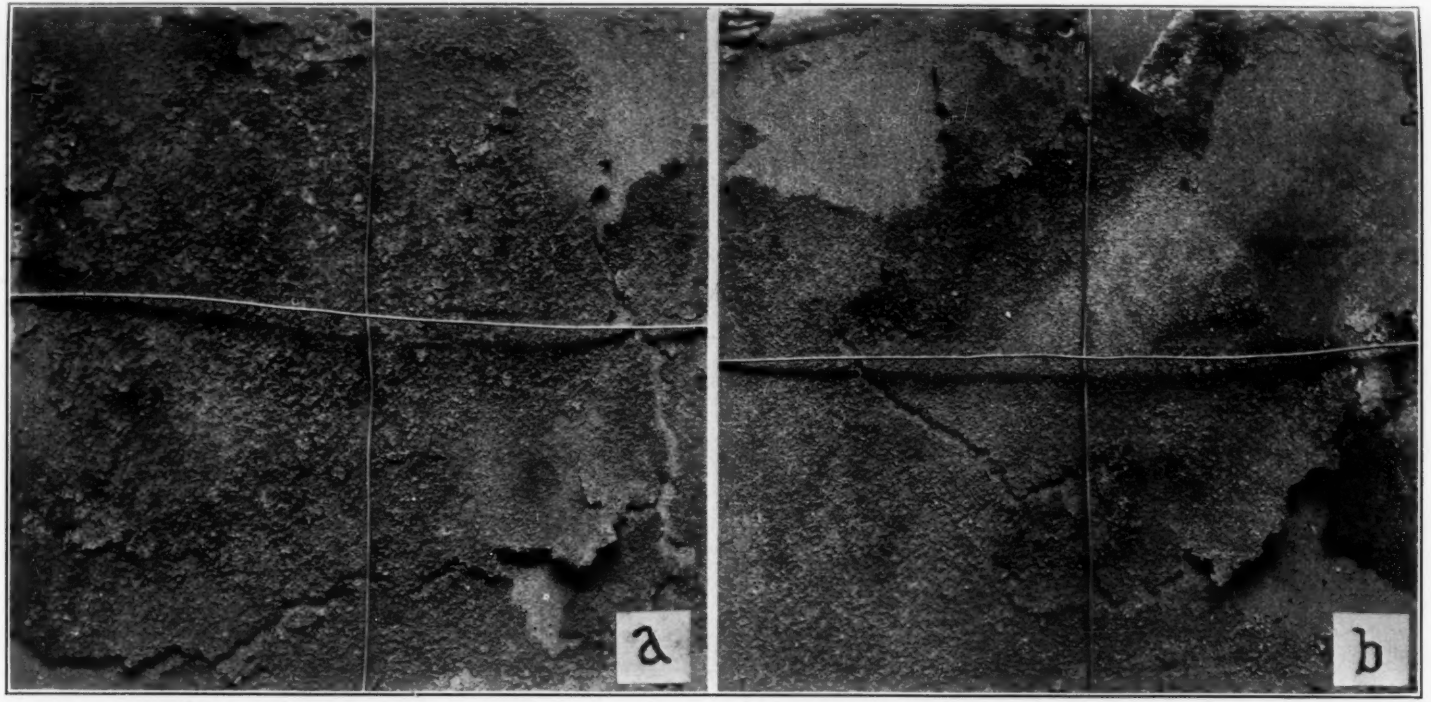

FIG. 22.—*Comparison of the effect produced by the presence of copper in the base metal of hot-dipped galvanized sheets upon the coat of iron rust formed by prolonged exposure in the simulated atmospheric corrosion test.* × *1*

a, copper-bearing steel base; weight of zinc coating, 1.50 oz./ft.² of sheet (No. 11, Table 1); *b*, noncopper-bearing steel base; weight of zinc coating, 2.54 oz./ft.² of sheet (No. 17, Table 1)

FIG. 23.—*Change in appearance of a 0.9-ounce coating after 2,450 hours' exposure to sodium chloride spray. (Material No. 3, specimen KH1–1, Table 2.)* × ¾

One type of corrosive attack was the formation of streaks extending from the upper edge downward and generally to the bottom edge, while the zinc coating lying between the streaks remained little affected. The breakdown of the coating occurred in these streaky areas, as evidenced by the formation of red-brown rust areas and spots (in this photograph, at the top and bottom ends of the central vertical streak, where indicated by arrows)

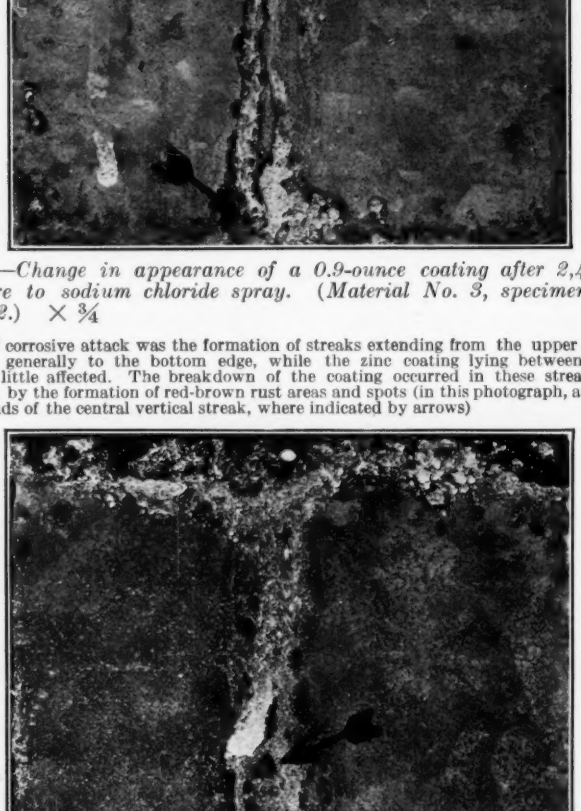

FIG. 24.—*Same specimen as in Figure 23, but showing reverse side.* × ¾

A number of specimens were corroded in a general manner, as manifested by a strong dulling of the surface and the formation of numerous very small pits over a portion of or the entire surface and usually on only one face of the specimen. There were formed, in addition, vertical streaks where the breaking down of the coating usually occurred. In this photograph, iron rust is shown present at two points (indicated by arrows) in the vertical streak as dark patches

should be kept in a vertical position, for it had been found [17] that specimens of zinc-plated and hot-dipped galvanized sheets placed in the salt spray box in a vertical position corroded more rapidly than those in a horizontal or an inclined position. Type (*b*) occurred in a large number of cases and apparently in a manner both capricious and independent of the kind of material, and type (*c*) in a number of cases, in some of which the isolated area formed the lower terminus of an initially started vertical steak. These three types of surface attack are illustrated in Figures 23, 24, 25, 26, and 29. The breaking down of the zinc coating, as evidenced by the formation of red-brown iron rust, occurred at the top, bottom, or along the central vertical streak in the great majority of cases, although there were quite a few cases where the failure point was first reached along one or more vertical steaks lying between the central part and either right or left edge of the specimen or in other locations apart from the central vertical streak.

The progressive corrosion of the zinc coating at the places covered by these three types of surface attack was evidently due to "differential aeration" [18] which had been set up first in the film of liquid that had formed at the point in question and later in the overlying layer of corrosion products resulting from the preceding stages of the corroding process. Evans has stated the general truth that "corrosion is likely to persist most readily in places to which oxygen has least access, provided that these inaccessible places are not far removed from places to which oxygen can penetrate freely." Here the outlying portion of the liquid film had free access to the oxygen of the atmosphere while the oxygen content of the inner portion of the film adjacent to the metal surface became impoverished soon after the initiation of the electrochemical reaction in which the metal surface acted as the anode and the outer portion of the film as the cathode. The soluble zinc chloride produced at the anode reacted with the alkali produced at the cathodic portion to form zinc hydroxide, which precipitated out at a point intermediate between the anodic and cathodic portions. The presence of this wall of insoluble hydroxide served as a barrier to the inward diffusion of the oxygen, and, consequently, the subsequent corrosion was localized in the shielded metal surface. In other words, the corrosion product in the form of the insoluble zinc hydroxide served to shield the underlying metal surface from the oxygen supply, and the corrosion, which would otherwise have been spread over the whole area, tended to become concentrated at this shielded, or anodic, area. The fact that the spray tests were stopped at intervals, as for over Sundays and holidays, and the specimens thus had a chance to get dry, probably

[17] See p. 28 of reference (b) cited in footnote 11.

[18] U. R. Evans, Corrosion of Metals, E. Arnold & Co., 2d ed.; 1926.

accounts, in part at least, for the spreading out of the corroded area, since a compact layer of dried corrosion products often tends to protect the metal just below it and to concentrate attack upon the areas immediately surrounding it.

(b) AMMONIUM CHLORIDE

Two aspects must necessarily be given to the results obtained with this solution because of a peculiar situation, the existence of which was not realized until toward the end of the tests. The plotted data in Figure 7 are divided roughly into two distinct groups, one along curve 1 and the other along curve 2. The specimens of the first group were put into test and had reached the failure point before the simulated atmospheric corrosion tests were started in close proximity (about 3 feet) to the spray box. The cases coming under this group are indicated in Table 4 by the reference mark (1) before the average values; there was, however, one case (KA 1 specimens) where the specimens were put into test at the same time but did not reach the failure point till a long time after the start of the simulated atmospheric corrosion tests. The data for the specimens having different weights of coating up to about 2.0 ounces plotted along curve 1 were quite consistent with the course of the curve drawn. These specimens showed a "life" about half as long as the corresponding specimens in the sodium chloride spray tests.

The specimens in the second group and also the annealed specimens (plotted as crossed circles) were put into test at different times after the start of the simulated atmospheric corrosion tests and were, in the majority of cases, still in test when these other tests were completed. There was much irregularity in the data plotted along curve 2 and in the region lying between the two curves, even in the data for the noncopper-bearing steel base specimens having about 0.8 ounce coating. The specimens with the heavier coatings, 2.0 and 2.5 ounce, showed a very much longer "life" than should have been expected from the course of curve 1.

It was suspected that this irregularity in results was due to conditions arising from the simultaneous operation of the simulated atmospheric corrosion test and the ammonium chloride spray test within a short distance of each other, even though in the latter the specimens were wholly inclosed. There was an occasional escape into the surrounding laboratory atmosphere of the gaseous mixture from the simulated atmospheric corrosion-test apparatus, especially while the tank covers were being exchanged before the washing stage. It should be added here that the sodium chloride spray box, which was kept in operation at the same time, was about 8 feet distant from the simulated atmospheric corrosion test apparatus and in the same direction as the ammonium chloride spray box. The sodium chloride spray test results did not show any such irregularities, even though

specimens of the same materials were put into test in both spray boxes at the same or nearly the same times. An examination of a number of specimens taken from both spray boxes, especially those that had been kept in for 3,000 or more hours, showed that there was present, in the case of the ammonium chloride spray specimens, but not of the sodium chloride spray ones, a thin transparent film which was spread over the uncorroded portions of the specimen faces and could easily be scraped off with a safety razor blade as a fine white powder. On scraping the white deposit of corrosion products off from the corroded areas on a number of the heavier zinc-coated specimens which appeared to have reached the failure point (4,000 or more hours), as judged by the presence of small rust spots on the surface of these deposits, the underlying metal surface showed no evidences of the coating having broken down. These specimens are reported in Table 4 as having a "life" of over 5,000 hours. It was concluded that the misleading presence of the rust spots was due to particles of iron rust that had been carried down by the stream of condensed spray from the suspension hole, which was rusted, lodged in some favorable crevice in the deposit and then covered over with a thin coat of corrosion products. Several of the specimens, from which the deposits of corrosion products had been scraped off, were put back into test and, after several hundred hours' additional exposure, the zinc coating was found to have broken down at some point within the area previously covered by the deposit of corrosion products.

Zinc has been reported[19] to be attacked several times as fast, in the absence of carbon dioxide, when immersed in a 1 per cent solution of ammonium chloride as in sodium chloride solution of the same strength, and, in the presence of carbon dioxide, at about the same rate for both solutions. According to Snyders,[20] zinc decomposes salt solutions, either concentrated or dilute, with the liberation of hydrogen gas and the formation of zinc oxide. This action is more pronounced if the oxide is soluble in the salt solution; this solubility is greatest in ammonium salts. The presence of oxide, without the addition of a carbonate, facilitates the solution of zinc in alkaline solutions. On the other hand, the presence of carbon dioxide retards, up to a certain point, the corrosive action by reason of the formation of a film of insoluble basic zinc carbonate which is spread over the surface.

It would seem that the explanation for the irregularity in the results obtained in the ammonium chloride spray test with those specimens, which were put into test after the simulated atmospheric corrosion tests

[19] Wagner, A., Ueber den Einfluss verschiedener Lösungen auf Metalle. Dingler's Polytech. J., **221**, p. 258: 1876. Also Comey's Dictionary of Chemical Solubilities: Inorganic. MacMillan Co., New York.

[20] Snyders, A. J. C., Die Chemische Wirkung von Wasser und von Salzlösungen auf Zink. Ber., **11** A, p. 936: 1878.

had been started, lies in the formation of a film of basic zinc carbonate that slowed down the otherwise relatively rapid attack of the ammonium chloride solution. In fact, as mentioned in a preceding paragraph, a thin transparent and strongly adherent film was found present on some of the ammonium chloride spray test specimens. Some of this film was scraped off, and the resulting white powder responded to a few qualitative tests for basic zinc carbonate and zinc oxide. Presumably the carbon dioxide gas, present in the atmosphere surrounding the spray box as a result of the escape of the gaseous mixture from the simulated atmospheric corrosion test apparatus, had reacted with the condensed ammonium chloride solution on the surfaces of the specimens to form this film of basic carbonate. Of course, any sulphur dioxide (or sulphurous acid) present would react with the zinc to form a zinc salt, but this gas was probably present in a considerably smaller proportion, and, therefore, the effect of the carbon dioxide would have preponderated. A similar action may have occurred in the sodium chloride spray box but to a much less degree, since the sodium chloride solution is more stable than the ammonium chloride solution.

The manner in which the zinc coating corroded and broke down was very similar to that described in Section V 2, (*a*), p. 287. Figures 27 to 31, inclusive, give typical illustrations of the corroding of the zinc coating in ammonium chloride spray.

Since it was clearly shown that the corroding attack produced by the ammonium chloride spray was entirely local in nature and not at all discriminating in bringing out the variations in the thickness of the coating on the specimen, no effort was made to repeat these tests for the purpose of straightening out the irregularity in the results. It is, however, obvious that due consideration must be given to the conditions surrounding the operation of the spray test in order that the possibility of interfering factors may be avoided.

VI. SUMMARY AND CONCLUSIONS

The purpose of this investigation was the comparison of the merits of two certain types of accelerated laboratory testing methods for evaluating the life of the zinc coating on hot-dip galvanized materials that have been employed by other investigators in testing zinc-coated materials. These two types of testing methods were the simulated atmospheric corrosion and the spray. The test specimens were exposed, in the first type, to a concentrated form of a moist acidic atmosphere which is found prevalent in industrial centers and some large cities and, in the second, to normal solutions of sodium chloride and ammonium chloride, used separately, in the form of a fog or mist. The "life" of the zinc coating was determined by noting the number of cycles (each 24-hour cycle consisting of three

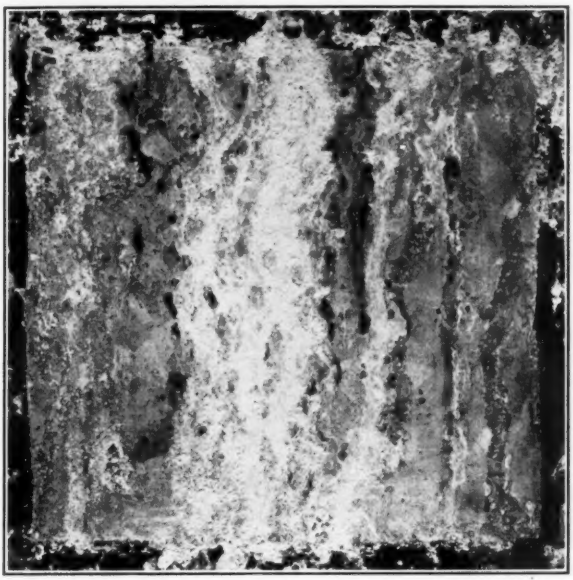

FIG. 25.—*Change in appearance of a 2.0-ounce coating after 2,180 hours' exposure to sodium chloride spray. (Material No. 14, specimen SB2–11, Table 2.)* × ¾

A number of specimens were heavily corroded in a manner similar to that shown here. The central vertical streak was heavily encrusted with corrosion products, and several iron rust spots were present in this streak, thus indicating that the coating had broken down at these points (these rust spots are not brought out in this photograph in a well-contrasted manner)

FIG. 26.—*Change in appearance of a specimen of lead-coated material after 1,560 hours' exposure to sodium chloride spray. (Material No. 35, specimen SSSL–111, Table 2.)* × ¾

Both the streaky and generally corroded types of corrosive attack occurred on this face of the lead-coated specimen. Numerous small iron rust spots were scattered above the lower edge and in portions of the different vertical streaks. The lead coat was roughened in the generally corroded area and in part along the streaks, while it remained smooth in the portions lying between the streaks

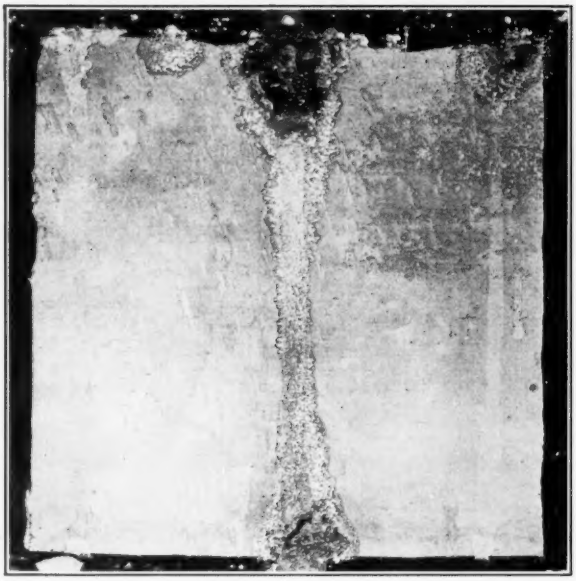

FIG. 27.—*Change in appearance of a 0.9-ounce coating after 2,560 hours' exposure to ammonium chloride spray. (Material No. 2, specimen SH2–1, Table 2.)* × ¾

A heavy deposit of iron rust is present at the top and bottom ends of the central streak and at the top of the streak near the right edge

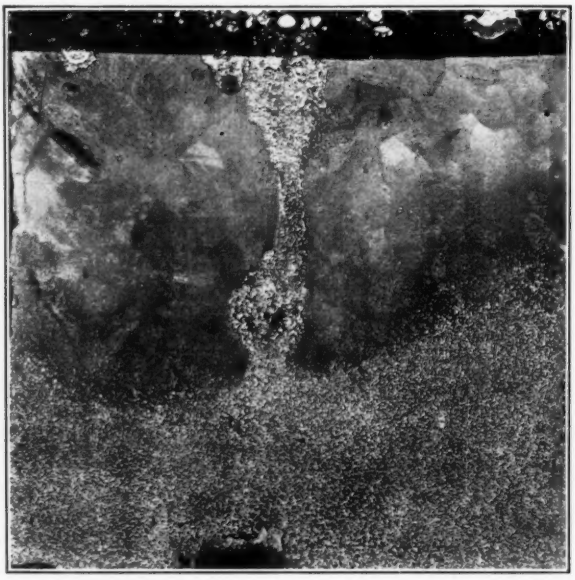

FIG. 28.—*Change in appearance of an 0.8-ounce coating after 1,070 hours' exposure to ammonium chloride spray. (Material No. 23, specimen KK1–11, Table 2.)* × ¾

The vertical streak at the center had formed before the general corroding of the lower half had developed. Clusters of small iron rust spots had formed in the top and middle of the vertical streak, and a considerable part of the corroded area in the lower half was covered with a yellow-colored rust. At the bottom of the vertical streak the coating had been entirely removed, thus leaving bare a good-sized area of the base metal, part of which was covered with an adherent coat of iron rust (shown very dark in the photograph)

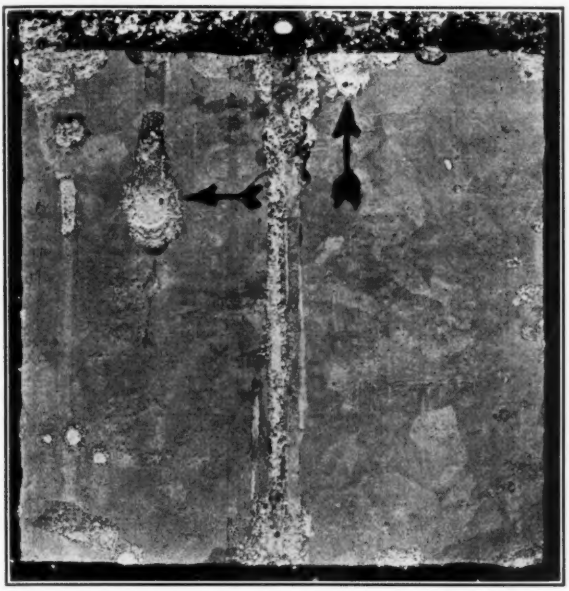

FIG. 29.—*Change in appearance of a 1.5-ounce coating after 1,530 hours' exposure to ammonium chloride spray. (Material No. 12, specimen KC2–11, Table 2.)* × ¾

The coating had broken down on localized corroded areas, as was evidenced by the presence of single small rust spots at the places indicated in the photograph by the arrows. The base metal was laid bare in one fair sized and several small areas at the top of the central vertical streak by the complete removal of the coating; these areas of exposed base metal are fairly well brought out in the photograph

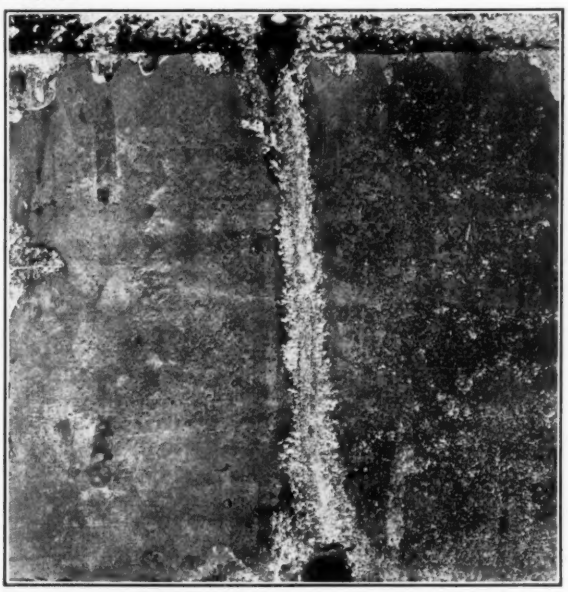

FIG. 30.—*Change in appearance of 1.2-ounce coating after 1,070 hours' exposure to ammonium chloride spray. (Material No. 7, specimen KE1–1, Table 2.)* × ¾

Fairly good-sized areas of the base metal have been laid bare at the top and bottom of the central vertical streak by the complete removal of the coating. Iron rust was present at the borders of these base metal areas. The right half of the specimen was corroded in a general manner, although no evidence of the coating as having broken down anywhere in this portion was present

UNIV OF

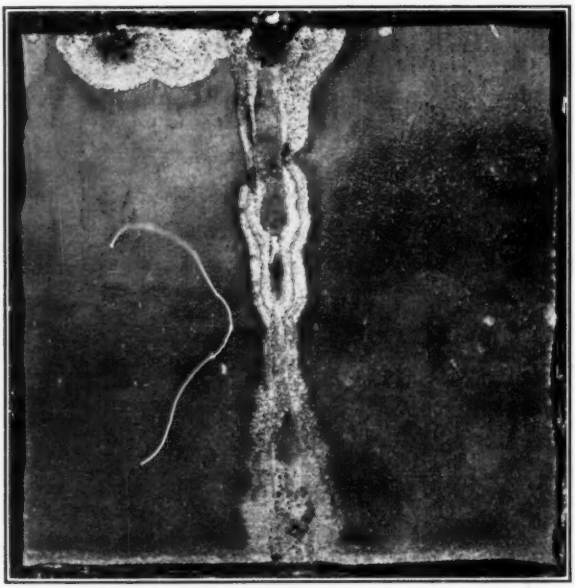

FIG. 31.—*Change in appearance of specimen of "commercially heat-treated" material after 1,125 hours' exposure to ammonium chloride spray. (Material No. 36, specimen SSSG–11, Table 2.)* × ¾

This photograph shows that about three-quarters of the light gray matte-like galvannealed coating had changed color to a blue-black, and that iron rust had formed at the top and bottom (as a cluster of small spots) of the vertical streak and at the upper edge near the left corner

stages: (*a*) 5 hours exposure to a warm moist gaseous mixture of, by volume, 5 parts CO_2, 1 part SO_2, and 94 parts air; (*b*) 1 hour to water spraying, emulating the action of rain; and (*c*) 18 hours air drying) for the first type and the number of hours for the second which were required to produce a breaking down of the coating as evidenced by the first definite appearances of iron rust due to the corroding of the underlying iron or steel base. No attempt was made to interpret the results of these tests in terms of service life in various types of atmospheres prevailing in different climates. Any satisfactory attempt at such an evaluation will have to await the results of long-time field tests on galvanized products carried out at various locations where different typical atmospherical conditions prevail. Fortunately, there is now in progress in this country, under the auspices of the American Society for Testing Materials, such a series of field tests on various classes of galvanized products.

In the simulated atmospheric corrosion tests a consistent relation was obtained between the "life" of the coating, represented by cycles, and the weight of the zinc coating. The time required to produce a breakdown of the coating was within reasonable limits for a laboratory testing method, about three to four weeks being required for sheet materials with 2.5-ounce coating exposed to the concentration of gases and for the comparatively short time per cycle employed in these tests. The rate of the loss in weight of the coating was found, experimentally, to vary from cycle to cycle for individual specimens, but that the average loss in weight per cycle and also the ratio of the initial weight of coating to the total loss in weight approached constant values, which were independent of the initial weight of the coating, for the series of tests.

In the spray tests, the results for the sodium chloride solution showed a quite consistent relationship between the "life" of the coating, expressed in hours, and the weight of coating. However, the time required for the breaking down of the coating was considerable, about 3,000 hours, or 125 days, being needed for specimens with a 2.5-ounce coating. In the tests with ammonium chloride solution the results obtained for about half of the specimens which were tested before the simulated atmospheric corrosion tests had been started in close proximity to the spray boxes showed about twice as short a "life" as for the corresponding specimens in the sodium chloride spray tests. The results for the remainder of the specimens, which were put into test during the progress of the simulated atmospheric corrosion tests, were complicated by the formation of a film of corrosion products which materially slowed down the rate of corrosion. The formation of this film is ascribed to the occasional presence in the laboratory atmosphere of gases that had come from the simulated atmospheric corrosion test apparatus.

The manner in which the zinc coating was attacked was altogether different in the two types of testing methods. In the simulated atmospheric corrosion test method the coating was removed in a progressive manner over the entire surface from the zinc metal layer down through the outer and inner iron-zinc alloy layers to the base metal, generally starting at the points where the coating was thinnest. This progressive removal of the coating was similar to that reported for galvanized materials exposed to the atmosphere under service conditions. With both solutions in the spray test method the specimens were corroded in an entirely local and capricious manner, depending on the distribution of the condensed spray over the surface of the specimen and usually along the vertical central portions where the specimen was suspended. Corrosion progressed at these points through differential aeration. The portions of the surface lying between the corroded areas oftentimes remained uncorroded. This absence of a selective corroding of the coating, whereby the thinnest portions of the coating are revealed, constitutes a serious drawback for the spray test method in comparing the merits of the two types of testing.

The presence of 0.2 per cent copper in the steel base metal produced no observable effect on the "life" of the zinc coating as compared with that of the coating on noncopper-bearing steel sheets.

The results for the sheet materials with imperfect coatings, such as gray galvanized, stringy, and blistered, were consistent in showing a somewhat lower "life" than the regular sheet materials of good quality in all the tests.

Results obtained with a number of hot-dip galvanized sheet specimens, which had been annealed at 500° C. (932° F.) for one-half hour for the purpose of converting as much of the zinc coating into an evenly distributed iron-zinc alloy as practicable, showed that this converted coating was somewhat more resistant than the normal nonannealed coating in the simulated atmospheric corrosion test but was decidedly less resistant in the sodium chloride spray test. The slower action in the former case seems possibly due to the absence of overlying portions of a zinc metal layer, whereby the general corrosive attack would have been accelerated by the reaction between the anodic zinc metal layer and the cathodic iron-zinc alloy layer. It appears probable that the more rapid action in the latter case is caused by a greater tendency for electrolytic action on the part of the alloy than of zinc metal in the presence of sodium chloride solution.

In the light of the above-reported results, the simulated atmospheric corrosion test method appears to give much promise as an accelerated laboratory corrosion testing method for zinc coatings that would be of value to the industry, particularly for development work where a comparative measure of the probable service behavior

under the severest atmospheric conditions of products coated by new or improved processes is to be desired. It is hardly to be recommended for routine testing wherein information as to the weight and uniformity in thickness of the coating is the sole objective, for the stripping tests now employed for this purpose are sufficiently adequate and less time consuming. There seems to be no reason why an automatically operated apparatus for the simulated atmospheric corrosion test method could not be developed, whereby the testing work would be facilitated to a marked degree. The spray test method, at least as used with normal solutions of sodium chloride and ammonium chloride as the corrodent, has failed to show any merits which would recommend it as an accelerated test method for evaluating the service life of hot-dip zinc coatings.

The authors wish to express their sincere appreciation to H. S. Rawdon and H. W. Gillett, of the division of metallurgy, Bureau of Standards, for helpful suggestions made in the course of this work.

WASHINGTON, May 4, 1928.

THE JULY, 1928, NUMBER OF THE JOURNAL

[VOL. 1, NO. 1]

contains the following Research Papers:

RP1. Accelerated tests of organic protective coatings. Percy H. Walker and E. F. Hickson.

RP2. Measurement of the tread movement of pneumatic tires and a discussion of the probable relation to tread wear. W. L. Holt and C. M. Cook.

RP3. Absolute methods in reflectometry. H. J. McNicholas.

RP4. Interferometer measurements of wave lengths in the vacuum arc spectra of titanium and other elements. C. C. Kiess.

RP5. Analysis of bauxite and of refractories of high alumina content. G. E. F. Lundell and J. I. Hoffman.

These will be available as separates for purchase from the Superintendent of Documents, Government Printing Office, Washington, D. C.

Bureau researches concern specifically fundamental science and the laws of matter and energy; physical constants and other basic data in the form of tables, equations, nomograms, or other graphs; the properties of materials, structures, and devices and their effective design and performance; the mitigation of injurious effects of such agencies as fire, corrosion, breakage; the promotion of efficiency by scientific measured control of processes through experimental and theoretical research in the fields of physics, chemistry, engineering, and the special technologies, such as:

Electricity
Magnetism
Radio communication
Photometry
Radioactivity
Length
Mass
Capacity
Density
Time
Radiometry
Spectroscopy
Colorimetry
Polarimetry
Atomic physics
Electrochemistry
Gas chemistry
Heat and power
Thermometry
Pyrometry
Fire resistance
Refrigeration
Mechanics
Sound
Aeronautics and aerodynamics
Metallurgy
Textiles, paper, leather, and rubber
Structural materials
Cement
Ceramics
Optical glass. etc.

Several hundred researches are in progress at the Bureau of Standards and the outlet for the results is the Bureau of Standards Journal of Research.